Faculty of Pharmaceutical, Biomedical, and Veterinary Sciences
Department of Veterinary Sciences

Juvenile Göttingen Minipigs as Pediatric Safety Testing Model for Antisense Oligonucleotides (ASOs)

PhD thesis submitted for the degree of Doctor of Veterinary Sciences (PhD) at the University of Antwerp to be defended by Allan Paulo Valenzuela

Supervisors:
Prof. Dr. Steven Van Cruchten
Dr. Miriam Ayuso Hernando

Antwerp, 2023

Table of Contents

List of Abbreviations

2’-MOE	2’-O-methoxyethyl
2’-OMe	2’-O-methyl
ADME	Absorption, distribution, metabolism, excretion
ALT	Alanine transaminase
APC	Alternative pathway of complement system
ApoB-100	Apolipoprotein B 100
aPTT	Activated partial thromboplastin time
ASGR1	Asialoglycoprotein receptor 1
ASO	Antisense oligonucleotides
AST	Aspartate aminotransferase
AUC	Area under the curve
BUN	Blood urea nitrogen
CFH	Complement factor H
CH50	50% hemolytic complement
C_{max}	Maximum concentration
CNS	Central nervous system
CRISPR	Clustered regularly interspaced short palindromic repeats
DAB	3, 3’-diaminobenzene
DART	Development and reproductive toxicology
DMPK	Drug metabolism and pharmacokinetics
DNase	deoxyribonuclease
dsDNA	Double-stranded DNA
EGF	epidermal growth factor
EMA	European Medicines Agency
ENPP1	Ectonucleotide pyrophosphatase/phosphodiesterase 1
FDA	Food and Drug Authority
GalNAc	N-acetylgalactosamine
GD	Gestational day
GFR	Glomerular filtration rate
GPVI	Glycoprotein VI
h	hours
H&E	Hematoxylin and eosin
ICH	International Conference on Harmonization
IgM	Immunoglobulin M
IHC	Immunohistochemistry
IP	Intraperitoneal
ISH	In situ hybridization
IV	Intravenous
JAS	Juvenile animal study
KIM1	Kidney injury molecule 1
LC-MS/MS	Liquid chromatography-tandem mass spectrometry
LDL	Low-density lipoprotein
LNA	Locked nucleic acid

min	minutes
MOA	Mechanism of action
mRNA	Messenger RNA
NBE	New biological entities
NCE	New chemical entities
NHP	Nonhuman primate
OD	Optical density
ON	Oligonucleotide
OND	ON-based drug
OSWG	Oligonucleotide Safety Working Group
PAS	Periodic acid-Schiff
PBPK	Physiologic-based pharmacokinetics
PC	Positive control
PCSK9	Proprotein convertase subtilisin/kexin type 9
PD	Pharmacodynamic
PDE1B	Phosphodiesterase 1B
PF4	Platelet factor 4
PIP	Pediatric investigation plan
PK	Pharmacokinetic
PND	Postnatal day
PO	Phosphodiester (unmodified)
PRP	Platelet-rich plasma
PRR	Pattern recognition receptor
PS	Phosphorothioate
PT	Prothrombin time
PTO	PS-modified ASOs
qPCR	Quantitative polymerase chain reaction
RNase H	Ribonuclease H
rpm	Revolutions per minute
RT	Room temperature
SC	Subcutaneous
siRNA	Small interfering RNA
ssDNA	Single-stranded DNA
SYK	Spleen tyrosine kinase
TCP	Thrombocytopenia
TLR	Toll-like receptor
T_{max}	Time to reach C_{max}
TREX1	3-prime repair exonuclease 1
TSP-1	Thrombospondin-1
WB	Whole blood
ΔTm	Melting temperature

Preface

The classical toolbox for drug discovery is continuously expanding beyond traditional small-molecule therapies and monoclonal antibodies. This includes oligonucleotide (ON)-based drugs (ONDs), such as antisense oligonucleotides (ASOs), which are designed to target RNA that enables selective modulation of currently difficult or even previously undruggable disease-related proteins. Currently, the development of ASOs is progressing for a wide range of indications, including cancers, viral infections, and rare genetic conditions, in adult and pediatric patients. Typically, nonhuman primates (NHPs) are used as the nonrodent model of choice for adult safety assessment of ASO drug candidates. In 2017, the adult Göttingen Minipig was characterized to be a suitable alternative non-rodent model in the adult safety assessment of ASOs. As authorities now also stimulate the development of drugs for pediatric indications, for which juvenile animal studies (JAS) may provide useful information, extending the work to qualify the juvenile Göttingen Minipig for pediatric safety assessment of ASOs has been suggested. Therefore, this thesis focuses on characterizing the juvenile Göttingen Minipig as a pediatric ASO safety testing model concerning its pharmacokinetic (PK), pharmacodynamic (PD), and safety profiles.

Chapter 1

General Introduction

1.1 Antisense oligonucleotides (ASOs)

ASOs belong to a large group of therapeutic ONs for which different mechanisms of action (MOA) are harnessed to exert their therapeutic potential. In particular, ASOs emerged as a clinically validated therapeutic modality that utilizes synthetic ONs to modulate the translation of disease-related proteins [1]. The use of synthetic ONs as therapeutic agents has progressed into broad applications concurrent with the development of ASOs and involves multiple modalities, including small interfering RNA (siRNA), mRNA, microRNA, non-coding RNA, long non-coding RNA, ribozymes, small nucleolar RNA, and nucleic acids used for immune modulation (e.g., aptamers), gene editing (i.e., CRISPR), and targeting toxic repeats [2]. These modalities and ASOs share characteristics such as native nucleotide components or analogs joined together by phosphodiester (PO) or modified linkages (see section 1.1.4.1). This thesis will focus on ASOs, and particularly on their PK/PD and safety profiles in the juvenile Göttingen Minipig. In this chapter, we will present a review of what ASOs are, beginning with a general perspective (1.1.1), followed by their therapeutic indications (section 1.1.2), types (classes) (section 1.1.3), modification chemistries, and design strategies (section 1.1.4). Afterward, a general description of their PK/PD (sections 1.1.5 – 6) and safety profiles (section 1.1.7) will be discussed. In addition, an overview of ASO nonclinical development and safety evaluation (section 1.2) will be presented, including perspectives on nonclinical pediatric ASO safety testing and species selection.

1.1.1 General perspectives: ASO history and general advances/challenges

Antisense-based pharmaceuticals have a variety of pharmacologic actions since they can potentially be designed to engage and modulate any RNA. As a result, clinical use (Table 1.1) and testing of ASOs encompass numerous medical conditions [1]. In 1998, the first marketing authorization for an ASO was granted to fomivirsen, indicated for cytomegalovirus retinitis in patients with AIDS. It took two decades for this approval to pass since the initial proof of the ASO concept in 1978 [2]. In the

beginning, the concept of antisense therapies was conceived as a DNA-like ON sequence capable of precisely binding to a complementary disease-related (m)RNA [2]. This began when Zamecnik and Stephenson showed in their seminal works that suppressing Rous Sarcoma viral replication and preventing chick fibroblasts' transformation into sarcoma cells could be achieved using a 13-mer unmodified single-stranded DNA (ssDNA) ON. As a result, this idea opened up novel strategies for developing treatments based on inhibiting or modulating protein translation [3]. Although the basic idea behind synthetic ONs as a therapeutic agent is straightforward, a thorough grasp of nucleic acid chemistry must be realized before it reaches the clinics.

On this account, it took 15 years for the subsequent approval of an ASO therapeutic to be witnessed in 2013. By the end of 2016, only two more ASOs had been granted approval by health authorities, while another four ASOs were approved by 2020 (Table 1.1) [4]. Evidently, this shows that the field took time to develop and get mature enough to produce safe and efficacious drugs qualified for marketing authorization. Nonetheless, the chemical toolbox gradually expanded and became more sophisticated throughout the years. ASOs that have advanced into clinical trials steadily increased in frequency in recent years. As more ASOs pass through stringer sequence screening and safety testing based on existing knowledge in this field, the pace of approvals will likely continue to speed up [5]. However, this promising drug modality still needs to address several challenges.

The main challenges the antisense therapeutic concept faced before reaching the clinics were primarily related to its physicochemical properties, such as nuclease instability and limited protein binding affinity (see section 1.1.4). Therefore, finding new analogs of ONs with enhanced nuclease resistance and protein binding for application in antisense investigations became the primary research objective in the past [2].

Table 1.1. List of currently approved oligonucleotide-based therapeutics. This table is adapted from Takakusa et al. (2023) [4].

Generic name	Type	Mechanism	Approval	Target	Indication
Fomivirsen	ASO	Translation block	US 1998 EU 1999	CMV IE2 mRNA	CMV retinitis
Pegaptanib	Aptamer (PEG)	Binding and blocking	US 2004 EU 2006 JP 2008	VEGF165 (protein)	Neovascular ARMD
Mipomersen	ASO (gapmer)	RNase H degradation	US 2013	ApoB-100 mRNA	HoFH
Eteplirsen	ASO	Splicing modulation	US 2016	Dystrophin pre-mRNA	DMD
Nusinersen	ASO	Splicing modulation	US 2016 EU 2017 JP 2017	SMN2 pre-mRNA	Spinal muscular atrophy
(CpG1018)1	CpG oligomer	Binding and activating	US 2017 EU 2021	TLR9 (protein)	HBV infection
Inotersen	ASO (gapmer)	RNase H degradation	US 2018 EU 2018	TTR mRNA	hATTR
Patisiran	siRNA (LNP)	RNAi	US 2018 EU 2018 JP 2019	TTR mRNA	hATTR
Volanesorsen	ASO (gapmer)	RNase H degradation	EU 2019	ApoCIII mRNA	FCS
Givosiran	siRNA (GalNAc)	RNAi	US 2019 EU 2020 JP 2021	ALAS1 mRNA	Acute hepatic porphyria
Golodirsen	ASO	Splicing modulation	US 2019	Dystrophin pre-mRNA	DMD
Viltolarsen	ASO	Splicing modulation	US 2020 JP 2020	Dystrophin pre-mRNA	DMD
Lumasiran	siRNA (GalNAc)	RNAi	US 2020 EU 2020	HAO1 mRNA	PH1
Inclisiran	siRNA (GalNAc)	RNAi	EU 2020 US 2021	PCSK9 mRNA	HeFH
Casimersen	ASO	Splicing modulation	US 2021	Dystrophin pre-mRNA	DMD
Vutrisiran	siRNA (GalNAc)	RNAi	US 2022	TTR mRNA	hATTR

Abbreviations: ASO, antisense oligonucleotide; US, United States; EU, European Union; CMV IE2, cytomegalovirus immediate early 2; PEG, polyethylene glycol; VEGF, vascular endothelial growth factor; ARMD, age-related macular degeneration; ApoB-100, apolipoprotein B 100; HoFH, homozygous familial hypercholesterolemia; DMD, Duchenne muscular dystrophy; SMN2, survival motor neuron 2; TLR9, Toll-like receptor 9; HBV, hepatitis B virus; TTR, transthyretin; hATTR, hereditary transthyretin amyloidosis; ApoCIII, apolipoprotein CIII; LNP, lipid nanoparticle; FCS, familial chylomicronemia syndrome; siRNA, small interfering RNA; GalNAc, N-Acetylgalactosamine; ALAS1, delta-aminolevulinate synthase 1; HAO1, hydroxyacid oxidase 1; PH1, primary hyperoxaluria type 1; PCSK9, proprotein convertase subtilisin kexin 9; HeFH, heterozygous familial hypercholesterolemia.

The synthesis of phosphorothioate (PS) ONs marked a significant advancement in the realm of ASO therapies in the mid-1980s [6,7]. PS-modified ASOs (PTOs) have more favorable physicochemical properties than unmodified ONs (e.g., nuclease resistance and increased protein binding affinity), making it a suitable modification basis for antisense therapeutics resulting in much higher cellular activity and a better PK profile [8] (see section 1.1.4.1.1). In light of these findings, the scientific community began to pay attention to antisense technology, and PTOs became the first generation of ASOs [2]. Nevertheless, this modification caused nonspecific off-target binding to other RNA sequences and proteins, which may result in adverse reactions [9] (see sections 1.1.7). The progression of PTOs from nonclinical to clinical investigations has offered an essential understanding of the characteristics of modified ASOs [2,10,11]. Improvements in PK profile and adverse reactions related to the PS backbone modification have been extensively investigated and categorized as 'class effects'. Considering the prevalent adverse reactions to PTOs, early development studies utilizing them persisted in growing [2]. Moreover, the duplex of a PTO with a complementary RNA induces RNase activity [12]. Hence, apart from the steric blocking and splicing modulation mechanisms, this allowed PTOs to be used in cleaving RNA strands causing translation inhibition [13] (see section 1.1.3).

Subsequently, medicinal chemists developed an array of modifications (e.g., 2'-O-methoxyethyl (2'-MOE) and locked nucleic acid (LNA)) to improve the different properties of ASOs, which will render them useful as therapeutic agents. Moreover, certain modifications can be combined in a chimeric pattern (e.g., gapmers) to further improve the desired ASO properties (see section 1.1.4.2). Applying these other ASO chemistries and modification patterns led to the second generation of ASOs [14].

Aside from drug metabolism (ASO degradation) and PK challenges, identifying toxicities or toxicological properties of ASOs poses another challenge in this field. As there are no specific guidelines for these emerging drug modalities (see section 1.2), designing the drug development and safety packages is more flexible for ASOs than small molecule drugs, which should be viewed as an opportunity instead of a problem. In general, the goal is to identify the adverse effects of ASOs (as discussed in section 1.1.7) through well-designed studies as early as possible. This warrants the use of in silico, in vitro, and suitable nonclinical animal models.

1.1.2 Indications

Currently, more than a dozen ONDs (of which nine are ASOs) have received marketing authorization (Table 1.1), while many others are in development for a wide range of indications, including malignant neoplasms and viral infections. Most of these diseases were previously untreatable with conventional drug modalities due to the innate difficulties in targeting the relevant proteins involved in their pathology [15]. Additionally, the majority of ON therapeutics that have received approval to date (e.g., eteplirsen, mipomersen, inotersen, and volanesorsen) are intended to treat rare, frequently genetic conditions. Since there is no viable alternative treatment, the appearance of certain safety signals in these circumstances has been determined to be acceptable based on risk: benefit analysis. This, however, will probably be different for certain recent initiatives that intend to target significantly larger populations with more prevalent diseases, such as the cholesterol-lowering siRNA (inclisiran) targeting Proprotein convertase subtilisin/kexin type 9 (*PCSK9*) transcript and for which alternative therapies are available [16]. On the other hand, ASOs can be customized to treat diseases unique to an individual, such as milasen, a splice-modulating ASO designed for an 8-year-old child with Batten disease, a fatal neurodegenerative disease [17]. Such tailored therapy will most certainly become a routine practice in the future as screening procedures in drug discovery improve and become more stringent [16].

Nonetheless, since ASOs could treat rare genetic conditions (among others) not just in the adult population but also in special populations, such as pediatrics (e.g., milasen), other pediatric indications of ASOs have also been explored [18–23]. For these indications, spinal muscular atrophy and Duchenne muscular dystrophy have been successfully treated [24–26]. In an overview of ASO candidates which have reached the clinic (either active/completed or discontinued), 31 of 136 clinical trials have a pediatric target population (birth to 17 years of age). Although these figures are non-exhaustive, as gathered in ClinicalTrials.gov during the conduct of this thesis, this shows the imbalance between adult and pediatric use of this technology and warrants future research to supplement the limited knowledge in refining and optimizing the design of drug development and safety packages for ASOs intended for pediatrics.

1.1.3 ASO characteristics and types

ASOs are designed to hybridize to RNA's sense strand (i.e., the strand coding for protein) [15] and are usually 8 to 50 nucleotides in length [27]. They bind to their cognate complementary RNA in a sequence-specific manner through the highly selective Watson–Crick base pairing [1]. This has the benefit of not requiring the identification of compounds with intricate ligand-protein binding sites, as in the case of small-molecule pharmaceuticals, and of high selectivity without being constrained to extracellular epitopes, as in the case of the majority of antibody therapies [28]. ONDs can exert their effects via a variety of mechanisms of action (Table 1.2).

In general, ASOs can be divided into two categories: enzyme-independent and enzyme-dependent oligonucleotides [1]. Steric-blocking ONs prevent the cellular machinery from accessing pre-mRNA or mRNA without triggering RNA enzymatic degradation, while other ASOs require enzyme-dependent degradation of the target mRNA (e.g., ribonuclease H (RNase H)-dependent ASOs) (Figure 1.1). Some of the principles that will be described in this thesis may be applicable to other OND modalities.

Table 1.2. Mechanism of action of nucleic acid-based therapeutics. The table is adapted from Lagos-Quintana (2016) [29].

Type of potential therapeutic nucleic acid		Mechanism of action
ASO	siRNA	RNA interference pathway*
	miRmimic	microRNA pathway
	antimiR	Inhibition of microRNAs
	RNase H-dependent ASO	RNase H-mediated RNA degradation pathway*
	Splicing modulators	Bind to pre-mRNA and modulate splicing, generally leading to exon skipping or inclusion.
	Steric translation/ transcription blockers	Bind to mRNA or genomic DNA and block translation or transcription, respectively
	Immunostimulatory ONs	Interact with receptors and proteins, which initiate immune signaling cascades leading to inflammatory reactions
Aptamers		Bind with high affinity and specificity to proteins modulating their function
Ribozymes/ DNAzymes		Catalytic nucleic acids that cleave target RNA
CRISPR guide RNAs		Base-pairing between sgRNA and target DNA causes double-strand breaks due to endonuclease activity of Cas9
mRNA		RNA transcripts that encode therapeutic protein, which will be translated in the cell

Abbreviations: ASO, antisense oligonucleotides, siRNA, small interfering RNA; ON, oligonucleotide; CRISPR, Clustered Regularly Interspaced Short Palindromic Repeats; Cas9, CRISPR-associated protein 9; *Enzyme-dependent ASOs.

1.1.3.1 *Enzyme-independent ASOs*

ASOs share the fundamental principle of target hybridization and modulation of RNA function. Basically, ASOs can bind to their target sequence and prevent translation (or pre-mRNA processing), impairing the target sequence's translation and hence, the ability to perform its function [30,31] (Figure 1.1). For instance, steric-blocking ONs may induce alternative splicing, correct defective RNA, enhance protein synthesis, or suppress gene expression without triggering RNA degradation [1]. Splice-switching ASOs, a type of steric-blocking ON, may improve the synthesis of a therapeutic splice variant (Figure 1.1) [15]. Typically, they target a specific or a subset of mutations and subsequently shift the protein synthesis towards the therapeutic isoforms, allowing the biological function that was formerly lacking or insufficient [3,15]. As a result, this ASO class could be used to treat numerous genetic diseases as opposed to conventional drugs that bind to proteins, which will unlikely increase its function.

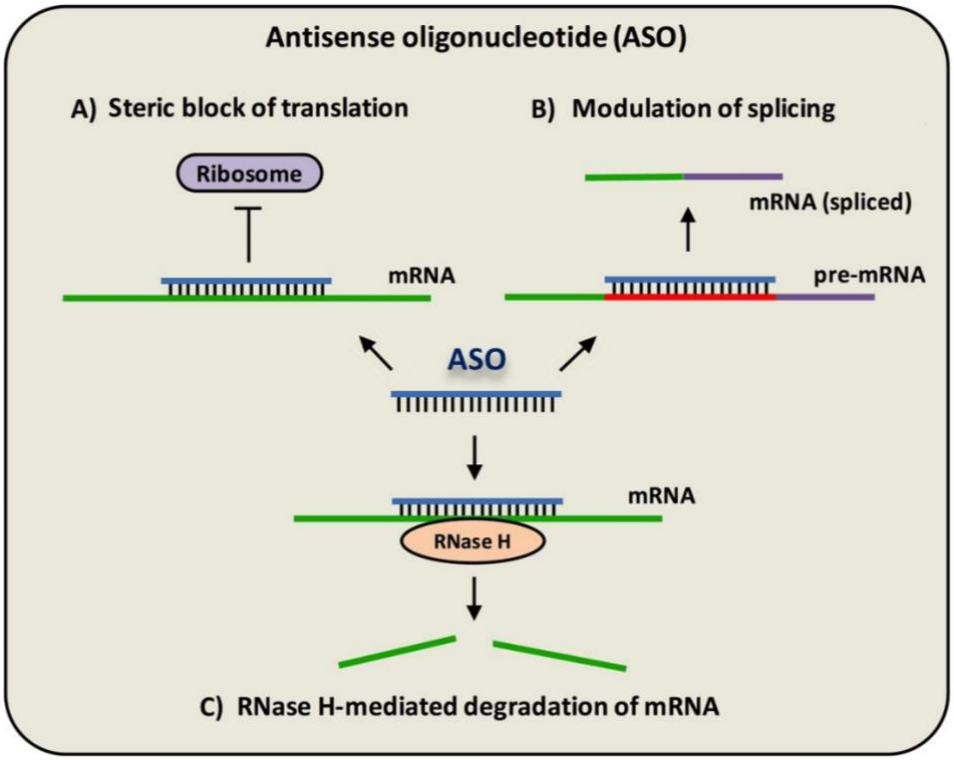

Figure 1.1. Three of the main mechanisms through which antisense oligonucleotides (ASOs) modulate gene expression: A) Steric block of translation, B) Splicing modulation, and C) RNase H-mediated mRNA degradation. This figure is adapted from Rossor et al., (2018) [32].

1.1.3.2 *Enzyme-dependent ASOs (RNase H mechanism)*

In contrast to the previously described ASO class, certain ASOs depend on enzymes to reduce RNA and protein levels to exert their therapeutic potential [15]. Upon entry into the cell and after engaging with its complementary target RNA sequence, the ASO that is now part of an RNA-DNA heteroduplex may induce cleavage of the target transcript through endogenous ribonucleases (i.e., RNase H) [33] (Figure 1.1). Hence, RNase H-dependent ASOs have been developed to facilitate the targeted degradation of a specific RNA sequence through the RNase H mechanism [34].

RNase H is a family of ubiquitously expressed endonucleases that particularly cleaves the RNA strand of a DNA/RNA heteroduplex [35], leaving 3'-hydroxyl and 5'-phosphate terminated metabolites, and subsequently releases the intact DNA strand (i.e., ASO). ASOs can modulate gene expression with such cleavage events as one binding interaction irreversibly destroys the target transcript [15].

Mammalian RNase H isoforms have distinctive functions, although overlap exists for the maintenance of genome stability [36]; RNase H1 is necessary for gene transcription (R-loop and Okazaki fragments processing) [8,37], whereas RNase H2 is thought to remove RNA primers during DNA replication [38]. RNase H1 is the key enzyme involved in ASO pharmacology for inhibiting RNA translation [39]. This has been supported by the works done by Wu et al., wherein downregulation and overexpression of both H1 and H2 variants confirmed that the H1 isoform is associated with ASO activity and its modulation affected antisense activity in a coordinated manner in both animal and in vitro models [37,39].

The heteroduplex formed through the interaction of ASO and the targeted RNA confers RNase H specificity in this mechanism. In particular, the N-terminus of this endonuclease contains the RNA binding domain, whereas the C-terminus has the catalytic domain, which is dependent on the existence of the 2'-hydroxyl on the ribose sugar for cleavage [3]. The catalytic region of the human RNase H1 establishes numerous crucial interactions with the heteroduplex's DNA and RNA strands, resulting in a seven-nucleotide footprint on the DNA-RNA hybrid [8]. Catalysis requires the presence of two metal ions (Mg^{2+} or Mn^{2+}), and RNase H interaction with the heteroduplex results in hydrolysis of the RNA strand at a point distal from the binding area [40,41]. Human RNase H1 has an Mg^{+2} preference for catalysis, while it is inhibited by Mn^{2+} [42].

The ASO must have a minimum of eight successive DNA bases for RNase H cleavage to be effective; this allows for the formation of an RNA-DNA hybrid upon binding, which in turn recruits RNase H and facilitates the target transcript cleavage [15]. More specifically, RNase H1 requires every nucleotide within its seven-nucleotide footprints to adapt several distinct conformations to support RNA cleavage [43,44]. This can be accomplished using unmodified (PO) DNA. However, due to nuclease instability, chemical and ASO sequence design modifications were needed to improve metabolic stability while still being compliant with RNase H1 biochemistry to facilitate RNA degradation [8]. Additionally, the ASO should remain intact so it can degrade other target transcripts, which in turn amplifies its potency.

1.1.4 OND chemistry and design

Unmodified ASOs, as previously stated, do not possess adequate nuclease stability [45] and are found to be unstable in cells and blood circulation, resulting in a relatively limited half-life and, thus, cannot be used as a therapeutic agent [5]. As a result, medicinal chemists have produced a plethora of chemical modifications to improve the enzymatic stability and biological effectiveness of antisense molecules [8]. Meanwhile, the quest for appropriate ASO design to support RNase H1 activity began [8,46] to optimize target RNA degradation. On the other hand, steric blockers (e.g., splicing modulators) benefited from chemistries with increased affinity (e.g., 2'-ribose and constrained nucleotides) that also enable the candidate sequence resistant to RNase H activity, as have been uniformly used (or in combination) in this ASO class [3].

In general, the antisense mechanism an ASO class can utilize after binding to its target RNA is determined by its chemical modification and design pattern specifications [47]. The chemistry and design variants within these ASO classes are maintained essentially the same, with just the nucleobase sequence changing to align with the target transcript. Certain chemical and design variants predominate over others, giving rise to common features shared across ASO classes [28]. The improvements brought by these chemistries and modification patterns regarding ASO PK/PD, together with the novel developments with the use of delivery systems, definitely advanced the field of ON therapeutics. These points will be described in the following sections.

1.1.4.1 *OND chemistry*

Major advances have been achieved in optimizing the balance between affinity and specificity, nuclease stability, distribution and elimination, cellular uptake and trafficking, and safety, depending on the chemistries utilized and how they were patterned in the sequence design [5,28]. While dozens of different sugar, base, and backbone modifications have been produced, ASOs often contain PS backbone and certain sugar moiety modifications that enhance their therapeutic characteristics [16,48]. Several of the most commonly used chemistry modifications can be seen in Figure 1.2. However, the focus in the following subsections would be limited to the PS backbone linkage modification, 2'-ribose-modified (i.e., 2'-O-methoxyethyl (2'-MOE)), and constrained sugar (i.e., locked nucleic acid (LNA)) chemistries. The latter two are among the most commonly used sugar-modified ON chemistries [5].

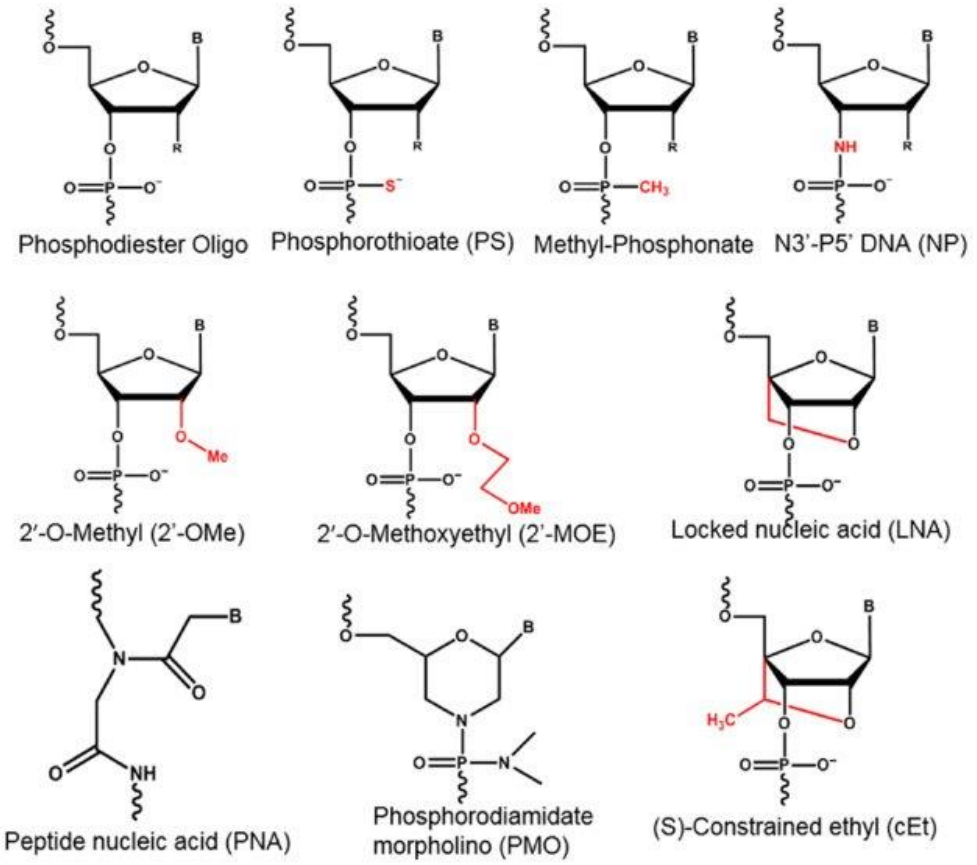

Figure 1.2. Overview of different chemical modifications of antisense oligonucleotides (ASOs). This figure is reproduced from Xiong et al. (2021) [49].

1.1.4.1.1 Phosphorothioate (PS) backbone linkages

One of the earliest and remains one of the most popular modifications is the substitution of sulfur for oxygen in the phosphate backbone leading to PTOs, which are much more stable than native DNA [1,8]. The PS linkage is chiral at phosphorus [8], resulting in two diastereomers (Sp and Rp stereoisomers). The increased stability of PTOs to nucleolytic degradation [50] is accounted for by the Sp configuration, which is highly resistant to nuclease activity, probably as a result of the sulfur being in closer proximity to the metal ions of nucleases [3]. Because of this, PTOs have enough stability in plasma, tissues, and cells following systemic administration, and this prevents degradation before they reach the target RNA [27].

An important advantage of incorporating PS linkages in the OND backbone is that it also enables to efficiently elicit RNase H cleavage of the target RNA [27]. Aside from that, PS modification also confers a substantial PK benefit by increasing the binding affinity to plasma proteins (see section 1.1.5.2.1). Nonetheless, the increased affinity to proteins due to its polyanionic nature can cause problems in the form of nonspecific toxic interactions with undesired proteins [51] (see section 1.1.7.2). On the other hand, the PS backbone lowers binding affinity to complementary nucleic acids, explaining why "first generation" ASOs based on PS DNA alone have low potency [2]. For each PS substitution, affinity for complementary nucleic acids is reduced (ΔTm −0.5 °C per modification) [8], and although small, the loss in affinity can become significant as the sequence becomes longer [8]. Thus, a chimeric design (“mixmers”) strategy (see section 1.1.4.2), in which high-affinity modifications compensating for the relatively low affinity of the PS backbone, can mitigate this drawback of PTOs [5]. As such, several modifications in the sugar moiety are commonly used in combination with the PS modification.

1.1.4.1.2 2’-ribose modification (e.g., 2’-MOE)

An important and popular set of modifications in the chemical toolbox for ONDs includes replacement of aliphatic residues at the 2’-position of the nucleoside sugar wherein this modification leads to molecules that are more RNA-like [1]. As such, the naturally occurring 2’-O-methyl (2’-OMe) chemistry has an improved binding affinity to target RNA, and also has good stability towards nuclease activity [52,53]. Studies carried out with this modification, however, showed less antisense activity compared with PTOs, when utilizing the RNase H-dependent mechanism [13]. Since then, dozens of variants have been tested yielding similar results [2]. In

addition, studies with sequences containing 2'-OMe in combination with PS backbone modification (as mixmers) showed attenuation on serum protein affinity [2]. Hence, indicating that the polyanionic nature of the PS backbone in 2'-OMe PS ASOs had contrasting properties than the all-PS variants [54]. As such, the safety profile of this chemistry is considered to be excellent and this insight was helpful in designing gapmer ASOs later on (see section 1.1.4.2).

In due course, medicinal chemists identified the 2'-MOE chemistry [55], in which an ethylene glycol moiety is appended to the 2'-hydroxyl group of the nucleic acid [56]. This variant stands out from the majority in terms of both nuclease stability and binding affinity (ΔTm = 0.9–1.7 °C per modification) [57]. Moreover, the enhanced hydration capacity brought by the ethylene glycol moiety in this chemistry reduces some of the nonspecific protein interactions observed with PS DNA ASOs [58]. Albeit this, there were some reports of complement activation and platelet count reduction in some specific 2'-MOE PS ASO sequences and implicate toxic interaction with certain serum proteins (see sections 1.1.7.2.1 and 1.1.7.2.3). On the other hand, fully substituting with 2'-MOE chemistry leads also to loss of the ability to recruit RNase H [8]. However, as they retain excellent base-pairing specificity and the ability to block the access of cellular machinery to pre-mRNA and mRNA without degrading the RNA, they can be utilized as steric-blocking ONs [15,59]. Nonetheless, both 2'-OMe and 2'-MOE residues are commonly used with PS backbone linkages to enhance its binding affinity while still allowing RNase H recognition [8].

1.1.4.1.3 Constrained sugars (e.g., LNA)

Another important modification is represented by reducing the conformational flexibility of nucleotides, which can lower the entropic penalty of binding and thus increase ON binding affinity to complementary RNA [60]. As such, locking the structure of the ribose sugar has been a highly successful approach in ON medicinal chemistry. These are collectively referred as bridged nucleic acids or constrained nucleotides [5].

Among those in this genre, LNAs are the most advanced in terms of applications [1,61–63]. In particular, LNA bridges the 2'-oxygen and 4'-carbon of the ribose, which led to a significant increase in complementary transcript affinity [64]. Particularly, every addition of an LNA nucleotide to a OND produces a dramatic increase in its binding affinity (ΔTm +3-8 °C per modification) as well as binding specificity for its target RNA [65–67]. However, LNA oligomers of eight or more nucleotides have

the tendency to aggregate, thereby limiting their therapeutic utility, which can be compensated by combining this with other chemistries. On the other hand, as LNA is not substrate for RNase H similar to 2'-ribose chemistries, it can be used for splicing modulation [2]. This is because of its very high binding affinity, which allows it to be used as the basis for shorter ONs than previously considered feasible [5]. As such, gapmers of 13–15 oligomers of nucleotides are now commonly used [59,68,69] unlike those utilized previously (≥ 18 nucleotides).

1.1.4.2 *OND design*

Based on previous experience with PTOs and other modified ASOs, it became evident that each one of the existing modifications have distinct desired qualities. However, all of them also lack one or more of the required characteristics for antisense therapy. This led to the idea that an optimal ASO could be designed using a combination of the different modifications (mixmers) [2] (see Figure 1.3). A typical chimeric pattern in RNase H-dependent ASOs consists of a central region that contains DNA-like nucleotides, while the flanking regions are modified with the aim of improving affinity to the target transcript. These mixmer ASOs are also called "gapmers" [8].

1.1.4.2.1 **Gapmer ASOs**

In general, most chemistries applied to a DNA strand do not support the RNase H antisense mechanism. So, when designing gapmers, ASOs should retain a region with DNA-like character [3], and therefore natural bases and sugars with a PS backbone linkages are usually utilized for the central gap region. The flanking region (also often referred as "wings") is typically two to five nucleotides in length and is comprised of modifications, which can protect the DNA-gap from exonuclease digestion while enhancing target affinity. Although the most sophisticated gapmer designs in clinical usage employ 2-ribose alterations such as 2'-MOE, more recent design iterations use higher-affinity modifications such as LNA [8]. On this account, inclusion of a particular modification can also improve the cleavage selectivity [70–72] of a particular gapmer, which would address the inherent mismatch tolerance of RNase H [73]. This is of interest for diseases caused by a dominant negative mutation where it would often be preferable to cleave one allele (i.e., producing toxic protein) while leaving another allele intact (i.e., desirable protein), like in Huntington's disease [5]. On the other hand, depending on the nature of the modification, the length of the RNase H binding site in the central gap may be longer. A typical gapmer design usually has 8–12 central DNA-like residues [3]. Nonetheless, it has been reported that as little as five

contiguous base regions were sufficient to maintain activity of a gapmer ASO [13,74]. Besides the length of the gapmer ASOs, high concentrations of PS ONs (PS load in gapmers) can inhibit RNase H activity [42,75]. Therefore, the use of PS linkages must be used strategically in an ASO gapmer to balance this effects together with the unwanted toxicities brought by its plasma protein binding propensity [76] (see section 1.1.7).

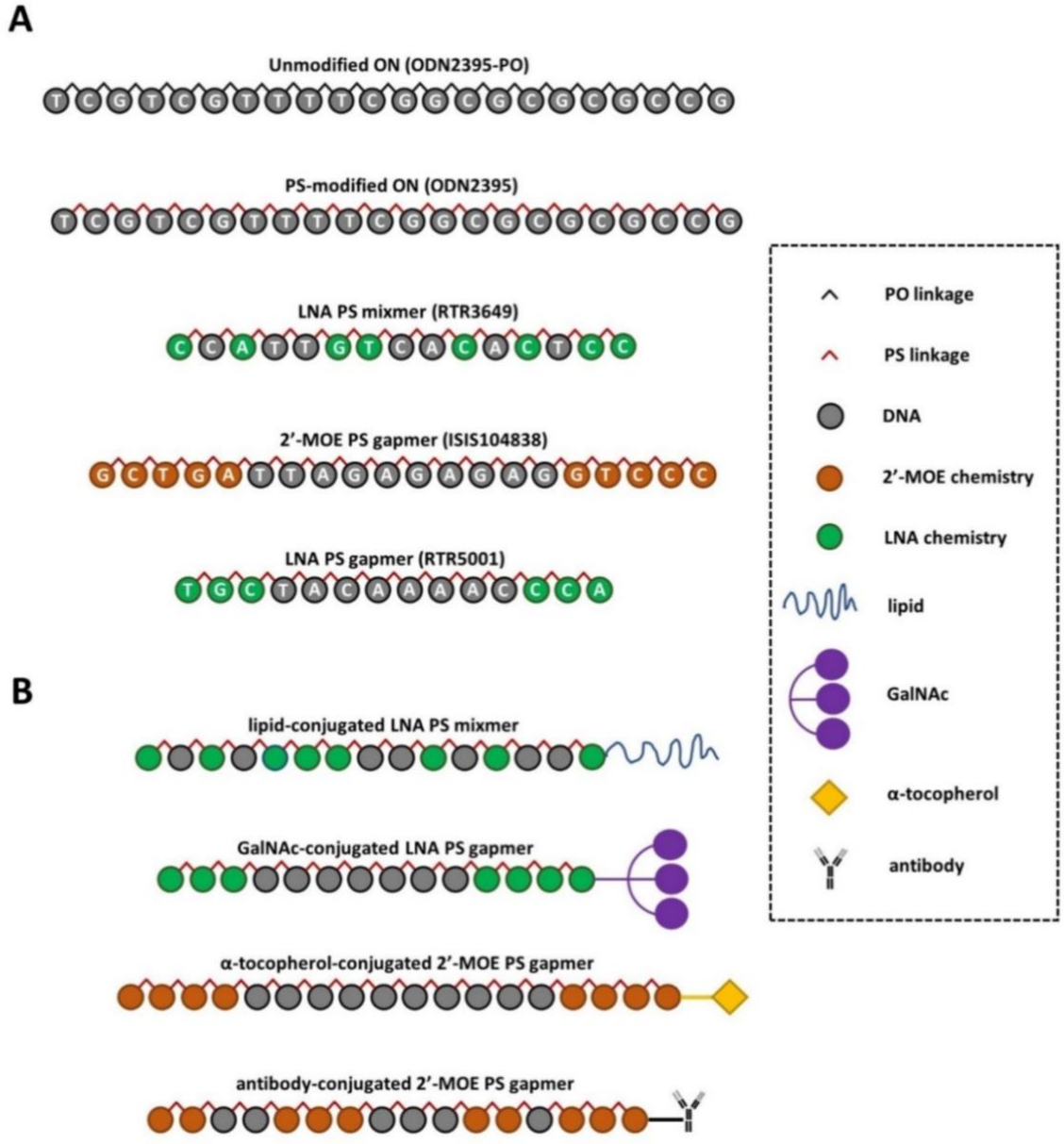

Figure 1.3. Overview of different design strategies (**A**) and delivery approaches (**B**) of antisense oligonucleotides (ASOs). Abbreviations: PO, phosphodiester; PS, phosphorothioate; LNA, locked nucleic acid; 2'-MOE, 2'-methoxyethyl; GalNAc, N-acetylgalactosamine.

The 2'-MOE gapmers are probably the most advanced and widely investigated ASOs in clinical use [2,8]. The enhanced potency and pharmacological effect duration effectively translates to lowered doses in clinical settings relative to first-generation PTOs [77]. Upon the discovery of the LNAs, LNA gapmers have shown increased potency in the liver and in extrahepatic tissues, thus expanding the range of tissues subject to antisense pharmacology (see section 1.1.5.3). The mechanisms by which LNA ASOs increase potency appear to be a combination of improved binding affinity for the target transcript and alterations in intracellular protein binding and trafficking [8]. On the other hand, LNA gapmers also demonstrated an increased propensity to cause hepatotoxicity [78] (see section 1.1.7.2.7) which can be prevented by small changes in sequence or structure [69,78,79]. While LNA chemistry has been widely used in the field of gapmer ASOs, only a few number of LNA-based ASOs have gone past early clinical investigations [8].

1.1.4.3 *OND delivery approaches*

A major challenge since the breakthrough of first-generation PTO drugs has been their inability to reach target tissues/cells [80]. For instance, sufficient level of the drug needs to reach tumors for a clinical response to be observed. Beyond the chemical modifications and design strategies within the ON molecules, delivery technologies have been investigated for optimizing ON trafficking into and within cells where they will find their intended target.

Systems to improve delivery include ligands or conjugates, as well as encapsulating agents [5,81]. As such, a number of chemical conjugates, including cholesterol [82], lipids [83], peptides [84], antibodies [85], and sugars [86] have been investigated for targeted in vivo delivery to increase selective cellular uptake and target tissues exposure [2,5]. In addition to the examples of organic nanoparticles mentioned above, research has also been conducted on inorganic nanomaterials and combinations of inorganic and organic nanomaterials [87]. One of the most characterized and popular targeting approach is N-acetylgalactosamine (GalNAc) conjugation (asialoglycoprotein receptor 1 (ASGR1)-mediated delivery to hepatocytes) that considerably increases selective hepatocyte uptake [88,89], thereby increasing ASO potency and efficacy, which proved to be transformative in clinical use [8].

1.1.5 Pharmacokinetics (PK)

Considering the specific OND mechanism, chemistry, and design, as well as delivery approaches, the PK can vary significantly between different OND classes (eg., aptamers vs ASOs) [16]. However, ONDs within the same class (i.e., ASO) that have the same chemistry and design (eg., LNA PS gapmers) demonstrate a relatively consistent and predictive 'class' behavior in terms of drug metabolism and pharmacokinetics (DMPK), and toxicity profiles (see section 1.1.7) [16,28]. This permits certain extrapolations since their class behavior is only marginally influenced by a particular sequence [90]. Such features facilitates a rational drug discovery approach for ONs of a given chemistry and design subclass [28]. This section focuses on the PK characteristics, and the influence of the physicochemical and structural properties of PS ASOs (1st and 2nd generation) in addition to administration routes [90].

1.1.5.1 *Route of administration*

In general, the majority of therapeutic ONs is administered via parenteral route to reach acceptable systemic exposures [28]. Initially, PTOs are mostly administered intravenously (IV) due to their proinflammatory tendency (see section 1.1.7.2.4) and inadequate nuclease stability when given subcutaneously (SC). Eventually, the use of 2'-MOE and LNA chemistries allowed SC route to be tolerable as this greatly improved their nuclease resistance and likewise alleviate the proinflammatory risk, likely due to less frequent dosing in the second generation ASOs [80]. On the other hand, the increased nucleolytic stability of gapmer ASOs also supports its potential oral delivery [91].

Reaching effective local concentrations in a broader range of tissues and cell types [47,48], together with achieving sufficient productive uptake in the target tissue itself [92] are ongoing challenges for ON therapeutics (see section 1.1.5.4). This could be addressed via direct administration of the compound to target organs such as the central nervous system (CNS), dermis, lungs, muscles, urinary bladder, or the eyes [28,90,93–97], which has been proven successful to reach clinically relevant tissue levels [98–105]. Moreover, the ease of quickly reaching therapeutically relevant concentrations after local administration coupled with slow clearance into the circulation allows lower and less frequent dosing, which in turn minimizes its systemic exposure [98,103,106].

Adverse effects, if any, are thus limited to locally administered tissues, with low risk of systemic toxicity.

1.1.5.2 *Absorption and plasma exposure*

Independent of the administration route, ASOs show similar kinetics after reaching the plasma compartment. ASOs are generally well-absorbed from the injection site (i.e., SC and intraperitoneal (IP)), although plasma ASO levels (e.g., maximum concentration (C_{max})) are lower compared to that of the IV route due to the gradual uptake from the IP and SC depot [80,90]. This enables for a larger concentration of ASO to bind plasma proteins and a reduced clearance of unbound ASOs [107,108]. Moreover, the time to reach maximum concentration (T_{max}) is longer after SC dosing. Accordingly, C_{max} was observed 3–4 hours (h) post-SC administration for mipomersen in patients and was thus similar to the T_{max} of 3 h observed for a PTO after SC administration [109,110]. Afterwards, the plasma concentration declines reflecting the tissue distribution phase, with the plasma half-life here depending on the chosen route of administration, chemical modification, and the specific ASO [111,112] (see section 1.1.5.3). This is then followed by a significantly slower elimination phase [28] (see section 1.1.5.5). Overall, the ASO plasma concentration versus time profile has been described as multiphasic [80].

The bioavailability for SC administered PTOs together with 2'-MOE and LNA ONs ranged from 26 to 100% of the exposure following IV administration [109,113,114]. For instance, the bioavailability of a 2'-MOE-modified ASO ranged from 80 to 100% in NHPs [111]. The bioavailability for the same ASO in healthy volunteers was 82% [110], confirming the results in NHPs. Interestingly, bioavailability was found to be dependent on formulation but not on the dose [114]. The C_{max} and the area under the curve (AUC)s are described to increase in a concentration/dose-dependent manner at doses used in the clinics, with peak levels not increasing after repeated administrations because ASOs distribute widely to tissues [113,115]. However, there are reports in animals showing that ASO plasma concentrations increase over proportionally with dose above certain levels, suggesting the involvement of saturable factors in ASO tissue distribution, with differences observed across species [111].

1.1.5.2.1 Protein binding

The PK differences seen among ASOs with different chemical modifications is at least partially a result of their altered protein binding capacities [116,117] and more or less not dependent on their nucleotide sequence [80]. For instance, the prominent polyanionic nature of PTOs enhance hydrophobicity and this results in a relatively higher nonspecific affinity to proteins [118,119]. Moreover, it was demonstrated that the prominent protein binding of second generation PS ASOs resembled those of first generation ONs. Newer ON modifications (e.g., 2'-MOE or LNA) are being utilized together with PS backbone linkages in nonclinical and clinical development [80,116].

The ability to enhance the interactions of ASOs with proteins could be simultaneously advantageous and detrimental [8,120] (see section 1.1.7.2). The nonspecific binding is exhibited in the quick absorption into the plasma from the injection site [121] as described earlier. Likewise, the association with cell-surface proteins promotes cellular uptake [5,8,27]. The binding of first and second generation ASOs to plasma proteins (e.g., albumin) also facilitates their extensive distribution to peripheral tissues [122]. Generally, plasma protein binding is not saturated at clinically relevant doses and this is related to the large binding capacity of plasma proteins [90]. The plasma protein binding of second-generation ASOs with PS backbone linkages was in the same range as PTOs with around 95% bound across most species, except mouse (85%) [116,123]. As such, PTOs are briefly sequestered in the plasma as they attached to hydrophilic sites of albumin and to a smaller extent to alpha2-macroglobulin [124]. Nonetheless, the binding affinity of ASOs to plasma α2-macroglobulin was observed to be higher than albumin [90]. It was demonstrated with gapmer ASOs that a two-fold increase in potency in α-2-macroglobin-knockout mice occurred, which might indicate that association with such proteins may steer the ASO toward less productive cellular or tissue compartments [125]. However, albumin seems to have a much greater nonspecific binding capacity for ONs, and together with its higher abundance in the plasma, it represents the main plasma protein ASOs associate with [126–128]. The transient and reversible (low affinity) association of PS ASOs and gapmer ASOs with plasma proteins also allows them to partition onto cell-surface proteins, which facilitates cellular uptake [129].

Another important benefit of ASO protein binding is that it also prevents the renal excretion of ASOs [80,130–132] (see section 1.1.5.5). Association with proteins in plasma minimizes kidney filtration (improved drug retention) and allows ASOs to circulate longer (better half-life) and

thereby distribute better to peripheral tissues [8]. Plasma protein binding and renal excretion rate are negatively correlated, with decreased protein binding leading to a higher rate of glomerular filtration and excretion [117,123]. In toxicity investigations, plasma protein binding can be saturated at high concentrations (particularly in mice), resulting in increased urinary excretion of the parent ASO [133].

Protein binding is also dependent on the ON length, with full-length ASOs excreted in the urine to a small extent, reflecting the low proportion of the unbound (or free fraction) form. Truncated/fragmented metabolites, with their significantly lower binding capacities, represent the major fraction in the urine [111,133]. Similarly, ON chemistries without the PS backbone also show lower protein binding and as a consequence are subject to rapid renal clearance [80]. As such, both 2'-MOE and LNA PO ONs are excreted faster in the urine as full-length sequences [134] due to their low plasma protein binding capacity, and this hinders their efficient tissue distribution.

1.1.5.3 *Distribution and tissue exposure*

The tissue distribution properties of PTOs and second-generation ASOs are generally comparable as they are rapidly and almost completely distributed from the plasma to the tissue compartments [80,111,133,135–138]. However, the initial half-life after the IV route is much faster (30-90 min) compared to the SC route due to the prolonged absorption from the injection site [111,112]. At clinically relevant doses, plasma concentrations in the distribution phase are generally in the μg/ml range [135]. The volume of distribution of ASO is often greater than two orders of magnitude larger than the blood volume. This suggests a widespread distribution and localization in peripheral tissues, while the total body clearance is low [113,139].

It is apparent from nonclinical studies that the plasma protein bounded ASOs distribute widely into most tissues following systemic administration for all animal species assessed [90]. Comparable tissue disposition between PTOs and chimeric ASOs have also been observed in mice and NHPs [2]. However, significant amounts of administered ASO accumulate in certain tissues after repeated dosing [140]. This is related to their increased in vivo stability, which results in longer tissue persistence [141,142], suggesting that tissue accumulation is a satiable event. In general, the kidney cortex accumulates the highest concentration and the liver receiving the highest total dose fraction [111,120,133,135,143–145].

To a lesser extent, ASOs are also taken up in other organs and tissues, including the spleen, lymph nodes, adipocytes (cell body), bone marrow, and vascular endothelium [68,111,122,145,146]. There is a low uptake in circulating blood cells in general, but ASOs readily accumulate in tissue macrophages. As such, ASO-containing macrophages can frequently be detected in many tissues, particularly in rodents [28]. Nonetheless, there is minimal uptake of systemically administered PS ASOs into organs such as the CNS and across the placenta [122,146–149]. The much lower exposures in most tissues explains, at least partly, the relative lack of toxicity observed in those organs other than liver and kidney (see section 1.1.7) [28].

There are reports pointing that the mode of ASO administration can also influence the ASO exposure in the kidney and liver tissues [150]. On the other hand, the organs to which ASOs distribute appear to depend on blood flow/perfusion. However, despite being highly vascularized, the relatively low uptake in lung, heart, and kidney glomerulus is clearly an effect of the protein binding properties of the ASOs [28,80]. In that capacity, the degree of plasma protein binding and length appear to be the critical factors for tissue uptake, where longer ONDs with PS linkages tend to reach higher concentrations in liver than in kidney and shorter sequences demonstrate an opposite pattern due to increased glomerular filtration brought by their less protein binding characteristics [123,124,151].

Regarding the chemistry, 2'-MOE partially modified PS ASOs and first-generation PTOs show similar, sequence-independent PK characteristics with regards to their in vivo disposition that is mainly dictated by their backbone chemistry [117]. On the other hand, LNAs are compartmentalized differently than other classes of ASOs, specifically within liver tissue, due to their more hydrophobic cyclic structure [152]. The distribution of LNA mixmers approximated that of PS ONDs. Nevertheless, they display substantially less protein binding and are mostly present in plasma as free molecules, being readily available for rapid tissue uptake [153,154]. Consequently, their accumulation in the kidney is less than that of PS ONs, whereas their uptake in the spleen, liver, and adrenal gland appears to be greater [153]. Furthermore, varied positioning of the LNA chemistry in the ASO strand alters its distribution and this may affect the relative ASO concentrations in a specific tissue [90,134,153]. For instance, the liver and kidney received the greatest concentrations of an all-LNA modified sequence, whereas the liver received up to 10-fold lower quantities of ASOs in a gapmer design featuring 2-5 LNA on each end of a 16-mer ASO [155].

On the other hand, the ON sequence might affect the uptake of LNA gapmers, which may be surprising with a given the design and chemistry. In one example, PS backboned 3–10–3 LNA gapmers against the same target that differed only in sequence, varied five-fold in liver concentration, and up to 25-fold in liver-to-kidney ratio [118].

To evaluate the efficacy and safety of a drug, it is crucial to evaluate parameters such as concentration and half-life in the tissue expressing the target transcript and plasma parameters. However, tissue biopsies are often unavailable in clinical research, hence nonclinical studies are the main source of this data. On the other hand, It might also be helpful to employ surrogate systems, such as the plasma trough concentration (see section 1.1.5.5), but these are limited by the strikingly non-homogenous uptake of PS backbone ONDs within a given organ [28,90]. ONDs' non-homogeneous tissue uptake qualities have significant effects on both PD and safety. In addition, cell-type uptake heterogeneity is observed in different organs, and despite extensive research, the molecular basis for these unique cell-specific differences in uptake remains incompletely understood [28].

1.1.5.4 *Cellular uptake*

Cellular uptake of ASOs in organs can be cell-type specific [80,156]. ONDs are typically taken up by phagocytically active cells (tissue macrophages) or tissues having fenestrated endothelium due to their molecular size and charge [28]. Accordingly in the kidneys, uptake is greatest in the proximal tubular epithelial cells of the convoluted tubule and considerably lower in the renal medulla [122,146,157]. Within the liver, non-parenchymal cells (Kupffer cells, and sinusoidal endothelial cells) contain 80–90% of the administered non-conjugated PS-containing ONDs and the remainder within hepatocytes [158,159]. Further evidence from kinetic studies shows that the hepatic cells that absorb most ASOs also absorb them the quickest [144]. However, gapmer ASOs tend to be more intrinsically active in hepatocytes than with nonparenchymal cells [160]. This is beneficial, as the majority of genes of therapeutic interest are expressed in hepatocytes [161].

It has been demonstrated that adding PS linkages to ASOs enhances cellular absorption, indicating that the kinetic behavior of ASOs in vivo is determined by the chemistry of their backbone [156,162]. Interestingly, ASOs with fewer PS links than those with a complete PS backbone exhibit greater cellular uptake [163–165]. Moreover, ASOs are detected in the cytoplasm of different cell

types within a very short time following administration, which appears to be a class effect and independent of sequence [90]. This increased the possibility that the innate ASO PK would provide preferential PD in certain organs that receive the highest concentration of the administered ASO dose [80]. For example, one of the first ASO targets in the liver that advanced to clinical testing was apolipoprotein B 100 (apoB-100) [166,167], the lipoprotein carrier of low-density lipoprotein (LDL) cholesterol and is needed for the assembly of circulating LDL cholesterol by the liver. Targeting apoB-100 displayed an ideal approach in lowering atherogenic particles linked with cardiovascular diseases [168]. Although this target is mainly expressed in the hepatocytes (not in nonparenchymal cells), antisense inhibition was validated in the clinics with mipomersen (Kynamro) [107,169], a 2'-MOE-modified PS gapmer. Thus, becoming the first systemically administered (SC) ASO approved by the US Food and Drug Authority (FDA) (January 2013).

Accordingly, this body of work offered insights on how targeted delivery to specific cell types (e.g., hepatocytes), may improve the ASO PK/PD properties in the liver. This demonstrated that the liver PK was related directly with ASO-mediated activity on the target transcript [133,170,171]. Subsequently, conjugation of a targeting ligand, such as GalNAc for hepatocyte-targeting ASOs have significantly improved uptake [172–174] and increases their potency by more than 30-fold over than unconjugated ASOs [175,176]. As a consequence, substantially lower dosages are needed and low-volume SC injections are given less often [175]. Other chemistries and delivery systems have now been introduced, which enhanced the potency of shorter ASO constructs (see section 1.1.4.1-3). This enables potency gains and enhances antisense activity not just in the liver but well beyond, such as in tumors [177] and muscle tissue [178].

As mentioned previously, the plasma protein binding of ASOs is transient as it is relatively low in affinity and it is a reversible interaction. This facilitates distribution to peripheral tissues [5,129] and subsequently allows the opportunity for the ON to contact cellular surface proteins, facilitating their binding to other acceptor sites leading to tissue uptake [5,27]. ASOs are seen to be linked with cellular surface proteins and extracellular matrix one hour following parenteral administration [126]. In addition, PS ONs have 100–1000 fold greater affinity for cell surface proteins than PO ONs [5]. Previous research shows a multitude of cell surface proteins where ASOs come into contact with, such as scavenger receptors, and trafficking proteins [179–181]. Accordingly, these works

have identified a number of cell type-specific nucleic acid-binding surface proteins [130,173] and the presence and abundance of these are crucial for cellular uptake [121,179].

It is reasonable that certain cell types have a specific set of cell-surface proteins that may engage and internalize ASOs, and research in this area is ongoing [182]. The mechanisms by which the ASOs traverse biological membranes to reach their intracellular target are not entirely known after ASO delivery. Cellular uptake leading to PD effects is often referred to as "productive uptake" [28,179,182]. Nevertheless, PS ONs may be delivered to hepatocytes through nonproductive intracellular routes that would likely result in trafficking to lysosomes [179]. Hence, the cellular mechanisms by which ONs reach their intracellular targets greatly influence ASO pharmacological activity [1] (see section 1.1.6). Each step may become rate-limiting and regulate the ASO cellular response according to their relative efficiency across different delivery mechanisms. Uptake by itself is insufficient; the ON needs to reach the correct subcellular compartments for activity (see section 1.1.6), e.g., the nucleus for splice modulation or RNase H activity [16]. The interactions of ASOs (i.e., gapmers) with intracellular proteins constitute an emerging field with interesting implications for the design of future generations of ONDs that utilize the control of intracellular protein recognition processes (e.g., PS ASOs interact with an array of cellular proteins) [51]. These interactions have the potential to modulate ASO activity and localization within cellular compartments [8,183–187]. However, these processes has been reviewed elsewhere [182,188] and not in the scope of this thesis.

1.1.5.5 *Metabolism and clearance*

The liver is considered the main site of ON metabolism due to its biodistribution characteristics [90]. Unlike conventional small molecular drugs, ASOs neither act as substrates for phase I (e.g., cytochrome P450) or phase II metabolizing enzymes (e.g., glucuronyl and sulfotransferases) or drug transporters (e.g., such as P-glycoprotein), nor inhibit or induce these proteins that are essential for small molecule metabolism, uptake, and excretion [133,189,190]. Hence, the drug–drug interaction potential of ASOs for these enzymes and transporters is negligible as established by clinical experience to date [191–194]. Instead, ASOs are hydrolyzed by endogenous nucleases in the circulation or tissue compartments [133,195]. These nucleases are phosphodiesterases that cleave the PO bonds of nucleic acids and can be classified as either exonucleases, which cleave one

nucleotide at the 3′- or 5′-end; or endonucleases, which cleave PO linkages in the middle of the nucleic acid chain [196].

Accordingly, unmodified (PO) ONs are metabolized within minutes in the blood, serum, or tissue [158,197], predominantly by exonucleolytic degradation, and the cleavage rate and extent are typically sequence-independent. Because of this, shorter metabolites are produced by gradual loss of one nucleotide after the other [90]. Replacing PO with PS linkages in the ASO backbone significantly protects the ON against nuclease activity (see section 1.1.4.1.1). For instance, enzymatic breakdown in the liver homogenate is over 20-fold slower for PS ONs their unmodified counterpart [197,198]. Moreover, ASOs with PS linkages have modest stability against exonucleases, but quite significant for endonucleases [8]. Accordingly, PTO degradation is mainly by exonucleases generating 3′ or 5′ shortened fragments, and minimally by endonucleases [80]. Therefore, the subsequent PTO metabolites may still have antisense activity. On the other hand, preincubation of liver homogenate with a PTO reduced subsequent enzymatic degradation of PO ONs [197]. Aside from chemical modification, sequence length affects metabolism rate. Nuclease substrates must have at least three inter-nucleotide links, with shorter sequences being degraded more slowly [90,197]. This suggests that initial metabolites from endonuclease degradation compete with full-length sequences for enzyme binding and hence, contribute to their stability.

Additional 2′-ribose modifications offers increased nuclease-resistance (see sections 1.1.4.1.2-3). Fully 2′-ribose modified ASOs are exclusively metabolized by exonucleases, mostly (but not solely) from the 3′-end [117]. Moreover, gapmer ONs further modified by terminal 2′-O-ribose or LNA chemistries blunt exonuclease degradation [90]. However, cleavage in the central gap region by endonucleases could still occur, which is then followed by exonuclease degradation of the unprotected ends of the metabolites [199]. Consequently, the metabolites of second generation ASOs produced from the initial endonuclease cleavage are too short to still have antisense activity [122]. Still, PS gapmers have multiple-week half-lives in animals and humans that correlate to long durations of activity [107,133,139,199,200].

Plasma clearance of PS-modified ASOs is attributed to the initial rapid tissue distribution and to a lesser extent to plasma metabolism [126,201]. In any case, the primary serum metabolite in general

result from 3’-exonucleolytic degradation. PS-modified ASOs is cleared nearly 10-fold slower compared to their unmodified counterparts[202,203] due to their extensive plasma protein binding (see section 1.1.5.2.1). On the other hand, intracellular degradation of full-PS ONs seems to be more varied and is cell type-dependent, with both 3’- and 5’-degradation profiles observed [76]. As such, within minutes after in vivo, shorter, base-depleted PS ON metabolites can be found [198]. For second generation ASOs, once they are distributed to various tissue compartments, they are generally degraded by endonucleases followed by exonucleases [122]. Therefore, expected putative metabolites, as well as tissue half-lives are dependent on enzymatic resistance of the ONs [90].

Species-specific differences in exonuclease or endonuclease activity may account for the variable half-lives on the tissues of different animals. For instance, an LNA-modified ASO had a half-life in the liver that was between 4 and 10 days in mice, compared to 2-4 weeks in NHPs and up to 5 weeks in humans [113]. The higher retention of second-generation ASOs in tissues reflects their longer half-lives. As increased tissue retention is required for a less frequent dosing regimen, several second-generation ASOs are injected weekly [204]. This is a major improvement to PTOs, for which continuous infusions up to several days are required to attain therapeutic concentrations [80].

After systemic treatment, only a small fraction of full-length OND is eliminated in the urine, while shorter metabolites produced by exonuclease digestion (in the case of PS ASOs and full 2'-ribose modified ASOs) are eventually cleared through the kidneys owing to their reduced plasma protein binding capacity [205] (see section 1.1.5.2.1). According to mass-balance studies, roughly 80% of the full dose is eliminated in the urine after 90 days for 2'-MOE gapmers [123]. Only a small percentage is found in feces and the remaining part can be found in the carcass [123].

The plasma elimination (terminal) half-life of ONs is determined by their tissue metabolism, the equilibration of parent ASOs and metabolites between tissues and blood, and renal excretion [111,122]. As such, this reflects tissue clearance, mostly after nuclease metabolism to shorter fragments [133,204] and may generally be between a few days for PTOs to several months for second generation ASOs, depending on their chemical modification pattern and the tissue [28]. At clinically relevant doses, plasma concentration of low ng/ml or pg/ml in the (post-distribution) elimination phase can be observed [123,204]. Accordingly, the steady-state plasma exposure

(plasma trough levels) during the elimination phase can be used to estimate tissue exposure, e.g., liver to plasma concentration ratio [123,145,204,206]. For instance, the plasma trough levels of the second-generation ASOs (i.e., mipomersen and drisapersen) increased after weekly injections due to their tissue half-lives being longer than one week [204,207].

1.1.6 Pharmacodynamics (PD)

PD is the collective term for the relationship between pharmaceuticals like ASOs and their biological targets, and how they influence the target to cause a pharmacological response. Therefore, the main goal of nonclinical and clinical research on the PD of ASOs has been on how the ASO affects target transcript (and/or target protein levels), downstream effects that come from target modulation, and therapeutic efficacy within a specific disease indication [80,205]. Moreover, establishing the PK/PD relationship is crucial in guiding the first dose in man and the dose and schedule optimization in later-stage clinical development. Thus, the existence therapeutic response markers as well as target selection and validation are fundamental. The criteria for these markers are extensive and are covered elsewhere [80].

Before ASOs can exert their pharmacological action on their target transcripts, three common processes need to happen: (i) access of ASOs to their action sites within the target cells, (ii) target RNA binding, and (iii) post-binding events (e.g., degradation of the RNA through endogenous enzymes) [1]. As mentioned in the PK section, productive and nonproductive uptake of ASOs could have an effect on its PD effect (see section 1.1.5.4). In vitro experiments showed that most cells readily take up PS ASOs. However, activity is seen only in a subset of these cells [179,182,184,185]. ASOs affinity for subcellular structures may also enhance or attenuate their biological effects [183,201,203] by determining their ability to reach the appropriate subcellular compartment. For instance, RNase H1 is located in both the nucleus and cytoplasm, thus ASO gapmers (with RNase H-dependent MOA) will act in both of these compartments [208], while splice-correcting ASOs are active only in the nucleus [28]. Therefore, among the mechanisms proposed for mild enhancement or inhibition/attenuation of ASO activity, changes in ASO subcellular distribution or interference with RNase H1 for binding to ASO/RNA duplexes were investigated [68,209]. More than 50 intracellular proteins interact with PS ASOs, according to several in vitro studies examining the kinetics and influence of ASO chemistry and delivery technique on subcellular localization and intracellular protein interactions [182]. As such, RNase H activity may be increased or decreased by

binding to different proteins. Some of these effects are linked to changes in subcellular ASO localization. Interestingly, binding affinity to a particular protein is determined by both the ASO sequence and the kind of ribose modification [28,119,182].

PD parameters are evaluated at the level of a target RNA/protein, or downstream biomarker (preferably at the cellular level), according to the MOA of an ASO. The primary PD endpoints to be assessed at the molecular level should be simple since binding of ASOs to their target leads to either transcript degradation, inhibition of translation, or splicing modification (see section 1.1.3). For instance, reduced mRNA and protein levels should be examined in particular for ASOs that cause mRNA degradation through the RNase H mechanism. Over half of the ASOs in late-stage clinical studies have been shown to inhibit their targets at the mRNA and/or protein levels in the relevant cell types in patients, such as those localized in the liver, muscle fibers, various solid tumors, lymph nodes, bone marrow, intestinal mucosa, and eosinophil progenitors and blood cells [80,210].

Abundance measurements of the target and any off-target mRNA may be made using a wide range of methods such as hybridization-based methods, quantitative polymerase chain reaction (qPCR)-based technologies, and RNA-sequencing methods. These techniques have been discussed in several studies [73,211,212] and have varying throughput capacities, benefits, and drawbacks. On the other hand, immunohistochemistry (IHC), immunofluorescence, Western blotting, and flow cytometry-based methods are used to quantify the abundance of the corresponding protein [210,213]. Assessing the PD effects of the ASO on the target is quite simple when the downstream biomarker is released into bodily fluids (e.g., the blood), and thus makes PD effect analyses straightforward [80]. Nevertheless, as ONs are species-specific, nonclinical development may be extremely challenging and need a variety of species-specific analogs or humanized mice models for a full pharmacological assessment [29] (see section 1.2.3).

1.1.7 Toxicology – Safety concerns

The understanding of the critical molecular mechanism for ASO PK/PD has evolved significantly as discussed in the previous sections. This is also true for the common toxicities experienced in the field. Key toxicological elements of ASO therapies will be summarized in the following sections.

In general, the chemistry of an ASO may have a variety of effects on its safety profile. For instance, adverse reactions (e.g., nonspecific polyanion-protein toxic-interactions) are anticipated to be reduced if a chemical modification decreases the required ASO dose. Nonetheless, ASOs may fold into various structures or attach to new proteins as a result of chemical modifications independent of the sequence, which might have adverse implications [214]. Meanwhile, the toxicity characteristics might vary across different OND classes based on the particular OND mechanism and design. At the same time, ONDs with the same MOA, chemistry, and design exhibit relatively similar behavior, permitting certain extrapolations across compounds within an OND class with the sole variable being the nucleobase sequence [16].

A similar profile of "class-related toxicities" was observed through early experience with PS and 2'-MOE ASOs (and subsequently with LNA ASOs), which is highly correlated with their PK characteristics [76,215]. Two primary toxicity mechanisms have been described for ASOs (see Figure 1.4). The most frequently observed is independent of the hybridization of the ASOs to RNA. The other mechanism is dependent of ASO hybridization to either target or other RNA sequences. Issues related to genotoxicity, carcinogenicity, immunotoxicity, as well as developmental and reproductive toxicity maybe also of relevance but are not further discussed in this thesis as they were not investigated.

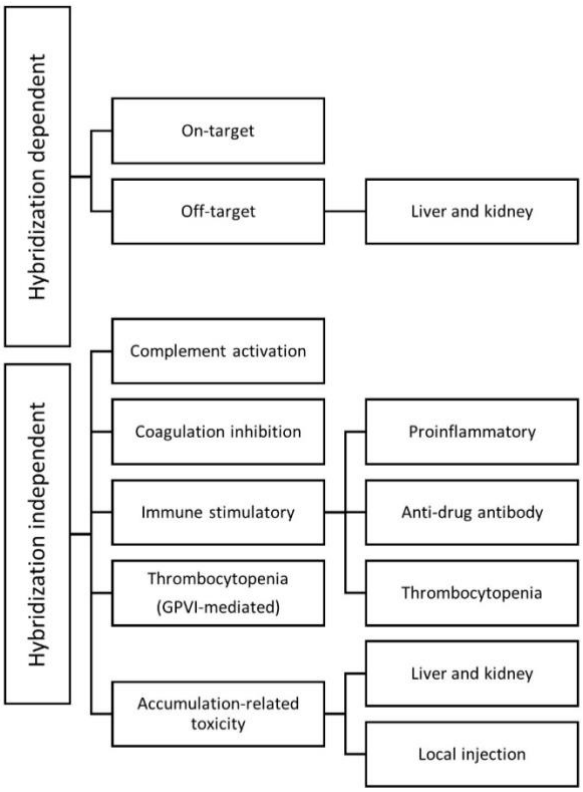

Figure 1.4. Schematic overview of the two primary OND-associated toxicities and the effects of Watson-Crick hybridization. Some of these toxicities have only been confirmed in animal studies. This figure is adapted from Andersson and Den Besten (2019) [28].

1.1.7.1 *Hybridization-dependent toxicities*

Concerns about on-target safety (exaggerated pharmacology and off-target interactions must be taken into account with every pharmaceutical modality. This is equivalent to Watson-Crick hybridization for ONDs to both the target RNA and non-target RNA transcript [28]. Exaggerated pharmacology is caused by the intended target RNA being inhibited to levels leading to adverse effects. Unintended RNA transcripts entirely or partially complementary to the ON sequence may likewise experience hybridization-dependent consequences. These are referred to as "off-target effects" [73,216].

Nonclinical efforts to comprehend and control these risks should take into account both the parent molecule and possibly active shortened-metabolites that are sometimes seen following exonuclease digestion of non-gapmer ASOs. These evaluations ideally begin early, during the discovery and design stages with ongoing monitoring throughout the development process to reduce the possibility of hybridization-dependent toxicities. [28].

1.1.7.1.1 Exaggerated pharmacology

Exaggerated pharmacology of ONDs, like with any medicinal platform, might result in toxicity via excessive or extended activity in the intended or non-intended organ [28]. It is often reported during the nonclinical safety studies necessary for first-in-human clinical trials in a drug development package [217]. To detect and analyze the possibility and possible impacts of on-target toxicities in any therapeutic modality, a full knowledge of the biology of the pharmacological target and the patient population is required [28]. Published examples include adverse liver effects found in patients treated with mipomersen as a result of excessive knockdown of the target apoB100 [218].

When evaluating on-target safety for ONDs, various considerations must be made in comparison to small-molecule and antibody medicines [219]. There are often just a few different organs and cell types that will undergo sufficient productive uptake for considerable on-target toxicity to occur. However, particular cells in the liver and kidney should always be examined for possible on-target adverse effects (see section 1.1.5.4). The evaluation of exaggerated pharmacology in pre-clinical phases poses an extra degree of complexity since ONDs are generally directed against a species-specific target transcript [217]. In circumstances when the clinical candidate's cross-species potency is inadequate, a surrogate OND (see section 1.2.3) that is active in one of the nonclinical models (often a rodent) may be utilized to facilitate on-target risk assessment [28].

1.1.7.1.2 Off-target toxicities

The relatively few cell types being amenable to sufficient productive uptake of ASOs also limit the number of organs and cell types susceptible to off-target effects. However, for ONDs that mainly exert their activity in the nucleus, such as ASO gapmers or splice-switching ASOs, off-target sequence analyses must include the introns of the unspliced pre-mRNA [220]. The inclusion of unspliced primary transcript sequences in specificity studies could dramatically increase the number of potential off-targets [73].

With improved mechanistic knowledge and the use of high-affinity chemistries (e.g., LNA) resulting in potent ASOs of shorter lengths, awareness of off-target hybridization and related toxicities has grown dramatically [221]. Accordingly, exaggerated RNase H-dependent off-target activity has been hypothesized as a possible explanation for the high-affinity ASO gapmers' sequence-dependent

hepato- and (perhaps) nephrotoxicity [222–224] (see sections 1.1.7.2.6-7). In line with this, due to the physiological function and minimal stringency requirements of RNase H1, RNase H-dependent ASOs present inherent specificity concerns [73].

In 2012, a subcommittee of the Oligonucleotide Safety Working Group (OSWG) on off-target analysis issued recommendations for assessing and managing potential hybridization-dependent off-target activities [225]. The fundamental processes in the risk assessment of hybridization-dependent off-target effects detailed in the 2012 recommendations are still applicable, despite the fact that advancement in the area has enhanced insights and knowledge on off-target effects [28]. However, off-target effect prediction should be carried out independently for each animal model utilized in experimental safety assessments owing to large sequence divergences across the species commonly employed in nonclinical evaluations (see section 1.2.3). Although functional annotation and sequence quality for lower mammals or primates are not on par with those of humans, the off-target effect analysis may still be useful, particularly when a species-specific phenotype is identified [73].

1.1.7.2 *Hybridization-independent toxicities*

Watson-Crick base pairing of ASOs to RNA is not the primary mechanism causing the majority of OND-induced toxicities; rather, tissue accumulation, proinflammatory processes, and/or protein binding (aptameric effects) are the primary causes [28]. Nevertheless, the sequence of ASOs can produce undesirable pharmacologic effects that are independent of hybridization [226–229], such as having unmethylated cytosine-guanine dinucleotide (CpG) motifs (cause immune activation through activation of Toll-like receptor (TLR) 9) [230].

On the other hand, the OND chemistry and design are substantially responsible for the majority of these toxicities [28]. PS ASOs, despite all of their advantages, may have unintended effects related to their physicochemical properties, which may occur by altering the degree of protein binding [216]. This is also true for those modifications that have reached clinical development and confer the greatest increase in potency, namely 2'-MOE [231] and LNA [232]. As these ONs still have PS linkages throughout the sequence, their toxicological properties are comparable to those outlined for PS ASOs [151,233].

Multiple mechanisms appear to be at play in some of the class-related toxicities. This is effectively demonstrated by the hepatotoxicity of gapmer ASOs (see section 1.1.7.2.7). This emphasizes the need to provide additional nuance to the OND class profile concept for novel OND classes with distinct properties. In the context of mechanisms and species translatability, a number of frequent observations are well understood. Aside from sporadic occurrences of thrombocytopenia recently described [234] (see section 1.1.7.2.3), no additional "new" toxicities or clinically relevant toxicological target organs have been added to the list of possible risks associated with ONDs. As a result, we can identify a recurring pattern of possible hazards associated with ASOs as a modality [28]. Figure 1.4 summarizes the major characteristics of several of these OND toxicities.

1.1.7.2.1 Complement activation

A well-characterized protein-binding feature of PS ASOs is activation of the alternative complement pathway [235]. The mechanism is through the inhibition of complement factor H (CFH) [236] an endogenous inhibitor of the alternative pathway of complement activation. The total amount of PS linkages (and hence PS OND length) and the impact of 2'-ribose modifications on protein-binding significantly affect complement activation, with sequence being less critical [215,237]. Complement activation is distinguished by the decrease in serum hemolytic potential (50% hemolytic complement, CH50 analysis) and concomitant transient increases in the liberation of complement split products Bb, C3a, and C5a at the cost of complement C3 protein [216].

Reduced levels of complement factors in circulation may impair the complement system's overall function and its part in innate immune surveillance, such as clearance of immune complexes. The ability of in vitro assays to predict in vivo concentration-effect relationships for specific split products of the alternative pathway (e.g., activated complement factor B (Bb)), is limited. Nevertheless, they can be used to screen toxic sequences and advance our understanding of structure-activity relationships. [28].

NHPs are known to be more sensitive to this adverse reaction than humans or other species [215,235–237]. This seems to be due to the reduced inherent inhibitory activity of NHP CFH relative to human CFH, rather than a greater binding affinity to CFH [237]. Complement inhibition for NHP factor H is threefold greater than that for the human protein. On the other hand, the lack of ON-induced complement activation in dogs provides support to the species variations in this effect of

PS ONs [216]. Nonetheless, it may also be seen in other species at high bolus IV doses (e.g., minipigs) [238], and man when given as prolonged infusion [239,240].

Acute toxicity to complement activation by ASOs is evidenced by marked clinical signs (lethargy and periorbital edema) together with hemodynamic changes (heart rate and blood pressure reduction) as well as hematologic effects (fluctuations in neutrophils) [235]. Accordingly, there were moderate to severe episodes of emesis, ataxia, and decreased motor activity in rhesus monkeys. This activation of the alternative complement pathway was demonstrated to be transient and plasma PS ASO concentration-dependent. [215]. It has been shown to occur primarily after rapid infusion of ONDs. The plasma PS ON activation threshold for NHPs has been characterized, i.e., when plasma concentrations reach or surpass 40–50 µg/ml [235].

Acute symptoms are often absent with SC administration or lower-dose IV infusions, although significant complement-related clinical symptoms and/or death have been reported in association with aggressive IV dosage regimens in NHPs [235]. Furthermore, persistent low-level activation of the alternative complement pathway in cynomolgus or rhesus monkeys eventually results to complement depletion, increased vulnerability to infectious diseases, and in certain circumstances, damage to the vascular system and kidney [215]. In contrast, no evidence of sustained/chronic complement activation or vascular inflammation in humans has been found in clinical studies to date [241], as high plasma concentrations can be avoided by controlling the dose and rate of administration. This underscores the importance of the clinical dosing regimen [110,236]. Moreover, even when circulating drug levels were comparable to or higher than those linked to complement activation in NHPs, acute complement activation is often not seen in clinical settings with SC injection at dosages up to 1000 mg/kg [237,241].

1.1.7.2.2 Coagulation cascade inhibition

Prolongation of the clotting time (i.e., activated partial thromboplastin times (aPTT)) is a well-known effect of PS ASOs [242–244] directly correlated to the PS content and extrapolates well across all species and different sequences [215,238,240,243,245]. This is the result of selective binding and interference with the intrinsic tenase complex (key activator of the intrinsic coagulation cascade) resulting in prolongation of the coagulation time of the intrinsic pathway [242,244].

Similar to complement activation, aPTT prolongation is closely correlated with plasma PS ASO concentrations, with most significant prolongation occurring at C_{max}. As a result, it is highly predictable but of limited clinical consequence since, at clinically relevant exposure levels, it is often not linked to an elevated risk of bleeding or other coagulation disorder symptoms. Compared to what is needed for complement activation, the plasma concentrations related to increased aPTT are lower (~10–15 µg/ml) [110,246]. The aPTT prolongation is transient and more prominent than prothrombin times (PT), demonstrating that the intrinsic pathway predominantly mediates the effect [216]. Prolongation of aPTT is common to many species and has been observed in mice, rat, and monkey [247–249]. Due to the lower plasma concentrations required to increase aPTT prolongation relative to complement activation, aPTT prolongation has been observed in humans. In these cases, neither altered coagulation status nor symptoms of bleeding were present [110,250]. Even after repeated dosing, the relative insignificance of the clinical manifestations of these coagulation changes is likely due to the minor scale and the transient nature of the aPTT change [240,250,251]. It is possible to avoid increased aPTT by controlling the administration of the PS ONs using dosing regimen (e.g., SC administration or longer IV infusions instead of bolus IV) in such a way that plasma concentrations remain below threshold [110,246] or by reducing the degree of protein binding through shorter ON length, chemical ribose and/or backbone modifications [28].

1.1.7.2.3 Thrombocytopenia (TCP)

Thrombocytopenia (TCP) is a common side effect of many pharmaceuticals and has also been observed with PS ONs [252]. After repeated doses of PS ASOs, dose-dependent decreases in platelet counts in mice and NHPs have been documented. [28,253]. The reductions were transient and reversible over courses of weeks or months depending on the half-life of the ASO [254]. In rodents, this effect is often accompanied by splenomegaly, which seems to be related with the proinflammatory effect of ASOs commonly observed in this species [28] (see section 1.1.7.2.4). TCP has also been reported in humans, following systemic administration of PS ONs in cancer patients [250,255–258].

The exact mechanism of the ASO-induced TCP is not known yet. It has been suggested that the mechanism may vary across species and between mild and severe occurrences [254]. The fact that three different ASOs covering two different MOA (RNase H1 and splice switching) and three different targets indicates that the TCP is not caused by exaggerated pharmacology. Moreover,

ASO-induced TCP is not linked to general bone marrow toxicity, reduced platelet production, or the existence of anti-drug antibodies [259,260]. Recent research has begun to give some insight into the interaction involving ASOs and platelets (both immune-mediated and non-immune-mediated [28]. We will tackle this specific adverse effect in detail in Chapter 4.

On the basis of extensive nonclinical NHP and clinical human experience with PS gapmer and non-gapmer ASOs, two separate phenotypic manifestations of platelet reductions are now recognized, each with distinct clinical impacts [28]. The more typical phenotype is characterized by a mild to moderate, dose-dependent, gradual, and non-progressive reduction in platelet count [253]. In this reproducible profile of platelet reduction, the platelet count often does not drop below the lower limit of normal (150,000 platelets per µl in humans). With prolonged therapy, platelet counts often stay within the normal range, do not further decrease, and are not linked to any signs of clotting dysfunction or an elevated risk of bleeding [261,262]. However, as the disease status (as well as the baseline platelet count) could affect the predisposition to platelet count alteration, proper assessment is still warranted to ensure ASO safety. The second phenotype is a severe TCP, which manifests at low incidence. These events are not seen across studies employing the same sequence and dosage levels, but their incidence rises with higher doses and longer treatment periods. Several observations, including repeated reductions in platelet counts in re-dosed monkeys, point to an immune-mediated mechanism [28].

1.1.7.2.4 Immune stimulation and proinflammatory effects

Immune-stimulatory effects have long been a prominent feature of ONs, wherein ample data from both animal toxicity research and early human clinical studies show that ASOs have proinflammatory properties [263] (see Figure 1.5).

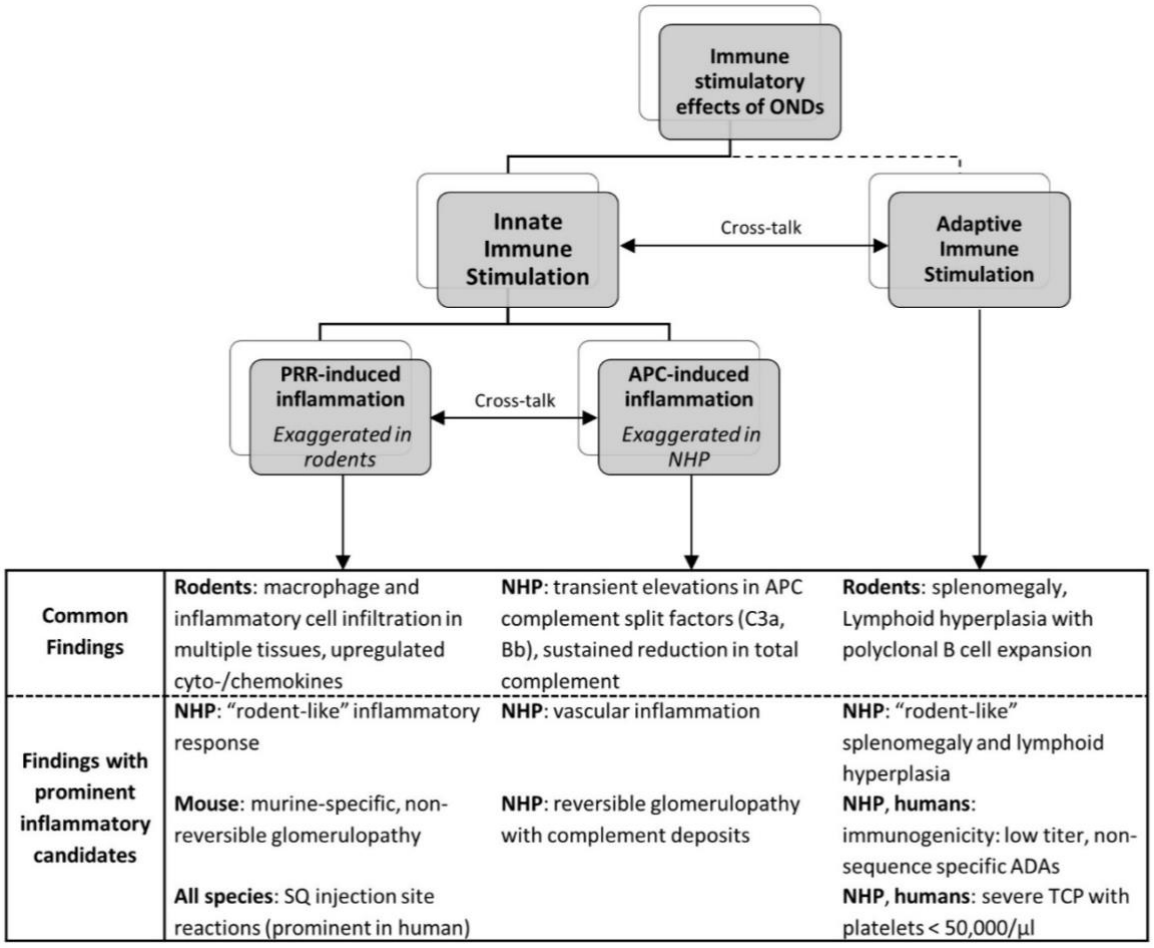

Common Findings	**Rodents**: macrophage and inflammatory cell infiltration in multiple tissues, upregulated cyto-/chemokines	**NHP**: transient elevations in APC complement split factors (C3a, Bb), sustained reduction in total complement	**Rodents**: splenomegaly, Lymphoid hyperplasia with polyclonal B cell expansion
Findings with prominent inflammatory candidates	**NHP**: "rodent-like" inflammatory response **Mouse**: murine-specific, non-reversible glomerulopathy **All species**: SQ injection site reactions (prominent in human)	**NHP**: vascular inflammation **NHP**: reversible glomerulopathy with complement deposits	**NHP**: "rodent-like" splenomegaly and lymphoid hyperplasia **NHP, humans**: immunogenicity: low titer, non-sequence specific ADAs **NHP, humans**: severe TCP with platelets < 50,000/µl

Figure 1.5. Immune stimulatory effects of ONDs – primary and secondary effects and pathologies related to immune stimulation. Abbreviations: PRR, pattern recognition receptor; NHP, nonhuman primate, ADA, antidrug antibodies; TCP, thrombocytopenia; APC, alternative pathway of complement; SC, subcutaneous. This figure is adapted from Andersson and Den Besten (2019) [28].

The proinflammatory characteristics of ONDs result from the activation of pattern-recognition receptors (PRR) within the innate immune system. The best characterized PRRs responsible for the recognition of synthetic ONDs are the membrane-bound TLRs, specifically the endosomal TLR3, TLR7 and TLR8, recognizing different RNA variants [264], and TLR9, which responds to unmethylated CpG motifs in DNA [265]. Other PRRs residing in the cytoplasm has also been described and tackled in detail elsewhere [266–269]. Binding to these different PRRs and activation of downstream signaling pathways distinguish between ON design, chemical modification of the base, ribose or backbone, and sequence, and therefore may not be applicable for all ONDs [28].

Responses may vary widely between species. In contrast to rodents, NHP, minipig, and human inflammatory responses are typically attenuated and less pronounced [215,238,248,249]. However,

prominent inflammatory responses, such as vasculitis, have been observed in NHPs [263,270], particularly with sequences that also show pronounced complement activation. On the other hand, the underlying mechanism for rodent sensitivity is not entirely understood but is assumed to involve variations in PRR expression, ligand selectivity, and signaling cascades [271,272]. In particular, rodents express the TLR9 receptor on more cell types [273] (B cells, dendritic cells, and monocytes) than humans and NHPs; thus it is likely that SC administration of these immunostimulatory ASO produced qualitatively distinct responses in mice as opposed to humans [254].

The immunomodulatory/stimulatory potential can be used deliberately to design nucleotide-based immunotherapies and vaccine adjuvants, often harboring so-called CpG motifs (proinflammatory ONDs) [99,274]. However, in most other cases these effects are unwanted. Accordingly, such proinflammatory effects had led to the rejection of a marketing authorization (e.g., Kyndrisa) [275]. Proinflammatory responses may involve production of antibodies to ssDNA (anti-drug antibodies) (i.e., mipomersen and drisapersen) or double-stranded DNA (dsDNA) [28,276], activation of the alternate complement pathway [235,277], hematological alterations including TCP [263,278], and stimulation of cytokine production [254,279–281]. In particular, patients in clinical trials have expressed complaints of fatigue, gastrointestinal disorders, chills, and fever, which are similar to those produced by the release of cytokines. Such immune responses ("flu-like symptoms") and local cutaneous injection site reactions have been seen in patients and led to cessation of therapy in some cases [282,283].

Local injection site reactions after SC administration have been reported and described as erythema, induration, itching, pain and sometimes ulceration or necrosis [275,284]. In general, ASO administration can lead to mononuclear cellular infiltrate at the administration site [249]. Although the pathophysiology of the local skin reactions remains unclear, it most likely includes the persistently high local concentration of the proinflammatory ONDs. Inflammatory SC injection site reactions in animal studies are less severe and mostly reversible, suggesting that SC tolerability is lower in humans, presumably due to species variations in SC skin composition, such as a higher adipocyte content in humans compared to laboratory animal species [28]. On the other hand, infiltration of mononuclear cells occurs not only at the administration site but also at systemic locations, such as in those organs that accumulates ASOs like the liver and kidney, and this may play

a role in the observed toxicity in these organs [249,263,285] (see section 1.1.7.2.5-7). Moreover, changes in spleen and lymph node weight were noted in some studies [285].

1.1.7.2.5 Accumulation-related toxicities

Toxicities in high-exposure organs is expected with ASOs in line to their tissue distribution (see section 1.1.5.3). Class-related toxicities in different tissues seem to be mostly associated to the proinflammatory potential of PS ONs, which leads to infiltrates of monocytes, lymphocytes, and fibroblasts [249,286] (see section 1.1.7.2.4). The ONs accumulate in the kidney and liver (among other organs) after systemic administration. Since the kidney represents the site with the highest OND concentration, it is potentially the primary target organ for toxicity [287]. On the other hand, the limited (or absent) absorption in other organs (e.g., brain, lung, gastrointestinal tract, eye, skeletal muscle, or heart muscle) is the reason for the very limited toxicities in these particular organs following systemic administration of ASOs [145]. However, exceptions such as the spleen and lymph nodes were observed as they are susceptible to dose-dependent proinflammatory effects of PS ONs, although they do not accumulate the highest concentration of the compounds [216].

The histologic hallmark of OND exposure and accumulation in tissues is the presence of basophilic granulation (under hematoxylin and eosin (H&E) stain), which has been observed in various tissues of animals treated with systemic PS ONs [145] as well as those that received it via inhalation [288,289]. Due to the fact that these granules disappear upon cessation of treatment and do not cause degenerative changes, they are considered non-adverse, adaptive changes [28]. The changes are reversible, but due to prolonged tissue half-life of the modified PS-ASOs, it may take weeks to months for these to resolve [278].

The organs presenting basophilic granulation are usually the principal sites of ON accumulation [76]. It is widely accepted that the granular material represents the ON's clearance and deposition in the cell type(s) where it is found. The granulation is usually observed in resident macrophages of the spleen, lymph nodes, and liver (see section 1.1.7.2.7), as well as in the proximal tubular cells of the kidney after systemic OND administration (see section 1.1.7.2.6) [216]. IHC evaluations of the kidney and liver reveal perivascular infiltrates and this often refer to “lymphohistiocytic cell infiltrates” [281]. The affected macrophages have been described as having

a “distended, weakly stained and finely vacuolated or granular cytoplasm” [263]. The liver resident macrophages (Kupffer cells) can appear reactive (hypertrophic) or proliferative (hyperplastic) [254]. The ON uptake by resident macrophages is frequently accompanied by a rise in macrophage number (histiocytosis), which induces the OND clearance process [216]. After local delivery via inhalation, a typical nonclinical toxicological finding is alveolar macrophage and histiocyte accumulations within the lungs of animals. These cells appear enlarged with cytoplasmic vacuolization containing basophilic granular material [98,288,289].

In multiple tissues of rodents that received high PS ASO doses, macrophages and histiocytes are frequently observed to have a foamy appearance. In contrast to the ASO-containing basophilic granules, the granular cytoplasm of activated macrophages is considered to contain cytokines. These are not generally observed in NHPs, owing to the greater rodent susceptibility to the proinflammatory properties of PS ASOs [263]. However, it is unknown if ASO uptake disturbs macrophage phagosomes. It has been proposed that alterations in tissue macrophages are caused by cellular activation and cytokine production in reaction to the ASO's proinflammatory character [270]. On the other hand, there is some evidence that the toxicity results from lysosomal breakdown or cytokine release by activated Kupffer cells (leading to hepatotoxicity) or mononuclear cells [215,235].

1.1.7.2.6 Nephrotoxicity

High local concentrations of ONs make the kidney one of the typical organs to observe toxicities related to various OND modalities [28,216,290], and this is particularly concentrated in the proximal tubular epithelium [157,287,291]. Changes in the proximal tubules are more common than in other tubular sections or the glomeruli. Renal toxicities are due to the buildup of ASOs (seen as basophilic granules) inside the proximal tubule's lysosomes, which causes the tubular absorptive capacity to be disrupted, leading to tubular proteinuria [215]. Accordingly, proteinuria was documented in drisapersen patients and was mainly modest in severity (primarily affecting low-molecular-weight proteins), reversible with brief treatment interruptions and neither progressing nor related with other renal impairment symptoms [262,292].

The pattern and distribution of these ON-containing basophilic granules in the tubular epithelium are similar to those of normal low molecular weight proteins [216]. The changes in tubular

morphology and function follow a predictable pattern in animal studies, with initial microscopic changes of cytoplasmic basophilic granules at low doses, which becomes associated with tubular atrophy, regeneration, and degeneration at high doses and tissue concentrations [215,233,293]. As such, functional tubular changes in NHPs are often seen only at several multiples of the clinically relevant dosage, as described for 2'-MOE gapmers [215,233]. Accordingly, NHPs appear to predict well for the tubular toxicity risk in humans [28].

Another prevalent change in the kidney after systemic ON treatment is the appearance of cytoplasmic vacuoles in the tubular epithelium (in formalin-fixed kidney sections). These vacuoles' existence is caused by osmotic imbalances caused by large concentrations of hydroscopic material (i.e., ONs) in the phagolysosomes [216]. Therefore, this is a fixation artefact that should not be mistaken as a degenerative change (i.e., vacuolar degeneration) [294]. Other changes have been reported at relatively high doses (more than 80 mg/kg/week) and high tissue concentration (as high as 2.6 mg/g), such as dose-dependent renal tubular atrophy and degeneration, although they are not considered function-limiting as these change were not accompanied by renal function abnormalities. When changes in renal function were identified in NHPs (increased urine protein/creatinine ratio), they were quickly reversed [233].

The mechanism for this mild, reversible tubular dysfunction is unclear. Still, it may be associated with transient and competitive interference with proximal tubular reabsorption of solutes, which includes proteins from the glomerular filtrate, as both ASOs and proteins are understood to be reabsorbed from the glomerular filtrate via scavenging-receptor-mediated endocytic processes. This would increase the excretion of low-molecular-weight proteins and, to a lesser degree, albumin, and the effect is easily reversed when the treatment is discontinued [262,294].

Except for those effects directly related to tissue accumulation, the tubular effects mentioned above are only slightly affected by the ON sequence. For ASOs with higher affinity modifications, a distinct pattern of tubular toxicity was observed [270], in which sequence tends to be more vital than tubular accumulation over a critical concentration threshold. This is evidenced by renal toxicity in rodents after only two weeks of dosing with 3–8–3 LNA gapmers that also caused hepatotoxicity [79]. On the other hand, acute tubular necrosis following three treatments of the LNA gapmer RTR5001 (5 mg/kg) is a clinical example of highly sequence-dependent renal toxicity [295].

Furthermore, human volunteers treated with an unusually short (12-mer) 2'-MOE gapmer intended to accumulate in the kidney and target the renal sodium-glucose cotransporter-2 transporter experienced acute tubular dysfunction as evidenced by a dose-dependent rise in serum creatinine and increased urinary excretion of β_2-microglobulin and kidney injury molecule-1 (KIM-1). Although a direct tubular effect has not been ruled out, it is likely that the intended pharmacology is the primary contributor, as serum creatinine levels stabilized with sustained treatment, indicating tubular adaptation [151,296].

Glomerular lesions are uncommon with PS ONDs and 2'-MOE gapmers [294]. However, glomerulopathies were detected (and reproducible) in three months or longer rodent and NHP toxicity trials utilizing 2'-OMe ASOs [263,297]. In general, these glomerular lesions were observed at or below the clinical doses/exposures and were unrelated to glomerular accumulation. Accordingly, they are distinguished by profound species differences: in mice, local inflammatory activity and murine-specific characteristics appeared to be significant determinants of the progressive and irreversible pathology [297]. On the other hand, the reversible lesions in NHPs showed evidence of chronic complement activation and ASO-induced inflammatory reactions [297], known to be triggered by ASOs when delivered to NHPs over a particular dosage threshold [140,270,298]. The fact that humans are less susceptible to ASO-induced complement activation and inflammatory mechanisms suggests that animal toxicity studies overpredict the clinical risk associated with glomerular lesions. Clinical experience supports this, with only a few of established ASO-related glomerulonephritis identified [28,292].

Overall, when detecting proteinuria in a patient, it is crucial to differentiate between the more medically manageable tubular toxicity and the more severe glomerular impairment [263]. Small or negligible levels of protein would be consistent with tubular effects and hence less clinically problematic, but substantial elevations or the presence of high molecular weight proteins may assist in identifying proteinuria of glomerular origin and risk of glomerulonephritis [254].

1.1.7.2.7 Hepatotoxicity

Following systemic treatment, the liver is another primary target organ for toxicity due to its high accumulation of PS ONs. In contrast to the kidney, where ONs are primarily located in the tubular epithelium, ONs are detectable in all liver cells [111,158,291]. Accordingly, single-cell necrosis and

Kupffer cell hypertrophy, as well as basophilic granules in the liver, have been observed in animal models at high dosages. [215,263,293]. The presence of the basophilic granules and hypertrophy of Kupffer cells demonstrates their normal function to clear foreign material and is usually not associated with hepatic dysfunction [216]. Further dose-dependent changes involve lymphohistiocytic cell infiltrates that may be linked to multifocal hepatocellular degeneration or single hepatocyte necrosis, consistent with the proinflammatory class effect of PS ONs [114] (see section 1.1.7.2.4). These changes tend to be accompanied by an elevation of serum transaminases (alanine transaminase (ALT)) and aspartate aminotransferase (AST)) and a decrease in albumin and cholesterol levels, which may indicate altered liver function [231,249]. On the other hand, a different and more severe form of liver toxicity not brought on by ASO accumulation nor proinflammatory effects has emerged with the development of ASO gapmers with high-affinity 2'-ribose modifications, such as LNA [299]. In cases with greater severity, changes are more profound with larger areas of apparent necrosis, evidenced by marked liver enzyme elevations, morbidity and mortality [78,300].

In general, this toxicity appears to be independent of local concentration or knockdown of the primary target mRNA and is not induced by metabolites or impurities [78,222,300]. Current evidence suggests off-target RNA knockdown plays a role in this gapmer-induced hepatotoxicities [28]. Three independent groups demonstrated that much of the hepatotoxicity of high-affinity gapmer ASOs results from RNase H-mediated cleavage of off-target transcripts (often within introns) [220,222,224,301]. Significant efforts have been made to better comprehend and define the specific ASO sequence component and sequence motifs that are linked with these hepatotoxic liabilities. Sequence motifs consisting two or three nucleotides were identified and correlate reasonably well with the toxic potential of the sequences [299,300]. In line with this, the precise location of the toxic sequence in the gapmer (gap vs. wings), the position of the LNA's in the wings and the gap size all influenced the toxicity profile [78,299,300].

Aside from liver accumulation related changes, hepatotoxicity observed in animals tends to be dependent on ASO sequence and chemistry, and the sensitivity of each species than the absolute concentration. Liver toxicity in rodents is more commonly reported, partly due to their sensitivity to the proinflammatory effects of ONDs, with increased lymphohistiocytic cell infiltrates as a key pathological feature. In general, NHPs are considered to better predict risks to clinically relevant

hepatotoxic effects associated with tissue accumulation [28]. The toxicities related with liver degeneration or necrosis in rodents have been demonstrated with LNA-modified ASOs at doses below those generally known to result in accumulation-related hepatic changes in other species [299,300]. The absence or mild liver findings in NHPs, often restricted to hypertrophy and basophilic granules in Kupffer cells, are consistent with the general lack of hepatic toxicities in clinical situations [215].

Rodent tolerability studies have shown to be an effective strategy for screening out these hepatotoxic candidates before moving on to the clinics [28]. Through careful sequence screening and selection, hepatoxicity has not been a general feature of most PTOs and newer generation ASOs in clinical settings [28,215], except for the toxicity secondary to exaggerated pharmacological inhibition of apoB-100 by mipomersen [218]. Another clinical case is the GalNAc-conjugated siRNA ALN-AAT, which was terminated after liver enzymes increased caused by an microRNA-like off-target activity in its Phase 1 trial [28].

1.2 ASO nonclinical development and safety evaluation

Various components of a drug development program could decide its success with regards to marketing approval. As for ON-based drugs, selection of sequence candidate during the discovery phase should weigh the balance between efficacy, clinical relevance of a target, and safety [16]. As mentioned earlier in this chapter, ASOs are designed with an assortment of chemical modifications dictated by its intended MOA. Based on this design, the probable PK/PD properties of a specific ASO candidate can be predicted. Potential safety issues identified as common 'class toxicities' profile usually correlate with the ASO PK properties [76,215]. With previous experience and the overall predictable behavior of ASOs, stringent screening processes can be applied. All these properties contribute to shorter timeframes from early pharmacological concepts to validation in the clinics for ON therapeutics when compared to other drug modalities [28,302].

1.2.1 Regulatory perspectives

The nonclinical development and general safety assessment of ONDs usually follows the nonclinical testing guidelines for small molecules (e.g., as small molecules for Food and Drug Authority (FDA); or as new chemical entities for European Medicines Agency (EMA)) as there is no formal guidelines

from health authorities in place for ONDs to date. Even though the small-molecule guideline recommendations from the International Conference on Harmonization (ICH M3 [R2]) does not directly address OND, the general principles may also apply to them as they are chemically synthesized (Table 1.3) and frequently involve not naturally-occurring chemical modifications [28,303]. On the other hand, some product attributes of ONDs are shared with biopharmaceutical agents such as larger size, predictive PK, longer half-life, and species and target specificity [304]. As ONDs are mentioned in the ICH S6 (R1) for biotechnology-derived pharmaceuticals, the principles from this guideline should also be taken into account in the nonclinical testing strategy of ONDs. Therefore, a hybrid approach between ICH M3 and S6 customized to a specific OND characteristic may satisfy the regulatory expectations and provide a scientifically sound safety evaluation [28].

Informally, a set of best practice recommendations (provided as series of white papers) were prepared by various consortia, such as the OSWG consisting of academics, regulators, and industry members. The OSWG presents very detailed discussions in these whitepapers on issues that were faced by both developers and regulatory reviewers of ON therapeutics. While these white papers do not represent the opinions of regulatory authorities, they do suggest a possible approach to resolving issues specific to ONDs that are not addressed in the current guidelines for small molecules and biopharmaceutical products [305].

Table 1.3. Comparison of product attributes across product classes. This table is reproduced from Schubert et al. (2012) [305].

	NCEs	**ONs**	**NBEs**
Molecular weight	Low (<1 kDa)	Mid (>6 kDa)	High (>30 kDa)
Manufacture	Chemical synthesis	Chemical synthesis	Biologically derived
Structure	Single entity	Single entity	Heterogenous
Tissue distribution	- Intra- and extracellular - Wide distribution	- Intra- and extracellular - Selected distribution	- Largely extracellular - Limited distribution
PK/ ADME	- Species-specific metabolites - Short half life	- Catabolized to nucleotides - Long acting	- Catabolized to amino acids - Long half life
Species specificity	Less likely	More likely	Often
Off-target toxicity	Often	Sometimes	Rarely

Abbreviations: NCEs, new chemical entities; ONs, oligonucleotides; NBEs, new biological entities; kDa, kilodalton; PK, pharmacokinetics; ADME, absorption, distribution, metabolism, and excretion.

1.2.2 Nonclinical safety assessment strategies

The general aim for nonclinical safety testing is to identify potential toxicities of ASO candidates to aid their use in the clinics. Developmental and reproductive toxicology, as well as juvenile animal studies may also be necessary for ONDs, depending on the indication(s) being pursued and the clinical phase of development. Beyond the typical considerations on general toxicology study design (e.g., species selection of relevant animal models), particular justifications unique to ONDs (e.g., exaggerated pharmacology assessment and use of surrogates) should be recognized [306]. Moreover, certain product attributes of the ON candidate (e.g., class, chemistry, and delivery system) also necessitate specific considerations when planning nonclinical studies and each OND could be assessed on a case-by-case basis [307].

The small molecule guideline defines the conduct of repeat-dose toxicity evaluation in two species (up to six months in one rodent and nine months in one non-rodent species) [308]. The main difference with this one as opposed to the biopharmaceutical guideline [309] is that a single species approach is allowed in the latter when sufficient justifications are provided (species selection will be discussed in section 1.2.3).

Nonetheless, only 29% of sponsors have experience with health authorities accepting a “leaner” (use of a single species) M3 (R2) approach for their ONs nonclinical regulatory packages upon first submission, according to the results from a survey across 22 companies developing therapeutic ONs performed in 2018 [310]. In cases where single (primarily non-rodent) species nonclinical safety programs were conducted, the following reasons necessitated it: (1) lack of cross-reactivity to pharmacologic target and (2) lack of feasibility of the clinical dose route in rodents (e.g., intrathecal dosing), and (3) low risk of systemic class-related or off-target toxicity based on route of administration. Correspondingly, 76% of the respondents in this survey had been requested at least once by health authorities for a study or readout (e.g., small molecule relevant assays and use of second species), which they had not included or planned to include. On this regard, 47% of the respondents had positive feedback after providing sufficient justification for a “leaner” ON-tailored approach [310]. This is an encouraging evidence that health authorities are open to a modified approach (hybrid with S6) when there is a clear and compelling scientific rationale. Still, the prevailing nonclinical regulatory packages that companies follow are still solely the principles of the two-species small molecule ICH M3 (R2) guideline [310] wherein 76% of the respondents have

always conducted toxicology testing in two species [16]. This is evidenced when respondents placed ICH S6 (R1) on the lower end of relevant guidelines with an overall mean relevance of 44%, as compared to the ICH M3 (R2) guideline that has 72% mean relevance [310].

A consensus report of the Reproductive subcommittee of the OSWG recommended the case-by-case approach to assess developmental and reproductive toxicology (DART) for ONDs, as well as for species selection [219,304,311], due to their unique product attributes discussed earlier. Therefore, when planning the DART program, ON developers should consider: the regulatory guidelines for both NCEs and NBEs [312,313], the intended patient population [306], the pharmacological effect of the specific ON [307], its function within the reproductive system, and the potential for exaggerated pharmacology during pregnancy and fetal development [314]. The shared attributes of ONDs to NCEs and NBEs also require considerations for its chemical characteristics, structural subclasses, MOA, and optimal exposure (including dosing regimen) when planning DART studies [304].

1.2.2.1 *Nonclinical safety testing for ASOs intended for Pediatrics*

Similar to the rational basis for the program development for DART studies, the specific product attributes of ONDs should also be considered when developing therapeutic ONs intended for the pediatric population. In comparison to adults, pediatric patients who can receive pharmaceuticals during periods of rapid growth and/or postnatal development of numerous organ system constitute a distinct population [315]. The immaturity and stage of maturation of human and animal organ systems during OND treatment can affect its PK/PD profiles, and/or off-target effects potentially leading to differences in safety and/or efficacy profiles between pediatric populations (as described in ICH E11) and/or when compared to adults [315]. Moreover, comparison of development across species can be challenging and is not uniform across different organ systems. Therefore, careful evaluation of these potential differences in the intended developmental age groups compared to adults and between species is warranted [316].

ICH S11 was devised to serve as a guideline in support to the development of pharmaceuticals intended for pediatric use [315]. The scope of this guideline includes small molecule therapeutics and biotechnology-derived pharmaceuticals as defined in ICH S6 and therefore may be applicable for antisense therapeutics [309]. Most of the general considerations in the guideline regarding the

design of a nonclinical juvenile animal study (JAS) can also be applied with the case-by-case approach. The level of maturity and function can potentially influence susceptibility to toxicity. Understanding differences across species during development (e.g., nuclease ontogeny) is needed not only to design the appropriate JAS but also to aid the translation of nonclinical toxicity findings of ONDs to human age categories [316].

To date, no white paper has been written about the conduct of JAS when previous nonclinical and adult human data are judged to be insufficient to support pediatric studies for ONDs. Normally, a JAS is included in the pediatric investigation plan (PIP) and is designed to investigate safety concerns that cannot be adequately addressed in other nonclinical studies or pediatric clinical trials, including potential long-term safety effects [315,317]. It should be noted that the most relevant safety data for pediatric studies ordinarily come from adult human exposure [316]. However, additional nonclinical investigations in juvenile animals are advisable depending on the identified safety concerns and the intended pediatric clinical use. This also depends on an integrated assessment (weight of evidence approach) based on the totality of the evidence, including the clinical context together with the pharmacology, PK (ADME), and nonclinical in vitro and in vivo animal, and clinical safety data (adult and/or pediatric) [315].

The requirement for JAS in a PIP are motivated by concerns regarding potential developmental toxicities, in view of the young age of the pediatric population to be investigated, lack of knowledge concerning the maturation of the pharmacological target, the lack of sufficient (non)clinical data, observed toxicities in the adult (non)clinical studies, and long duration of the intended treatments [317]. Primary or secondary pharmacological properties of a pharmaceutical can be responsible for unwanted side effects. Moreover, further nonclinical investigation in juvenile animals should be considered for ONDs even though they have high selectivity and specificity for their target sequence, as potential adverse effects can stem out from exaggerated pharmacology [315]. Furthermore, both on-target and off-target pharmacology can be an important predictor of developmental effects for all classes of pharmaceuticals, including ONDs. During development, genes can have very distinct functions than in adults, and modulation of an array of pharmaceutical targets has been linked to developmental implications [313,318].

1.2.3 Species selection

The selection of animal models requires careful consideration [319] for the proper safety evaluation of an OND candidate including the general assessments common for toxicology studies, together with particular types of endpoints to assess potential toxicities that have been reported previously for other ONDs [306]. As such, an ideal animal model(s) should be representative of humans with regard to PK, metabolism, sensitivity to toxicity, and pharmacologic effects [313]. Specific considerations for species selection for ASO DART studies had been described elsewhere, while the ICH guideline S11 for pharmaceuticals in general is being considered for JAS in support of the development of ONDs intended for pediatrics.

In general, toxicity studies for ONDs are performed in a rodent and a non-rodent species, similar to small molecules [16] as evidenced by the prevailing nonclinical regulatory packages that most companies follow [310]. This is in line with the recommendation of the Japanese Research Working Group as ONDs often cause hybridization-independent off-target toxicities and sensitivity to these effects may vary between species [307]. Therefore, when assessing the off-target toxicities of ONDs, M3(R2) should be the reference as there are similarities between ONDs and NCEs. On the other hand, S6(R1) should be referred to for assessing on-target toxicities of ONDs. Accordingly, the consensus of the Subcommittees of the OSWG (DART, Safety Pharmacology, Formulated ON) recommends that at least one pharmacologically relevant species (responsive to the ON candidate pharmacologic activity) should be used for safety testing of ONDs that are directed against 'host targets' (i.e., human gene products or pathways) [304,311,320]. This is also consistent with recommendations by the Exaggerated Pharmacology subcommittee of OSWG in evaluating the potential for toxicities induced by the intended pharmacologic activity of a candidate ON [219].

Characterization of cross-species pharmacologic activity is critical for species routinely employed in toxicological assessments, especially for species that have traditionally been used for OND safety assessment, such as NHPs [219,321]. In case that two or more species are available for appropriate testing of on-target effects, toxicity studies should, in principle, be conducted in both, one rodent and one non-rodent [307]. However, it is the experience of the members of the Exaggerated Pharmacology Subcommittee that the pharmacologic activity of an OND is often achievable only in one species, owing to the ON sequence specificity and the precise sequence homology requirement for successful downregulation of an expressed gene [320,321]. Accordingly, sequence differences

may lead to inadequate activity of the clinical OND candidate in animal test species when evaluating potential hybridization-dependent on and off-target toxicities [319].

If a second pharmacologically relevant species is unavailable (e.g., mouse or rat), then the second species should typically be used to test only for chemistry-related effects (class effects) or other types of non-mechanism-based effects. As is the case with antibody therapeutics, toxicological testing of a particular candidate in a non-pharmacologically relevant species could be avoided if sufficient justifications are provided (e.g., previously well-studied drug class) [320,321]. In addition to using previous knowledge of the biological function encoded by the target sequence, in silico and/or in vitro microarray analyses could be used to assess the risk of on-target toxicities [307]. Similarly, the sponsor may recommend carrying out an extra in vivo toxicity study with a surrogate (active animal analog) before clinical studies or proceeding directly to the clinical phase without such data. This decision may be made on a case-by-case basis depending on previous available information [307]. When no pharmacologically responsive animal species can be identified for the clinical candidate, a satellite group receiving a single dose of a surrogate to assess on-target toxicities could be helpful for hazard identification. A similar study design has been proposed by S6(R1) and in a white paper by Kornbrust et al. [219,307]. However, there are very few instances when ON exaggerated pharmacology that translated into significant toxicity was reported in animals. Therefore it is essential to consider this before considering the use of analogs. Exaggerated pharmacology evaluation for ONs requires careful planning and close attention to a number of criteria in order to provide useful safety data while minimizing the possibility of causing unrelated effects that might be misinterpreted as exaggerated pharmacology [219]. In addition, off-target effects or class effects resulting from a clinical candidate's chemistry should not be assessed based on findings from a surrogate [307].

Information on the toxicity profile of many types of ONs that is often dominated by nonspecific “class effects” [76,129,276], if available, may be useful for selecting an animal species for toxicity studies and interpreting the results. As such, except for complement activation, rodents are more susceptible to OND toxicity than NHPs in a study of OND toxicity in individual animal species [307]. This information proved helpful in extrapolating nonclinical animal toxicity results to foresee the onset of adverse reactions in humans [278]. Other safety issues, such as proinflammatory

indications, exhibit rather poor interspecies translation but may still be important to evaluate and select against in regulatory toxicology studies to increase the probability of success [319].

Moreover, one aspect influencing the species selection would be variations in OND metabolism across species. Since the nuclease resistance and metabolite profiles of ONDs can be evaluated in vitro or in vivo, selecting an animal species with a metabolic profile comparable to that of humans would be suitable if species-specific metabolite differences are identified [307]. If such data is known for an OND in the same class, an animal species with a PK profile comparable to humans should be chosen. For instance, PS ASOs showed PK profiles in nonclinical animal studies (except in mice) which correlated well with human PK [307].

1.2.3.1 *Rodents*

Mice and rats have been used as the rodent species for OND toxicity testing, and the selection criteria seems to be company- and program-specific [306]. For ASOs, relevant pharmacological activity is relative to the sequence homology degree between the drug candidate and the target transcript across species. The degree of homology between rodents and humans (or rodents and NHPs), is frequently poor. As a result, a rodent-active surrogate may be required to allow pharmacology investigations in rodent species. The rodent surrogate OND can then address the potential toxicities related to exaggerated pharmacological activity by including it as a distinct treatment group in the toxicity evaluation for the human-active OND [306].

Although the rat is the most commonly used rodent when investigating small molecule toxicities, rat-specific lesions such as Chronic Progressive Nephropathy [215,263] are exacerbated by the high kidney concentrations following systemic PS ASO administration. Chronic Progressive Nephropathy has no human relevance, however it may cause issues in chronic toxicity investigations [16,322]. On the other hand, treatment of mice with high doses of PS ASOs resulted in elevated levels of circulating cytokines and chemokines [269,286] and dose-dependent lymphoid hyperplasia with spleen and lymph node enlargement and lymphohistiocytic cell infiltration often detected in different organs [263,279,321]. In line with this, there is growing proof that the intensity and range of anatomic pathologies produced by immunostimulatory ONs in rodents do not indicate human responses [219]. Thus, although rodents have been commonly utilized for in vivo toxicity screening, they are thought to be more susceptible to immune stimulation and specific

lesions such as Chronic Progressive Nephropathy, which does not necessarily translate to humans [319].

1.2.3.2 *Non-rodents*

The primary non-rodent species for OND safety evaluation has been the NHP, often a macaque species such as the cynomolgus monkey [306]. The reason for this is due to the highest likelihood of sequence-dependent crossover on activity (due to high degree or complete RNA sequence homology) and a robust historical background data [16]. The former enables the exaggerated pharmacology evaluation in the clinical candidate's general toxicity study in NHPs. However, for those ASOs that depend on hybridization for MOA, high degree of homology does not ensure activity across species as single base mismatches may significantly diminish or eliminate activity. Hence, some evidence of pharmacological activity (in vitro or in vivo) in the species selected for the nonclinical program may be required [306].

Other non-rodents have been evaluated, including the minipig [16,238,310], regarding ASO safety assessment. On the other hand, the high cost of production in the early days of OND development encouraged the selection of NHP owing to their smaller body weight than the dog (∼2.4 vs. ∼8–10 kg). Alternative non-rodent species have also been utilized for certain indications or administration methods, such as dermal applications (minipig and rabbit) or intraocular injections (rabbit and dog) [306]. Nevertheless, regulatory-based review papers have focused on using NHPs for toxicity assessment, reinforcing the need to include an NHP species for nearly every OND program [303,323]. Accordingly, the PK properties and sensitivity to proinflammatory effects of NHPs, generally appear to appropriately represent human responses. In part, it was presumed that the similarity of NHPs to humans indicated a high degree of relevance of the findings to human safety. However, this relationship remains a subject of continual assessment. In turn, considering the particular attributes of the drug candidate, an alternative to NHP may be more relevant and/or practical for general toxicity assessment, presuming sufficient evidence of pharmacological activity for the chosen non-rodent species. As stated previously, even if the OND has substantial cross-species activity for general toxicology and exaggerated pharmacology evaluation, regulatory authorities may expect some testing in NHPs unless a solid rationale is provided [306].

1.3 The Göttingen Minipig as a safety testing model

Göttingen Minipigs are one of the most often used purpose-bred pigs in Europe. Recent studies have provided data supporting the predictive value of minipigs in the nonclinical development of pharmaceuticals [324,325] as the minipig exhibits many similarities to human anatomy, physiology, biochemistry, and pathophysiological responses [326,327].

Pigs have a higher genetic similarity to humans than rodent and canine models. In 2005, the first entire pig reference genome sequence assembly was made accessible, containing approximately 2500 Mb in size organized in 18 autosomal and two sex chromosomes of comparable sizes to those of humans [328]. Considering the similarities with humans and the good body of information available for the minipig, the model has the potential to be used in the development of biopharmaceuticals, ONDs, and possibly in silico toxicology studies [326].

Transgenic technology can be readily applied in minipigs [326,327]. For instance, humanized Göttingen Minipigs are now available [327] and this allows the safety assessment of human IgG-based therapeutic antibodies. This can be beneficial also for safety testing of antibody-ON conjugates (AOCs). As the Göttingen Minipig genome has been sequenced [329,330], it is possible to make homologous ASOs that cross-react in minipigs, which permits the study of toxicities linked to the pharmacologic target. In essence, pharmacological target homology is essential for showing the pharmacological effects of ASO candidates in the relevant nonclinical species. As such, the recent sequencing of the minipig genome is crucial in considering this model as a potential alternative non-rodent species [238].

1.3.1 The adult Göttingen Minipig as a safety testing model for ASOs

Concerning the use of minipigs as an adult non-rodent toxicity model, only 14% of RNase-H-based ASOs and 20–40% of other ASO subclasses were tested in this model [310]. In 2017, the adult Göttingen Minipig was reported to be a suitable alternative model for NHPs in the adult safety assessment of ASO drugs [238]. In this study, four different model LNA PS ASOs, all with known safety profiles, were administered subcutaneously to minipigs using similar study designs and read-outs as in earlier NHP studies. Administration of the four LNA PS ASOs resulted in similar PK/PD and safety profile in minipigs as in NHPs upon subacute systemic exposure [238].

ASOs are well-absorbed in the circulation following SC administration. Similar to other species, plasma exposure increased roughly dose-proportionally, and ASOs were rapidly cleared from circulation [123,238]. In both species (minipigs and NHPs), LNA PS ASOs (e.g., RTR5001) are distributed and taken up by peripheral tissues such as the liver and kidney. For most of the investigated LNA PS ASOs, there was an exposure saturation in the kidneys. In general, kidney exposure was significantly higher compared to the liver, as previously described [68,145,238].

Target engagement and pharmacologic effect had also been demonstrated in the minipigs [238]. However, among the four model ASOs assessed, only one of the compounds (i.e., RTR5001, see Table 1.4) showed pharmacologic activity in the minipigs. A decrease in LDL cholesterol after repeated administration of RTR5001 (20 mg/kg) (targeting the *PCSK9* transcript) had been observed similar to NHPs [331]. Likewise, *PCSK9* expression in minipig livers was significantly reduced even though there is a single mismatch (end-standing) in the minipig sequence. Accordingly, PCSK9 is a protease that degrades LDL receptors in the liver, thereby has a role in controlling plasma LDL cholesterol levels [332]. Furthermore, no additional on- and off-target effects or non-hybridization-dependent toxicities were identified in the adult minipigs for the four tested LNA PS ASOs [238].

Table 1.4. Nonclinical and clinical information of RTR5001, one of the four model ASOs evaluated for safety testing in adult Göttingen Minipigs.

RTR5001 compound information		**Remarks and references**
Sequence	'5-T*G*C*t*a*c*a*a*a*a*c*C*C*A*-3' (upper-case, LNA monomers; lower-case, DNA monomers; *, PS linkages)	See section 1.1.4.1.1 for PS; and 1.1.4.1.3 for LNA modification information.
Design	LNA PS gapmer (RNase H-dependent ASO)	See section 1.1.4.2.1 for LNA gapmer characteristics.
Indication	Familial Hypercholesterolemia: a genetic disease characterized by elevated plasma LDL cholesterol. LDL cholesterol deposits in blood vessels, increasing the risk of premature cardiovascular disease.	[333,334]
Pharmacologic target	*PCSK9* mRNA (mainly expressed in the liver): PCSK9 functions by increasing the degradation rate of LDL receptor (binds LDL in the circulation) and secondarily by preventing LDL clearance (increases circulating LDL cholesterol).	[335]
Available information in nonclinical (Göttingen	***Göttingen Minipig*:** Three minipigs (adult females, 4-6 months) per dose level group received a SC dose (inguinal region, left and right alternated) of 6 or 20 mg/kg on days 1, 6, 11, and 16 at a dose	[238,331,336]

Minipig and NHPs) and clinical study designs (e.g., dosing regimen)	volume of 0.25 mL/kg. Two animals served as concurrent controls (phosphate-buffered saline). ***Cynomolgus monkey*:** Three monkeys per dose level group received subcutaneous doses of 0, 6, or 20 mg/kg on days 1, 6, 11, and 16. Single-dose study. Six monkeys received a 10 mg/kg SC dose with subsequent killing of single monkeys at days 4, 7, 14, 21, 28, and 56 after dosing. Multiple-dose study. Five monkeys were initially SC dosed with 20 mg/kg, followed by four weekly 5 mg/kg maintenance doses. Forty-eight hours after the last dose (day 30), three monkeys were sacrificed, and the remaining two were monitored for an additional 8-week recovery period. ***Human*:** Randomized, ascending dose, double-blind, and placebo-controlled (0.9% saline), with an RTR5001:placebo ratio of 6:2 per cohort (24 healthy volunteers). The drug was administered SC in the abdominal region as three weekly doses of 0.5, 1.5, or 5 mg/kg on study days 1, 8, and 15 (150 mg/ml RTR5001 dissolved in water for injection; injection volumes ≤3 ml administered in a single injection and volumes >3ml in two injections). The 0.5 mg/kg/week starting dose was 4-fold lower than the maximum recommended starting dose of 2.0 mg/kg/week, based on the NOAEL of 20 mg/kg per dose, with an applied safety factor of 10.	
Pharmacokinetic profile		
Plasma exposure	***Göttingen Minipigs*:** AUC and C_{max} values increased roughly dose-proportionally. Mean $AUC_{0\text{-}24h}$ (µg*h/mL): 25.3±4.3 (Day 1, 6 mg/kg); 120.0±26.9 (Day 1, 20 mg/kg); 23.6±4.1 (Day 16, 6 mg/kg); 111.1±21.9 (Day 16, 20 mg/kg). Mean C_{max} (µg/mL): 3.8±1.2 (Day 1, 6 mg/kg); 15.1±1.6 (Day 1, 20 mg/kg); 3.3±1.0 (Day 16, 6mg/kg); 15.6±3.5 (Day 16, 20 mg/kg). Plasma exposure over repeated administration remained unchanged and rapidly cleared from circulation, resulting in a concentration of 2-3 orders of magnitude lower than C_{max} after 24 hours. ***Cynomolgus monkey*:** Mean $AUC_{0\text{-}24h}$ (µg*h/mL): 27.0±8.4 (Day 1, 6 mg/kg); 128.0±26.0 (Day 1, 20 mg/kg); 25.8±8.4 (Day 16, 6 mg/kg); 117.0±16.0 (Day 16, 20 mg/kg). Mean C_{max} (µg/mL): 5.34±2.6 (Day 1, 6 mg/kg); 12.9±2.0 (Day 1, 20 mg/kg); 3.55±1.7 (Day 16, 6mg/kg); 10.9±1.0 (Day 16, 20 mg/kg). No available data on the single and multiple-dose studies. ***Human*:** Mean $AUC_{0\text{-}24h}$ (µg*h/mL): 1.8 (Day 1, 0.5mg/kg); 5.0 (Day 1, 1.5mg/kg); 23.0 (Day 1, 5.0mg/kg). Mean C_{max} (µg/mL): 0.3 (Day 1, 0.5mg/kg); 0.8 (Day 1, 1.5mg/kg); 2.4 (Day 1, 5.0mg/kg). T_{max}: 1.7±0.5 (0.5 mg/kg), 1.2±0.4 (1.5 mg/kg), and 2.5±2.7 (5.0 mg/kg) hours post-dose. High binding affinity of RTR5001 (>95%) to human serum albumin.	See section 1.1.5.2 for further details about ASO plasma exposure. [238,336]
Distribution	***Göttingen Minipig*:** Liver and kidney tissue levels increased dose-dependently after administration (partitioned to a markedly higher concentration in the kidney cortex than in	See section 1.1.5.3 for further details about ASO

	the liver). The presence of RTR5001 was demonstrated by immunohistochemistry and in situ hybridization in the cytoplasm of tubular epithelial cells in the kidneys, Kupffer cells in the liver, and macrophages in the lymph nodes. Accumulation of RTR5001 in the proximal tubular cells in kidneys resulted in cytoplasmic basophilic granules. Kidney cortex exposure: 0, 164, and 555 µg/g at 0, 6, and 20 mg/kg, respectively. Liver exposure: 0, 38, and 74 µg/g at 0, 6, and 20 mg/kg, respectively. ***Cynomolgus monkey*:** Kidney cortex exposure: 0, 386, and 602 µg/g at 0, 6, and 20 mg/kg, respectively. Liver exposure: 0, 65, and 177 µg/g at 0, 6, and 20 mg/kg, respectively. Liver exposure (multiple doses, 20 mg/g initial dose followed by four weekly doses of 5 mg/kg, day 30): 58.0±17 µg/g. RTR5001 uptake is most prominent in the proximal tubules of the kidneys. ***Human*:** No available data.	distribution. [238,295,331]
Metabolism and Excretion (terminal elimination)	***Göttingen Minipig*:** No available data. ***Cynomolgus monkey*:** liver tissue half-life, at least six days (single dose). The plasma half-life during recovery (multiple doses) is estimated to be at least seven days. ***Humans*:** Plasma half-life (terminal phase) was estimated to be seven days. The total amount of RTR5001 in urine increased more than dose-proportionally. During the first 24 hours after administration, only 1-3% of the dose was excreted in the urine (approximately corresponding to the unbound fraction).	See section 1.1.5.5 (ASO metabolism and excretion) for further details. [331,336]
<u>Pharmacologic activity profile</u>		
Göttingen Minipigs:	At 20 mg/kg: statistically significant ($p < 0.05$) decrease (up to -53%) in mean serum LDL cholesterol, together with a decline of mean total cholesterol (-20 to 30%) on days 12 and 17; and decreased triglyceride levels on day 17. *PCSK9* mRNA expression levels in the liver were markedly and dose-dependently reduced (measured by quantitative PCR) by up to 72% after SC dosing despite the single end-standing mismatch in the minipig sequence of RTR5001. By in situ hybridization, a reduced *PCSK9* mRNA expression was confirmed wherein minimal to mild cytoplasmic staining for *PCSK9* was present in hepatocytes of control minipigs, and no or only minimal staining was present in minipigs dosed with 20 mg/kg RTR5001.	[238]
Nonhuman primates (Cynomolgus monkey):	Decrease in total cholesterol and triglyceride levels at 20 mg/kg, and reduction in LDL cholesterol at ≥6 mg/kg. Single dose, 10 mg/kg: LDL cholesterol levels decreased continuously over the first three weeks, with a maximum reduction of 50% at day 21, the effect diminished slowly, and at day 56, LDL cholesterol had returned to pre-dose levels. Multiple doses: significant reduction in serum PCSK9 protein levels was observed (24 hours after the first dose). At day 7, an 85% reduction of PCSK9 protein level was seen and maintained for the treatment period. This translated into decreased LDL cholesterol (and total cholesterol, while HDL	[238,331]

	cholesterol was unaffected). However, the reduction was delayed and was observed only from day four onwards (an average of 50% below pre-dose level, with 70% in the highest responder). Liver *PCSK9* mRNA expression compared to controls was 85% lower. Liver LDL receptor protein levels (analyzed by western blot) increased by 67%. For recovery period monitoring, circulating LDL cholesterol increased gradually to 65% of the pre-dose level during the first four weeks. At the recovery period termination (day 84), liver *PCSK9* mRNA expression level was similar to the pre-dose levels.	
Humans:	Plasma PCSK9 protein concentration decreased (37.2 – 58.5%), reaching a level of significance ($p<0.0001$) when compared with placebo at the highest dose levels. The maximal decrease in PCSK9 level was achieved one week after the last dose (from 302±80 ng/ml at baseline to 156±85 ng/ml on day 21, at 5 mg/kg). LDL cholesterol dose-dependently decreased (25%) with a maximal effect reached two weeks after the last dose (from 3.8±0.8 mmol/L at baseline to 2.9±1.1mmol/L on day 29, for 5 mg/kg). LDL cholesterol returned to baseline nine weeks after the last dose administration. HDL cholesterol, VLDL cholesterol, and triglycerides are not affected by treatment.	[336]
Toxicity profile		
In-life observation and Clinical pathology	***Göttingen Minipig*:** All animals survived until the scheduled sacrifice. No RTR5001-related clinical signs or injection site reactions, and no changes in hematology, coagulation parameters, and cytokines were observed. On day 17 (after four doses) at 20 mg/kg, one minipig showed an increase in serum creatinine (1.6-fold) and blood urea nitrogen (BUN; 1.8-fold); another minipig showed a rise in BUN only (1.2-fold). Urinary changes at 20 mg/kg: increased urinary volume with a concomitant increase of N-acetyl-beta-D-glucosaminidase, sodium, and calcium normalized to creatinine. ***Cynomolgus monkey*:** Increase WBC count, neutrophils, and monocytes were observed at 20 mg/kg. Single and multiple dose studies: no significant effect in liver and kidney toxicology markers (e.g., alanine aminotransferase, aspartate aminotransferase, urea, creatinine, glucose). ***Human*:** One subject dosed at the highest dose (5 mg/kg per dose) experienced acute (transient) tubular necrosis five days after the last dose (serum creatinine level from 0.81 mg/dL at baseline to 2.67 mg/dL, and this coincide with the presence of WBC, granular cast, and minimal hematuria on urine microscopy). This patient's serum creatinine peaked at 3.81 mg/dL one week after the last dose before returning to baseline levels 44 days upon conservative treatment. Kidney injury urine markers started to increase after the first dose, and a 4-fold increase was observed for β_2-microglobulin, while 24-fold for α-GST and 60-fold for KIM-1 were observed in samples taken before the last dose administration. No	[238,331,336]

	clinically relevant effects on serum creatinine levels were observed in the 0.5 and 1.5 mg/kg per dose groups, while thr 5 mg/kg dose induced a transient increase in serum creatinine (four out of six subjects). Average serum creatinine in the high-dose group started to increase after the last administration and peaked approximately ten days after the final dose (from 84±12 to 106±15 µmol/L; reference ranges are 64-104 µmol/L for males and 49-90 µmol/L for females) before gradually declining to baseline levels. Increases in serum creatinine (9%, p=0.02), urinary β_2-microglobulin (200%, p=0.01), urinary KIM-1 (55%, p=0.2), and urinary α-GST (280%, p=0.004) were observed at the highest dose level tested, with serum creatinine and urinary KIM-1 reaching the peak at the fourth week.	
Gross and anatomic pathology	***Göttingen Minipig*:** increased weights and pale discoloration of the kidneys. Red discoloration of the injection sites (corresponds to histologic findings of inflammation and acute hemorrhage). ***Cynomolgus monkey*:** No observed gross effects in the single and multiple dose studies. ***Human*:** Injection site reactions (44% of the treated subjects, 0/6, 3/6, and 5/6 in the 0.5, 1.5, and 5 mg/kg dosing groups, and none in placebo-treated subjects).	[238,331,336]
Accumulation-related and proinflammatory toxicities	***Göttingen Minipig*:** In the kidneys, mild to moderate dilatation of the proximal renal tubules and mild to moderate tubular degeneration/regeneration were seen in 2 of 3 minipigs at 20 mg/kg. Tubular degeneration consists of proximal tubular cell vacuolation, necrosis of tubular cells, and occasional apoptotic/necrotic cells in the lumen. In the liver, minimal single-cell necrosis was observed in 1 of 3 minipigs dosed at 20 mg/kg. In the mandibular, mesenteric, and inguinal (draining) lymph nodes, minimal to mild macrophage vacuolation was observed (≥ 6 mg/kg). At the injection site, increased SC inflammation was characterized by the presence of macrophages, lymphocytes, and granulocytes (at 6 and 20 mg/kg); necrosis, edema, and hemorrhages were also observed when compared with controls. ***Cynomolgus monkey*:** No histological changes in the livers of treated monkeys. Basophilic tubular granules at ≥ 6 mg/kg, tubular dilatation/atrophy in 1 of 3 at 20 mg/kg. In the lymph nodes, sinus histiocytosis (vacuolated/stippled) at ≥ 6 mg/kg). At the injection site, increase severity of inflammation, edema, and hemorrhages when compared with controls. ***Human*:** Acute multifocal tubular necrosis (cause unclear, but hypothesized as off-target effect) and signs of oligonucleotide accumulation were observed in a (healthy) subject five days after the three weekly doses were given. Histopathologic examination showed several foci of severe tubular injury with total denudation, nuclear apoptosis, and eosinophilic epithelial degeneration with shedding into the tubular lumen, which also contained debris with granular material. The interstitium showed focal edema and	[28,238,295,331,336]

	lymphocytic infiltrates. Electron microscopy showed cell necrosis, vacuolization, and cytoskeleton collapse, commonly seen in toxic tubular damage.	
Aptameric effects	Complement activation, coagulation cascade inhibition, and platelet count reduction were not observed in adult minipigs, NHPs, and humans.	See sections 1.1.7.2.1; 1.1.7.2.2; and 1.1.7.2.3 for further information about these adverse effects by ASOs. [238,295,331,336]

Abbreviations: PS, phosphothioate; LNA, locked nucleic acid; SC, subcutaneous; LDL, low-density lipoprotein; HDL, high-density lipoprotein; VLDL, very low density lipoprotein; PCSK9, proprotein convertase subtilisin/kexin 9; NOAEL, no observed adverse effect level; C_{max}, maximum concentration; AUC, area under the graph; α-GST, α-glutathione S-transferase; KIM-1, kidney injury molecule-1.

In general, minipigs showed very good comparability in toxicity profile versus NHPs. Effects on the coagulation and platelet count, were comparable to those observed in NHPs. On the other hand, the minipig did not predict the clinical features of human injection site reactions better than the NHPs, but histopathological similarities were observed between the two species. Typical of the class-wide toxicity profile of ASOs (e.g. RTR5001) [238], the kidney, liver, and lymphoid tissues were also observed to be the main target tissues of toxicity in the minipigs, similar to NHPs. However, minipigs appeared more sensitive to the high-dose kidney toxicity of most of the selected ASOs than NHPs. In particular, one minipig dosed with RTR4955 showed a mesangioproliferative glomerulonephritis, a lesion not previously observed in NHPs for the four LNA PS ASOs. On the other hand, activation of the complement system was seen at plasma C_{max} values of approximately 500 µg/mL RTR2996 in the minipigs [238]. In contrast, activation of the complement system in NHPs was reported with threshold ASO plasma levels of 70–80 µg/mL [298]. Although this warrants more data, this finding could suggest a lower sensitivity of minipigs to this effect in terms of complement activation than NHPs and thus possibly a higher relevance to human safety evaluation since NHPs are known to be over predictive [337].

1.3.2 The Göttingen Minipig in pediatric drug development

Besides species similarity, welfare considerations, technical feasibility, and rapid postnatal development [324,326,338] make the juvenile minipigs a promising model for safety assessment of pharmaceuticals, including ONDs. The ICH S11 guidelines on nonclinical safety testing in support of the development of pediatric pharmaceuticals also state that there are many similarities between human and Göttingen Minipig regarding organ development [315]. In addition, the EMA has established different age categories within the pediatric population and this information is available

in the public domain [339]. Detailed information about these similarities, differences, as well as advantages, and disadvantages of the model are reviewed elsewhere [338].

With the recent advances in genetic engineering along with the inherent characteristics of (mini)pigs, different (mini)pig models representing active disease states have become available [338]. As such, these models mostly account for genetic disorders (e.g., Duchenne muscular dystrophy [340], cystic fibrosis [341,342], and hereditary tyrosinemia type 1 [343]. Moreover, other disease models are available for the pigs/piglets, such as inflammatory bowel disease [344], and nonalcoholic fatty liver disease [338], wherein antisense therapy application has been explored [345–347]. In particular, Duchenne muscular dystrophy, which is of interest for pediatric indications, has been already been treated successfully with ASOs [24,26].

Pigs and humans share many developmental milestones as both species show similar differences between adult and juvenile populations. In particular, the patterns of development of the gastrointestinal tract (GIT) including the liver, cardiovascular, CNS systems, and eye are remarkably comparable in both species. On the other hand, the development of the renal, immune, and reproductive systems occur relatively earlier and quicker in humans than in pigs [338]. Nonetheless, the pig shares more similarities with humans in ontogenic changes in PK than other species, including the dog [348]. Despite attempts to further characterize ADME processes in minipigs (especially in neonatal and juvenile piglets) for their use in drug development studies [326,349,350], no information is available yet about the ontogeny of nucleases responsible to ASO degradation in the different tissue compartments in the minipigs. Likewise, no data is present regarding the effect of age in the PK, PD, and safety of ASOs in the Göttingen Minipig. Therefore, further research is necessary. The main focus of this thesis will be on the evaluation of an LNA PS gapmer, RTR5001, of which its characteristics, PK/PD, and safety profiles are described on Table 1.4 (see section 1.3.1).

1.4 References

1. Ming, X. Cellular Pharmacology of Antisense Oligonucleotides. In *Oligonucleotide-Based Drugs and Therapeutics*; 2018.
2. Agrawal, S.; Gait, M.J. CHAPTER 1: History and Development of Nucleotide Analogues in Nucleic Acids Drugs. In *RSC Drug Discovery Series*; 2019; Vol. 2019-January.
3. Aartsma-Rus, A.; Jackson, A.L.; Levin, A.A. Mechanisms of Oligonucleotide Actions. In *Oligonucleotide-Based Drugs and Therapeutics*; Ferrari, N, Seguin, R., Ed.; John Wiley & Sons, Inc.: New Jersey, 2018; pp. 1–38 ISBN 9781119070290.

4. Takakusa, H.; Iwazaki, N.; Nishikawa, M.; Yoshida, T.; Obika, S.; Inoue, T. Drug Metabolism and Pharmacokinetics of Antisense Oligonucleotide Therapeutics: Typical Profiles, Evaluation Approaches, and Points to Consider Compared with Small Molecule Drugs. *Nucleic Acid Ther* **2023**, doi:10.1089/nat.2022.0054.
5. Watts, J.K. The Medicinal Chemistry of Antisense Oligonucleotides. In *Oligonucleotide-Based Drugs and Therapeutics*; Ferrari, N, Seguin, R., Ed.; John Wiley & Sons, Inc.: New Jersey, 2018; pp. 39–69 ISBN 9781119070290.
6. De Clercq, E.; Eckstein, F.; Merigan, T.C. Interferon Induction Increased through Chemical Modification of a Synthetic Polyribonucleotide. *Science (1979)* **1969**, *165*, doi:10.1126/science.165.3898.1137.
7. Stec, W.J.; Zon, G.; Egan, W.; Stec, B. Automated Solid-Phase Synthesis, Separation, and Stereochemistry of Phosphorothioate Analogues of Oligodeoxyribonucleotides. *J Am Chem Soc* **1984**, *106*, doi:10.1021/ja00332a054.
8. Seth, P.P.; Swayze, E.E. CHAPTER 3: The Medicinal Chemistry of RNase H-Activating Antisense Oligonucleotides. In *RSC Drug Discovery Series*; 2019; Vol. 2019-January.
9. Gura, T. Antisense Has Growing Pains. *Science (1979)* 1995, *270*.
10. Agrawal, S.; Kandimalla, E.R. Antisense Therapeutics: Is It as Simple as Complementary Base Recognition? *Molecular Medicine* 2000, *6*.
11. Agrawal, S. Importance of Nucleotide Sequence and Chemical Modifications of Antisense Oligonucleotides. *Biochimica et Biophysica Acta - Gene Structure and Expression* 1999, *1489*.
12. Walder, R.Y.; Walder, J.A. Role of RNase H in Hybrid-Arrested Translation by Antisense Oligonucleotides. *Proceedings of the National Academy of Sciences* **1988**, *85*, 5011–5015, doi:10.1073/pnas.85.14.5011.
13. Monia, B.P.; Lesnik, E.A.; Gonzalez, C.; Lima, W.F.; McGee, D.; Guinosso, C.J.; Kawasaki, A.M.; Cook, P.D.; Freier, S.M. Evaluation of 2'-Modified Oligonucleotides Containing 2'-Deoxy Gaps as Antisense Inhibitors of Gene Expression. *Journal of Biological Chemistry* **1993**, *268*, doi:10.1016/s0021-9258(19)85268-7.
14. Gait, M.J.; Agrawal, S. Introduction and History of the Chemistry of Nucleic Acids Therapeutics. In *Methods in Molecular Biology*; 2022; Vol. 2434.
15. Liu, Z.; Corey, D.R. CHAPTER 2: Mechanisms of Antisense Oligonucleotides. In *RSC Drug Discovery Series*; 2019; Vol. 2019-January.
16. Andersson, P. Preclinical Safety Assessment of Therapeutic Oligonucleotides. In *Methods in Molecular Biology*; 2022; Vol. 2434.
17. Kim, J.; Hu, C.; Moufawad El Achkar, C.; Black, L.E.; Douville, J.; Larson, A.; Pendergast, M.K.; Goldkind, S.F.; Lee, E.A.; Kuniholm, A.; et al. Patient-Customized Oligonucleotide Therapy for a Rare Genetic Disease. *New England Journal of Medicine* **2019**, *381*, doi:10.1056/nejmoa1813279.
18. Scoto, M.; Finkel, R.; Mercuri, E.; Muntoni, F. Genetic Therapies for Inherited Neuromuscular Disorders. *Lancet Child Adolesc Health* **2018**, *2*, 600–609, doi:10.1016/S2352-4642(18)30140-8.
19. Abreu, N.J.; Waldrop, M.A. Overview of Gene Therapy in Spinal Muscular Atrophy and Duchenne Muscular Dystrophy. *Pediatr Pulmonol* **2021**, *56*, 710–720, doi:10.1002/ppul.25055.
20. Aoki, Y.; Wood, M.J.A. Emerging Oligonucleotide Therapeutics for Rare Neuromuscular Diseases. *J Neuromuscul Dis* **2021**, *Pre-press*, 1–16, doi:10.3233/jnd-200560.
21. Martinovich, K.M.; Shaw, N.C.; Kicic, A.; Schultz, A.; Fletcher, S.; Wilton, S.D.; Stick, S.M. The Potential of Antisense Oligonucleotide Therapies for Inherited Childhood Lung Diseases. *Mol Cell Pediatr* **2018**, *5*, 3, doi:10.1186/s40348-018-0081-6.
22. Ashrafi, M.R.; Amanat, M.; Garshasbi, M.; Kameli, R.; Nilipour, Y.; Heidari, M.; Rezaei, Z.; Tavasoli, A.R. An Update on Clinical, Pathological, Diagnostic, and Therapeutic Perspectives of Childhood Leukodystrophies. *Expert Rev Neurother* **2020**, *20*, 65–84, doi:10.1080/14737175.2020.1699060.
23. Oren, Y.S.; Irony-Tur Sinai, M.; Golec, A.; Barchad-Avitzur, O.; Mutyam, V.; Li, Y.; Hong, J.; Ozeri-Galai, E.; Hatton, A.; Leibson, C.; et al. Antisense Oligonucleotide-Based Drug Development for Cystic Fibrosis Patients Carrying the 3849+10 Kb C-to-T Splicing Mutation. *Journal of Cystic Fibrosis* **2021**, *In Press*, doi:10.1016/j.jcf.2021.06.003.
24. Dhuri, K.; Bechtold, C.; Quijano, E.; Pham, H.; Gupta, A.; Vikram, A.; Bahal, R. Antisense Oligonucleotides: An Emerging Area in Drug Discovery and Development. *J Clin Med* **2020**, *9*, 2004, doi:10.3390/jcm9062004.
25. Osredkar, D.; Jílková, M.; Butenko, T.; Loboda, T.; Golli, T.; Fuchsová, P.; Rohlenová, M.; Haberlova, J. Children and Young Adults with Spinal Muscular Atrophy Treated with Nusinersen. *European Journal of Paediatric Neurology* **2021**, *30*, 1–8, doi:10.1016/j.ejpn.2020.11.004.
26. Hoffman, E.P. Pharmacotherapy of Duchenne Muscular Dystrophy. *Handb Exp Pharmacol* **2020**, *261*, 25–37, doi:10.1007/164_2019_256.
27. Bennett, C.F.; Swayze, E.E. RNA Targeting Therapeutics: Molecular Mechanisms of Antisense Oligonucleotides as a Therapeutic Platform. *Annu Rev Pharmacol Toxicol* **2010**, *50*, 259–293, doi:10.1146/annurev.pharmtox.010909.105654.
28. Andersson, P.; Den Besten, C. Preclinical and Clinical Drug-Metabolism, Pharmacokinetics and Safety of Therapeutic Oligonucleotides. In *RSC Drug Discovery Series*; Agrawal, Sudhir, Gait, M., Ed.; Royal Society of Chemistry: UK, 2019; Vol. 2019-Janua, pp. 474–517 ISBN 978-1-78801-571-4.

29. Lagos-Quintana, M. Oligonucleotide-Based Therapeutics, Development and Regulatory Challenges, Rheinischen Friedrich-Wilhelms-Universität: Bonn, 2016.
30. Kole, R. Modification of Pre-MRNA Splicing by Antisense Oligonucleotides. *Acta Biochim Pol* 1997, *44*.
31. Kole, R.; Vacek, M.; Williams, T. Modification of Alternative Splicing by Antisense Therapeutics. *Oligonucleotides* 2004, *14*.
32. Rossor, A.M.; Reilly, M.M.; Sleigh, J.N. Antisense Oligonucleotides and Other Genetic Therapies Made Simple. *Pract Neurol* **2018**, *18*, doi:10.1136/practneurol-2017-001764.
33. Donis-Keller, H. Site Specific Enzymatic Cleavage of RNA. *Nucleic Acids Res* **1979**, *7*, doi:10.1093/nar/7.1.179.
34. Gazzoli, I.; Aartsma-Rus, A. Splice-Switching Oligonucleotides. In *Oligonucleotide-Based Drugs and Therapeutics*; 2018.
35. Cerritelli, S.M.; Crouch, R.J. Ribonuclease H: The Enzymes in Eukaryotes. *FEBS Journal* 2009, *276*.
36. Amon, J.D.; Koshland, D. RNase H Enables Efficient Repair of R-Loop Induced DNA Damage. *Elife* **2016**, *5*, doi:10.7554/elife.20533.
37. Lima, W.F.; Murray, H.M.; Damle, S.S.; Hart, C.E.; Hung, G.; De Hoyos, C.L.; Liang, X.H.; Crooke, S.T. Viable RNaseH1 Knockout Mice Show RNaseH1 Is Essential for R Loop Processing, Mitochondrial and Liver Function. *Nucleic Acids Res* **2016**, *44*, doi:10.1093/nar/gkw350.
38. Chapados, B.R.; Chai, Q.; Hosfield, D.J.; Qiu, J.; Shen, B.; Tainer, J.A. Structural Biochemistry of a Type 2 RNase H: RNA Primer Recognition and Removal during DNA Replication. *J Mol Biol* **2001**, *307*, doi:10.1006/jmbi.2001.4494.
39. Wu, H.; Lima, W.F.; Zhang, H.; Fan, A.; Sun, H.; Crooke, S.T. Determination of the Role of the Human RNase H1 in the Pharmacology of DNA-like Antisense Drugs. *Journal of Biological Chemistry* **2004**, *279*, 17181–17189, doi:10.1074/jbc.M311683200.
40. Nowotny, M.; Yang, W. Stepwise Analyses of Metal Ions in RNase H Catalysis from Substrate Destabilization to Product Release. *EMBO Journal* **2006**, *25*, doi:10.1038/sj.emboj.7601076.
41. Nowotny, M.; Gaidamakov, S.A.; Crouch, R.J.; Yang, W. Crystal Structures of RNase H Bound to an RNA/DNA Hybrid: Substrate Specificity and Metal-Dependent Catalysis. *Cell* **2005**, *121*, doi:10.1016/j.cell.2005.04.024.
42. Wu, H.; Lima, W.F.; Crooke, S.T. Properties of Cloned and Expressed Human RNase H1. *Journal of Biological Chemistry* **1999**, *274*, 28270–28278, doi:10.1074/jbc.274.40.28270.
43. Østergaard, M.E.; Nichols, J.; Dwight, T.A.; Lima, W.; Jung, M.E.; Swayze, E.E.; Seth, P.P. Fluorinated Nucleotide Modifications Modulate Allele Selectivity of SNP-Targeting Antisense Oligonucleotides. *Mol Ther Nucleic Acids* **2017**, *7*, doi:10.1016/j.omtn.2017.02.001.
44. Lima, W.F.; Wu, H.; Nichols, J.G.; Prakash, T.P.; Ravikumar, V.; Crooke, S.T. Human RNase H1 Uses One Tryptophan and Two Lysines to Position the Enzyme at the 3′-DNA/5′-RNA Terminus of the Heteroduplex Substrate. *Journal of Biological Chemistry* **2003**, *278*, doi:10.1074/jbc.M306543200.
45. Stein, C.A.; Cohen, J.S. Oligodeoxynucleotides as Inhibitors of Gene Expression: A Review. *Cancer Res* **1988**, *48*.
46. Furdon, P.J.; Dominski, Z.; Kole, R. RNase H Cleavage of RNA Hybridized to Oligonucleotides Containing Methylphosphonate, Phosphorothioate and Phosphodiester Bonds. *Nucleic Acids Res* **1989**, *17*, doi:10.1093/nar/17.22.9193.
47. Brad Wan, W.; Seth, P.P. The Medicinal Chemistry of Therapeutic Oligonucleotides. *J Med Chem* 2016, *59*.
48. Khvorova, A.; Watts, J.K. The Chemical Evolution of Oligonucleotide Therapies of Clinical Utility. *Nat Biotechnol* 2017, *35*.
49. Xiong, H.; Veedu, R.N.; Diermeier, S.D. Recent Advances in Oligonucleotide Therapeutics in Oncology. *Int J Mol Sci* **2021**, *22*, 3295, doi:10.3390/ijms22073295.
50. Stein, C.A.; Subasinghe, C.; Shinozuka, K.; Cohen, J.S. Physicochemical Properties of Phospborothioate Oligodeoxynucleotides. *Nucleic Acids Res* **1988**, *16*, doi:10.1093/nar/16.8.3209.
51. Brown, D.A.; Kang, S.H.; Gryaznov, S.M.; DeDionisio, L.; Heidenreich, O.; Sullivan, S.; Xu, X.; Nerenberg, M.I. Effect of Phosphorothioate Modification of Oligodeoxynucleotides on Specific Protein Binding. *Journal of Biological Chemistry* **1994**, *269*, 26801–26805, doi:https://doi.org/10.1016/S0021-9258(18)47090-1.
52. Yu, D.; Iyer, R.P.; Shaw, D.R.; Lisziewicz, J.; Li, Y.; Jiang, Z.; Roskey, A.; Agrawal, S. Hybrid Oligonucleotides: Synthesis, Biophysical Properties, Stability Studies, and Biological Activity. *Bioorg Med Chem* **1996**, *4*, doi:10.1016/0968-0896(96)00160-5.
53. Rettig, G.R.; Behlke, M.A. Progress toward in Vivo Use of SiRNAs-II. *Molecular Therapy* 2012, *20*.
54. Shaw, D.R.; Rustagi, P.K.; Kandimalla, E.R.; Manning, A.N.; Jiang, Z.; Agrawal, S. Effects of Synthetic Oligonucleotides on Human Complement and Coagulation. *Biochem Pharmacol* **1997**, *53*, doi:10.1016/S0006-2952(97)00091-9.
55. Altmann, K.H.; Bévierre, M.O.; De Mesmaeker, A.; Moser, H.E. The Evaluation of 2′- and 6′-Substituted Carbocyclic Nucleosides as Building Blocks for Antisense Oligonucleotides. *Bioorg Med Chem Lett* **1995**, *5*, doi:10.1016/0960-894X(95)00050-4.
56. Teplova, M.; Minasov, G.; Tereshko, V.; Inamati, G.B.; Cook, P.D.; Manoharan, M.; Egli, M. Crystal Structure and Improved Antisense Properties of 2′-O-(2- Methoxyethyl)-RNA. *Nat Struct Biol* **1999**, *6*, doi:10.1038/9304.

57. Pallan, P.S.; Ittig, D.; Héroux, A.; Wawrzak, Z.; Leumann, C.J.; Egli, M. Crystal Structure of Tricyclo-DNA: An Unusual Compensatory Change of Two Adjacent Backbone Torsion Angles. *Chemical Communications* **2008**, doi:10.1039/b716390h.
58. Gao, W.Y.; Han, F.S.; Storm, C.; Egan, W.; Cheng, Y.C. Phosphorothioate Oligonucleotides Are Inhibitors of Human DNA Polymerases and RNase H: Implications for Antisense Technology. *Mol Pharmacol* **1992**, *41*.
59. Murray, S.; Ittig, D.; Koller, E.; Berdeja, A.; Chappell, A.; Prakash, T.P.; Norrbom, M.; Swayze, E.E.; Leumann, C.J.; Seth, P.P. TricycloDNA-Modified Oligo-2′-Deoxyribonucleotides Reduce Scavenger Receptor B1 MRNA in Hepatic and Extra-Hepatic Tissues-a Comparative Study of Oligonucleotide Length, Design and Chemistry. *Nucleic Acids Res* **2012**, *40*, doi:10.1093/nar/gks273.
60. Kool, E.T. Preorganization of DNA: Design Principles for Improving Nucleic Acid Recognition by Synthetic Oligonucleotides. *Chem Rev* **1997**, *97*, doi:10.1021/cr9603791.
61. Veedu, R.N.; Wengel, J. Locked Nucleic Acids: Promising Nucleic Acid Analogs for Therapeutic Applications. *Chem Biodivers* 2010, *7*.
62. Watts, J.K. Locked Nucleic Acid: Tighter Is Different. *Chemical Communications* **2013**, *49*, doi:10.1039/c3cc40340h.
63. Koch, T. LNA Antisense: A Review. *Curr Phys Chem* **2013**, *3*, doi:10.2174/1877946811303010009.
64. Wengel, J.; Petersen, M.; Nielsen, K.E.; Jensen, G.A.; Håkansson, A.E.; Kumar, R.; Sørensen, M.D.; Rajwanshi, V.K.; Bryld, T.; Jacobsen, J.P. LNA (Locked Nucleic Acid) and the Diastereoisomeric α-L-LNA: Conformational Tuning and High-Affinity Recognition of DNA/RNA Targets. *Nucleosides Nucleotides Nucleic Acids* **2001**, *20*, doi:10.1081/NCN-100002312.
65. Vester, B.; Wengel, J. LNA (Locked Nucleic Acid): High-Affinity Targeting of Complementary RNA and DNA. *Biochemistry* **2004**, *43*, doi:10.1021/bi0485732.
66. Singh, S.K.; Nielsen, P.; Koshkin, A.A.; Wengel, J. LNA (Locked Nucleic Acids): Synthesis and High-Affinity Nucleic Acid Recognition. *Chemical Communications* **1998**, doi:10.1039/a708608c.
67. Koshkin, A.A.; Singh, S.K.; Nielsen, P.; Rajwanshi, V.K.; Kumar, R.; Meldgaard, M.; Olsen, C.E.; Wengel, J. LNA (Locked Nucleic Acids): Synthesis of the Adenine, Cytosine, Guanine, 5-Methylcytosine, Thymine and Uracil Bicyclonucleoside Monomers, Oligomerisation, and Unprecedented Nucleic Acid Recognition. *Tetrahedron* **1998**, *54*, doi:10.1016/S0040-4020(98)00094-5.
68. Straarup, E.M.; Fisker, N.; Hedtjärn, M.; Lindholm, M.W.; Rosenbohm, C.; Aarup, V.; Hansen, H.F.; Ørum, H.; Hansen, J.B.R.; Koch, T. Short Locked Nucleic Acid Antisense Oligonucleotides Potently Reduce Apolipoprotein B MRNA and Serum Cholesterol in Mice and Non-Human Primates. *Nucleic Acids Res* **2010**, *38*, 7100–7111, doi:10.1093/nar/gkq457.
69. Seth, P.P.; Siwkowski, A.; Allerson, C.R.; Vasquez, G.; Lee, S.; Prakash, T.P.; Wancewicz, E. V.; Witchell, D.; Swayze, E.E. Short Antisense Oligonucleotides with Novel 2′-4′ Conformationaly Restricted Nucleoside Analogues Show Improved Potency without Increased Toxicity in Animals. *J Med Chem* **2009**, *52*, doi:10.1021/jm801294h.
70. Østergaard, M.E.; Southwell, A.L.; Kordasiewicz, H.; Watt, A.T.; Skotte, N.H.; Doty, C.N.; Vaid, K.; Villanueva, E.B.; Swayze, E.E.; Bennett, C.F.; et al. Rational Design of Antisense Oligonucleotides Targeting Single Nucleotide Polymorphisms for Potent and Allele Selective Suppression of Mutant Huntingtin in the CNS. *Nucleic Acids Res* **2013**, *41*, doi:10.1093/nar/gkt725.
71. Southwell, A.L.; Skotte, N.H.; Kordasiewicz, H.B.; Østergaard, M.E.; Watt, A.T.; Carroll, J.B.; Doty, C.N.; Villanueva, E.B.; Petoukhov, E.; Vaid, K.; et al. In Vivo Evaluation of Candidate Allele-Specific Mutant Huntingtin Gene Silencing Antisense Oligonucleotides. *Molecular Therapy* **2014**, *22*, doi:10.1038/mt.2014.153.
72. Østergaard, M.E.; Kumar, P.; Nichols, J.; Watt, A.; Sharma, P.K.; Nielsen, P.; Seth, P.P. Allele-Selective Inhibition of Mutant Huntingtin with 2-Thio- and C5- Triazolylphenyl-Deoxythymidine-Modified Antisense Oligonucleotides. *Nucleic Acid Ther* **2015**, *25*, doi:10.1089/nat.2015.0547.
73. Kitson, J.D.A.; Kamola, P.J.; Kane, L. Hybridization-Dependent Effects. In *Oligonucleotide-Based Drugs and Therapeutics*; 2018.
74. Crooke, S.T.; Lemonidis, K.M.; Neilson, L.; Griffey, R.; Lesnik, E.A.; Monia, B.P. Kinetic Characteristics of Escherichia Coli RNase H1: Cleavage of Various Antisense Oligonucleotide-RNA Duplexes. *Biochemical Journal* **1995**, *312*, doi:10.1042/bj3120599.
75. Gao, W.; Stein, C.A.; Cohen, J.S.; Dutschman, G.E.; Cheng, Y. Effect of Phosphorothioate Homo-Oligodeoxynucleotides on Herpes Simplex Virus Type 2-Induced DNA Polymerase. *Journal of Biological Chemistry* **1989**, *264*, doi:10.1016/s0021-9258(18)60494-6.
76. Levin, A.A. A Review of Issues in the Pharmacokinetics and Toxicology of Phosphorothioate Antisense Oligonucleotides. **1999**, *1489*, 69–84.
77. Wengel, J. Synthesis of 3′-C- and 4′-C-Branched Oligodeoxynucleotides and the Development of Locked Nucleic Acid (LNA). *Acc Chem Res* **1999**, *32*, doi:10.1021/ar980051p.

78. Swayze, E.E.; Siwkowski, A.M.; Wancewicz, E. V.; Migawa, M.T.; Wyrzykiewicz, T.K.; Hung, G.; Monia, B.P.; Bennett, C.F. Antisense Oligonucleotides Containing Locked Nucleic Acid Improve Potency but Cause Significant Hepatotoxicity in Animals. *Nucleic Acids Res* **2007**, *35*, doi:10.1093/nar/gkl1071.
79. Stanton, R.; Sciabola, S.; Salatto, C.; Weng, Y.; Moshinsky, D.; Little, J.; Walters, E.; Kreeger, J.; Dimattia, D.; Chen, T.; et al. Chemical Modification Study of Antisense Gapmers. *Nucleic Acid Ther* **2012**, *22*, doi:10.1089/nat.2012.0366.
80. Lightfoot, H.; Schneider, A.; Hall, J. Pharmacokinetics and Pharmacodynamics of Antisense Oligonucleotides. In *Oligonucleotide-Based Drugs and Therapeutics*; Ferrari, N, Seguin, R., Ed.; John Wiley & Sons, Inc.: New Jersey, 2018; pp. 107–136 ISBN 9781119070290.
81. Juliano, R.L.; Ming, X.; Nakagawa, O. The Chemistry and Biology of Oligonucleotide Conjugates. *Acc Chem Res* **2012**, *45*, doi:10.1021/ar2002123.
82. Letsinger, R.L.; Zhang, G.; Sun, D.K.; Ikeuchi, T.; Sarin, P.S. Cholesteryl-Conjugated Oligonucleotides: Synthesis, Properties, and Activity as Inhibitors of Replication of Human Immunodeficiency Virus in Cell Culture. *Proc Natl Acad Sci U S A* **1989**, *86*, doi:10.1073/pnas.86.17.6553.
83. Shen, G.; Fang, H.; Song, Y.; Bielska, A.A.; Wang, Z.; Taylor, J.S.A. Phospholipid Conjugate for Intracellular Delivery of Peptide Nucleic Acids. *Bioconjug Chem* **2009**, *20*, doi:10.1021/bc900048y.
84. Lemaitre, M.; Bayard, B.; Lebleu, B. Specific Antiviral Activity of a Poly(L-Lysine)-Conjugated Oligodeoxyribonucleotide Sequence Complementary to Vesicular Stomatitis Virus N Protein MRNA Initiation Site. *Proc Natl Acad Sci U S A* **1987**, *84*, doi:10.1073/pnas.84.3.648.
85. Zhang, K.; Hao, L.; Hurst, S.J.; Mirkin, C.A. Antibody-Linked Spherical Nucleic Acids for Cellular Targeting. *J Am Chem Soc* **2012**, *134*, doi:10.1021/ja306854d.
86. Sun, C.; Ridderstråle, K.; Höglund, A.S.; Larsson, L.G.; Jansson, C. Sweet Delivery - Sugar Translocators as Ports of Entry for Antisense Oligodeoxynucleotides in Plant Cells. *Plant Journal* **2007**, *52*, doi:10.1111/j.1365-313X.2007.03287.x.
87. Falzarano, M.S.; Passarelli, C.; Ferlini, A. Nanoparticle Delivery of Antisense Oligonucleotides and Their Application in the Exon Skipping Strategy for Duchenne Muscular Dystrophy. *Nucleic Acid Ther* 2014, *24*.
88. Prakash, T.P.; Graham, M.J.; Yu, J.; Carty, R.; Low, A.; Chappell, A.; Schmidt, K.; Zhao, C.; Aghajan, M.; Murray, H.F.; et al. Targeted Delivery of Antisense Oligonucleotides to Hepatocytes Using Triantennary N-Acetyl Galactosamine Improves Potency 10-Fold in Mice. *Nucleic Acids Res* **2014**, *42*, doi:10.1093/nar/gku531.
89. Nair, J.K.; Willoughby, J.L.S.; Chan, A.; Charisse, K.; Alam, M.R.; Wang, Q.; Hoekstra, M.; Kandasamy, P.; Kelin, A. V.; Milstein, S.; et al. Multivalent N -Acetylgalactosamine-Conjugated SiRNA Localizes in Hepatocytes and Elicits Robust RNAi-Mediated Gene Silencing. *J Am Chem Soc* **2014**, *136*, doi:10.1021/ja505986a.
90. Dirin, M.; Winkler, J. Tissue Distribution, Metabolism, and Clearance. In *Oligonucleotide-Based Drugs and Therapeutics*; Ferrari, N, Seguin, R., Ed.; John Wiley & Sons, Inc.: New Jersey, 2018; pp. 137–151 ISBN 9781119070290.
91. Wang, H.; Cai, Q.; Zeng, X.; Yu, D.; Agrawal, S.; Zhang, R. Antitumor Activity and Pharmacokinetics of a Mixed-Backbone Antisense Oligonucleotide Targeted to the RIα Subunit of Protein Kinase A after Oral Administration. *Proc Natl Acad Sci U S A* **1999**, *96*, doi:10.1073/pnas.96.24.13989.
92. Dowdy, S.F. Overcoming Cellular Barriers for RNA Therapeutics. *Nat Biotechnol* 2017, *35*.
93. de Smet, M.D.; Meenken, C.; Van Den Horn, G.J. Fomivirsen – a Phosphorothioate Oligonucleotide for the Treatment of CMV Retinitis. *Ocul Immunol Inflamm* **1999**, *7*, doi:10.1076/ocii.7.3.189.4007.
94. Miller, T.M.; Pestronk, A.; David, W.; Rothstein, J.; Simpson, E.; Appel, S.H.; Andres, P.L.; Mahoney, K.; Allred, P.; Alexander, K.; et al. An Antisense Oligonucleotide against SOD1 Delivered Intrathecally for Patients with SOD1 Familial Amyotrophic Lateral Sclerosis: A Phase 1, Randomised, First-in-Man Study. *Lancet Neurol* **2013**, *12*, doi:10.1016/S1474-4422(13)70061-9.
95. Bogdahn, U.; Stockhammer, G.; Mahapatra, A.K.; Venkataramana, N.K.; Oliushine, V.E.; Parfenov, V.E.; Poverennova, I.E.; Hau, P.; Jachimczak, P.; Heinrichs, H.; et al. Phase III Sapphire Study in High-Grade Gliomas: Targeted Therapy with TGF-Beta2 Inhibitor Trabedersen Based on Results of a Randomized Phase IIB Study. *Neuro Oncol* **2010**, *12*.
96. Imaoka, H.; Campbell, H.; Babirad, I.; Watson, R.M.; Mistry, M.; Sehmi, R.; Gauvreau, G.M. TPI ASM8 Reduces Eosinophil Progenitors in Sputum after Allergen Challenge. *Clinical and Experimental Allergy* **2011**, *41*, doi:10.1111/j.1365-2222.2011.03816.x.
97. Goemans, N.M.; Tulinius, M.; van den Akker, J.T.; Burm, B.E.; Ekhart, P.F.; Heuvelmans, N.; Holling, T.; Janson, A.A.; Platenburg, G.J.; Sipkens, J.A.; et al. Systemic Administration of PRO051 in Duchenne's Muscular Dystrophy.[Erratum Appears in N Engl J Med. 2011 Oct 6;365(14):1361]. *New England Journal of Medicine* **2011**, *364*.
98. Fey, R.A.; Templin, M. V.; McDonald, J.D.; Yu, R.Z.; Hutt, J.A.; Gigliotti, A.P.; Henry, S.P.; Reed, M.D. Local and Systemic Tolerability of a 2'O-Methoxyethyl Antisense Oligonucleotide Targeting Interleukin-4 Receptor-α Delivery by Inhalation in Mouse and Monkey. *Inhal Toxicol* **2014**, *26*, doi:10.3109/08958378.2014.907587.

99. Jackson, S.; Candia, A.F.; Delaney, S.; Floettmann, S.; Wong, C.; Campbell, J.D.; Kell, S.; Lum, J.; Hessel, E.M.; Traquina, P.; et al. First-in-Human Study With the Inhaled TLR9 Oligonucleotide Agonist AZD1419 Results in Interferon Responses in the Lung, and Is Safe and Well-Tolerated. *Clin Pharmacol Ther* **2018**, *104*, doi:10.1002/cpt.938.
100. Querbes, W.; Ge, P.; Zhang, W.; Fan, Y.; Costigan, J.; Charisse, K.; Maier, M.; Nechev, L.; Manoharan, M.; Kotelianski, V.; et al. Direct CNS Delivery of SiRNA Mediates Robust Silencing in Oligodendrocytes. *Oligonucleotides* **2009**, *19*, doi:10.1089/oli.2008.0165.
101. Khorkova, O.; Wahlestedt, C. Oligonucleotide Therapies for Disorders of the Nervous System. *Nat Biotechnol* **2017**, *35*, doi:10.1038/nbt.3784.
102. Solano, E.C.R.; Kornbrust, D.J.; Beaudry, A.; Foy, J.W.D.; Schneider, D.J.; Thompson, J.D. Toxicological and Pharmacokinetic Properties of QPI-1007, a Chemically Modified Synthetic SiRNA Targeting Caspase 2 MRNA, Following Intravitreal Injection. *Nucleic Acid Ther* **2014**, *24*, doi:10.1089/nat.2014.0489.
103. Leeds, J.M.; Henry, S.P.; Bistner, S.; Scherrill, S.; Williams, K.; Levin, A.A. Pharmacokinetics of an Antisense Oligonucleotide Injected Intravitreally in Monkeys. *Drug Metabolism and Disposition* **1998**, *26*.
104. Henry, S.P.; Danis, R.P. Potential Therapeutic Application of Antisense Oligonucleotides in the Treatment of Ocular Diseases. *Expert Opin Pharmacother* 2001, *2*.
105. Henry, S.P.; Miner, R.C.; Drew, W.L.; Fitchett, J.; York-Defalco, C.; Rapp, L.M.; Levin, A.A. Antiviral Activity and Ocular Kinetics of Antisense Oligonucleotides Designed to Inhibit CMV Replication. *Invest Ophthalmol Vis Sci* **2001**, *42*.
106. Leeds, J.M.; Henry, S.P.; Truong, L.; Zutshi, A.; Levin, A.A.; Kornbrust, D. Pharmacokinetics of a Potential Human Cytomegalovirus Therapeutic, a Phosphorothioate Oligonucleotide, after Intravitreal Injection in the Rabbit. *Drug Metabolism and Disposition* **1997**, *25*.
107. Kastelein, J.J.P.; Wedel, M.K.; Baker, B.F.; Su, J.; Bradley, J.D.; Yu, R.Z.; Chuang, E.; Graham, M.J.; Crooke, R.M. Potent Reduction of Apolipoprotein B and Low-Density Lipoprotein Cholesterol by Short-Term Administration of an Antisense Inhibitor of Apolipoprotein B. *Circulation* **2006**, *114*, doi:10.1161/CIRCULATIONAHA.105.606442.
108. Yu, R.Z.; Baker, B.; Chappell, A.; Geary, R.S.; Cheung, E.; Levin, A.A. Development of an Ultrasensitive Noncompetitive Hybridization-Ligation Enzyme-Linked Immunosorbent Assay for the Determination of Phosphorothioate Oligodeoxynucleotide in Plasma. *Anal Biochem* **2002**, *304*, doi:10.1006/abio.2002.5576.
109. Crooke, S.T.; Geary, R.S. Clinical Pharmacological Properties of Mipomersen (Kynamro), a Second Generation Antisense Inhibitor of Apolipoprotein B. *Br J Clin Pharmacol* **2013**, *76*, 269–276, doi:10.1111/j.1365-2125.2012.04469.x.
110. Sewell, K.L.; Geary, R.S.; Baker, B.F.; Glover, J.M.; Mant, T.G.K.; Yu, R.Z.; Tami, J.A.; Dorr, F.A. Phase I Trial of ISIS 104838, a 2′-Methoxyethyl Modified Antisense Oligonucleotide Targeting Tumor Necrosis Factor-α. *Journal of Pharmacology and Experimental Therapeutics* **2002**, *303*, doi:10.1124/jpet.102.036749.
111. Geary, R.S.; Yu, R.Z.; Watanabe, T.; Henry, S.P.; Hardee, G.E.; Chappell, A.; Matson, J.; Sasmor, H.; Cummins, L.; Levin, A.A. Pharmacokinetics of a Tumor Necrosis Factor-α Phosphorothioate 2′-O-(2-Methoxyethyl) Modified Antisense Oligonucleotide: Comparison across Species. *Drug Metabolism and Disposition* **2003**, *31*, 1419–1428, doi:10.1124/dmd.31.11.1419.
112. Talbot, D.C.; Ranson, M.; Davies, J.; Lahn, M.; Callies, S.; André, V.; Kadam, S.; Burgess, M.; Slapak, C.; Olsen, A.L.; et al. Tumor Survivin Is Downregulated by the Antisense Oligonucleotide LY2181308: A Proof-of-Concept, First-in-Human Dose Study. *Clinical Cancer Research* **2010**, *16*, doi:10.1158/1078-0432.CCR-10-1932.
113. Lundin, K.E.; Hansen, B.R.; Persson, R.; Bramsen, J.B.; Koch, T.; Wengel, J.; Smith, C.I.E. Biological Activity and Biotechnological Aspects of Locked Nucleic Acids. *Adv Genet* **2013**, *82*, 47–107, doi:10.1016/B978-0-12-407676-1.00002-0.
114. Leeds, J.M.; Henry, S.P.; Geary, R.; Burckin, T.; Levin, A.A. Comparison of the Pharmacokinetics of Subcutaneous and Intravenous Administration of a Phosphorothioate Oligodeoxynucleotide in Cynomolgus Monkeys. *Antisense Nucleic Acid Drug Dev* **2000**, *10*, doi:10.1089/oli.1.2000.10.435.
115. Lanford, R.E.; Hildebrandt-Eriksen, E.S.; Petri, A.; Persson, R.; Lindow, M.; Munk, M.E.; Kauppinen, S.; Rum, H. Therapeutic Silencing of MicroRNA-122 in Primates with Chronic Hepatitis C Virus Infection. *Science (1979)* **2010**, *327*, 198–201, doi:10.1126/science.1178178.
116. Geary, R.S.; Watanabe, T.A.; Truong, L.; Freier, S.; Lesnik, E.A.; Sioufi, N.B.; Sasmor, H.; Manoharan, M.; Levin, A.A. Pharmacokinetic Properties of 2′-O-(2-Methoxyethyl)-Modified Oligonucleotide Analogs in Rats. *Journal of Pharmacology and Experimental Therapeutics* **2001**, *296*, 890–897.
117. Dirin, M.; Winkler, J. Influence of Diverse Chemical Modifications on the ADME Characteristics and Toxicology of Antisense Oligonucleotides. *Expert Opin Biol Ther* 2013, *13*.
118. Hagedorn, P.H.; Persson, R.; Funder, E.D.; Albæk, N.; Diemer, S.L.; Hansen, D.J.; Møller, M.R.; Papargyri, N.; Christiansen, H.; Hansen, B.R.; et al. Locked Nucleic Acid: Modality, Diversity, and Drug Discovery. *Drug Discov Today* **2018**, *23*, 101–114, doi:10.1016/j.drudis.2017.09.018.

119. Vickers, T.A.; Crooke, S.T. Development of a Quantitative BRET Affinity Assay for Nucleic Acid-Protein Interactions. *PLoS One* **2016**, *11*, doi:10.1371/journal.pone.0161930.
120. Agrawal, S. Antisense Oligonucleotides: Towards Clinical Trials. *Trends Biotechnol* 1996, *14*.
121. Wang, L.; Prakash, R.K.; Stein, C.A.; Koehn, R.K.; Ruffner, D.E. Progress in the Delivery of Therapeutic Oligonucleotides: Organ/Cellular Distribution and Targeted Delivery of Oligonucleotides in Vivo. *Antisense Nucleic Acid Drug Dev* 2003, *13*.
122. Geary, R.S. Antisense Oligonucleotide Pharmacokinetics and Metabolism. *Expert Opin Drug Metab Toxicol* **2009**, *5*, 381–391, doi:10.1517/17425250902877680.
123. Levin, A.A.; Yu, R.Z.; Geary, R.S. Basic Principles of the Pharmacokinetics of Antisense Oligonucleotide Drugs. In *Antisense Drug Technology: Principles, Strategies, and Applications, Second Edition*; Crooke, S.T., Ed.; CRC Press: USA, 2007; pp. 183–216 ISBN 9780849387968.
124. Watanabe, T.A.; Geary, R.S.; Levin, A.A. Plasma Protein Binding of an Antisense Oligonucleotide Targeting Human ICAM-1 (ISIS 2302). *Oligonucleotides* **2006**, *16*, 169–180, doi:10.1089/oli.2006.16.169.
125. Shemesh, C.S.; Yu, R.Z.; Gaus, H.J.; Seth, P.P.; Swayze, E.E.; Bennett, F.C.; Geary, R.S.; Henry, S.P.; Wang, Y. Pharmacokinetic and Pharmacodynamic Investigations of ION-353382, a Model Antisense Oligonucleotide: Using Alpha-2-Macroglobulin and Murinoglobulin Double-Knockout Mice. *Nucleic Acid Ther* **2016**, *26*, doi:10.1089/nat.2016.0607.
126. Meibohm, B. *Pharmacokinetics and Pharmacodynamics of Biotech Drugs: Principles and Case Studies in Drug Development*; 2006;
127. Wartlick, H.; Spänkuch-Schmitt, B.; Strebhardt, K.; Kreuter, J.; Langer, K. Tumour Cell Delivery of Antisense Oligonuclceotides by Human Serum Albumin Nanoparticles. *Journal of Controlled Release* **2004**, *96*, 483–495, doi:10.1016/j.jconrel.2004.01.029.
128. Srinivasan, S.K.; Tewary, H.K.; Iversen, P.L. Characterization of Binding Sites, Extent of Binding, and Drug Interactions of Oligonucleotides with Albumin. *Antisense Res Dev* **1995**, *5*, 131–139, doi:10.1089/ard.1995.5.131.
129. Geary, R.S.; Yu, R.Z.; Levin, A.A. Pharmacokinetics of Phosphorothioate Antisense Oligodeoxynucleotides. *Current Opinion in Investigational Drugs* 2001, *2*.
130. Miller, C.M.; Donner, A.J.; Blank, E.E.; Egger, A.W.; Kellar, B.M.; Østergaard, M.E.; Seth, P.P.; Harris, E.N. Stabilin-1 and Stabilin-2 Are Specific Receptors for the Cellular Internalization of Phosphorothioate-Modified Antisense Oligonucleotides (ASOs) in the Liver. *Nucleic Acids Res* **2016**, *44*, 2782–2794, doi:10.1093/nar/gkw112.
131. Freier, S.M.; Altmann, K.H. The Ups and Downs of Nucleic Acid Duplex Stability: Structure-Stability Studies on Chemically-Modified DNA:RNA Duplexes. *Nucleic Acids Res* **1997**, *25*, doi:10.1093/nar/25.22.4429.
132. Eckstein, F. Phosphorothioate Oligodeoxynucleotides: What Is Their Origin and What Is Unique about Them? *Antisense Nucleic Acid Drug Dev* 2000, *10*.
133. Yu, R.Z.; Kim, T.W.; Hong, A.; Watanabe, T.A.; Gaus, H.J.; Geary, R.S. Cross-Species Pharmacokinetic Comparison from Mouse to Man of a Second-Generation Antisense Oligonucleotide, ISIS 301012, Targeting Human Apolipoprotein B-100. *Drug Metabolism and Disposition* **2007**, *35*, 460–468, doi:10.1124/dmd.106.012401.
134. Fluiter, K.; ten Asbroek, A.L.M.A.; de Wissel, M.B.; Jakobs, M.E.; Wissenbach, M.; Olsson, H.; Olsen, O.; Oerum, H.; Baas, F. In Vivo Tumor Growth Inhibition and Biodistribution Studies of Locked Nucleic Acid (LNA) Antisense Oligonucleotides. *Nucleic Acids Res* 2003, *31*.
135. Yu, R.Z.; Geary, R.S.; Monteith, D.K.; Matson, J.; Truong, L.; Fitchett, J.; Levin, A.A. Tissue Disposition of 2′-O-(2-Methoxy) Ethyl Modified Antisense Oligonucleotides in Monkeys. *J Pharm Sci* **2004**, *93*, doi:10.1002/jps.10473.
136. Dutta, S.; Karol, M.D.; Cohen, T.; Jones, R.M.; Mant, T. Comparison of Pharmacokinetics and Tissue Disposition of an Antisense Phosphorothioate Oligonucleotide Targeting Human Ha-Ras MRNA in Mouse and Monkey. *J Pharm Sci* **2001**, *90*, doi:10.1002/1520-6017(200102)90:2<182::AID-JPS9>3.0.CO;2-F.
137. Phillips, J.A.; Craig, S.J.; Bayley, D.; Christian, R.A.; Geary, R.; Nicklin, P.L. Pharmacokinetics, Metabolism, and Elimination of a 20-Mer Phosphorothioate Oligodeoxynucleotide (CGP 69846A) after Intravenous and Subcutaneous Administration. *Biochem Pharmacol* **1997**, *54*, doi:10.1016/S0006-2952(97)00190-1.
138. Crooke, S.T.; Graham, M.J.; Zuckerman, J.E.; Brooks, D.; Conklin, B.S.; Cummins, L.L.; Greig, M.J.; Guinosso, C.J.; Kornbrust, D.; Manoharan, M.; et al. Pharmacokinetic Properties of Several Novel Oligonucleotide Analogs in Mice. *Journal of Pharmacology and Experimental Therapeutics* **1996**, *277*.
139. Hildebrandt-Eriksen, E.S.; Aarup, V.; Persson, R.; Hansen, H.F.; Munk, M.E.; Ørum, H. A Locked Nucleic Acid Oligonucleotide Targeting MicroRNA 122 Is Well-Tolerated in Cynomolgus Monkeys. *Nucleic Acid Ther* **2012**, *22*, 152–161, doi:10.1089/nat.2011.0332.
140. Shen, L.; Engelhardt, J.A.; Hung, G.; Yee, J.; Kikkawa, R.; Matson, J.; Tayefeh, B.; Machemer, T.; Giclas, P.C.; Henry, S.P. Effects of Repeated Complement Activation Associated with Chronic Treatment of Cynomolgus Monkeys with 2′-O-Methoxyethyl Modified Antisense Oligonucleotide. *Nucleic Acid Ther* **2016**, *26*, 236–249, doi:10.1089/nat.2015.0584.

141. Zhang, R.; Iyer, R.P.; Yu, D.; Tan, W.; Zhang, X.; Lu, Z.; Zhao, H.; Agrawal, S. Pharmacokinetics and Tissue Disposition of a Chimeric Oligodeoxynucleoside Phosphorothioate in Rats after Intravenous Administration. *Journal of Pharmacology and Experimental Therapeutics* **1996**, *278*.
142. Zhang, R.; LU, Z.; Zhao, H.; Zhang, X.; Diasio, R.B.; Habus, I.; Jiang, Z.; Iyer, R.P.; Yu, D.; Agrawal, S. In Vivo Stability, Disposition and Metabolism of a "Hybrid" Oligonucleotide Phosphorothioate in Rats. *Biochem Pharmacol* **1995**, *50*, doi:10.1016/0006-2952(95)00159-W.
143. Raoof, A.A.; Chiu, P.; Ramtoola, Z.; Cumming, I.K.; Teng, C.; Weinbach, S.P.; Hardee, G.E.; Levin, A.A.; Geary, R.S. Oral Bioavailability and Multiple Dose Tolerability of an Antisense Oligonucleotide Tablet Formulated with Sodium Caprate. *J Pharm Sci* **2004**, *93*, doi:10.1002/jps.20051.
144. Geary, R.S.; Wancewicz, E.; Matson, J.; Pearce, M.; Siwkowski, A.; Swayze, E.; Bennett, F. Effect of Dose and Plasma Concentration on Liver Uptake and Pharmacologic Activity of a 2'-Methoxyethyl Modified Chimeric Antisense Oligonucleotide Targeting PTEN. *Biochem Pharmacol* **2009**, *78*, 284–291, doi:10.1016/j.bcp.2009.04.013.
145. Geary, R.S.; Norris, D.; Yu, R.; Bennett, C.F. Pharmacokinetics, Biodistribution and Cell Uptake of Antisense Oligonucleotides. *Adv Drug Deliv Rev* **2015**, *87*, 46–51, doi:10.1016/j.addr.2015.01.008.
146. Hung, G.; Xiao, X.; Peralta, R.; Bhattacharjee, G.; Murray, S.; Norris, D.; Guo, S.; Monia, B.P. Characterization of Target MRNA Reduction through in Situ RNA Hybridization in Multiple Organ Systems Following Systemic Antisense Treatment in Animals. *Nucleic Acid Ther* **2013**, *23*, doi:10.1089/nat.2013.0443.
147. Soucy, N. V.; Riley, J.P.; Templin, M. V.; Geary, R.; De Peyster, A.; Levin, A.A. Maternal and Fetal Distribution of a Phosphorothioate Oligonucleotide in Rats after Intravenous Infusion. *Birth Defects Res B Dev Reprod Toxicol* **2006**, *77*, doi:10.1002/bdrb.20067.
148. Henry, S.P.; Denny, K.H.; Templin, M. V.; Yu, R.Z.; Levin, A.A. Effects of an Antisense Oligonucleotide Inhibitor of Human ICAM-1 on Fetal Development in Rabbits. *Birth Defects Res B Dev Reprod Toxicol* **2004**, *71*, doi:10.1002/bdrb.20024.
149. Henry, S.P.; Denny, K.H.; Templin, M. V.; Yu, R.Z.; Levin, A.A. Effects of Human and Murine Antisense Oligonucleotide Inhibitors of ICAM-1 on Reproductive Performance, Fetal Development, and Post-Natal Development in Mice. *Birth Defects Res B Dev Reprod Toxicol* **2004**, *71*, doi:10.1002/bdrb.20023.
150. Heemskerk, H.; De Winter, C.; Van Kuik, P.; Heuvelmans, N.; Sabatelli, P.; Rimessi, P.; Braghetta, P.; Van Ommen, G.J.B.; De Kimpe, S.; Ferlini, A.; et al. Preclinical PK and PD Studies on 2'-O-Methyl-Phosphorothioate RNA Antisense Oligonucleotides in the Mdx Mouse Model. *Molecular Therapy* **2010**, *18*, doi:10.1038/mt.2010.72.
151. Zanardi, T.A.; Han, S.C.; Jeong, E.J.; Rime, S.; Yu, R.Z.; Chakravarty, K.; Henry, S.P. Pharmacodynamics and Subchronic Toxicity in Mice and Monkeys of ISIS 388626, a Second-Generation Antisense Oligonucleotide That Targets Human Sodium Glucose Cotransporter 2. *Journal of Pharmacology and Experimental Therapeutics* **2012**, *343*, doi:10.1124/jpet.112.197426.
152. Greenberger, L.M.; Horak, I.D.; Filpula, D.; Sapra, P.; Westergaard, M.; Frydenlund, H.F.; Albæk, C.; Schrøder, H.; Ørum, H. A RNA Antagonist of Hypoxia-Inducible Factor-1α, EZN-2968, Inhibits Tumor Cell Growth. *Mol Cancer Ther* **2008**, *7*, doi:10.1158/1535-7163.MCT-08-0510.
153. Corey, D.R. Chemical Modification: The Key to Clinical Application of RNA Interference? *Journal of Clinical Investigation* 2007, *117*.
154. Moulds, C.; Lewis, J.G.; Froehler, B.C.; Grant, D.; Huang, T.; Milligan, J.F.; Matteucci, M.D.; Wagner, R.W. Site and Mechanism of Antisense Inhibition by C-5 Propyne Oligonucleotides. *Biochemistry* **1995**, *34*, doi:10.1021/bi00015a015.
155. Laxton, C.; Brady, K.; Moschos, S.; Turnpenny, P.; Rawal, J.; Pryde, D.C.; Sidders, B.; Corbau, R.; Pickford, C.; Murray, E.J. Selection, Optimization, and Pharmacokinetic Properties of a Novel, Potent Antiviral Locked Nucleic Acid-Based Antisense Oligomer Targeting Hepatitis C Virus Internal Ribosome Entry Site. *Antimicrob Agents Chemother* **2011**, *55*, 3105–3114, doi:10.1128/AAC.00222-11.
156. Jason, T.L.H.; Koropatnick, J.; Berg, R.W. Toxicology of Antisense Therapeutics. *Toxicol Appl Pharmacol* 2004, *201*.
157. Butler, M.; Stecker, K.; Bennett, C.F. Cellular Distribution of Phosphorothioate Oligodeoxynucleotides in Normal Rodent Tissues. *Laboratory Investigation* **1997**, *77*.
158. Graham, M.J.; Crooke, S.T.; Monteith, D.K.; Cooper, S.R.; Lemonidis, K.M.; Stecker, K.I.M.K.; Martin, M.J.; Crooke, R.M. In Vivo Distribution and Metabolism of a Phosphorothioate Oligonucleotide within Rat Liver after Intravenous Administration. **1998**, *286*, 447–458.
159. Graham, M.J.; Crooke, S.T.; Lemonidis, K.M.; Gaus, H.J.; Templin, M. V.; Crooke, R.M. Hepatic Distribution of a Phosphorothioate Oligodeoxynucleotide within Rodents Following Intravenous Administration. *Biochem Pharmacol* **2001**, *62*, doi:10.1016/S0006-2952(01)00669-4.
160. Donner, A.J.; Wancewicz, E. V.; Murray, H.M.; Greenlee, S.; Post, N.; Bell, M.; Lima, W.F.; Swayze, E.E.; Seth, P.P. Co-Administration of an Excipient Oligonucleotide Helps Delineate Pathways of Productive and Nonproductive Uptake of Phosphorothioate Antisense Oligonucleotides in the Liver. *Nucleic Acid Ther* **2017**, *27*, doi:10.1089/nat.2017.0662.
161. Sehgal, A.; Vaishnaw, A.; Fitzgerald, K. Liver as a Target for Oligonucleotide Therapeutics. *J Hepatol* 2013, *59*.

162. Eckstein, F. Phosphorothioates, Essential Components of Therapeutic Oligonucleotides. *Nucleic Acid Ther* 2014, *24*.
163. Agrawal, S.; Tan, W.; Cai, Q.; Xie, X.; Zhang, R. In Vivo Pharmacokinetics of Phosphorothioate Oligonucleotides Containing Contiguous Guanosines. In Proceedings of the Antisense and Nucleic Acid Drug Development; 1997; Vol. 7.
164. Agrawal, S.; Iadarola, P.L.; Temsamani, J.; Zhao, Q.; Shaw, D.R. Effect of G-Rich Sequences on the Synthesis, Purification, Hybridization, Cell Uptake, and Hemolytic Activity of Oligonucleotides. *Bioorg Med Chem Lett* **1996**, *6*, doi:10.1016/0960-894X(96)00403-9.
165. Djavanbakht Samani, T.; Jolles, B.; Laigle, A. Best Minimally Modified Antisense Oligonucleotides According to Cell Nuclease Activity. *Antisense Nucleic Acid Drug Dev* **2001**, *11*, doi:10.1089/108729001300338654.
166. Merki, E.; Graham, M.J.; Mullick, A.E.; Miller, E.R.; Crooke, R.M.; Pitas, R.E.; Witztum, J.L.; Tsimikas, S. Antisense Oligonucleotide Directed to Human Apolipoprotein B-100 Reduces Lipoprotein(a) Levels and Oxidized Phospholipids on Human Apolipoprotein B-100 Particles in Lipoprotein(a) Transgenic Mice. *Circulation* **2008**, *118*, doi:10.1161/CIRCULATIONAHA.108.786822.
167. Crooke, R.M.; Graham, M.J.; Lemonidis, K.M.; Whipple, C.P.; Koo, S.; Perera, R.J. An Apolipoprotein B Antisense Oligonucleotide Lowers LDL Cholesterol in Hyperlipidemic Mice without Causing Hepatic Steatosis. *J Lipid Res* **2005**, *46*, doi:10.1194/jlr.M400492-JLR200.
168. Geary, R.S.; Baker, B.F.; Monia, B.P. CHAPTER 4: Antisense Technology: Liver Targeting and beyond for Drug Discovery. In *RSC Drug Discovery Series*; 2019; Vol. 2019-January.
169. Santos, R.D.; Raal, F.J.; Donovan, J.M.; Cromwell, W.C. Mipomersen Preferentially Reduces Small Low-Density Lipoprotein Particle Number in Patients with Hypercholesterolemia. *J Clin Lipidol* **2015**, *9*, doi:10.1016/j.jacl.2014.12.008.
170. Zhang, H.; Cook, J.; Nickel, J.; Yu, R.; Stecker, K.; Myers, K.; Dean, N.M. Reduction of Liver Fas Expression by an Antisense Oligonucleotide Protects Mice from Fulminant Hepatitis. *Nat Biotechnol* **2000**, *18*, doi:10.1038/78475.
171. Yu, R.Z.; Zhang, H.; Geary, R.S.; Graham, M.; Masarjian, L.; Lemonidis, K.; Crooke, R.; Dean, N.M.; Levin, A.A. Pharmacokinetics and Pharmacodynamics of an Antisense Phosphorothioate Oligonucleotide Targeting Fas MRNA in Mice. *Journal of Pharmacology and Experimental Therapeutics* **2001**, *296*.
172. Tanowitz, M.; Hettrick, L.; Revenko, A.; Kinberger, G.A.; Prakash, T.P.; Seth, P.P. Asialoglycoprotein Receptor 1 Mediates Productive Uptake of N-Acetylgalactosamine-Conjugated and Unconjugated Phosphorothioate Antisense Oligonucleotides into Liver Hepatocytes. *Nucleic Acids Res* **2017**, *45*, doi:10.1093/nar/gkx960.
173. Schmidt, K.; Prakash, T.P.; Donner, A.J.; Kinberger, G.A.; Gaus, H.J.; Low, A.; Østergaard, M.E.; Bell, M.; Swayze, E.E.; Seth, P.P. Characterizing the Effect of GalNAc and Phosphorothioate Backbone on Binding of Antisense Oligonucleotides to the Asialoglycoprotein Receptor. *Nucleic Acids Res* **2017**, *45*, doi:10.1093/nar/gkx060.
174. Prakash, T.P.; Yu, J.; Migawa, M.T.; Kinberger, G.A.; Wan, W.B.; Østergaard, M.E.; Carty, R.L.; Vasquez, G.; Low, A.; Chappell, A.; et al. Comprehensive Structure-Activity Relationship of Triantennary N-Acetylgalactosamine Conjugated Antisense Oligonucleotides for Targeted Delivery to Hepatocytes. *J Med Chem* **2016**, *59*, doi:10.1021/acs.jmedchem.5b01948.
175. Graham, M.J.; Lee, R.G.; Brandt, T.A.; Tai, L.-J.; Fu, W.; Peralta, R.; Yu, R.; Hurh, E.; Paz, E.; McEvoy, B.W.; et al. Cardiovascular and Metabolic Effects of ANGPTL3 Antisense Oligonucleotides . *New England Journal of Medicine* **2017**, *377*, doi:10.1056/nejmoa1701329.
176. Viney, N.J.; van Capelleveen, J.C.; Geary, R.S.; Xia, S.; Tami, J.A.; Yu, R.Z.; Marcovina, S.M.; Hughes, S.G.; Graham, M.J.; Crooke, R.M.; et al. Antisense Oligonucleotides Targeting Apolipoprotein(a) in People with Raised Lipoprotein(a): Two Randomised, Double-Blind, Placebo-Controlled, Dose-Ranging Trials. *The Lancet* **2016**, *388*, doi:10.1016/S0140-6736(16)31009-1.
177. MacLeod, A.R.; Crooke, S.T. RNA Therapeutics in Oncology: Advances, Challenges, and Future Directions. *J Clin Pharmacol* **2017**, *57*, doi:10.1002/jcph.957.
178. Jauvin, D.; Chrétien, J.; Pandey, S.K.; Martineau, L.; Revillod, L.; Bassez, G.; Lachon, A.; McLeod, A.R.; Gourdon, G.; Wheeler, T.M.; et al. Targeting DMPK with Antisense Oligonucleotide Improves Muscle Strength in Myotonic Dystrophy Type 1 Mice. *Mol Ther Nucleic Acids* **2017**, *7*, doi:10.1016/j.omtn.2017.05.007.
179. Koller, E.; Vincent, T.M.; Chappell, A.; De, S.; Manoharan, M.; Bennett, C.F. Mechanisms of Single-Stranded Phosphorothioate Modified Antisense Oligonucleotide Accumulation in Hepatocytes. *Nucleic Acids Res* **2011**, *39*, 4795–4807, doi:10.1093/nar/gkr089.
180. Frey, P.A.; Sammons, R.D. Bond Order and Charge Localization in Nucleoside Phosphorothioates. *Science (1979)* 1985, *228*.
181. Weidner, D.A.; Valdez, B.C.; Henning, D.; Greenberg, S.; Busch, H. Phosphorothioate Oligonucleotides Bind in a Non Sequence-Specific Manner to the Nucleolar Protein C23/Nucleolin. *FEBS Lett* **1995**, *366*, doi:10.1016/0014-5793(95)00517-D.
182. Crooke, S.T.; Wang, S.; Vickers, T.A.; Shen, W.; Liang, X.H. Cellular Uptake and Trafficking of Antisense Oligonucleotides. *Nat Biotechnol* 2017, *35*, 230–237.

183. Liang, X.H.; Sun, H.; Shen, W.; Crooke, S.T. Identification and Characterization of Intracellular Proteins That Bind Oligonucleotides with Phosphorothioate Linkages. *Nucleic Acids Res* **2015**, *43*, 2927–2945, doi:10.1093/nar/gkv143.
184. Wang, S.; Sun, H.; Tanowitz, M.; Liang, X.H.; Crooke, S.T. Intra-Endosomal Trafficking Mediated by Lysobisphosphatidic Acid Contributes to Intracellular Release of Phosphorothioate-Modified Antisense Oligonucleotides. *Nucleic Acids Res* **2017**, *45*, doi:10.1093/nar/gkx231.
185. Miller, C.M.; Wan, W.B.; Seth, P.P.; Harris, E.N. Endosomal Escape of Antisense Oligonucleotides Internalized by Stabilin Receptors Is Regulated by Rab5C and EEA1 during Endosomal Maturation. *Nucleic Acid Ther* **2018**, *28*, doi:10.1089/nat.2017.0694.
186. Wang, S.; Sun, H.; Tanowitz, M.; Liang, X.H.; Crooke, S.T. Annexin A2 Facilitates Endocytic Trafficking of Antisense Oligonucleotides. *Nucleic Acids Res* **2016**, *44*, doi:10.1093/nar/gkw595.
187. Bailey, J.K.; Shen, W.; Liang, X.H.; Crooke, S.T. Nucleic Acid Binding Proteins Affect the Subcellular Distribution of Phosphorothioate Antisense Oligonucleotides. *Nucleic Acids Res* **2017**, *45*, doi:10.1093/nar/gkx709.
188. Crooke, S.T.; Vickers, T.A.; Liang, X.H. Phosphorothioate Modified Oligonucleotide-Protein Interactions. *Nucleic Acids Res* **2021**, *48*, 5235–5253, doi:10.1093/NAR/GKAA299.
189. Shemesh, C.S.; Yu, R.Z.; Warren, M.S.; Liu, M.; Jahic, M.; Nichols, B.; Post, N.; Lin, S.; Norris, D.A.; Hurh, E.; et al. Assessment of the Drug Interaction Potential of Unconjugated and GalNAc3-Conjugated 2′-MOE-ASOs. *Mol Ther Nucleic Acids* **2017**, *9*, doi:10.1016/j.omtn.2017.08.012.
190. Yu, R.Z.; Gunawan, R.; Post, N.; Zanardi, T.; Hall, S.; Burkey, J.; Kim, T.W.; Graham, M.J.; Prakash, T.P.; Seth, P.P.; et al. Disposition and Pharmacokinetics of a GalNAc3-Conjugated Antisense Oligonucleotide Targeting Human Lipoprotein (a) in Monkeys. *Nucleic Acid Ther* **2016**, *26*, doi:10.1089/nat.2016.0623.
191. Yu, R.Z.; Geary, R.S.; Flaim, J.D.; Riley, G.C.; Tribble, D.L.; VanVliet, A.A.; Wedel, M.K. Lack of Pharmacokinetic Interaction of Mipomersen Sodium (ISIS 301012), a 2′-O-Methoxyethyl Modified Antisense Oligonucleotide Targeting Apolipoprotein B-100 Messenger RNA, with Simvastatin and Ezetimibe. *Clin Pharmacokinet* **2009**, *48*, 39–50, doi:10.2165/0003088-200948010-00003.
192. Geary, R.S.; Bradley, J.A.D.; Watanabe, T.; Kwon, Y.; Wedel, M.; Van Lier, J.J.; VanVliet, A.A. Lack of Pharmacokinetic Interaction for ISIS 113715, a 2′-0- Methoxyethyl Modified Antisense Oligonucleotide Targeting Protein Tyrosine Phosphatase 1B Messenger RNA, with Oral Antidiabetic Compounds Metformin, Glipizide or Rosiglitazone. *Clin Pharmacokinet* **2006**, *45*, doi:10.2165/00003088-200645080-00003.
193. Geary, R.S.; Henry, S.P.; Grillone, L.R. Fomivirsen: Clinical Pharmacology and Potential Drug Interactions. *Clin Pharmacokinet* 2002, *41*.
194. Laskin, J.J.; Nicholas, G.; Lee, C.; Gitlitz, B.; Vincent, M.; Cormier, Y.; Stephenson, J.; Ung, Y.; Sanborn, R.; Pressnail, B.; et al. Phase I/II Trial of Custirsen (OGX-011), an Inhibitor of Clusterin, in Combination with a Gemcitabine and Platinum Regimen in Patients with Previously Untreated Advanced Non-Small Cell Lung Cancer. *Journal of Thoracic Oncology* **2012**, *7*, doi:10.1097/JTO.0b013e31823f459c.
195. Griffey, R.H.; Greig, M.J.; Gaus, H.J.; Liu, K.; Monteith, D.; Winniman, M.; Cummins, L.L. Characterization of Oligonucleotide Metabolism in Vivo via Liquid Chromatography/Electrospray Tandem Mass Spectrometry with a Quadrupole Ion Trap Mass Spectrometer. *Journal of Mass Spectrometry* **1997**, *32*, 305–313, doi:10.1002/(SICI)1096-9888(199703)32:3<305::AID-JMS482>3.0.CO;2-R.
196. Yang, W. Nucleases: Diversity of Structure, Function and Mechanism. *Q Rev Biophys* **2011**, *44*, 1–93, doi:10.1017/S0033583510000181.
197. Crooke, R.M.; Graham, M.J.; Martin, M.J.; Lemonidis, K.M.; Wyrzykiewiecz, T.A.D.; Cummins, L.L. Metabolism of Antisense Oligonucleotides in Rat Liver Homogenates. *J Pharmacol Exp Ther* **2000**, *292*, 140–149.
198. Gilar, M.; Belenky, A.; Smisek, D.L.; Bourque, A.; Cohen, A.S. Kinetics of Phosphorothioate Oligonucleotide Metabolism in Biological Fluids. *Nucleic Acids Res* **1997**, *25*, 3615–3620, doi:10.1093/nar/25.18.3615.
199. Baek, M.S.; Yu, R.Z.; Gaus, H.; Grundy, J.S.; Geary, R.S. In Vitro Metabolic Stabilities and Metabolism of 2′-O-(Methoxyethyl) Partially Modified Phosphorothioate Antisense Oligonucleotides in Preincubated Rat or Human Whole Liver Homogenates. *Oligonucleotides* **2010**, *20*, doi:10.1089/oli.2010.0252.
200. Gupta, N.; Fisker, N.; Asselin, M.C.; Lindholm, M.; Rosenbohm, C.; Ørum, H.; Elmén, J.; Seidah, N.G.; Straarup, E.M. A Locked Nucleic Acid Antisense Oligonucleotide (LNA) Silences PCSK9 and Enhances LDLR Expression In Vitro and In Vivo. *PLoS One* **2010**, *5*, 1–9, doi:10.1371/journal.pone.0010682.
201. Tillman, L.G.; Geary, R.S.; Hardee, G.E. Oral Delivery of Antisense Oligonucleotides in Man. *J Pharm Sci* **2008**, *97*, 225–236, doi:10.1002/jps.21084.
202. Ho, S.P.; Scully, M.S.; Krauthauser, C.M.; Wexler, E.J.; Stow, M.D.; Dinchuk, J.E.; Kerr, J.S.; Friedman, P.A. Antisense Oligonucleotides Selectively Regulate Aspartyl β-Hydroxylase and Its Truncated Protein Isoform in Vitro but Distribute Poorly into A549 Tumors in Vivo. *Journal of Pharmacology and Experimental Therapeutics* **2002**, *302*, doi:10.1124/jpet.302.2.795.
203. Shoeman, R.L.; Hartig, R.; Huang, Y.; Grub, S.; Traub, P. Fluorescence Microscopic Comparison of the Binding of Phosphodiester and Phosphorothioate (Antisense) Oligodeoxyribonucleotides to Subcellular Structures, Including

Intermediate Filaments, the Endoplasmic Reticulum, and the Nuclear Interior. *Antisense Nucleic Acid Drug Dev* **1997**, *7*, doi:10.1089/oli.1.1997.7.291.

204. Yu, R.Z.; Lemonidis, K.M.; Graham, M.J.; Matson, J.E.; Crooke, R.M.; Tribble, D.L.; Wedel, M.K.; Levin, A.A.; Geary, R.S. Cross-Species Comparison of in Vivo PK/PD Relationships for Second-Generation Antisense Oligonucleotides Targeting Apolipoprotein B-100. *Biochem Pharmacol* **2009**, *77*, 910–919, doi:10.1016/j.bcp.2008.11.005.
205. Yu, R.Z.; Geary, R.S.; Levin, A.A. Pharmacokinetics and Pharmacodynamics of Antisense Oligonucleotides. In *Pharmacokinetics and Pharmacodynamics of Biotech Drugs: Principles and Case Studies in Drug Development*; Meibohm, B., Ed.; Wiley-VCH: Weinheim, Germany, 2006; pp. 93–115 ISBN 3-527-31408-39.
206. Geary, R.S.; Yu, R.Z.; Siwkowski, A.; Levin, A.A. Pharmacokinetic/Pharmacodynamic Properties of Phosphorothioate 2′-O-(2-Methoxyethyl)-Modified Antisense Oligonucleotides in Animals and Man. In *Antisense Drug Technology: Principles, Strategies, and Applications, Second Edition*; Crooke, S.T., Ed.; CRC Press: USA, 2007; pp. 305–326 ISBN 9780849387968.
207. Goemans, N.M.; Tulinius, M.; van den Akker, J.T.; Burm, B.E.; Ekhart, P.F.; Heuvelmans, N.; Holling, T.; Janson, A.A.; Platenburg, G.J.; Sipkens, J.A.; et al. Systemic Administration of PRO051 in Duchenne's Muscular Dystrophy. *New England Journal of Medicine* **2011**, *364*, 1513–1522, doi:10.1056/nejmoa1011367.
208. Liang, X.H.; Sun, H.; Nichols, J.G.; Crooke, S.T. RNase H1-Dependent Antisense Oligonucleotides Are Robustly Active in Directing RNA Cleavage in Both the Cytoplasm and the Nucleus. *Molecular Therapy* **2017**, *25*, 2075–2092, doi:10.1016/j.ymthe.2017.06.002.
209. Weers, J.G.; Bell, J.; Chan, H.K.; Cipolla, D.; Dunbar, C.; Hickey, A.J.; Smith, I.J. Pulmonary Formulations: What Remains to Be Done? *J Aerosol Med Pulm Drug Deliv* 2010, *23*.
210. Lightfoot, H.L.; Hall, J. Target MRNA Inhibition by Oligonucleotide Drugs in Man. *Nucleic Acids Res* 2012, *40*.
211. Arikawa, E.; Sun, Y.; Wang, J.; Zhou, Q.; Ning, B.; Dial, S.L.; Guo, L.; Yang, J. Cross-Platform Comparison of SYBR® Green Real-Time PCR with TaqMan PCR, Microarrays and Other Gene Expression Measurement Technologies Evaluated in the MicroArray Quality Control (MAQC) Study. *BMC Genomics* **2008**, *9*, doi:10.1186/1471-2164-9-328.
212. Forreryd, A.; Johansson, H.; Albrekt, A.-S.; Lindstedt, M. *Evaluation of High Throughput Gene Expression Platforms Using a Genomic Biomarker Signature for Prediction of Skin Sensitization*; 2014;
213. Olsen, A.L.; Davies, J.M.; Medley, L.; Breen, D.; Talbot, D.C.; McHugh, P.J. Quantitative Analysis of Survivin Protein Expression and Its Therapeutic Depletion by an Antisense Oligonucleotide in Human Lung Tumors. *Mol Ther Nucleic Acids* **2012**, *1*, doi:10.1038/mtna.2012.19.
214. Shen, W.; Liang, X.H.; Sun, H.; Crooke, S.T. 2′-Fluoro-Modified Phosphorothioate Oligonucleotide Can Cause Rapid Degradation of P54nrb and PSF. *Nucleic Acids Res* **2015**, *43*, doi:10.1093/nar/gkv298.
215. Henry, S.P.; Kim, T.W.; Kramer-Stickland, K.; Zanardi, T.A.; Fey, R.A.; Levin, A.A. Toxicologic Properties of 2′-o-Methoxyethyl Chimeric Antisense Inhibitors in Animals and Man. In *Antisense Drug Technology: Principles, Strategies, and Applications, Second Edition*; 2007.
216. Ferrari, N. Hybridization-Independent Effects. In *Oligonucleotide-Based Drugs and Therapeutics*; 2018.
217. Guimond, A.; Kornbrust, D. Exaggerated Pharmacology. In *Oligonucleotide-based Drugs and Therapeutics*; Ferrari, N., Seguin, R., Eds.; John Wiley and Sons: Hoboken NJ USA, 2019; pp. 243–255.
218. Hashemi, N.; Odze, R.D.; McGowan, M.P.; Santos, R.D.; Stroes, E.S.G.; Cohen, D.E. Liver Histology during Mipomersen Therapy for Severe Hypercholesterolemia. *J Clin Lipidol* **2014**, *8*, doi:10.1016/j.jacl.2014.08.002.
219. Kornbrust, D.; Cavagnaro, J.; Levin, A.; Foy, J.; Pavco, P.; Gamba-Vitalo, C.; Guimond, A. Oligo Safety Working Group Exaggerated Pharmacology Subcommittee Consensus Document. *Nucleic Acid Ther* **2013**, *23*, doi:10.1089/nat.2012.0399.
220. Kamola, P.J.; Kitson, J.D.A.; Turner, G.; Maratou, K.; Eriksson, S.; Panjwani, A.; Warnock, L.C.; Douillard Guilloux, G.A.; Moores, K.; Koppe, E.L.; et al. In Silico and in Vitro Evaluation of Exonic and Intronic Off-Target Effects Form a Critical Element of Therapeutic ASO Gapmer Optimization. *Nucleic Acids Res* **2015**, *43*, doi:10.1093/nar/gkv857.
221. Hagedorn, P.H.; Hansen, B.R.; Koch, T.; Lindow, M. Managing the Sequence-Specificity of Antisense Oligonucleotides in Drug Discovery. *Nucleic Acids Res* 2017, *45*.
222. Burel, S.A.; Hart, C.E.; Cauntay, P.; Hsiao, J.; Machemer, T.; Katz, M.; Watt, A.; Bui, H.H.; Younis, H.; Sabripour, M.; et al. Hepatotoxicity of High Affinity Gapmer Antisense Oligonucleotides Is Mediated by RNase H1 Dependent Promiscuous Reduction of Very Long Pre-MRNA Transcripts. *Nucleic Acids Res* **2015**, *44*, 2093–2109, doi:10.1093/nar/gkv1210.
223. Dieckmann, A.; Hagedorn, P.H.; Burki, Y.; Brügmann, C.; Berrera, M.; Ebeling, M.; Singer, T.; Schuler, F. A Sensitive In Vitro Approach to Assess the Hybridization-Dependent Toxic Potential of High Affinity Gapmer Oligonucleotides. *Mol Ther Nucleic Acids* **2018**, *10*, doi:10.1016/j.omtn.2017.11.004.
224. Kasuya, T.; Hori, S.I.; Watanabe, A.; Nakajima, M.; Gahara, Y.; Rokushima, M.; Yanagimoto, T.; Kugimiya, A. Ribonuclease H1-Dependent Hepatotoxicity Caused by Locked Nucleic Acid-Modified Gapmer Antisense Oligonucleotides. *Sci Rep* **2016**, *6*, doi:10.1038/srep30377.

225. Lindow, M.; Vornlocher, H.P.; Riley, D.; Kornbrust, D.J.; Burchard, J.; Whiteley, L.O.; Kamens, J.; Thompson, J.D.; Nochur, S.; Younis, H.; et al. Assessing Unintended Hybridization-Induced Biological Effects of Oligonucleotides. *Nat Biotechnol* 2012, *30*.
226. Bennett, C.F.; Chiang, M. yi; Wilson-lingardo, L.; Wyatt, J.R. Sequence Specific Inhibition of Human Type II Phospholipase A2, Enzyme Activity by Phosphorothioate Oligonucleotides. *Nucleic Acids Res* **1994**, *22*, doi:10.1093/nar/22.15.3202.
227. Maltese, J. yves; Sharma, H.W.; Vassilev, L.; Narayanan, R. Sequence Context of Antisense RelA/NF-KB Phosphorothioates Determines Specificity. *Nucleic Acids Res* **1995**, *23*, doi:10.1093/nar/23.7.1146.
228. Stein, C.A. Phosphorothioate Antisense Oligodeoxynucleotides: Questions of Specificity. *Trends Biotechnol* **1996**, *14*, doi:10.1016/0167-7799(96)20006-X.
229. Krieg, A.M.; Stein, C.A. Phosphorothioate Oligodeoxynucleotides: Antisense or Anti-Protein? *Antisense Res Dev* 1995, *5*.
230. Haas, T.; Metzger, J.; Schmitz, F.; Heit, A.; Müller, T.; Latz, E.; Wagner, H. The DNA Sugar Backbone 2′ Deoxyribose Determines Toll-like Receptor 9 Activation. *Immunity* **2008**, *28*, doi:10.1016/j.immuni.2008.01.013.
231. Henry, S.P.; Geary, R.S.; Yu, R.; Levin, A.A. Drug Properties of Second-Generation Antisense Oligonucleotides: How Do They Measure up to Their Predecessors? *Current Opinion in Investigational Drugs* 2001, *2*.
232. Ørum, H.; Wengel, J. Locked Nucleic Acids: A Promising Molecular Family for Gene-Function Analysis and Antisense Drug Development. *Curr Opin Mol Ther* **2001**, *3*.
233. Henry, S.P.; Johnson, M.; Zanardi, T.A.; Fey, R.; Auyeung, D.; Lappin, P.B.; Levin, A.A. Renal Uptake and Tolerability of a 2′-O-Methoxyethyl Modified Antisense Oligonucleotide (ISIS 113715) in Monkey. *Toxicology* **2012**, *301*, 13–20, doi:10.1016/j.tox.2012.06.005.
234. Chi, X.; Gatti, P.; Papoian, T. Safety of Antisense Oligonucleotide and SiRNA-Based Therapeutics. *Drug Discov Today* 2017, *22*.
235. Henry, S.P.; Beattie, G.; Yeh, G.; Chappel, A.; Giclas, P.; Mortari, A.; Jagels, M.A.; Kornbrust, D.J.; Levin, A.A. Complement Activation Is Responsible for Acute Toxicities in Rhesus Monkeys Treated with a Phosphorothioate Oligodeoxynucleotide. *Int Immunopharmacol* **2002**, *2*, doi:10.1016/S1567-5769(02)00142-X.
236. Henry, S.P.; Giclas, P.C.; Leeds, J.; Pangburn, M.; Auletta, C.; Levin, A.A.; Kornbrust, D.J. Activation of the Alternative Pathway of Complement by a Phosphorothioate Oligonucleotide: Potential Mechanism of Action. *Journal of Pharmacology and Experimental Therapeutics* **1997**, *281*.
237. Shen, L.; Frazer-Abel, A.; Reynolds, P.R.; Giclas, P.C.; Chappell, A.; Pangburn, M.K.; Younis, H.; Henry, S.P. Mechanistic Understanding for the Greater Sensitivity of Monkeys to Antisense Oligonucleotide-Mediated Complement Activation Compared with Humans. *Journal of Pharmacology and Experimental Therapeutics* **2014**, *351*, doi:10.1124/jpet.114.219378.
238. Braendli-Baiocco, A.; Festag, M.; Erichsen, K.D.; Persson, R.; Mihatsch, M.J.; Fisker, N.; Funk, J.; Mohr, S.; Constien, R.; Ploix, C.; et al. The Minipig Is a Suitable Non-Rodent Model in the Safety Assessment of Single Stranded Oligonucleotides. *Toxicological Sciences* **2017**, *157*, 112–128, doi:10.1093/toxsci/kfx025.
239. Rudin, C.M.; Fleming, G.F.; Mani, S.; Stadler, W.M.; Schumm, P.; Ratain, M.J.; Holmlund, J.; Monia, B.P.; Johnston, J.F.; Geary, R.; et al. Phase I Trial of ISIS 5132, an Antisense Oligonucleotide Inhibitor of c-Raf-1, Administered by 24-Hour Weekly Infusion to Patients with Advanced Cancer. *Clinical Cancer Research* **2001**, *7*.
240. Advani, R.; Lum, B.L.; Fisher, G.A.; Halsey, J.; Geary, R.S.; Holmlund, J.T.; Kwoh, T.J.; Dorr, F.A.; Sikic, B.I. A Phase I Trial of Aprinocarsen (ISIS 3521/LY900003), an Antisense Inhibitor of Protein Kinase C-α Administered as a 24-Hour Weekly Infusion Schedule in Patients with Advanced Cancer. *Invest New Drugs* **2005**, *23*, doi:10.1007/s10637-005-2906-0.
241. Crooke, S.T.; Baker, B.F.; Kwoh, T.J.; Cheng, W.; Schulz, D.J.; Xia, S.; Salgado, N.; Bui, H.H.; Hart, C.E.; Burel, S.A.; et al. Integrated Safety Assessment of 2′-O-Methoxyethyl Chimeric Antisense Oligonucleotides in NonHuman Primates and Healthy Human Volunteers. *Molecular Therapy* **2016**, *24*, doi:10.1038/mt.2016.136.
242. Sheehan, J.P.; Phan, T.M. Phosphorothioate Oligonucleotides Inhibit the Intrinsic Tenase Complex by an Allosteric Mechanism. *Biochemistry* **2001**, *40*, doi:10.1021/bi002396x.
243. Henry, S.P.; Novotny, W.; Leeds, J.; Auletta, C.; Kornbrust, D.J. Inhibition of Coagulation by a Phosphorothioate Oligonucleotide. *Antisense Nucleic Acid Drug Dev* **1997**, *7*, doi:10.1089/oli.1.1997.7.503.
244. Sheehan, J.P.; Lan, H.C. Phosphorothioate Oligonucleotides Inhibit the Intrinsic Tenase Complex. *Blood* **1998**, *92*, doi:10.1182/blood.v92.5.1617.417k13_1617_1625.
245. Chen, H.X.; Marshall, J.L.; Ness, E.; Martin, R.R.; Dvorchik, B.; Rizvi, N.; Marquis, J.; McKinlay, M.; Dahut, W.; Hawkins, M.J. A Safety and Pharmacokinetic Study of a Mixed-Backbone Oligonucleotide (GEM231) Targeting the Type I Protein Kinase a by Two-Hour Infusions in Patients with Refractory Solid Tumors. *Clinical Cancer Research* **2000**, *6*.
246. Yacyshyn, B.R.; Chey, W.Y.; Goff, J.; Salzberg, B.; Baerg, R.; Buchman, A.L.; Tami, J.; Yu, R.; Gibiansky, E.; Shanahan, W.R. Double Blind, Placebo Controlled Trial of the Remission Inducing and Steroid Sparing Properties of an ICAM-

1 Antisense Oligodeoxynucleotide, Alicaforsen (ISIS 2302), in Active Steroid Dependent Crohn's Disease. *Gut* **2002**, *51*, doi:10.1136/gut.51.1.30.

247. Webb, M.S.; Tortora, N.; Cremese, M.; Kozlowska, H.; Blaquiere, M.; Devine, D. V.; Kornbrust, D.J. Toxicity and Toxicokinetics of a Phosphorothioate Oligonucleotide against the C-Myc Oncogene in Cynomolgus Monkeys. *Antisense Nucleic Acid Drug Dev* **2001**, *11*, doi:10.1089/108729001300338681.
248. Monteith, D.K.; Geary, R.S.; Leeds, J.M.; Johnston, J.; Monia, B.P.; Levin, A.A. Preclinical Evaluation of the Effects of a Novel Antisense Compound Targeting C-Raf Kinase in Mice and Monkeys. *Toxicological Sciences* **1998**, *46*, doi:10.1006/toxs.1998.2527.
249. Henry, S.P.; Taylor, J.; Midgley, L.; Levin, A.A.; Kornbrust, D.J. Evaluation of the Toxicity of ISIS 2302, a Phosphorothioate Oligonucleotide, in a 4-Week Study in CD-1 Mice. *Antisense Nucleic Acid Drug Dev* **1997**, *7*, doi:10.1089/oli.1.1997.7.473.
250. Desai, A.A.; Schilsky, R.L.; Young, A.; Janisch, L.; Stadler, W.M.; Vogelzang, N.J.; Cadden, S.; Wright, J.A.; Ratain, M.J. A Phase I Study of Antisense Oligonucleotide GTI-2040 given by Continuous Intravenous Infusion in Patients with Advanced Solid Tumors. *Annals of Oncology* **2005**, *16*, doi:10.1093/annonc/mdi178.
251. Kandimalla, E.R.; Shaw, D.R.; Agrawal, S. Effects of Phosphorothioate Oligodeoxyribonucleotide and Oligoribonucleotides on Human Complement and Coagulation. *Bioorg Med Chem Lett* **1998**, *8*, doi:10.1016/S0960-894X(98)00368-0.
252. Narayanan, P.K.; Henry, S.; Li, N. Drug-Induced Thrombocytopenia: Mechanisms and Relevance in Preclinical Safety Assessment. *Curr Opin Toxicol* 2019, *17*.
253. Henry, S.P.; Narayanan, P.; Shen, L.; Bhanot, S.; Younis, H.S.; Burel, S.A. Assessment of the Effects of 2'-Methoxyethyl Antisense Oligonucleotides on Platelet Count in Cynomolgus Nonhuman Primates. *Nucleic Acid Ther* **2017**, *27*, doi:10.1089/nat.2017.0666.
254. Seguin, R. Class-Related Proinflammatory Effects. In *Oligonucleotide-Based Drugs and Therapeutics*; Ferrari, N, Seguin, R., Ed.; John Wiley & Sons, Inc.: New Jersey, 2018; pp. 227–242 ISBN 9781119070290.
255. Paz-Ares, L.; Douillard, J.Y.; Koralewski, P.; Manegold, C.; Smit, E.F.; Reyes, J.M.; Chang, G.C.; John, W.J.; Peterson, P.M.; Obasaju, C.K.; et al. Phase III Study of Gemcitabine and Cisplatin with or without Aprinocarsen, a Protein Kinase C-Alpha Antisense Oligonucleotide, in Patients with Advanced-Stage Non-Small-Cell Lung Cancer. *Journal of Clinical Oncology* **2006**, *24*, doi:10.1200/JCO.2005.04.3299.
256. Chi, K.N.; Siu, L.L.; Hirte, H.; Hotte, S.J.; Knox, J.; Kollmansberger, C.; Gleave, M.; Guns, E.; Powers, J.; Walsh, W.; et al. A Phase I Study of OGX-011, a 2'-Methoxyethyl Phosphorothioate Antisense to Clusterin, in Combination with Docetaxel in Patients with Advanced Cancer. *Clinical Cancer Research* **2008**, *14*, doi:10.1158/1078-0432.CCR-07-1310.
257. Plummer, R.; Vidal, L.; Griffin, M.; Lesley, M.; De Bono, J.; Coulthard, S.; Sludden, J.; Siu, L.L.; Chen, E.X.; Oza, A.M.; et al. Phase I Study of MG98, an Oligonucleotide Antisense Inhibitor of Human DNA Methyltransferase 1, given as a 7-Day Infusion in Patients with Advanced Solid Tumors. *Clinical Cancer Research* **2009**, *15*, doi:10.1158/1078-0432.CCR-08-2859.
258. Grossman, S.A.; Alavi, J.B.; Supko, J.G.; Carson, K.A.; Priet, R.; Dorr, F.A.; Grundy, J.S.; Holmlund, J.T. Efficacy and Toxicity of the Antisense Oligonucleotide Aprinocarsen Directed against Protein Kinase C-α Delivered as a 21-Day Continuous Intravenous Infusion in Patients with Recurrent High-Grade Astrocytomas. *Neuro Oncol* **2005**, *7*, doi:10.1215/S1152851703000353.
259. Narayanan, P.; Shen, L.; Curtis, B.R.; Bourdon, M.A.; Nolan, J.P.; Gupta, S.; Hoffmaster, C.; Zhou, F.; Christian, B.; Schaubhut, J.L.; et al. Investigation into the Mechanism(s) That Leads to Platelet Decreases in Cynomolgus Monkeys during Administration of ISIS 104838, a 20-MoE-Modified Antisense Oligonucleotide. *Toxicological Sciences* **2018**, *164*, doi:10.1093/toxsci/kfy119.
260. Sewing, S.; Roth, A.B.; Winter, M.; Dieckmann, A.; Bertinetti-Lapatki, C.; Tessier, Y.; McGinnis, C.; Huber, S.; Koller, E.; Ploix, C.; et al. Assessing Single-Stranded Oligonucleotide Drug-Induced Effects in Vitro Reveals Key Risk Factors for Thrombocytopenia. *PLoS One* **2017**, *12*, 1–18, doi:10.1371/journal.pone.0187574.
261. Crooke, S.T.; Baker, B.F.; Witztum, J.L.; Kwoh, T.J.; Pham, N.C.; Salgado, N.; McEvoy, B.W.; Cheng, W.; Hughes, S.G.; Bhanot, S.; et al. The Effects of 2'-O-Methoxyethyl Containing Antisense Oligonucleotides on Platelets in Human Clinical Trials. *Nucleic Acid Ther* **2017**, *27*, doi:10.1089/nat.2016.0650.
262. Goemans, N.M.; Tulinius, M.; Van Den Hauwe, M.; Kroksmark, A.K.; Buyse, G.; Wilson, R.J.; Van Deutekom, J.C.; De Kimpe, S.J.; Lourbakos, A.; Campion, G. Long-Term Efficacy, Safety, and Pharmacokinetics of Drisapersen in Duchenne Muscular Dystrophy: Results from an Open-Label Extension Study. *PLoS One* **2016**, *11*, doi:10.1371/journal.pone.0161955.
263. Frazier, K.S. Antisense Oligonucleotide Therapies:The Promise and the Challenges from a Toxicologic Pathologist's Perspective. *Toxicol Pathol* **2015**, *43*, 78–89, doi:10.1177/0192623314551840.
264. Meng, Z.; Lu, M. RNA Interference-Induced Innate Immunity, off-Target Effect, or Immune Adjuvant? *Front Immunol* 2017, *8*.
265. Krieg, A.M. Therapeutic Potential of Toll-like Receptor 9 Activation. *Nat Rev Drug Discov* 2006, *5*.

266. Broz, P.; Monack, D.M. Newly Described Pattern Recognition Receptors Team up against Intracellular Pathogens. *Nat Rev Immunol* 2013, *13*.
267. Sledz, C.A.; Holko, M.; De Veer, M.J.; Silverman, R.H.; Williams, B.R.G. Activation of the Interferon System by Short-Interfering RNAs. *Nat Cell Biol* **2003**, *5*, doi:10.1038/ncb1038.
268. Ablasser, A.; Bauernfeind, F.; Hartmann, G.; Latz, E.; Fitzgerald, K.A.; Hornung, V. RIG-I-Dependent Sensing of Poly(DA:DT) through the Induction of an RNA Polymerase III-Transcribed RNA Intermediate. *Nat Immunol* **2009**, *10*, doi:10.1038/ni.1779.
269. Paz, S.; Hsiao, J.; Cauntay, P.; Soriano, A.; Bai, L.; Machemer, T.; Xiao, X.; Guo, S.; Hung, G.; Younis, H.; et al. The Distinct and Cooperative Roles of Toll-Like Receptor 9 and Receptor for Advanced Glycation End Products in Modulating in Vivo Inflammatory Responses to Select CpG and Non-CpG Oligonucleotides. *Nucleic Acid Ther* **2017**, *27*, doi:10.1089/nat.2017.0668.
270. Engelhardt, J.A.; Fant, P.; Guionaud, S.; Henry, S.P.; Leach, M.W.; Louden, C.; Scicchitano, M.S.; Weaver, J.L.; Zabka, T.S.; Frazier, K.S. Scientific and Regulatory Policy Committee Points-to-Consider Paper∗: Drug-Induced Vascular Injury Associated with Nonsmall Molecule Therapeutics in Preclinical Development: Part 2. Antisense Oligonucleotides. *Toxicol Pathol* 2015, *43*.
271. Jurk, M.; Kritzler, A.; Schulte, B.; Tluk, S.; Schetter, C.; Krieg, A.M.; Vollmer, J. Modulating Responsiveness of Human TLR7 and 8 to Small Molecule Ligands with T-Rich Phosphorothiate Oligodeoxynucleotides. *Eur J Immunol* **2006**, *36*, doi:10.1002/eji.200535806.
272. Barchet, W.; Wimmenauer, V.; Schlee, M.; Hartmann, G. Accessing the Therapeutic Potential of Immunostimulatory Nucleic Acids. *Curr Opin Immunol* 2008, *20*.
273. Puig, M.; Tosh, K.W.; Schramm, L.M.; Grajkowska, L.T.; Kirschman, K.D.; Tami, C.; Beren, J.; Rabin, R.L.; Verthelyi, D. TLR9 and TLR7 Agonists Mediate Distinct Type I IFN Responses in Humans and Nonhuman Primates in Vitro and in Vivo. *J Leukoc Biol* **2011**, *91*, doi:10.1189/jlb.0711371.
274. Holtick, U.; Scheulen, M.E.; Von Bergwelt-Baildon, M.S.; Weihrauch, M.R. Toll-like Receptor 9 Agonists as Cancer Therapeutics. *Expert Opin Investig Drugs* 2011, *20*.
275. Mustonen, E.K.; Palomäki, T.; Pasanen, M. Oligonucleotide-Based Pharmaceuticals: Non-Clinical and Clinical Safety Signals and Non-Clinical Testing Strategies. *Regulatory Toxicology and Pharmacology* **2017**, *90*, 328–341, doi:10.1016/j.yrtph.2017.09.028.
276. Levin, A.; Henry, S.; Monteith, D.; Templin, M. Toxicity of Antisense Oligonucleotides. In *Antisense Drug Technology*; 2001.
277. Galbraith, W.M.; Hobson, W.C.; Giclas, P.C.; Schechter, P.J.; Agrawal, S. Complement Activation and Hemodynamic Changes Following Intravenous Administration of Phosphorothioate Oligonucleotides in the Monkey. *Antisense Res Dev* **1994**, *4*, doi:10.1089/ard.1994.4.201.
278. Levin, A.A.; Henry, S.P. Toxicology of Oligonucleotide Therapeutics and Understanding the Relevance of the Toxicities. In *Preclinical Safety Evaluation of Biopharmaceuticals: A Science-Based Approach to Facilitating Clinical Trials*; 2007.
279. Krieg, A.M. CpG Motifs in Bacterial DNA and Their Immune Effects. *Annu Rev Immunol* 2002, *20*.
280. Klinman, D.M.; Yi, A.K.; Beaucage, S.L.; Conover, J.; Krieg, A.M. CpG Motifs Present in Bacterial DNA Rapidly Induce Lymphocytes to Secrete Interleukin 6, Interleukin 12, and Interferon γ. *Proc Natl Acad Sci U S A* **1996**, *93*, doi:10.1073/pnas.93.7.2879.
281. Henry, S.P.; Templin, M. V.; Gillett, N.; Rojko, J.; Levin, A.A. Correlation of Toxicity and Pharmacokinetic Properties of a Phosphorothioate Oligonucleotide Designed to Inhibit ICAM-1. In Proceedings of the Toxicologic Pathology; 1999; Vol. 27.
282. Hovingh, K.; Besseling, J.; Kastelein, J. Efficacy and Safety of Mipomersen Sodium (Kynamro). *Expert Opin Drug Saf* 2013, *12*.
283. Flaim, J.D.; Grundy, J.S.; Baker, B.F.; McGowan, M.P.; Kastelein, J.J.P. Changes in Mipomersen Dosing Regimen Provide Similar Exposure with Improved Tolerability in Randomized Placebo-Controlled Study of Healthy Volunteers. *J Am Heart Assoc* **2014**, *3*, doi:10.1161/JAHA.113.000560.
284. van Meer, L.; Moerland, M.; Gallagher, J.; van Doorn, M.B.A.; Prens, E.P.; Cohen, A.F.; Rissmann, R.; Burggraaf, J. Injection Site Reactions after Subcutaneous Oligonucleotide Therapy. *Br J Clin Pharmacol* 2016.
285. Henry, S.; Stecker, K.; Brooks, D.; Monteith, D.; Conklin, B.; Bennett, C.F. Chemically Modified Oligonucleotides Exhibit Decreased Immune Stimulation in Mice. *Journal of Pharmacology and Experimental Therapeutics* **2000**, *292*.
286. Monteith, D.K.; Henry, S.P.; Howard, R.B.; Flournoy, S.; Levin, A.A.; Bennett, C.F.; Crooke, S.T. Immune Stimulation a Class Effect of Phosphorothioate Oligodeoxynucleotides in Rodents. *Anticancer Drug Des* **1997**, *12*.
287. Oberbauer, R.; Schreiner, G.F.; Meyer, T.W. Renal Uptake of an 18-Mer Phosphorothioate Oligonucleotide. In Proceedings of the Kidney International; 1995; Vol. 48.

288. Guimond, A.; Viau, E.; Aubé, P.; Renzi, P.M.; Paquet, L.; Ferrari, N. Advantageous Toxicity Profile of Inhaled Antisense Oligonucleotides Following Chronic Dosing in Non-Human Primates. *Pulm Pharmacol Ther* **2008**, *21*, doi:10.1016/j.pupt.2008.08.001.
289. Templin, M. V.; Levin, A.A.; Graham, M.J.; Aberg, P.M.; Axelsson, B.I.; Butler, M.; Geary, R.S.; Bennett, C.F. Pharmacokinetic and Toxicity Profile of a Phosphorothioate Oligonucleotide Following Inhalation Delivery to Lung in Mice. *Antisense Nucleic Acid Drug Dev* **2000**, *10*, doi:10.1089/oli.1.2000.10.359.
290. Carver, M.P.; Charleston, J.S.; Shanks, C.; Zhang, J.; Mense, M.; Sharma, A.K.; Kaur, H.; Sazani, P. Toxicological Characterization of Exon Skipping Phosphorodiamidate Morpholino Oligomers (PMOs) in Non-Human Primates. *J Neuromuscul Dis* **2016**, *3*, doi:10.3233/JND-160157.
291. Ferdinandi, E.S.; Vassilakos, A.; Lee, Y.; Lightfoot, J.; Fitsialos, D.; Wright, J.A.; Young, A.H. Preclinical Toxicity and Toxicokinetics of GTI-2040, a Phosphorothioate Oligonucleotide Targeting Ribonucleotide Reductase R2. *Cancer Chemother Pharmacol* **2011**, *68*, doi:10.1007/s00280-010-1473-z.
292. Goemans, N.; Mercuri, E.; Belousova, E.; Komaki, H.; Dubrovsky, A.; McDonald, C.M.; Kraus, J.E.; Lourbakos, A.; Lin, Z.; Campion, G.; et al. A Randomized Placebo-Controlled Phase 3 Trial of an Antisense Oligonucleotide, Drisapersen, in Duchenne Muscular Dystrophy. *Neuromuscular Disorders* **2018**, *28*, doi:10.1016/j.nmd.2017.10.004.
293. Monteith, D.K.; Horner, M.J.; Gillett, N.A.; Butler, M.; Geary, R.; Burckin, T.; Ushiro-Watanabe, T.; Levin, A.A. Evaluation of the Renal Effects of an Antisense Phosphorothioate Oligodeoxynucleotide in Monkeys. *Toxicol Pathol* **1999**, *27*, doi:10.1177/019262339902700306.
294. Engelhardt, J.A. Comparative Renal Toxicopathology of Antisense Oligonucleotides. *Nucleic Acid Ther* 2016, *26*.
295. Van Poelgeest, E.P.; Swart, R.M.; Betjes, M.G.H.; Moerland, M.; Weening, J.J.; Tessier, Y.; Hodges, M.R.; Levin, A.A.; Burggraaf, J. Acute Kidney Injury during Therapy with an Antisense Oligonucleotide Directed against PCSK9. *American Journal of Kidney Diseases* **2013**, *62*, 796–800, doi:10.1053/j.ajkd.2013.02.359.
296. van Meer, L.; van Dongen, M.; Moerland, M.; de Kam, M.; Cohen, A.; Burggraaf, J. Novel SGLT2 Inhibitor: First-in-Man Studies of Antisense Compound Is Associated with Unexpected Renal Effects. *Pharmacol Res Perspect* **2017**, *5*, doi:10.1002/prp2.292.
297. Frazier, K.S.; Sobry, C.; Derr, V.; Adams, M.J.; Besten, C. Den; Kimpe, S. de; Francis, I.; Gales, T.L.; Haworth, R.; Maguire, S.R.; et al. Species-Specific Inflammatory Responses as a Primary Component for the Development of Glomerular Lesions in Mice and Monkeys Following Chronic Administration of a Second-Generation Antisense Oligonucleotide. *Toxicol Pathol* **2014**, *42*, doi:10.1177/0192623313505781.
298. Henry, S.P.; Jagels, M.A.; Hugli, T.E.; Manalili, S.; Geary, R.S.; Giclas, P.C.; Levin, A.A. Mechanism of Alternative Complement Pathway Dysregulation by a Phosphorothioate Oligonucleotide in Monkey and Human Serum. *Nucleic Acid Ther* **2014**, *24*, 326–335, doi:10.1089/nat.2014.0491.
299. Burdick, A.D.; Sciabola, S.; Mantena, S.R.; Hollingshead, B.D.; Stanton, R.; Warneke, J.A.; Zeng, M.; Martsen, E.; Medvedev, A.; Makarov, S.S.; et al. Sequence Motifs Associated with Hepatotoxicity of Locked Nucleic Acid - Modified Antisense Oligonucleotides. *Nucleic Acids Res* **2014**, *42*, 4882–4891, doi:10.1093/nar/gku142.
300. Hagedorn, P.H.; Yakimov, V.; Ottosen, S.; Kammler, S.; Nielsen, N.F.; Høg, A.M.; Hedtjärn, M.; Meldgaard, M.; Møller, M.R.; Ørum, H.; et al. Hepatotoxic Potential of Therapeutic Oligonucleotides Can Be Predicted from Their Sequence and Modification Pattern. *Nucleic Acid Ther* **2013**, *23*, doi:10.1089/nat.2013.0436.
301. Kamola, P.J.; Maratou, K.; Wilson, P.A.; Rush, K.; Mullaney, T.; McKevitt, T.; Evans, P.; Ridings, J.; Chowdhury, P.; Roulois, A.; et al. Strategies for In Vivo Screening and Mitigation of Hepatotoxicity Associated with Antisense Drugs. *Mol Ther Nucleic Acids* **2017**, *8*, doi:10.1016/j.omtn.2017.07.003.
302. Arechavala-Gomeza, V.; Garanto, A. Antisense RNA Therapeutics: A Brief Overview. In *Methods in Molecular Biology*; 2022; Vol. 2434.
303. Black, L.E.; Farrelly, J.G.; Cavagnaro, J.A.; Ahn, C.H.; Degeorge, J.J.; Taylor, A.S.; Defelice, A.F.; Jordan, A. Regulatory Considerations for Oligonucleotide Drugs: Updated Recommendations for Pharmacology and Toxicology Studies. *Antisense Res Dev* **1994**, *4*, doi:10.1089/ard.1994.4.299.
304. Cavagnaro, J.; Berman, C.; Kornbrust, D.; White, T.; Campion, S.; Henry, S. Considerations for Assessment of Reproductive and Developmental Toxicity of Oligonucleotide-Based Therapeutics. *Nucleic Acid Ther* 2014, *24*.
305. Schubert, D.; Levin, A.A.; Kornbrust, D.; Berman, C.L.; Cavagnaro, J.; Henry, S.; Seguin, R.; Ferrari, N.; Shrewsbury, S.B. The Oligonucleotide Safety Working Group (OSWG). *Nucleic Acid Ther* 2012, *22*.
306. Younis, H.S.; Templin, M.; Whitely, L.O.; Kornbrust, D.; Kim, T.W.; Henry, S.P. Overview of the Nonclinical Development Strategies and Class-Effects of Oligonucleotide-Based Therapeutics. In *A Comprehensive Guide to Toxicology in Preclinical Drug Development*; 2013.
307. Hirabayashi, Y.; Maki, K.; Kinoshita, K.; Nakazawa, T.; Obika, S.; Naota, M.; Watanabe, K.; Suzuki, M.; Arato, T.; Fujisaka, A.; et al. Considerations of the Japanese Research Working Group for the ICH S6 & Related Issues Regarding Nonclinical Safety Assessments of Oligonucleotide Therapeutics: Comparison with Those of Biopharmaceuticals. *Nucleic Acid Ther* **2021**, *31*, doi:10.1089/nat.2020.0879.

308. M3(R2); ICH, E. ICH M3(R2) - Guidance on Non-Clinical Safety Studies for the Conduct of Human Clinical Trials and Marketing Authorization for Pharmaceuticals. *International Conference on Harmonisation* **2013**, doi:EMA/CPMP/ICH/286/1995.
309. ICH ICH S6 (R1) - Preclinical Safety Evaluation of Biotechnology-Derived Pharmaceuticals. *Gl* **1997**, *Step 5*.
310. Tessier, Y.; Achanzar, W.; Mihalcik, L.; Amuzie, C.; Andersson, P.; Parry, J.D.; Moggs, J.; Whiteley, L.O. Outcomes of the European Federation of Pharmaceutical Industries and Associations Oligonucleotide Working Group Survey on Nonclinical Practices and Regulatory Expectations for Therapeutic Oligonucleotide Safety Assessment. *Nucleic Acid Ther* **2021**, *31*, doi:10.1089/nat.2020.0892.
311. Berman, C.L.; Cannon, K.; Cui, Y.; Kornbrust, D.J.; Lagrutta, A.; Sun, S.Z.; Tepper, J.; Waldron, G.; Younis, H.S. Recommendations for Safety Pharmacology Evaluations of Oligonucleotide- Based Therapeutics. *Nucleic Acid Ther* 2014, *24*.
312. Cavagnaro, J.A. The Principles of ICH S6 and the Case-by-Case Approach. In *Preclinical Safety Evaluation of Biopharmaceuticals: A Science-Based Approach to Facilitating Clinical Trials*; 2007.
313. White, T.E.K.; Cavagnaro, J. Reproductive and Developmental Toxicity Testing Strategies for Oligonucleotide-Based Therapeutics. In *Oligonucleotide-Based Drugs and Therapeutics*; 2018.
314. Henck, J.W.; Hilbish, K.G.; Serabian, M.A.; Cavagnaro, J.A.; Hendrickx, A.G.; Agnish, N.D.; Kung, A.H.C.; Mordenti, J. Reproductive Toxicity Testing of Therapeutic Biotechnology Agents. In Proceedings of the Teratology; 1996; Vol. 53.
315. ICH S11 NONCLINICAL SAFETY TESTING IN SUPPORT OF DEVELOPMENT OF PAEDIATRIC PHARMACEUTICALS. *ICH Consensus Guideline* **2020**.
316. European Medicines Agency ICH Topic E11: Clinical Investigation of Medicinal Products in the Pediatric Population. *Prescrire Int* **2001**.
317. Carleer, J.; Karres, J. Juvenile Animal Studies and Pediatric Drug Development: A European Regulatory Perspective. *Birth Defects Res B Dev Reprod Toxicol* **2011**, *92*, 254–260, doi:10.1002/bdrb.20310.
318. Faustman, E.M.; Gohlke, J.M.; Ponce, R.A.; Lewandowski, T.A.; Seeley, M.R.; Whittaker, S.G.; Griffith, W.C. Experimental Approaches to Evaluate Mechanisms of Developmental Toxicity. In *Developmental and Reproductive Toxicology: A Practical Approach*; 2005.
319. Goyenvalle, A.; Jimenez-Mallebrera, C.; Van Roon, W.; Sewing, S.; Krieg, A.M.; Arechavala-Gomeza, V.; Andersson, P. Considerations in the Preclinical Assessment of the Safety of Antisense Oligonucleotides. *Nucleic Acid Ther* 2023, *33*.
320. Marlowe, J.L.; Akopian, V.; Karmali, P.; Kornbrust, D.; Lockridge, J.; Semple, S. Recommendations of the Oligonucleotide Safety Working Group's Formulated Oligonucleotide Subcommittee for the Safety Assessment of Formulated Oligonucleotide-Based Therapeutics. *Nucleic Acid Ther* 2017, *27*.
321. Monteith, D.K.; Levin, A.A. Synthetic Oligonucleotides: The Development of Antisense Therapeutics. In Proceedings of the Toxicologic Pathology; 1999; Vol. 27.
322. Hard, G.C.; Johnson, K.J.; Cohen, S.M. A Comparison of Rat Chronic Progressive Nephropathy with Human Renal Disease-Implications for Human Risk Assessment. *Crit Rev Toxicol* 2009, *39*.
323. Black, L.E.; Degeorge, J.J.; Cavagnaro, J.A.; Jordan, A.; Ahn, C. ho Regulatory Considerations for Evaluating the Pharmacology and Toxicology of Antisense Drugs. *Antisense Res Dev* **1993**, *3*, doi:10.1089/ard.1993.3.399.
324. Bode, G.; Clausing, P.; Gervais, F.; Loegsted, J.; Luft, J.; Nogues, V.; Sims, J. The Utility of the Minipig as an Animal Model in Regulatory Toxicology. *J Pharmacol Toxicol Methods* **2010**, *62*, 196–220, doi:10.1016/j.vascn.2010.05.009.
325. Ganderup, N.C.; Harvey, W.; Mortensen, J.T.; Harrouk, W. The Minipig as Nonrodent Species in Toxicology - Where Are We Now? In Proceedings of the International Journal of Toxicology; 2012; Vol. 31.
326. Forster, R.; Bode, G.; Ellegaard, L.; van der Laan, J.W. The RETHINK Project on Minipigs in the Toxicity Testing of New Medicines and Chemicals: Conclusions and Recommendations. *J Pharmacol Toxicol Methods* **2010**, *62*, 236–242, doi:10.1016/j.vascn.2010.05.008.
327. Flisikowska, T.; Egli, J.; Flisikowski, K.; Stumbaum, M.; Küng, E.; Ebeling, M.; Schmucki, R.; Georges, G.; Singer, T.; Kurome, M.; et al. A Humanized Minipig Model for the Toxicological Testing of Therapeutic Recombinant Antibodies. *Nat Biomed Eng* **2022**, *6*, doi:10.1038/s41551-022-00921-2.
328. Wernersson, R.; Schierup, M.H.; Jørgensen, F.G.; Gorodkin, J.; Panitz, F.; Stærfeldt, H.H.; Christensen, O.F.; Mailund, T.; Hornshøj, H.; Klein, A.; et al. Pigs in Sequence Space: A 0.66X Coverage Pig Genome Survey Based on Shotgun Sequencing. *BMC Genomics* **2005**, *6*, doi:10.1186/1471-2164-6-70.
329. Heckel, T.; Schmucki, R.; Berrera, M.; Ringshandl, S.; Badi, L.; Steiner, G.; Ravon, M.; Küng, E.; Kuhn, B.; Kratochwil, N.A.; et al. Functional Analysis and Transcriptional Output of the Göttingen Minipig Genome. *BMC Genomics* **2015**, *16*, 1–19, doi:10.1186/s12864-015-2119-7.
330. Vamathevan, J.J.; Hall, M.D.; Hasan, S.; Woollard, P.M.; Xu, M.; Yang, Y.; Li, X.; Wang, X.; Kenny, S.; Brown, J.R.; et al. Minipig and Beagle Animal Model Genomes Aid Species Selection in Pharmaceutical Discovery and Development. *Toxicol Appl Pharmacol* **2013**, *270*, 149–157, doi:10.1016/j.taap.2013.04.007.

331. Lindholm, M.W.; Elmén, J.; Fisker, N.; Hansen, H.F.; Persson, R.; Møller, M.R.; Rosenbohm, C.; Ørum, H.; Straarup, E.M.; Koch, T. PCSK9 LNA Antisense Oligonucleotides Induce Sustained Reduction of LDL Cholesterol in Nonhuman Primates. *Molecular Therapy* **2012**, *20*, 376–381, doi:10.1038/mt.2011.260.
332. Horton, J.D.; Cohen, J.C.; Hobbs, H.H. Molecular Biology of PCSK9: Its Role in LDL Metabolism. *Trends Biochem Sci* 2007, *32*.
333. Fahed, A.C.; Nemer, G.M. Familial Hypercholesterolemia: The Lipids or the Genes? *Nutr Metab (Lond)* 2011, *8*.
334. Sjouke, B.; Kusters, D.M.; Kastelein, J.J.P.; Hovingh, G.K. Familial Hypercholesterolemia: Present and Future Management. *Curr Cardiol Rep* **2011**, *13*, doi:10.1007/s11886-011-0219-9.
335. Krieg, A.M. Targeting LDL Cholesterol with LNA. *Mol Ther Nucleic Acids* 2012, *1*.
336. Van Poelgeest, E.P.; Hodges, M.R.; Moerland, M.; Tessier, Y.; Levin, A.A.; Persson, R.; Lindholm, M.W.; Dumong Erichsen, K.; Ørum, H.; Cohen, A.F.; et al. Antisense-Mediated Reduction of Proprotein Convertase Subtilisin/Kexin Type 9 (PCSK9): A First-in-Human Randomized, Placebo-Controlled Trial. *Br J Clin Pharmacol* **2015**, *80*, 1350–1361, doi:10.1111/bcp.12738.
337. Henry, S.P.; Seguin, R.; Cavagnaro, J.; Berman, C.; Tepper, J.; Kornbrust, D. Considerations for the Characterization and Interpretation of Results Related to Alternative Complement Activation in Monkeys Associated with Oligonucleotide-Based Therapeutics. *Nucleic Acid Ther* **2016**, *26*, 210–215, doi:10.1089/nat.2015.0593.
338. Ayuso, M.; Buyssens, L.; Stroe, M.; Valenzuela, A.; Allegaert, K.; Smits, A.; Annaert, P.; Mulder, A.; Carpentier, S.; Van Ginneken, C.; et al. The Neonatal and Juvenile Pig in Pediatric Drug Discovery and Development. *Pharmaceutics* **2021**, *13*, 44, doi:10.3390/pharmaceutics13010044.
339. Rose, K.; Van Den Anker, J.N. *Guide to Paediatric Clinical Research*; 2006;
340. Klymiuk, N.; Blutke, A.; Graf, A.; Krause, S.; Burkhardt, K.; Wuensch, A.; Krebs, S.; Kessler, B.; Zakhartchenko, V.; Kurome, M.; et al. Dystrophin-Deficient Pigs Provide New Insights into the Hierarchy of Physiological Derangements of Dystrophic Muscle. *Hum Mol Genet* **2013**, *22*, doi:10.1093/hmg/ddt287.
341. Rogers, C.S.; Hao, Y.; Rokhlina, T.; Samuel, M.; Stoltz, D.A.; Li, Y.; Petroff, E.; Vermeer, D.W.; Kabel, A.C.; Yan, Z.; et al. Production of CFTR-Null and CFTR-ΔF508 Heterozygous Pigs by Adeno-Associated Virus - Mediated Gene Targeting and Somatic Cell Nuclear Transfer. *Journal of Clinical Investigation* **2008**, *118*, doi:10.1172/JCI34773.
342. Steines, B.; Dickey, D.D.; Bergen, J.; Excoffon, K.J.D.A.; Weinstein, J.R.; Li, X.; Yan, Z.; Abou Alaiwa, M.H.; Shah, V.S.; Bouzek, D.C.; et al. CFTR Gene Transfer with AAV Improves Early Cystic Fibrosis Pig Phenotypes. *JCI Insight* **2016**, *1*, doi:10.1172/jci.insight.88728.
343. Hickey, R.D.; Nicolas, C.T.; Allen, K.; Mao, S.; Elgilani, F.; Glorioso, J.; Amiot, B.; VanLith, C.; Guthman, R.; Du, Z.; et al. Autologous Gene and Cell Therapy Provides Safe and Long-Term Curative Therapy in A Large Pig Model of Hereditary Tyrosinemia Type 1. *Cell Transplant* **2019**, *28*, doi:10.1177/0963689718814188.
344. Ziv, Y.; Nevler, A.; Willenz, E.; Doron, O.; Zbar, A.; Shperber, A.; Sandbank, J. A Novel Porcine Model for Chemically Inducible Crohn's-like Reaction. *Israel Medical Association Journal* **2015**, *17*.
345. Marafini, I.; Monteleone, G. Inflammatory Bowel Disease: New Therapies from Antisense Oligonucleotides. *Ann Med* 2018, *50*.
346. Lu, K.; Fan, Q.; Zou, X. Antisense Oligonucleotide Is a Promising Intervention for Liver Diseases. *Front Pharmacol* 2022, *13*.
347. Cansby, E.; Nuñez-Durán, E.; Magnusson, E.; Amrutkar, M.; Booten, S.L.; Kulkarni, N.M.; Svensson, L.T.; Borén, J.; Marschall, H.U.; Aghajan, M.; et al. Targeted Delivery of Stk25 Antisense Oligonucleotides to Hepatocytes Protects Mice Against Nonalcoholic Fatty Liver Disease. *CMGH* **2019**, *7*, doi:10.1016/j.jcmgh.2018.12.004.
348. Roth, W.J.; Kissinger, C.B.; McCain, R.R.; Cooper, B.R.; Marchant-Forde, J.N.; Vreeman, R.C.; Hannou, S.; Knipp, G.T. Assessment of Juvenile Pigs to Serve as Human Pediatric Surrogates for Preclinical Formulation Pharmacokinetic Testing. *AAPS Journal* **2013**, *15*, doi:10.1208/s12248-013-9482-6.
349. Gad, SC; Dincer, Z; Svendsen, O. *Animal Models in Toxicology*; 2nd ed.; CRC Taylor and Francis: New York, 2007; ISBN 9780824754075.
350. Suenderhauf, C.; Parrott, N. A Physiologically Based Pharmacokinetic Model of the Minipig: Data Compilation and Model Implementation. *Pharm Res* 2013, *30*.

Chapter 2

Aims of the Doctoral Thesis

In accordance with EU law, it is required to replace, reduce, and refine animal use for research purposes (the "3Rs" concept), with a particular emphasis on limiting the use of nonhuman primates (NHPs). However, new drug modalities such as ASOs are frequently intended to interact with human targets with high specificity, which is why NHPs are often the selected species in the safety testing of these drug candidates. Nonetheless, other animal models are also being explored.

Significant efforts have already been made to advance scientific knowledge and comprehension of the value of minipigs as an alternative animal model for the safety testing of pharmaceuticals. In fact, the adult Göttingen Minipig has recently been recognized as a suitable alternative to NHPs in the safety testing of ASOs. On the other hand, potential differences in PK, PD, and off-target effects of ON-based therapeutics in pediatric patients may lead to differences in safety and/or efficacy profiles of a candidate ASO between pediatric populations and adults. Expanding the translational knowledge to juvenile minipigs for pediatric indications will advance the use of this animal model in the safety testing of ASOs in pediatric drug development. As the minipig presents multiple advantages in view of developmental pharmacology, drug discovery, and safety testing, as well as shares many similar developmental milestones with humans, we hypothesize that the juvenile minipig is a suitable model in nonclinical safety testing of ASOs intended for pediatric populations. However, no data is available on the PK/PD, toxicological, and metabolic profiles of ASOs in juvenile minipigs. To test our hypothesis, the following research objectives were addressed:

1. Assess potential differences in exposure/toxicity and pharmacologic effect of a model ASO in the juvenile Göttingen Minipig, following weekly dosing starting on postnatal day (PND) 1 for up to 8 weeks. This was done using an antisense LNA/PS/LNA gapmer (RTR5001) that had been previously characterized in adult Göttingen Minipigs and NHPs, in which the kidney and the liver were the primary target organs (Chapter 3).
2. To further explore the findings of the in vivo study with regard to the toxicokinetic and pharmacologic effects of ASOs; we evaluated the ontogeny of nuclease expression and activity in blood, kidney, and liver tissues obtained from the study animals and in additional

tissues from a biobank (gestational day (GD) 84-86, 108; PND 1, 3, 7, 28; and adults). To that end, we assessed the relative gene transcription (by qPCR) and activity (by activity assays using three isosequential ASOs (i.e., unmodified, all-PS, and LNA gapmer)) of identified key nucleases responsible for ASO metabolism and pharmacologic activity (Chapter 3).

3. To further understand ASO-induced thrombocytopenia (TCP), in vitro platelet activity and aggregometry assays were performed in Göttingen Minipigs. A panel of ASOs with different sequences and modifications (i.e., unmodified, all-PS, LNA gapmer, and 2'-MOE gapmer) with known platelet response phenotypes in NHPs and humans were employed as tool ASOs. The mechanism for direct platelet activation identified in humans was characterized in adult Göttingen Minipig samples. To extend this work to the juvenile minipigs, the ontogeny of proteins (i.e., glycoprotein VI (GPVI) and platelet factor 4 (PF4)) implicated in ASO-induced TCP mechanisms were studied (Chapter 4).
4. Collate and analyze the data obtained from objectives 1-3 and compare it to existing adult minipig, NHP, and human data (Chapters 3 and 4). This will expand the translational knowledge in juvenile Göttingen Minipigs versus human pediatric populations (Chapter 5).

Chapter 3

Safety Testing of an Antisense Oligonucleotide Intended for Pediatric Indications in the Juvenile Göttingen Minipig, Including an Evaluation of the Ontogeny of Key Nucleases

Allan Paulo Valenzuela, Claire Tardiveau, Miriam Ayuso Hernando, Laura Buyssens, Chloé Bars, Chris Van Ginneken, Pierluigi Fant, Isabelle Leconte, Annamaria Braendli-Baiocco, Neil Parrott, Georg Schmitt, Yann Tessier, Paul Barrow, and Steven Van Cruchten.

Adapted from *Pharmaceutics 2021, 13(9), 1442*.

Abstract: The adult Göttingen Minipig is an acknowledged model for safety assessment of antisense oligonucleotide (ASO) drugs developed for adult indications. To assess whether the juvenile Göttingen Minipig is also a suitable nonclinical model for pediatric safety assessment of ASOs, we performed an 8-week repeat-dose toxicity study in different age groups of minipigs ranging from 1 to 50 days of age. The animals received a weekly dose of a phosphorothioated locked-nucleic-acid-based ASO that was assessed previously for toxicity in adult minipigs. The endpoints included toxicokinetic parameters, in-life monitoring, clinical pathology, and histopathology. Additionally, the ontogeny of key nucleases involved in ASO metabolism and pharmacologic activity was investigated using quantitative polymerase chain reaction and nuclease activity assays. Similar clinical chemistry and toxicity findings were observed; however, differences in plasma and tissue exposures as well as pharmacologic activity were seen in the juvenile minipigs when compared with the adult data. The ontogeny study revealed a differential nuclease expression and activity, which could affect the metabolic pathway and pharmacologic effect of ASOs in different tissues and age groups. These data indicate that the juvenile Göttingen Minipig is a promising nonclinical model for safety assessment of ASOs intended to treat disease in the human pediatric population.

3.1 Introduction

Antisense oligonucleotides (ASOs) belong to a therapeutic modality designed to treat specific diseases by selectively modulating the gene expression of disease-associated proteins. Usually 12–24 nucleotides in length, ASOs are designed to hybridize with a specific and complementary mRNA, resulting in inhibition of protein translation [1]. Currently, more than a dozen RNA-targeting therapeutics are authorized for use, while many others are in development for various indications for which no or limited treatment options are available [2–4].

One mechanism by which ASOs inhibit RNA translation is through RNA degradation by the RNase H-dependent cleavage mechanism [5,6]. RNase H-dependent ASOs utilize a ubiquitous endogenous ribonuclease that specifically hydrolyzes the RNA strand in the RNA–DNA heteroduplexes. This antisense mechanism remains one of the most utilized despite the rapid advancements in RNA-targeted therapeutics [7,8]. After parenteral administration, ASOs transiently bind to plasma proteins before getting biodistributed rapidly to peripheral tissues. The plasma protein interaction supports tissue bioavailability and reduces renal clearance [9,10]. As observed across several mammalian species, the highest tissue concentration is reached primarily in the kidney and liver, with a long elimination phase from those tissues [11,12]. Accumulation-related changes in these organs are commonly observed in nonclinical testing of ASOs together with hematological alterations, immunostimulation, and coagulopathy [13].

Unlike conventional small molecule drugs, ASOs do not appear to be a substrate for cytochrome P450 enzymes [14,15]. Instead, ASOs are hydrolyzed by endogenous nucleases in the blood and other tissue compartments [16,17]. Nucleases are phosphodiesterases that cleave the phosphodiester bonds (P-O) of nucleic acids and can be classified as either exonucleases, which cleave one nucleotide at the 3’- or 5’-end; or endonucleases, which cleave P-O in the middle of the nucleic acid chain [18]. ASOs are metabolized by 3’-exonucleases while in circulation [19–21]. Once ASOs reach the various tissue compartments, they are generally metabolized by endonucleases followed by exonucleases [21]. Unmodified ASOs containing P-O bonds are inherently susceptible to nucleolytic degradation and have poor intrinsic binding affinity and biodistribution, which make these ASOs not suitable as therapeutic agents. This led to the development of first-generation ASOs with backbone chemistry modifications, e.g., phosphorothioate (PS), so-called phosphorothioate

antisense oligonucleotides (PTOs) [22,23]. PTOs later included additional modifications of the nucleotide sugar moiety, e.g., locked-nucleic acids (LNAs) in the flanking regions. This modification pattern, termed as gapmers, results in greater nuclease resistance and improved pharmacokinetics and potency [24] while still ensuring the activation of RNase H [25–27]. Currently, additional modifications are being investigated to further improve intracellular uptake of ASOs and delivery to the target tissues by e.g., covalently binding them to a carrier or ligand [23,28,29].

To date, no specific guidelines regulate the nonclinical safety testing of ASO drug candidates. The nonclinical testing guidelines for small molecule drugs are applicable since ASOs are manufactured by chemical synthesis. Thus, repeat-dose toxicity studies in both a rodent and a non-rodent are generally required [30], for which one needs to be pharmacologically relevant. Classically, nonhuman primates (NHPs) are the preferred non-rodent model for this class of compounds when the candidate ASO does not hybridize in dogs. However, the adult Göttingen Minipig appears to be a suitable alternative to NHPs, as it showed a similar safety profile in a previous study [31]. Moreover, with the sequencing of the Göttingen Minipig genome [32,33], it has become feasible to synthesize homologous ASOs that cross-react in swine to allow the evaluation of adverse effects related to the pharmacological target (exaggerated pharmacology). In essence, pharmacological target homology is crucial for demonstrating pharmacological effects of ASO candidates in the relevant nonclinical species. Still, only 14% of RNase-H-based ASOs and 20–40% of other ASO subclasses were tested in minipigs for non-rodent toxicity studies. ASOs are also of interest for pediatric indications, including neuromuscular diseases [34–36], such as spinal muscular atrophy [37] and Duchenne muscular dystrophy [38], which have already been treated successfully [6]. Moreover, ASOs are also being explored for the treatment of several other diseases in children such as retinopathy of prematurity [39], leukodystrophies [40], and inherited lung diseases [41]. Consequently, more repeat-dose toxicity studies in juvenile animals may be required/expected before starting pediatric clinical trials, depending on the intended pediatric age group(s), duration of treatment, etc. [42]. This is motivated by concerns of increased susceptibility of juveniles to toxicities due to, for instance, differences in absorption, distribution, metabolism, and excretion (ADME) [43]. Generally, minipigs and humans share many developmental milestones [42]. Moreover, both species show comparable differences between adult and juvenile populations. Therefore, the juvenile minipig as a model species presents multiple advantages in view of developmental pharmacology, drug discovery, and drug safety testing [44]. For ASOs, the juvenile

minipig is a promising model due to its biological similarity to humans, technical feasibility, welfare considerations, and rapid postnatal development [45,46]. However, to date, there are no data available on the pharmacodynamic, toxicological, and metabolic profiles of ASOs in the juvenile minipig.

To qualify the use of the juvenile Göttingen Minipig for pediatric safety assessment of ASOs, knowledge of the ontogeny of the key nucleases responsible for ASO metabolism and pharmacologic activity is pivotal. The functional immaturity of nucleases for ASO metabolism may result in high ASO exposure, resulting in more severe or additional toxicities in young individuals. On the other hand, the functional immaturity of RNase H may lead to low or absent ASO pharmacologic activity or could mask potential exaggerated pharmacology or off-target effects. Juvenile animal studies are designed to detect such effects and thus provide valuable safety data for the human pediatric population.

The goal of this study was to assess potential differences in exposure/toxicity and pharmacologic effect (i.e., reduce total and LDL cholesterol) of a model ASO in the juvenile Göttingen Minipig, following weekly dosing starting on postnatal day (PND) 1 for up to 8 weeks. This was done using an antisense LNA/PS/LNA gapmer (RTR5001) that had been previously characterized in adult Göttingen Minipigs and NHPs, in which the kidney and the liver were the primary organs of distribution/toxicity [31,47]. The ontogeny of nuclease expression and activity was assessed in blood, kidney, and liver tissues obtained from the study animals and in additional tissues from a biobank (gestational day (GD) 84–86, 108; PND 1, 3, 7, 28; and adults). Quantitative polymerase chain reaction (qPCR) and activity assays were performed using three isosequential ASOs (i.e., unmodified, all-PS, LNA/PS/LNA gapmer) to explore the findings of the in vivo study with regard to the toxicokinetic and pharmacologic effects of ASOs.

3.2 Materials and methods

3.2.1 Antisense oligonucleotides (ASOs)

RNase H-active antisense LNA/PS/LNA gapmer (RTR5001) with the 14-base pair sequence 5’-TGCtacaaaacCCA-3’ (upper-case, LNA monomers; lower-case, PS DNA monomers) was provided by Roche Innovation Center (Copenhagen, DK). RTR5001 targets the proprotein convertase

subtilisin/kexin 9 (*PCSK9*) mRNA (NCBI reference sequence: NM_174936.3) that is mainly expressed in the liver (therapeutic target organ) [48]. This model ASO matches the human sequence while having a single end-standing mismatch to the minipig sequence, which does not ablate its pharmacology in swine [31]. Two additional isosequential variants (unmodified and all-PS-modified) in desalted form were procured from Integrated DNA Technologies (Leuven, BE).

3.2.2 Study design

Two experiments were set up: (1) an in vivo 8-week repeat-dose toxicity study in juvenile Göttingen Minipigs (from now on referred to as the in vivo study; Figure 3.1A); and (2) an investigation of the ontogeny of nuclease gene expression and activity in the blood, kidney, and liver of different juvenile and adult Göttingen Minipigs (from now on referred to as the biobank study; Figure 3.1B). In-life monitoring, toxicokinetic parameters, clinical and anatomic pathology (including immunohistochemistry and in situ hybridization) after model ASO (RTR5001) administration were investigated in the in vivo study. Then, the ontogeny of nucleases was evaluated in blood and tissue samples from the in vivo study together with additional samples from our biobank.

3.2.3 In vivo study

The in vivo repeat-dose toxicity study of RTR5001 in animals was carried out at Charles River Laboratories France Safety Assessment SAS. The test facility is accredited by the Association for Assessment and Accreditation of Laboratory Animal Care, and the study was conducted according to standard operating procedures in accordance with the Organization for Economic Cooperation and Development Good Laboratory Practice. The welfare and treatment of animals were in accordance with the following: Guide for the care and use of laboratory animals, 2011; Decree no. 2013–118 relating to the protection of animals used in scientific experiments described in the Journal Officiel de la République Française on 1 February 2013; and Directive 2010/63/EU of the European Parliament and of the Council of 22 September 2010 on the protection of animals used for scientific purposes.

Four multiparous pregnant Göttingen Minipig sows aged between 21 and 32 months old were supplied by Ellegaard Göttingen Minipigs A/S (Dalmose, Denmark). The sows were acclimatized to the study housing conditions for three weeks before the predicted parturition date. After birth, the

piglets were given 1 mL of iron intramuscularly within 24 h and were allowed to suckle the dam until weaning. Sows were identified by ear tags and the piglets by transponder implants. Each sow and her litter were housed separately in 4 m^2 pens with anti-crush protection until PND 28 (weaning). After weaning, the litters were grouped by sex in two 6 m^2 pens.

A

***In vivo* samples (i.e. kidney, liver, blood)**

Age	Control group			Treatment group		
	Female	Male	N	Female	Male	N
PND 2	2	2	4	1	1	2
PND 9	1	1	2	1	1	2
PND 16	1	1	2	1	1	2
PND 23	1	-	1	2	1	3
PND 29	1	-	1	1	1	2
PND 37	1	1	2	1	1	2
PND 43	2	-	2	1	-	1
PND 51	2	-	2	1	1	2

→ **Clinical evaluation: hematology, coagulation, clinical chemistry, urinalysis**

→ **RTR5001 exposure assessment (LC-MS/MS) in plasma, kidney, and liver**

→ **Anatomic Pathology, immunohistochemistry, and *in situ* hybridization**

→ **Nuclease gene expression analysis (qPCR)**
- 3'-exonucleases in blood, kidney, and liver (*ENPP1*, *PDE1B*, *TREX1)*
- Endonucleases in kidney and liver (*DNASE1*, *DNASE2*)
- Ribonuclease Hs in kidney and liver (*RNASEH1*, *RNASEH2A*)

→ **Nuclease activity assay (towards isosequential ASOs)**
- Plasma nuclease activity assay

B

Biobank samples

Age	Kidney			Liver			Blood/Plasma		
	Female	Male	N	Female	Male	N	Female	Male	N
GD 84-86	4	4	8	4	4	8	-	-	-
GD 108	4	4	8	4	4	8	-	-	-
PND 1	5	5	10	5	5	10	-	-	-
PND 3	3	5	8	4	4	8	-	-	-
PND 7	3	5	8	4	4	8	-	-	-
PND 28	4	4	8	4	4	8	-	-	-
Adult	8	4	12	8	4	12	4	4	8

Nuclease gene expression analysis (qPCR)
- 3'-exonucleases in blood, kidney, and liver (*ENPP1*, *PDE1B*, *TREX1)*
- Endonucleases in kidney and liver (*DNASE1*, *DNASE2*)
- Ribonuclease H in kidney and liver (*RNASEH1*, *RNASEH2A*)

Nuclease activity assay (towards isosequential ASOs)
- Plasma nuclease activity assay (adult plasma samples only)
- Tissue nuclease activity assay (kidney and liver)

Figure 3.1. Schematic diagram of the study design illustrating the samples used and main experimental approaches. (A) In vivo study sample distribution over the different developmental stages, experimental groups, and sex. (B) Biobank study sample distribution over different juvenile and adult stages, and sex. Downstream usage of samples for the different assays are represented by arrows. GD: gestational day; PND: postnatal day; qPCR: quantitative polymerase chain reaction; ENPP1: ectonucleotide pyrophosphatase/phosphodiesterase 1; PDE1B: Phosphodiesterase 1B; TREX1: three-prime repair exonuclease 1; DNASE1 and DNASE2: deoxyribonuclease 1 and 2; RNASEH1 and RNASEH2A: ribonuclease H 1 and 2 subunit A; LC-MS/MS: liquid chromatography coupled with tandem mass spectrometry.

Thirty-two piglets from the four litters were randomly allocated to a control and an RTR5001 treatment group. RTR5001 was administered subcutaneously caudal to the pinna (left and right alternated) at a dose of 20 mg/kg and a volume of 2.5 mL/kg on PND 1, followed by seven weekly doses (i.e., PND 8, 15, 22, 28, 36, 42, and 50). Control animals received the same volume of vehicle (sterile 0.9% NaCl). A homogenous distribution of the litters across the different groups was ensured by randomly allocating piglets from the same litter to the different studied time points (i.e., 24 h after each dosing: PND 2, 9, 16, 23, 29, 37, 43, and 51) (Figure 3.1A). Control and treated animals were humanely killed at their designated time points by intravenous injection of sodium pentobarbital followed by exsanguination.

3.2.3.1 *In-life monitoring*

The following parameters and endpoints were closely monitored throughout the study period: mortality, clinical observations, body weight development, food consumption, and physical development. Body weight was measured daily from PND 1 to 7 and then twice per week until the end of the study period. All piglets were checked for landmarks of physical development (i.e., pinna unfolding, incisor eruption, and eye opening) from birth until PND 1–2, by which point all piglets had attained all three milestones.

3.2.3.2 *Tissue sampling*

Liver and kidney samples for bioanalytical examination, gene expression, and nuclease activity assays were harvested, weighed, and immediately snap-frozen in liquid nitrogen before storage at −80 °C. Blood samples were collected from the unfasted piglets during necropsy from the external jugular vein. Blood samples for the gene expression experiment were collected with EDTA-K_2 as anticoagulant and centrifuged (1000× *g*) for 15 min at 4 °C. The sediments (buffy coat and RBC) were mixed with 1 mL lysis buffer DL (Nucleospin® RNA Blood Midi). Blood samples for the nuclease activity assay were collected with sodium citrate as an anticoagulant and centrifuged (15,000× *g*) for 5 min at 4 °C. The plasma samples were aliquoted and stored at −80 °C. Blood was collected with EDTA-K_2 as anticoagulant and centrifuged (1800× *g*) for 10 min at 4 °C for plasma exposure assessment at several time points (0, 1, 3, 6, 24 h) after each dosing and throughout the study.

3.2.3.3 *Exposure assessment*

Plasma, liver, and kidney cortex tissue were analyzed by liquid chromatography coupled to tandem mass spectrometry (LC-MS/MS) using an LC Shimadzu system coupled with an API 6500+ Mass Spectrometer (AB Sciex, Framingham, MA, USA). Before analysis, tissue samples were homogenized with water (dilution factor 4), and the aliquot homogenates were diluted 5-fold in minipig blank plasma before sample preparation. The RTR5001 quantification was performed against a minipig plasma calibration curve from 1.00 to 1000 nM. The performance of sample analysis was monitored by analyzing quality control samples in minipig plasma spiked with a known concentration (2.00, 50.0, and 750 nM) of RTR5001. Fifty µL of calibration standards, quality control samples (freshly prepared in minipig plasma), and tissue homogenate samples diluted in minipig blank plasma were treated for protein denaturation with 150 µL of 4 M guanidine thiocyanate after the addition of 10 µL of the internal standard (1000 ng/mL or 5000 ng/mL in water RTR78464). After vigorous mixing

(20 min at 1600 rpm), 200 µL of a water/hexafluoroisopropanol (HFIP)/diisopropylethylamine (DIPEA) solution (100:4:0.2, *v*/*v*/*v*) were added, followed by mixing (15 min at 1500 rpm). Afterward, a clean-up step was performed using solid-phase extraction cartridges (Waters, OASIS HLB, 30 µm) after elution and evaporation to dryness (30–45 min at 40 °C under nitrogen). The samples were reconstituted in 100 µL of water/methanol/HFIP/DIPEA 950/50/5/3.5 (*v*/*v*/*v*/*v*) mobile phase. After vortex mixing (10 min at 1500 rpm), an aliquot (20 µL) was injected into the analytical column (Xbridge Oligonucleotide BRH C18, 2.1 × 50 mm, 2.5 µm (Waters Corporation, Milford, MA, USA)) kept at 60 °C. The analyte and internal standard were separated from matrix interferences using gradient elution from water/methanol/HFIP/DIPEA 950/50/5/3.5 (*v*/*v*/*v*/*v*) to water/methanol/HFIP/DIPEA 100/900/5/3.5 (*v*/*v*/*v*/*v*) within 4 min at a flow rate of 0.4 mL/min. Mass spectrometric detection was carried out on an AB-Sciex 6500+ mass spectrometer using selected reaction monitoring (SRM) in the negative ion mode. The selected ion reactions (*m*/*z*) were 658.8/134.0 for RTR5001 and 670.8/95.0 for RTR78464 internal standard. Detection was accomplished utilizing ion spray MS/MS in negative ion SRM mode. As determined from the analysis of quality control samples, the precision and accuracy of the assay were satisfactory throughout the study. Plasma exposure data were subjected to noncompartmental pharmacokinetic evaluation, and maximum plasma concentration (C_{max}) and area under the curve (0–24 h) (AUC_{0-24h}) values were determined. One animal from PND 16 was excluded from the exposure assessment analysis due to a sampling error.

3.2.3.4 *Clinical pathology*

Blood samples were used to assess hematology, coagulation, clinical chemistry parameters, and total complement activity (CH50). Additionally, urine was also collected at necropsy and used for urinalysis and urine chemistry assessment. Hematology parameters were determined using an ADVIA 120/2120 system (Siemens, Erlangen, Germany), coagulation parameters were determined with a STA R Max system (Stago, Asnières sur Seine, France), clinical chemistry parameters were determined with an AU680 system (Beckman Coulter, Brea, CA, USA), and CH50 was measured with an in vitro liposome immunoassay CH 50 Autokit (Fujifilm WAKO, Neuss, Germany) on a biochemistry analyzer AU680 system (Beckman Coulter, Brea, CA, USA). For CH50, four treated and four control animals were sampled before RTR5001 administration, 15 min, and 24 h after dosing on each treatment day until PND 28. On PND 36 and 42, four control and only three treated animals were sampled. On PND 50, only two animals per group were sampled. CH50 values were compared

with the before-administration values above the lower limit of detection on PND 8, as CH50 levels were not detectable before and after the first dose at PND 1. Urinary chemistry parameters were measured with an AU680 system (Beckman Coulter, Brea, CA, USA). In the results section, only significantly altered parameters when compared with control and/or pre-dosing values are presented.

3.2.3.5 *Necropsy, anatomic pathology, immunohistochemistry, in situ hybridization*

A complete post-mortem examination was performed, and an extensive list of tissues and organs was fixed and preserved in 10% neutral buffered formalin, embedded in paraffin, sectioned, mounted on glass slides, and stained with hematoxylin and eosin (H&E). The kidney histologic sections were additionally stained with Periodic Acid-Schiff (PAS). Histopathological evaluation was performed for all slides.

Immunohistochemistry. Immunohistochemistry (IHC) to localize ASOs in the kidney (PND 2, 9, 16, 23, 29, 37, 43, and 51), liver (PND 51), and mandibular and retropharyngeal lymph node (PND 2, 43, and 51) samples were performed using a Ventana Discovery Ultra® immunostainer (Ventana Medical Systems, Tucson, AZ, USA). Formalin-fixed and paraffin-embedded tissue sections (3–4 µm thick) of selected animals were deparaffinized, and an anti-ASO pAb2 rabbit polyclonal antibody (synthesized ad hoc by Creative Biolabs) diluted 1:100 was used as a primary antibody (32 min) in a standard protocol using the Ventana Chromo Map DAB® kit (760-159, Ventana). A Discovery OmniMap anti-Rabbit HRP (760-4311, Ventana) was used as a secondary antibody (8 min). No pretreatment was performed. A Discovery Inhibitor (760-4840, Ventana) and S-Block (760-4212, Ventana) (4 min) were selected, and sections were counterstained with hematoxylin.

In situ hybridization. In situ hybridization (ISH) was used to detect and localize RTR5001 in the kidney (PND 2, 9, 16, 23, 29, 37, 43, and 51), liver (PND 51), and lymph node samples (PND 2, 43, and 51). Briefly, tissue sections were deparaffinized and pre-treated with ISH-protease 3 (780-4149, Ventana). Following hybridization with the specific probe, sections were incubated with anti-DIG HRP enzyme conjugate (760-4822, Ventana) in conjunction with a tyramide-based Amplification BF Kit (760-226, Ventana) and anti-BF HRP (760-4828, Ventana). The DISCOVERY Purple kit (760-229, Ventana) was used as chromogen, and specific staining signals were identified as purple punctate dots or diffuse staining present in the cytoplasm. RNA diluent and LNA DIG-labeled U6 probes

(provided by Qiagen) were used as negative and positive controls, respectively. Sections were counterstained with hematoxylin II (790-2208, Ventana).

3.2.4 Biobank study

Snap-frozen liver and kidney samples from different untreated developing and adult female minipigs that were previously collected by Van Peer et al. [49] together with the kidney, liver, and blood samples from four adult males provided by Ellegaard Göttingen Minipig A/S (Dalmose, Denmark), and four adult females provided by Charles River Laboratories France Safety Assessment SAS (Saint-Germain-Nuelles, France) were used in the gene expression and nuclease activity assays for the biobank study. The following age groups were investigated: gestational day (GD) 84–86 and 108; postnatal day (PND) 1, 3, 7, and 28; and adults (aged 14–33 months). GD 84–86 and 108 represent 75 and 95% of gestation length in the minipig, respectively, therefore limiting the fetal age groups to the third trimester of pregnancy. PND 28, which is usually the weaning age in piglets in nonclinical settings, is roughly equivalent to the first year of life in children [42]. Both sexes were equally represented for each tissue and age group except for the kidney samples at PND 3 and 7, and adult kidney and liver samples (Figure 3.1B).

3.2.5 Gene expression

The gene expression analysis was first conducted on the biobank samples (*N* = 62), and then, a second analysis was performed on samples from the in vivo study, including biobank adult samples (*N* = 44). The expression profile of seven nuclease genes was assessed and was selected to provide comprehensive coverage of the key endogenous nucleases implicated in ASO metabolism and pharmacologic activity (see Table 3.1). This included three exonucleases, as ASOs are reported to be degraded by 3'-exonucleases while in circulation and after tissue biodistribution [19,20], and two endonucleases as the digestion of ASOs by these enzymes serve as the initial cleavage event in tissues for modified ASOs [50]. The gene expression profiles of the two isoforms of RNase H in mammalian cells were also evaluated, considering that RNases H hydrolyze RNA in the RNA–DNA hybrids [51]. RNase H1 has been identified as responsible for target RNA degradation in the ASO-driven cleavage mechanism [52]. However, as the definite role of RNase H2 is still unclear, depending on its subcellular localization in specific cell type [53], it was also included in our key nuclease list. Blood samples were evaluated for the relative expression of the exonuclease genes,

whereas both exonuclease and endonuclease (both DNase and RNase H isoforms) were evaluated for liver and kidney samples.

Total RNA was isolated using RNeasy® Plus Mini kit (74134, Qiagen, Hilden, Germany) from all liver and kidney samples, and a Nucleospin® RNA Blood Midi kit (740210.20, Macherey-Nagel, Düren, Germany) was used for the blood samples in EDTA-K_2 anticoagulant following the manufacturers' instructions. The concentration and purity (OD260/280) of the isolated total RNA were measured directly by UV-Vis Spectrophotometer (NanoDrop Technologies, Wilmington, DE, USA), and the RNA quality was evaluated by running the total RNA in gel electrophoresis, wherein intact rRNA subunits (28S and 18S) were observed, indicating minimal degradation. After extraction, 1 µg of total RNA was reverse transcribed using qScript® cDNA Supermix (95048-500, Quantabio, Beverly, MA, USA) and random hexamers in Q qPCR instrument version 1.0 (Quantabio, Beverly, MA, USA) in a total volume of 20 µL. The first-strand cDNA synthesized was diluted 1/10 with nuclease-free water prior to qPCR.

The primers for the target genes were designed using ApE software v2.0.55 (M Wayne, Madera, CA, USA), ensuring the specificity and inclusion of all transcript variants available on GENBANK and/or ENSEMBL pig sequences. Primers were designed to span different exons to prevent genomic DNA amplification. Primer pair specificities were verified with the Primer-BLAST tool (https://www.ncbi.nlm.nih.gov/tools/primer-blast/, accessed on 01 October 2018), and PCR product sizes were confirmed with gel electrophoresis. Primer sequences and details (i.e., amplicon length, efficiencies) are listed in Table 3.1. Transcript quantification was performed using a PerfeCTa SYBR Green Fastmix (95072-05K, Quantabio, Beverly, MA, USA) on a Q qPCR instrument version 1.0 (Quantabio, Beverly, MA, USA) in 48-well reaction plates. The qPCR reactions were prepared in a total volume of 20 µL containing 1 µL of cDNA (1/10 dilution), 10 µL SYBR Green Fastmix, and 400 nM for both forward and reverse primers. No-template controls were used for each batch of mixes. The thermocycling program followed a fast 2-step cycling protocol wherein an activation step of 95 °C for 1 min was set, which was followed by 50 cycles of 95 °C for 5 s and 60 °C for 30 s when fluorescence was acquired. A melt curve analysis was generated to check PCR specificity that starts from 72 until 95 °C at a ramp rate of 0.3 °C/s, and wherein single peaks confirmed the specific amplification of the genes. All samples were run in triplicates.

Table 3.1. Primer design for qPCR, gene details, and PCR efficiencies in the three analyzed tissues: blood (B), kidney (K), and liver (L).

Symbol	Name	Acc. Number	Rationale of Inclusion	Primer (5'–3')	Amplicon Length	E% (B)	E% (K)	E% (L)
ENPP1	Ectonucleotide Pyrophosphate/ Phosphodiesterase 1	XM_021087933	human orthologue identified as the plasma 3'-exonuclease responsible for PS degradation [20]	(f) CAGATCATGGCATGGAACAAGGCA (r) TGGTTTGGTTCCTGGCAAGAAAG	135	101	103	97
PDE1B	Phosphodiesterase 1B	XM_003126207	bovine orthologue was reported to show a similar 3'-exonuclease activity on PS oligonucleotide to that of the human plasma [57]	(f) GACTCGGCACAACCTCATCA (r) CAGTGGACCGTCTGGGTAAC	147	94	100	93
TREX1	Three prime repair exonuclease 1	XM_021070628	major and most abundant 3'-exonuclease in mammalian cells [58,59]	(f) CCTGCCTGCTGTTCGGCTC (r) GGCTCTCCAGGGCACATCTAT	175	94	106	98
DNASE1	Deoxyribonuclease 1	NM_213991	well-characterized role in DNA degradation [60,61]	(f) GGGATCTGGAGGACATCATGCT (r) CGACCACGATCCTGTCATAGGC	177	-	97	88
DNASE2	Deoxyribonuclease 2	NM_214196	well-characterized role in DNA degradation [60,61]	(f) GGAGGAGGTAGTCAAGGGCCA (r) GCCAGAGTACAGGTCGTCTCC	133	-	90	97
RNASEH1	Ribonuclease H1	NM_001243681	demonstrated its role for ASO pharmacologic activity [52]	(f) GCCAGGCCATCCTTTAAATGTAGG (r) CCCAGCTAGTGATGCCATTGATGG	170	-	98	96
RNASEH2A	Ribonuclease H2 subunit A	NM_001244444	isoform of ribonuclease H in mammalian cells, capable of degrading target RNA in cell lysates [8,53]	(f) TTTGTGGGCTGGGCATTGGA (r) ACAAACACCTGGGCCACTTTC	158	-	101	89

f, forward; r, reverse; E%, primer % efficiency.

Data were analyzed using the Q-qPCR software v1.0.2 (Quantabio, Beverly, MA, USA). Ct values were used for the analysis of gene expression. Primer amplification efficiencies (E) were determined for each gene in each tissue by calculating the slope of a four-point, five-fold dilution standard curve of a pool of cDNA samples. Gene expression, relative to the most highly expressed sample, was calculated by the ΔΔCt method using reference genes to normalize the expression of target genes. A panel of six commonly used reference genes of which the primer sequences were previously described by Nygard et al. [54] was tested with the geNorm software [55] to evaluate their expression stability among the different age groups, between sexes, and between organs (kidney and liver). Hypoxanthine phosphoribosyltransferase 1 (*HPRT1*) and TATA-box binding protein (*TBP*) were identified as the most stable genes across the different age and sex groups per organ, and they were first used to normalize the data separately for the liver and kidney samples. To allow comparison between kidney and liver data, *HPRT1* and *TBP* were identified to be stable in both the liver and kidney samples for the postnatal age and sex groups, limiting the comparison to postnatal stages. On the other hand, glyceraldehyde 3-phosphate dehydrogenase (*GAPDH*) and *HPRT1* were identified as stable and used to normalize the target gene expression for the blood samples.

3.2.6 Plasma nuclease activity

Frozen plasma samples from our biobank and the in vivo study with sodium citrate as anticoagulant were thawed and diluted 1/5 with phosphate-buffered saline (PBS) (pH 7.2). The three isosequential model ASOs were incubated with the plasma in parallel at 37 °C and a final concentration of 20 ng/µL. Five 5 µL-aliquots were taken at time points 0, 15, 30, 60, and 180 min for the unmodified sequence (RTR5001_PO), and 0, 1, 3, 6, and 24 h for the all-PS (RTR5001_PS) and LNA/PS/LNA gapmer (RTR5001). The enzymatic reaction was quenched by adding an equal volume of formamide-containing Gel loading Buffer II (AM8547, Ambion, Oudeschoot, The Netherlands) to the aliquots before storage at −80 °C for further polyacrylamide gel electrophoresis analysis. The samples were thawed and heated at 95 °C for 5 min before the intact and digested oligonucleotides were separated on a 15% denaturing nucleic acid Mini-PROTEAN polyacrylamide gel electrophoresis (4566056, Bio-Rad Laboratories, Hercules, CA, USA) for 50 min at 200 V. Similar to the study of Wahlestedt et al. [56], the gels were subsequently stained with SYBR Gold Nucleic Acid Gel Stain (S-11494, Molecular Probes, Eugene, OR, USA) to directly visualize the oligonucleotides. The gels were visualized and photographed in Gel Doc XR+ System (Bio-Rad Laboratories, Hercules, CA, USA). Densitometric analysis was performed using Image Lab software

version 5.1 (Bio-Rad Laboratories, Hercules, CA, USA), wherein the volume density of the major band corresponding to the intact oligonucleotide was calculated in each lane and corrected for background. The volume density of the sample from 0 min/h time point was set as the reference value for each incubation. Plasma nuclease activity was obtained as the percentage of degraded ASO fraction for each incubation time relative to the volume density of the 0 min/h time point. Data from the 15 min (RTR5001_PO) or 1 h (RTR5001_PS, RTR5001) incubation time point was used to evaluate age and sex effects.

3.2.7 Tissue nuclease activity

Total protein was extracted from the frozen liver and kidney biobank samples using T-PER Tissue Protein Extraction Reagent (78510, Thermo-Fischer Scientific, Waltham, MA, USA) supplemented with Halt Protease Inhibitor Cocktail (87785, Thermo-Fischer Scientific, Waltham, MA, USA) following the manufacturer's instructions. Contaminating nucleic acid in the crude tissue extract was precipitated using 2% streptomycin sulfate (S6501-5G, Sigma-Aldrich, Saint Louis, MO, USA), and carry-over streptomycin in the protein extract was removed using Bio-Spin 6 columns (732–6228, Bio-Rad Laboratories, Hercules, CA, USA). The protein content of the tissue extract was determined using a Pierce BCA Protein Assay kit (23225, Thermo-Fischer Scientific, Waltham, MA, USA), and the samples were adjusted to a protein concentration of 1 µg/µl using the T-PER reagent before storage at −80 °C. Incubation of the three isosequential model ASOs with the adjusted tissue protein extract and nuclease activity analysis were as described for the plasma nuclease activity assay. Reaction rates for the liver and kidney homogenates were also computed for the 15 min (RTR5001_PO) or 1 h (RTR5001_PS, RTR5001) incubation time point wherein the relative volume degraded is divided by incubation time.

3.2.8 Statistical analysis

To evaluate the effect of age and sex on nuclease gene expression and activity, data on the biobank liver and kidney samples were fitted first to a linear mixed model. The fixed factors of the model for this analysis consisted of age and sex, together with their interaction. Then, a second analysis for the in vivo study samples was performed for genes that did not have sex or age–sex interaction on the initial analysis. Age was the only fixed factor included in the model for the second analysis. Treatment as an effect was not included, as it is not expected to affect nuclease gene expression.

To account for the dependence between observation among littermates, sow was set as a random effect on the model. Run-by-plates (gene expression) or run-by-gel (activity assay) were added as a random factor to the model to correct for inter-run variability. The starting model was gradually simplified using stepwise backward modeling, wherein all non-significant effects were removed step by step. Post hoc analysis with Tukey's honest significance test was used when comparing the different age groups. When an age–sex interaction was detected, the effect of age was evaluated separately for both sexes. To evaluate the difference in gene expression and nuclease activity reaction rates between the kidney and liver samples per age group, organ, sex, and their interaction were used as fixed factors in the model. A non-parametric Spearman rank correlation test was performed to identify the correlation between nuclease gene expressions and activity toward the isosequential ASOs and between the exposure parameters and mean plasma albumin concentration for the investigational toxicity study. For the other in vivo parameters, no statistical analyses were performed due to limited sample size, except for the complement activity. To evaluate the effect of age, treatment, and their interaction on complement activity, data were fitted to a linear mixed model with Dunnett's multiple comparison test using PND 8 control (predose value) as reference. The model included age, treatment, and their interactions as fixed factors. Animals nested into the treatment group were set as a random effect to account for repeated measures for each subject. A p-value smaller than 0.05 was considered statistically significant. Variables were log- or square-root transformed when needed to meet normality and/or homoscedasticity assumptions. Statistical analysis and graphs were done using JMP® Pro 15 (SAS Institute, Cary, NC, USA) and GraphPad Prism 8 (La Jolla, CA, USA).

3.3 Results

3.3.1 Exposure assessment and tissue biodistribution

Based on the limited number of treated animals per group, only descriptive results for the temporal trends of RTR5001 concentrations in the plasma, kidney, and liver are presented. For the plasma $AUC_{0–24h}$ and C_{max}, comparable values after the first four SC administrations (PND 2, 9, 16, and 23) were observed (Figures 3.2A and S3.1). A relatively higher $AUC_{0–24h}$ value at PND 29 was seen after the fifth dosing. This was followed by a slight decrease that remained relatively unchanged from the sixth until the eighth dose (PND 37, 43, and 51). In contrast, C_{max} increased gradually after the

fifth dose. The highest C_{max} value was reached after the last dose, and it was 2.3-fold higher than the C_{max} after the initial dose at PND 1. After 24 h post-administration, RTR5001 was rapidly cleared from the blood circulation, resulting in concentrations two to three orders of magnitude lower than the C_{max}. Plasma trough levels measured directly before RTR5001 administration were relatively low at PND 1, 8, 22, 28, and 36, whereas slightly higher concentrations were seen at PND 15, 42, and 50 (Figure S3.1).

The RTR5001 concentration in the kidney (Figure 3.2B) was steady following the first three dosing days (PND 2, 9, and 16). Afterwards, a higher concentration was observed through the fourth to sixth doses (PND 23, 29, 37), which was followed by a drop in concentration by about half for the seventh (PND 43) and eighth (PND 51) doses. In contrast, a gradual increase in concentration of RTR5001 was observed in the liver, reaching a plateau between the sixth and seventh doses (PND 37 and 43) (Figure 3.2C), which was followed by a lower concentration after the final dose (PND 51). Generally, the compound distributed more in the kidney than in the liver except at PND 43. Spearman's rank correlation analysis on the three exposure panels showed a high correlation between plasma $AUC_{0–24h}$ and the liver exposure levels ($p < 0.0001$, $r = 0.8436$, $n = 15$) but failed to detect a significant correlation between plasma $AUC_{0–24h}$ and the kidney exposure levels ($p = 0.8101$, $r = 0.0679$).

3.3.2 In-life observation and clinical pathology

All animals survived up to the scheduled humane killing, and RTR5001 was clinically well-tolerated at 20 mg/kg/dose. There were no treatment-related effects on the physical development of piglets (i.e., pinna unfolding, eye opening, and incisor eruption), body weight, and no injection site reactions were observed for any RTR5001-treated animals.

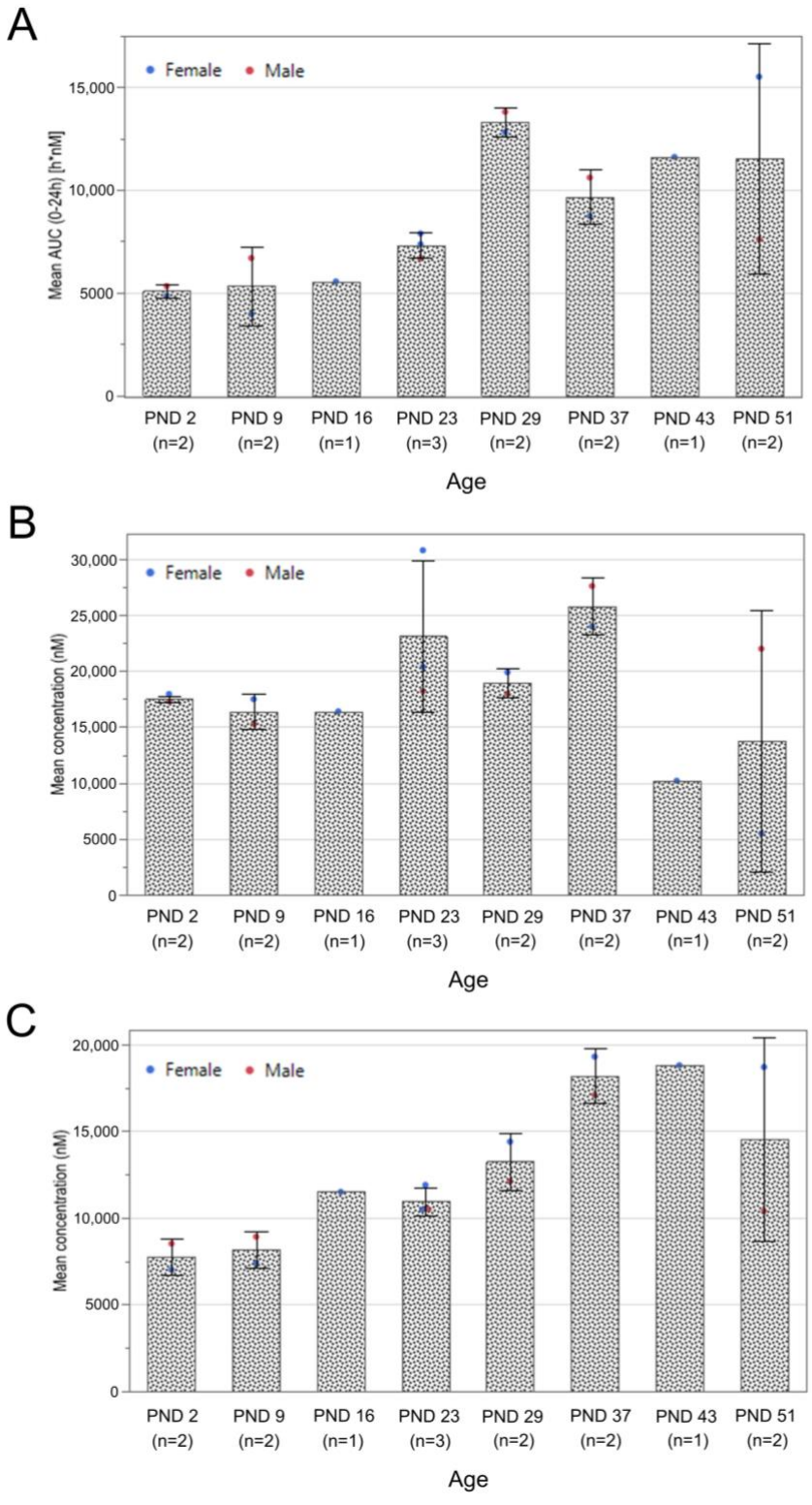

Figure 3.2. Mean ± SD exposure levels in the (**A**) plasma, (**B**) kidney cortex, and (**C**) liver after repeated SC administration of RTR5001 to different developing minipigs at 20 mg/kg dose level. The exposure in plasma (bound and unbound proportion) was measured as AUC of plasma concentration over a time interval of 0 to 24 h.

The administration of RTR5001 led to a minimal to mild increase in white blood cells (neutrophils and lymphocytes) and a minimal to mild increase in fibrinogen. No changes for coagulation parameters were noted (see Table 3.2). Moreover, a mild increase in aspartate aminotransferase (AST) was observed, but no effect was seen on urinalysis or urine chemistry parameters (see Table 2). The total complement activity measured by CH50 was not detectable before and after the initial dosing at PND 1. Activity levels on PND 8 until PND 22 between control and treated animals were comparable. However, RTR5001 caused a significantly increased CH50 on the pre-dose values from weaning onwards compared to PND 8 control group (p = 0.0364), and it did not differ statistically over time (p = 0.9397). On the other hand, there was no significant change in total complement activity 15 min post-RTR5001 administration within each age group (Figure 3.3).

Table 3.2. Clinical pathology evaluation overview. Comparison with published adult data [31] after RTR5001 administration.

Parameters	**Age**						
	PND 2 (*n* = 2)	**PND 23 (*n* = 3)**	**PND 29 (*n* = 2)**	**PND 37 (*n* = 2)**	**PND 43 (*n* = 1)**	**PND 51 (*n* = 2)**	**Adult (4–6 mos) (*n* = 3)**
Hematology		Minimal to mild ↑ WBC, lymphocytes		Minimal to mild ↑ WBC, neutrophils, lymphocytes	Minimal to mild ↑ WBC, neutrophils		
Clinical chemistry	Mild ↑ AST	Minimal to mild ↑ fibrinogen	Mild ↑ AST	Minimal to mild ↑ fibrinogen	Mild ↑ AST; minimal ↓ CHOL, LDL, minimal to mild ↑ fibrinogen	Minimal ↓ CHOL, LDL	↓ CHOL, LDL, trig; ↑ crea in 1 of 3, BUN
Urinalysis							↑ Na/Crea, Ca/Crea
Total complement activity	Not detectable		↑ CH50	↑ CH50	↑ CH50	↑ CH50	No data

PND 9 (n = 2) and PND 16 (n = 1) are not shown as no significant finding was observed. Abbreviations: AST, aspartate aminotransferases; BUN, blood urea nitrogen; Ca, calcium; CH50, 50% hemolytic complement activity; CHOL, total cholesterol; Crea, creatinine; LDL, low-density lipoprotein; Na, sodium; PND, postnatal day; trig, triglycerides; WBC, white blood cells.

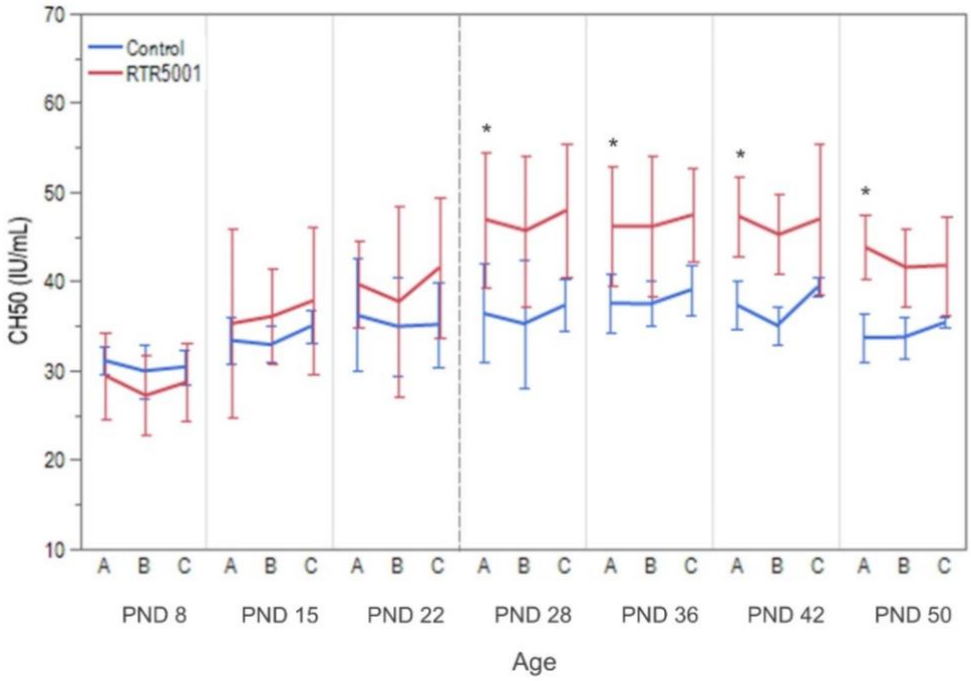

Figure 3.3. Mean ± SD total complement (CH50) activity measured in the serum of control and RTR5001-treated minipigs in different juvenile age groups: pre-dose (A), 15 min post-dose (B), and 24 h post-dose (C) of RTR5001. The same animals were tested (control: *n* = 4; RTR5001-treated: *n* = 4) from PND 1 until PND 28, and reduced at PND 36 and 42 (control: *n* = 4; RTR5001-treated: *n* = 3), and PND 50 (control: *n* = 2; RTR5001-treated: *n* = 2) accordingly. Broken line indicates weaning time (at PND 28) for the piglets. Differences between age, experimental groups, and their interactions before RTR5001 administration were determined using a mixed model with Dunnett's multiple comparison tests. *p* value < 0.05 when compared to PND 8 control (pre-dose value) was considered significant (*). CH50 was not significantly reduced 15 min post-RTR5001 administration within each age group, but it was significantly higher for the pre-dose values of PND 28 until 50 compared to the PND 8 control group after repeated administration of RTR5001.

The serum total cholesterol and low-density lipoprotein (LDL) cholesterol levels of both control and treated groups remained stable from PND 2 to PND 9 (Figure 3.4). Both parameters gradually increased until PND 23 before gradually decreasing back to the basal level again on PND 43 and 51. In contrast, a peak triglyceride level was observed at PND 2 before an initial drop on PND 9 that stayed stable until PND 29 (Figure 3.4). Another drop could be observed at PND 37 and remained stable until PND 51. No overt decrease in the three parameters (total cholesterol, LDL cholesterol, and triglycerides) was observed in treated groups after the first six weekly doses. In contrast, values for both LDL- and total cholesterol panels in the treated animals were higher at PND 23, 29, and 37 compared with the controls. However, when the total cholesterol values were compared with published control data in Göttingen Minipigs [62], only values at PND 23 were above the normal

range. Afterwards, decreases on PND 43 and PND 51 for total cholesterol (44% and 19% lower, respectively) and LDL cholesterol (74% and 44% lower, respectively) were seen for the treated animals when compared with control animals in the study and with previous data [62].

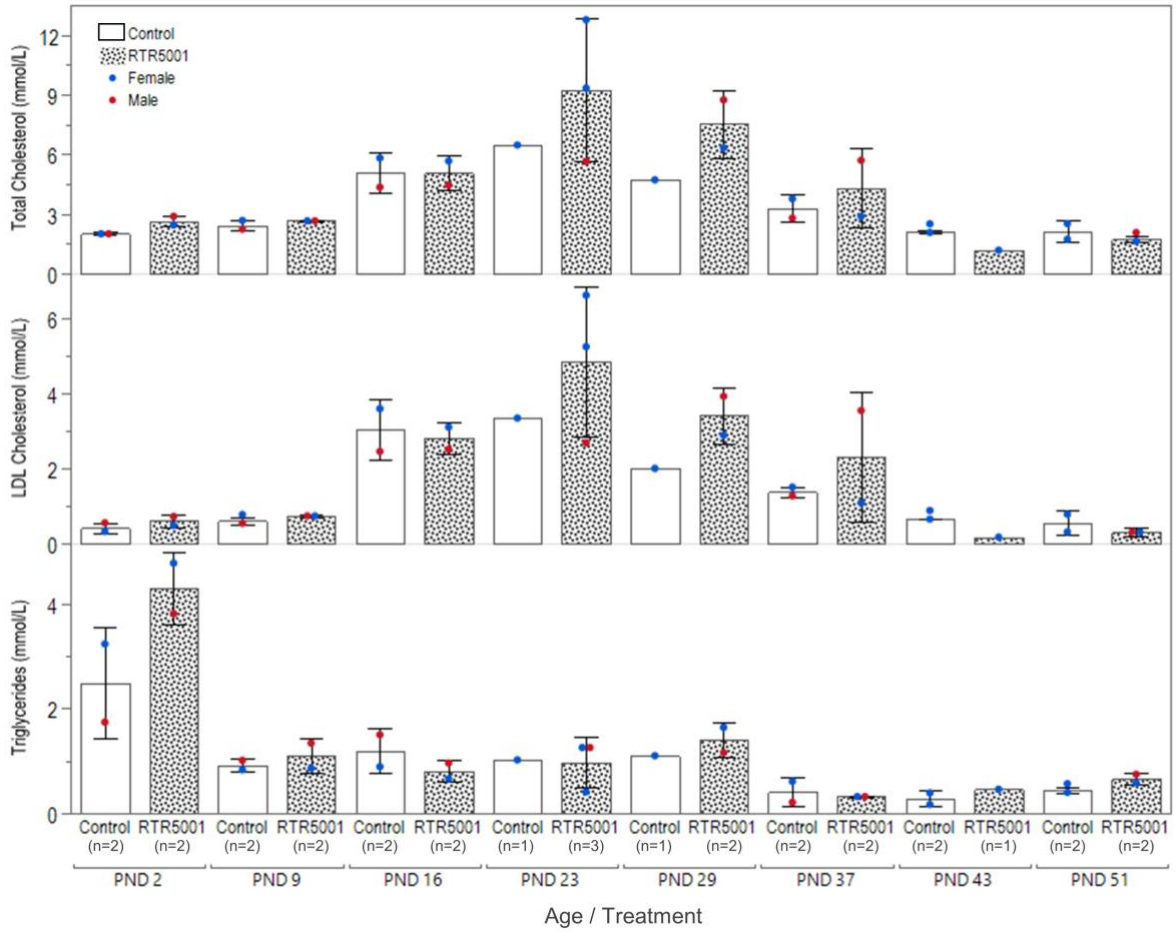

Figure 3.4. Mean ± SD level of serum total cholesterol, LDL cholesterol, and triglycerides in control and RTR5001-treated minipigs in the different juvenile age groups.

No treatment-related effects were observed in the mean plasma albumin concentration, but an age-related effect was observed (Figure 3.5). A gradual increase in both control and treated groups was observed, reaching the highest concentration at PND 37. A slight decrease was observed at PND 43, which remained unchanged at PND 51. Spearman's rank correlation analysis showed high correlations between the mean plasma albumin concentration and AUC_{0-24h} ($p < 0.0121$, $r = 0.6286$, $n = 15$), kidney exposure levels ($p < 0.0218$, $r = 0.5857$, $n = 15$), and liver exposure levels ($p < 0.0055$, $r = 0.6774$, $n = 15$).

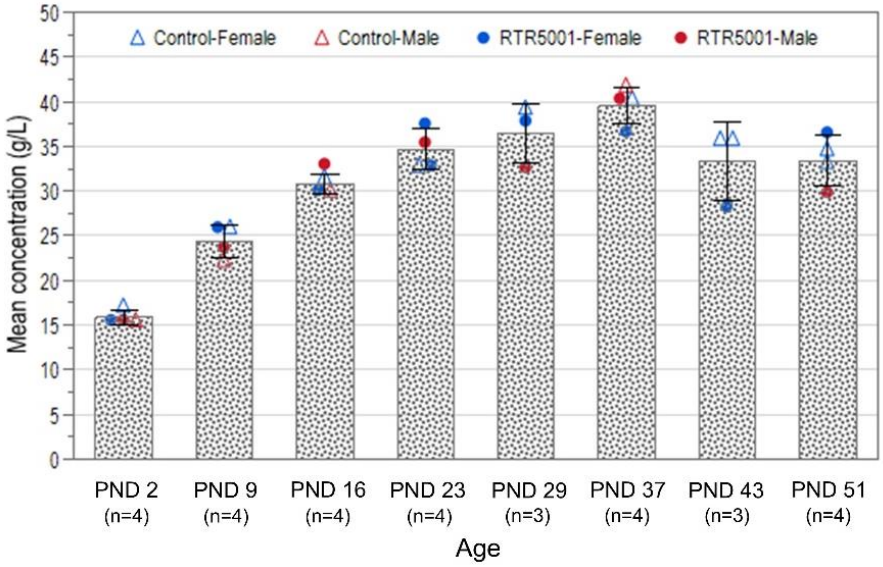

Figure 3.5. Mean ± SD plasma albumin concentration in control and RTR5001-treated juvenile minipigs in the different juvenile age groups.

3.3.3 Anatomic pathology, immunohistochemistry, and in situ hybridization

The repeated SC administration of RTR5001 did not cause any relevant gross lesions except at the injection sites. After microscopic evaluation, RTR5001-related histopathological findings were observed in the kidney, lymph nodes, and injection sites.

In the kidneys (Figure 3.6A-B), RTR5001-related minimal tubular degeneration/regeneration was observed at PND 23 onwards. At PND 43 and 51, the tubular changes were minimal to mild in severity and were accompanied by mononuclear cell infiltration, glomerulosclerosis, fibrosis, basophilic granules, and hyaline casts in the renal cortical region. Only scattered and barely visible basophilic granules considered to reflect the oligonucleotide uptake were observed in the cytoplasm of the epithelial cells lining the renal tubules at PND 51.

In the lymph nodes (Figure 3.6C), foamy/granular macrophages were observed in the retropharyngeal lymph node at PND 37, and in the mandibular, mesenteric, and superficial cervical lymph nodes at PND 43 and 51. There were no changes in the lymphoid tissue of these lymph nodes. Brown pigment consistent with iron deposits was observed in the examined lymph nodes.

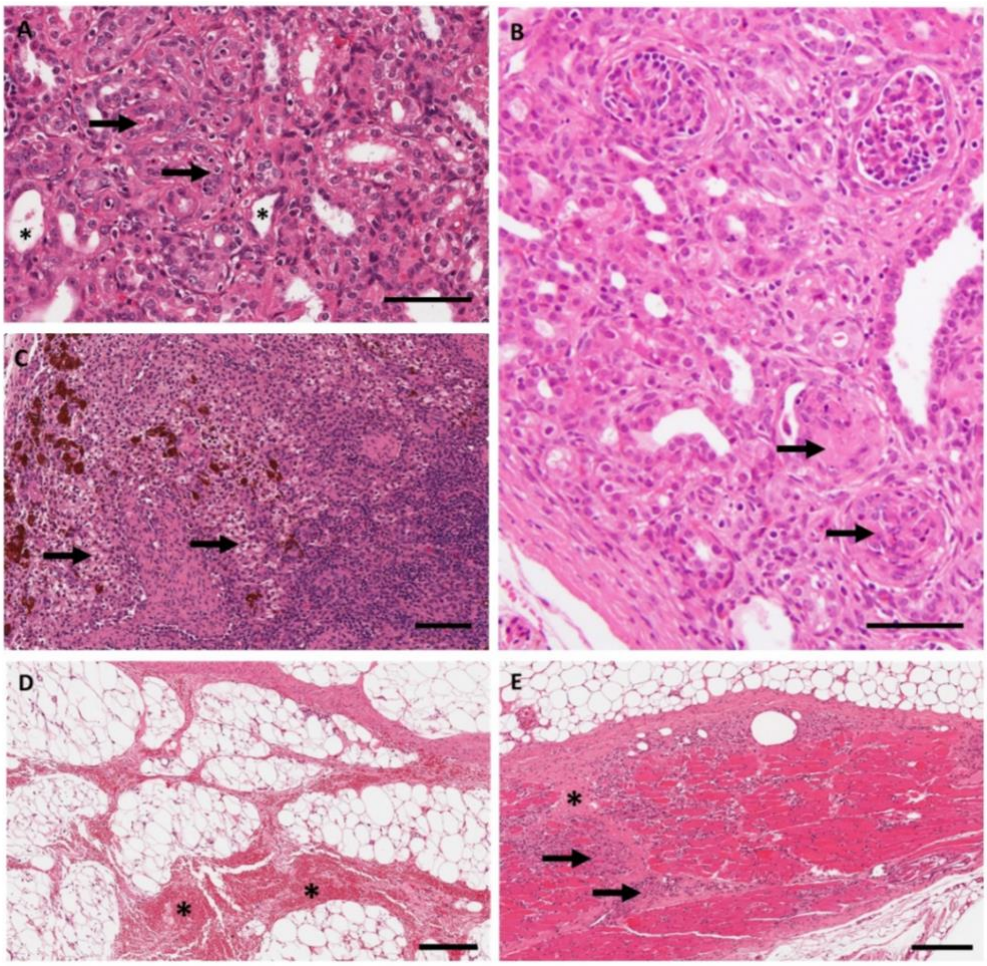

Figure 3.6. Histopathology findings. (**A**) Kidney, PND 43, H&E; Necrosis of tubular cells (arrow), tubular degeneration (asterisk). (**B**) Kidney, PND 51, H&E; Interstitial fibrosis and inflammatory cell infiltration, and glomerulosclerosis (arrow), (**C**) Lymph node, PND 51, H&E; Foamy macrophages (arrow) and brown pigment in the sinus macrophages due to intramuscular iron injection. (**D**) Injection site, PND 37 (control), H&E; Hemorrhage (asterisk) in the subcutaneous adipose tissue. (**E**) Injection site, PND 43 (treated), H&E; Inflammation (arrow) and fibrosis (asterisk) of the panniculus muscle. (Scale bar: (**A**–**C**) = 100 μM; (**D**,**E**) = 200 μM).

At the injection sites, gross and microscopic findings were at a higher incidence in the treated groups (69%) than in the control (21%) animals. Dark foci were observed in control and treated animals, and they were correlated microscopically with dermal and/or subcutaneous inflammation and hemorrhages, which were accompanied by inflammation and/or degeneration of the panniculus muscle (Figure 3.6D-E). The severity of the inflammatory changes was slightly higher (minimal to mild) in treated piglets at PND 43 and 51 compared to the other sacrifice time points where the severity was generally minimal. In control animals, the inflammation was acute, and no

fibrosis was observed. No basophilic granules or foamy/granular macrophages were observed at injection sites.

Immunohistochemistry and in situ hybridization revealed the presence of RTR5001 in the renal tubular cells, Kupffer cells, and lymph node macrophages of juvenile minipigs treated with RTR5001 (Figure 3.7).

Immunohistochemistry for RTR5001 demonstrated pronounced positive cytoplasmic staining in the renal cortical tubular cells already after the first administration of RTR5001, and there was no apparent increase over time. In the youngest minipigs (PND 2, 9, and 16), the renal tubules in the outer cortex below the capsule were not stained (Figure 3.7A-B). This area contains smaller and immature nephrons that lack differentiation, and therefore may not yet be functional at that age [63]. In the animals with the highest degree of tubular degeneration/regeneration at histopathological evaluation of the H&E sections (PND 23, 43, and 51), fewer tubules were stained, and the staining was irregularly distributed compared to the non-affected kidneys (Figure S3.2). Positive staining was characterized by brown granules in the cytoplasm of tubular cells. In situ hybridization for RTR5001 demonstrated positive cytoplasmic reaction in the renal tubular cells. Positive staining was characterized by purple, punctate dots and diffuse staining in the cytoplasm of tubular cells.

In the liver, positive staining in Kupffer cells was observed by ISH (Figure 3.7C) and IHC (Figure 3.7D), as evident by purple and brown pigments, respectively. However, the brown positive stain was partially due to intramuscular administration of iron, which is routinely done in newborn minipigs to prevent iron-deficiency anemia [64].

In the lymph nodes (mandibular and retropharyngeal), positively stained macrophages in the sinus were observed in both IHC- and ISH-stained slides (Figure 3.7E-F). This corresponded to the presence of foamy/granular macrophages observed in the lymph node sinus at histopathological evaluation of the H&E sections. Similar to the liver, brown pigments consistent with iron-containing hemosiderin deposits were observed in the sinus macrophages of lymph nodes stained by ISH. In IHC, this pigment could not be distinguished from the brown DAB staining.

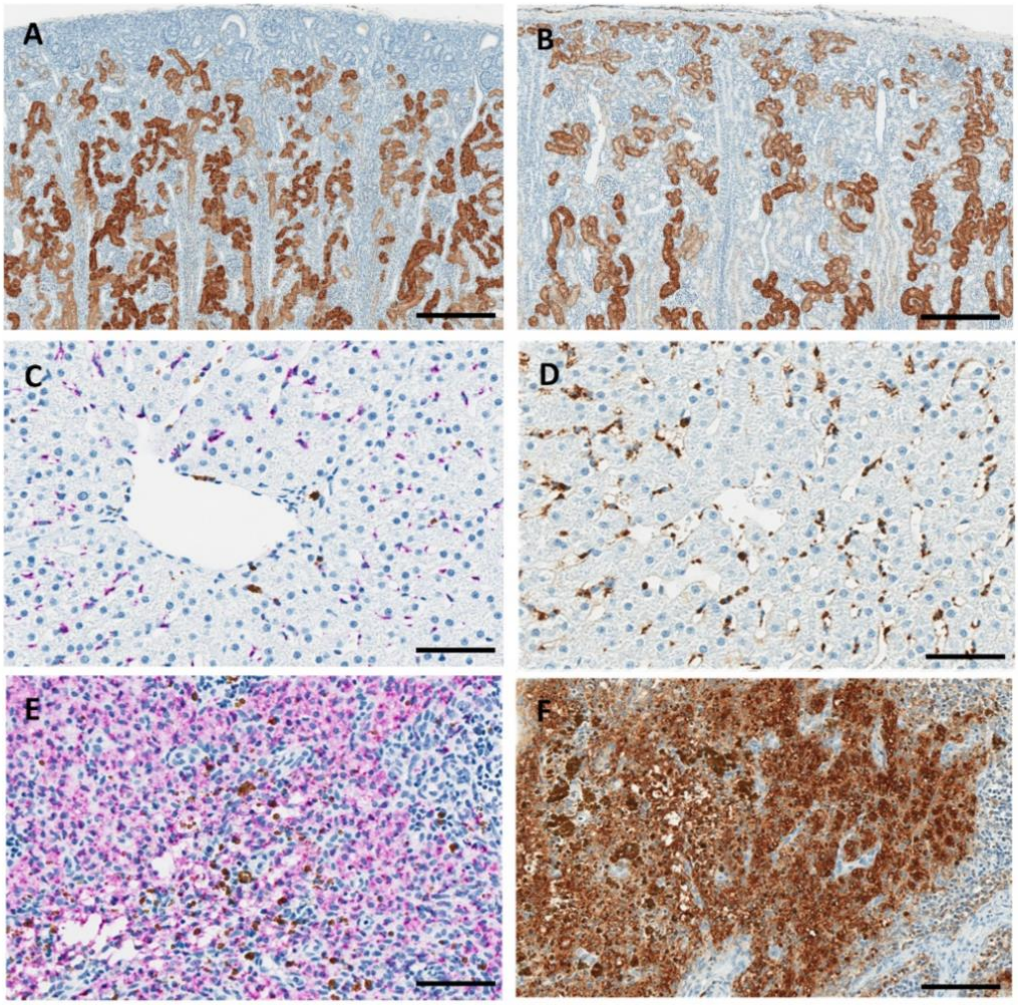

Figure 3.7. Immunohistochemistry and in situ hybridization. (**A**) Kidney, PND 2; immunohistochemistry for RTR5001. Accumulation of RTR5001 into the proximal tubular cells (brown staining). Renal tubular cells of the outer cortex below the capsule are not stained. (**B**) Kidney, PND 37; immunohistochemistry for RTR5001. Accumulation of RTR5001 in the tubular cells including the outer cortex. (**C**) Liver, PND 51; in situ hybridization for RTR5001. Accumulation of LNA into the Kupffer cells (purple staining) and brown pigment (iron deposits). (**D**) Liver, PND 51; Immunohistochemistry for RTR5001. Presence of brown staining due to accumulation of LNA in Kupffer cells and presence of iron pigment deposits cannot be differentiated, unlike with ISH-stained sections (image C). (**E**) Lymph node, PND 43; in situ hybridization for RTR5001. Accumulation of RTR5001 into the vacuolated macrophages (purple staining) and brown pigment (iron deposits) in sinus macrophages. (**F**) Lymph node, PND 43; immunohistochemistry for RTR5001 Accumulation of RTR5001 and presence of iron pigment deposits. (Scale bar: (**A**,**B**) = 100 µM; (**C**–**F**) = 50 µM).

3.3.4 Ontogeny of nuclease gene expression and activity in the blood

Low expression of the three 3'-exonuclease genes was observed in the blood derived from the youngest age groups from the in vivo study (Figure 3.8). *ENNP1* expression level showed a transient mild increase at PND 29, and the highest level was reached at PND 51 (p = 0.0002). Afterwards, *ENNP1* expression dropped to the same level as the youngest groups. This is in contrast to the *PDE1B* expression, which continued to increase and reached the highest level in adulthood (p = 0.0176). The highest *TREX1* expression level was also observed at the adult group (p = 0.0001), but no clear maturation profile was observed for the older juvenile stages.

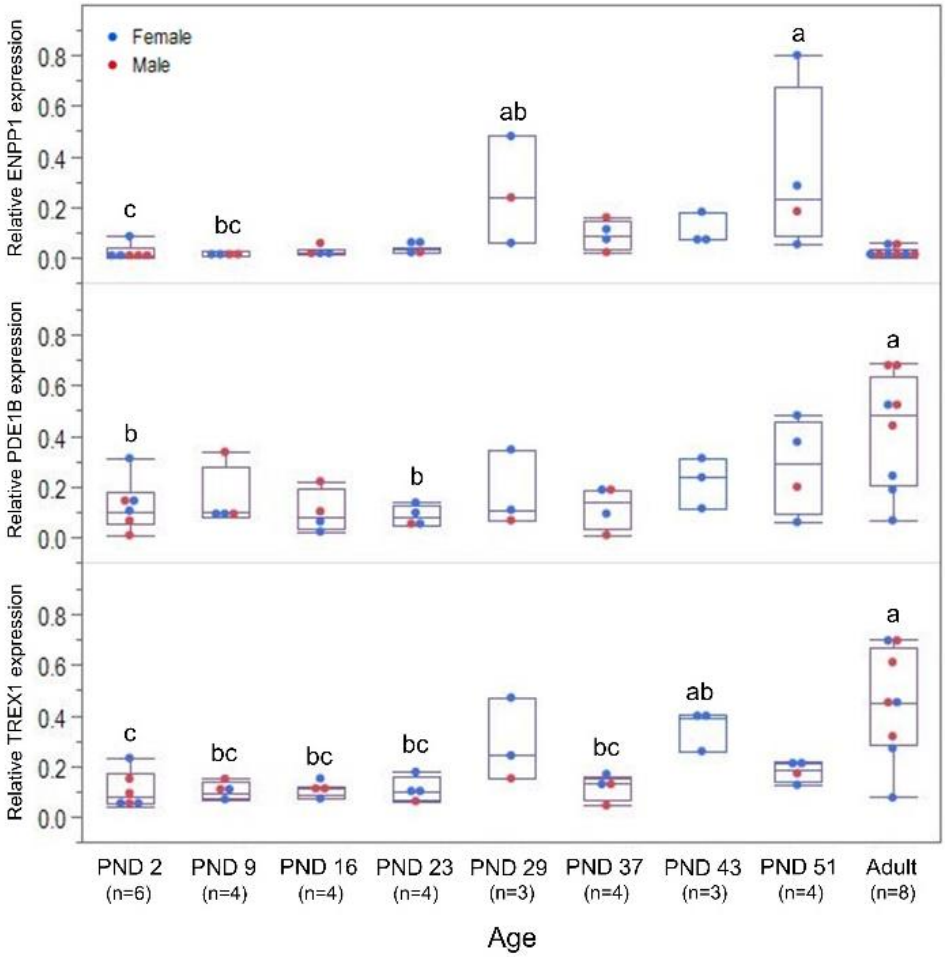

Figure 3.8. Relative gene expression of 3'-exonucleases: *ENPP1*, *PDE1B*, and *TREX1* in the blood over time in the developing and adult Göttingen Minipig. Age groups not sharing the same letter within each gene panel show significantly different gene expression (p < 0.05).

Regarding nuclease activity, the unmodified (PO) ASO was almost completely metabolized in the assay within three hours (Figure 3.9A, left panel), whereas the two modified ASOs exhibited stability against the endogenous nucleases in the plasma. This was markedly observed with the LNA/PS/LNA gapmer and, to a lesser degree, with the all-PS after 24 h of incubation. When looking at the degradation of the different ASOs after 15 min (PO) or 1 h (PS, LNA/PS/LNA) incubation with plasma, no statistically significant difference between the age groups was detected (PO: $p = 0.6323$; PS: $p = 0.0507$; LNA/PS/LNA: $p = 0.8182$) (Figure 3.9A, right panel).

3.3.5 Ontogeny of nuclease gene expression and activity in the kidney and liver

In general, higher expression of the endonuclease and exonuclease candidate genes were observed in kidney than in liver samples from our biobank (Figure S3.3). A similar ontogeny profile was observed for both members of the DNase endonuclease family in the kidney, in which they exhibited a significantly lower expression at PND 3 than in the adult group (*DNASE1*: $p = 0.0046$; *DNASE2*: $p = 0.0387$; Figure 3.10A, left panel). A gradual increase was observed after PND 3 and eventually reached the highest levels at the adult stage. In contrast, liver *DNASE1* exhibited a significantly higher expression at GD 108 than the postnatal age groups, with GD 84–86 and adults showing intermediate values ($p = 0.0112$). A downregulation after birth was observed for liver *DNASE1* expression, and it remained the same until PND 28. Moreover, a sex–age interaction was detected in liver *DNASE2* expression ($p = 0.0001$); i.e., males exhibited a gradual decrease from PND 1, reaching the lowest level at the adult stage ($p = 0.0001$). In contrast, expression in females reached the lowest level at PND 28, before increasing again in adulthood ($p = 0.0001$).

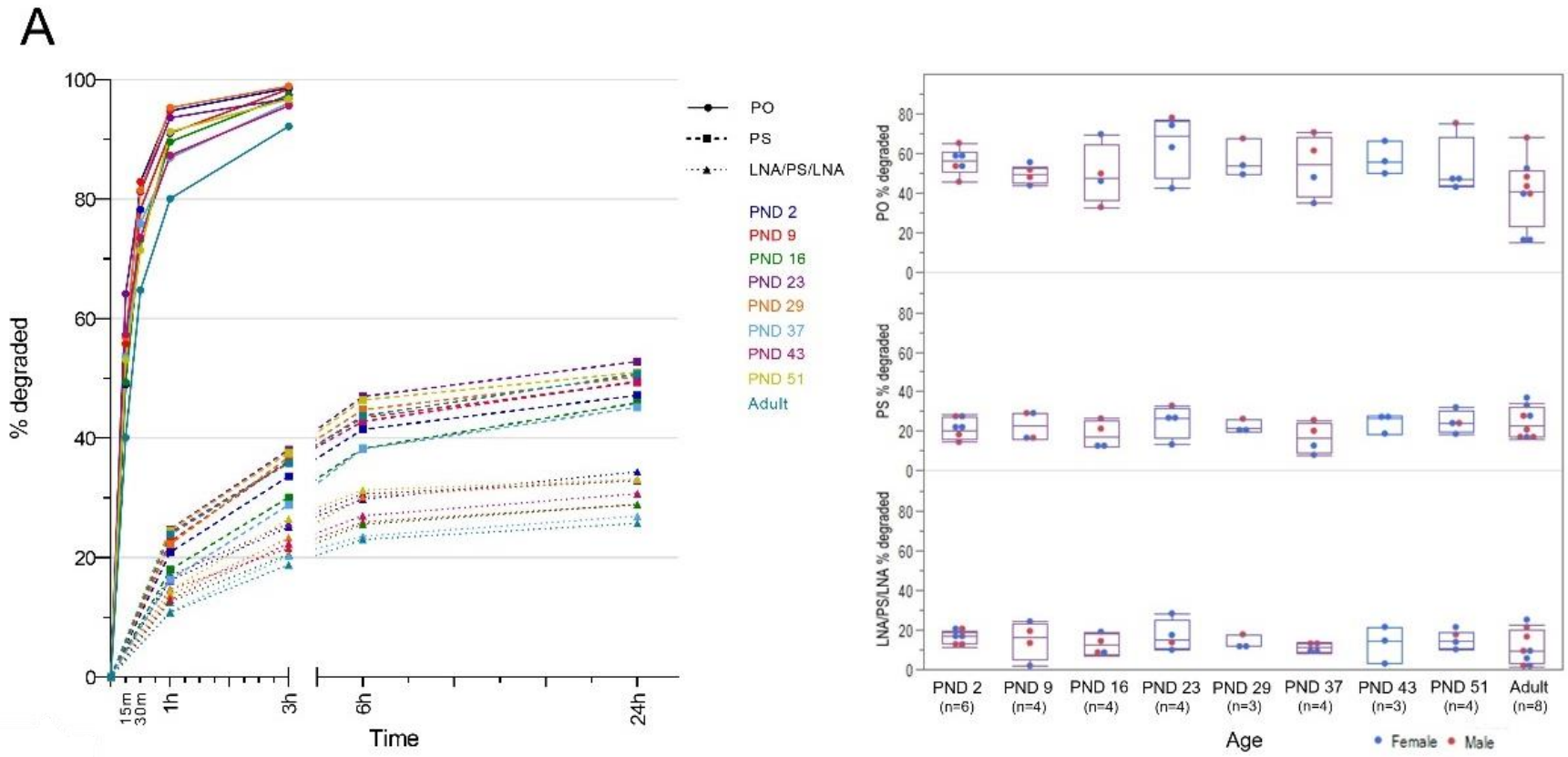
A
% degraded
100
80
60
40
20
0
15m
30m
1h
3h
6h
24h
Time
PO
PS
LNA/PS/LNA
PND 2
PND 9
PND 16
PND 23
PND 29
PND 37
PND 43
PND 51
Adult
PO % degraded
PS % degraded
LNA/PS/LNA % degraded
PND 2 (n=6)
PND 9 (n=4)
PND 16 (n=4)
PND 23 (n=4)
PND 29 (n=3)
PND 37 (n=4)
PND 43 (n=3)
PND 51 (n=4)
Adult (n=8)
Age
Female
Male

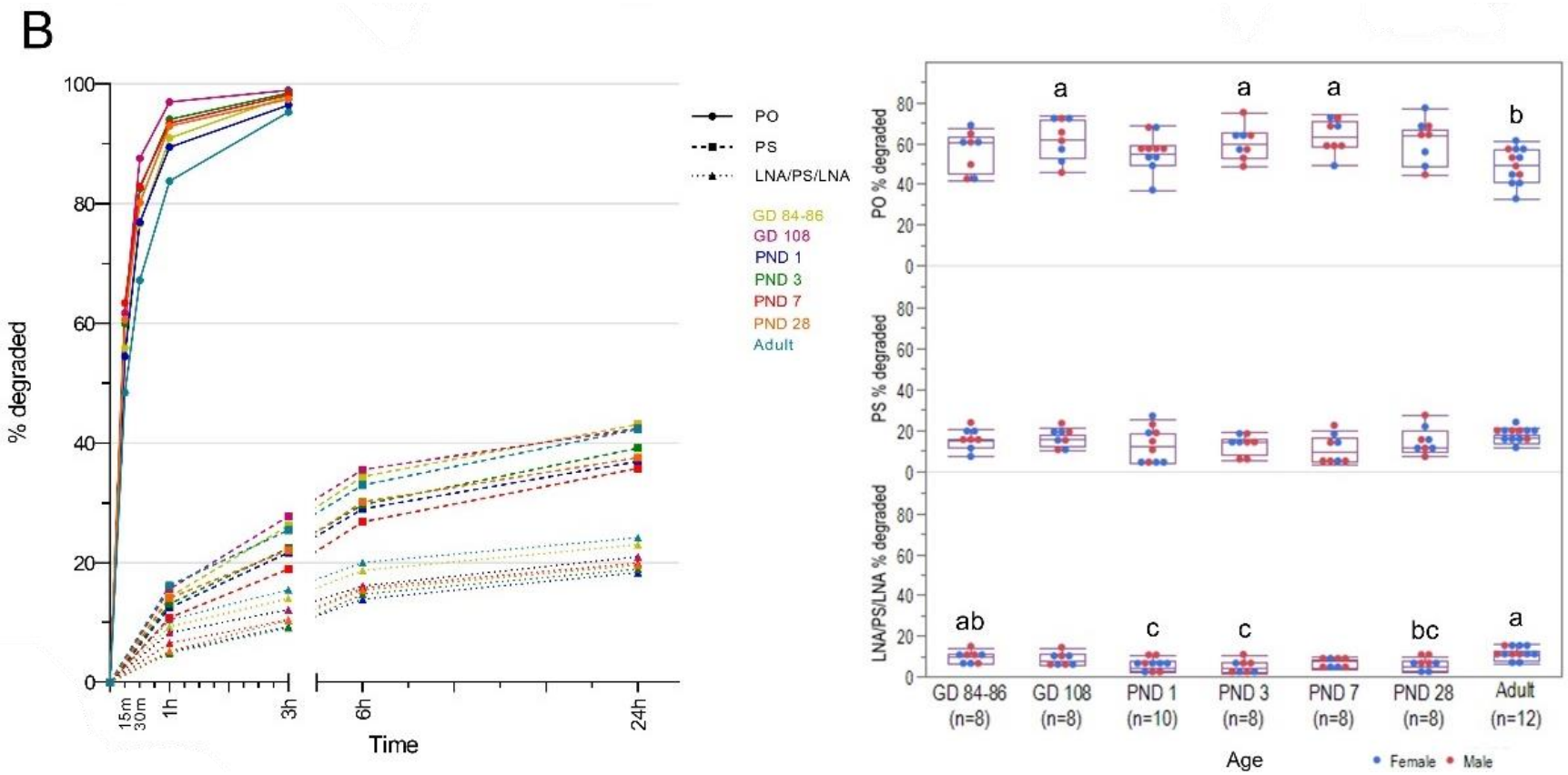
B
% degraded
Time
15m
30m
1h
3h
6h
24h
PO
PS
LNA/PS/LNA
GD 84-86
GD 108
PND 1
PND 3
PND 7
PND 28
Adult
PO % degraded
PS % degraded
LNA/PS/LNA % degraded
a
a
a
b
ab
c
c
bc
a
GD 84-86 (n=8)
GD 108 (n=8)
PND 1 (n=10)
PND 3 (n=8)
PND 7 (n=8)
PND 28 (n=8)
Adult (n=12)
Age
Female
Male

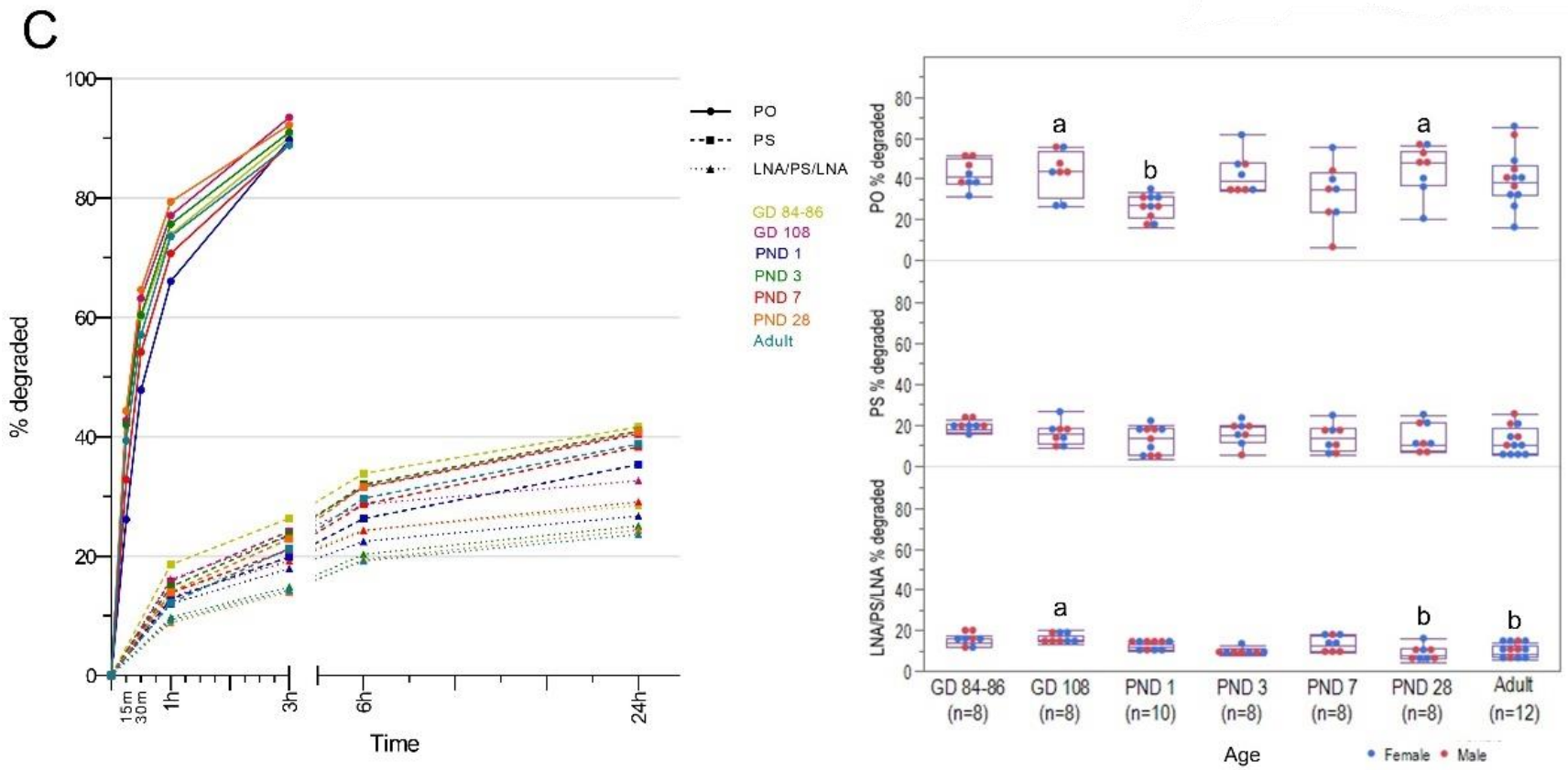
C
% degraded
Time
15m
30m
1h
3h
6h
24h
PO
PS
LNA/PS/LNA
GD 84-86
GD 108
PND 1
PND 3
PND 7
PND 28
Adult
PO % degraded
PS % degraded
LNA/PS/LNA % degraded
a
b
GD 84-86 (n=8)
GD 108 (n=8)
PND 1 (n=10)
PND 3 (n=8)
PND 7 (n=8)
PND 28 (n=8)
Adult (n=12)
Age
Female
Male

Figure 3.9. Degradation of isosequential ASOs: unmodified (PO), all-PS (PS), and LNA/PS/LNA gapmer (RTR5001) in (**A**) plasma, (**B**) kidney, and (**C**) liver over time in the developing and adult Göttingen Minipig. Nuclease activity is represented by the percentage of degraded ASO fraction for each incubation time on the left panel: PO (0, 115, 30, 60, 180 min), PS and LNA/PS/LNA (0, 1, 3, 6, 24 h). The rate of ASO degradation for the two modified sequences slowed down between 6 and 24h of incubation. The degraded ASO fraction percentages at the 15 min (PO) and 1 h (PS, LNA/PS/LNA) time points between different age groups are presented in the right panels. Age groups not sharing the same letter are significantly different ($p < 0.05$).

The 3'-exonucleases in the kidney and liver presented ontogeny profiles that were different from the ones of the endonucleases (Figure 3.10B). Kidney *ENPP1* showed its lowest expression at PND 3, which was followed by an increase to its highest level at PND 7, while the other age groups showed intermediate values ($p = 0.0142$). Liver *ENPP1* remained lowly expressed from PND 3 until PND 28 before increasing to a higher level in adulthood that was comparable to the expression at the fetal stages until PND 1 ($p = 0.0001$). On the other hand, *PDE1B* expression remained unchanged throughout development in both kidney and liver ($p = 0.0581$; $p = 0.0720$, respectively). A sex–age interaction in *TREX1* expression was detected in both organs (kidney: $p = 0.0299$; liver: $p = 0.0001$, respectively). Kidney *TREX1* expression in males exhibited a higher level at PND 28 than in the perinatal stages, with other age groups showing intermediate values ($p = 0.0117$). Kidney *TREX1* expression remained low for the first week of life in females, before gradually increasing until adulthood ($p = 0.0001$). Similarly, a higher expression of *TREX1* was seen in the adult female liver samples ($p = 0.0001$). Meanwhile, a lower liver *TREX1* expression in adult males was observed compared to GD 108, with the other age groups showing values in between ($p = 0.0295$). These observed ontogeny profiles in the biobank samples are mostly in congruence with the expression patterns seen in the samples from the in vivo study (Figure S3.4A-B).

A

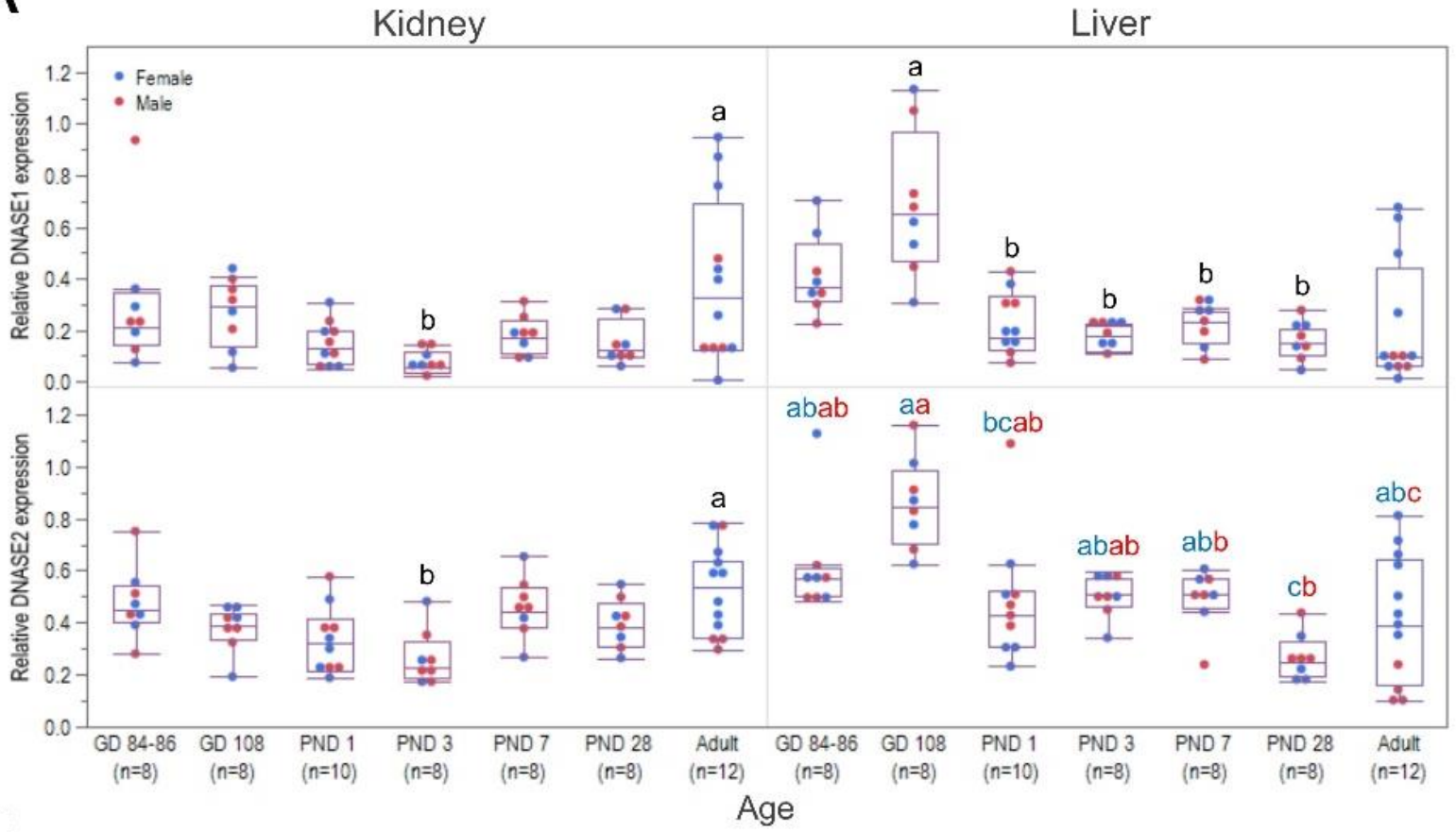
Kidney
Liver
Female
Male
Relative DNASE1 expression
Relative DNASE2 expression
0.0
0.2
0.4
0.6
0.8
1.0
1.2
a
b
abab
aa
bcab
ababab
abb
cb
abc
GD 84-86 (n=8)
GD 108 (n=8)
PND 1 (n=10)
PND 3 (n=8)
PND 7 (n=8)
PND 28 (n=8)
Adult (n=12)
Age

B

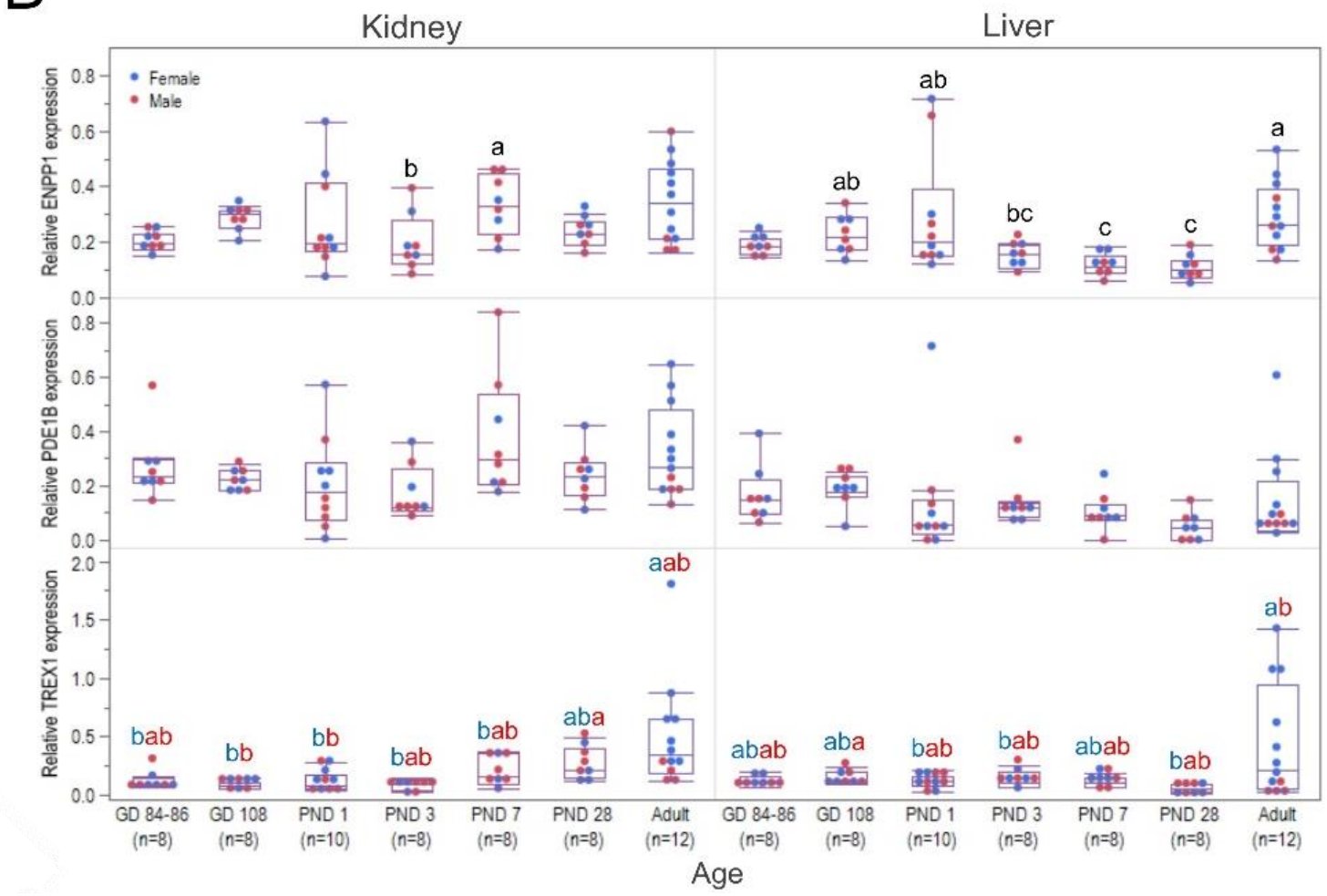
Kidney
Liver
Female
Male
Relative ENPP1 expression
Relative PDE1B expression
Relative TREX1 expression
0.0
0.2
0.4
0.6
0.8
1.0
1.5
2.0
b
a
ab
ab
bc
c
c
a
bab
bb
bb
bab
bab
aba
aab
abab
aba
bab
bab
abab
bab
ab
GD 84-86 (n=8)
GD 108 (n=8)
PND 1 (n=10)
PND 3 (n=8)
PND 7 (n=8)
PND 28 (n=8)
Adult (n=12)
Age

C

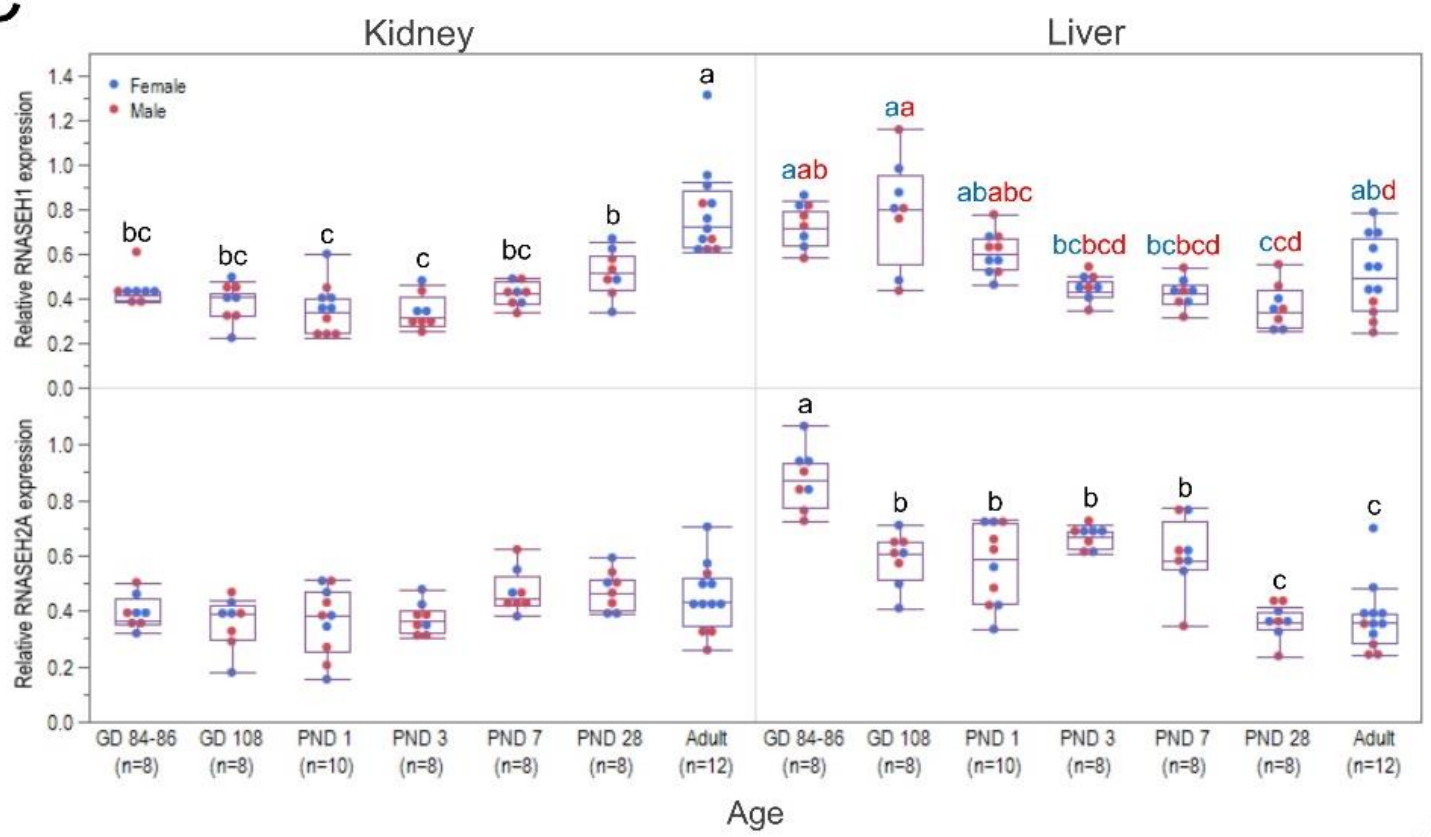
Kidney
Liver
Female
Male
Relative RNASEH1 expression
Relative RNASEH2A expression
1.4
1.2
1.0
0.8
0.6
0.4
0.2
0.0
bc
bc
c
c
bc
b
a
aab
aa
ababc
bcbcd
bcbcd
ccd
abd
a
b
b
b
b
c
c
GD 84-86 (n=8)
GD 108 (n=8)
PND 1 (n=10)
PND 3 (n=8)
PND 7 (n=8)
PND 28 (n=8)
Adult (n=12)
Age

Figure 3.10. Relative gene expression of nucleases for ASO metabolism and pharmacologic activity over time in the developing and adult Göttingen Minipig. Endonucleases: *DNASE1* and *DNASE2* (**A**); 3'-exonucleases: *ENPP1*, *PDE1B*, and *TREX1* (**B**); and *RNASEH1* and *RNASEH2A* (**C**) were evaluated in kidney and liver. Age groups not connected by same letter are significantly different ($p < 0.05$). When sex–age interaction was detected, the gene expression differences between age groups were evaluated separately for females and males. Same colored letters belong to the same sex, and age groups not sharing the same letters are significantly different ($p < 0.05$).

The stability of the two modified isosequential ASOs and marked susceptibility of PO ASO to nuclease activity in the kidney and liver homogenates were similar to what was observed in the plasma (Figure 3.9B-C, left panels). However, reaction rates toward the PO ASO in the kidney homogenates were significantly higher than in the liver except in the adult group (Figure S3.5). The rate of PS ASO degradation was observed to be higher in the liver at GD 84–86, whereas it was seen higher in the kidney for the adult group. The opposite observations for PO ASO were seen in the LNA/PS/LNA gapmer, wherein degradation generally proceeded faster in the liver of the fetal and juvenile age groups. A relatively higher activity toward PO ASO was observed at GD 108 and PND 3–7 in the kidney ($p = 0.0001$), while higher activity was seen at GD 108 and PND 28 in the liver ($p = 0.0156$) (Figure 3.9B-C, right panels). On the other hand, lower activity in the kidney was observed in the adult group, whereas it was detected immediately after birth in the liver homogenates. No statistically significant difference was observed among the different age groups in terms of activity toward the isosequential all-PS ASO (kidney: $p = 0.4758$; liver: $p = 0.3568$). Degradation of the LNA/PS/LNA gapmer in the kidney was slower at PND 1–3, but it gradually accelerated until adulthood ($p = 0.0001$). In contrast, higher activity in the liver was seen at GD 108, and a lower activity was seen at PND 28 and in the adult group ($p = 0.0033$). Spearman's rank correlation analysis on all age groups together showed a moderate correlation between liver DNASE1 expression and the activity toward the LNA/PS/LNA gapmer in the liver ($p < 0.00026$, $r = 0.4175$).

3.3.6 Ontogeny of ribonuclease H expression in the kidney and liver

Kidney *RNASEH1* expression showed a postnatal maturation profile reaching the highest level in adulthood ($p = 0.0001$). No maturation profile was noted for kidney *RNASEH2A* ($p = 0.1458$). In contrast, the liver expression of the two ribonuclease Hs displayed a gradual decrease postnatally (Figure 3.10C). A sex–age interaction was detected in the expression of *RNASEH1* in the liver ($p = 0.0011$). Although both males and females showed lower expression at PND 3 than in the gestational period, this lower expression was detected until PND 28 ($p = 0.0001$) and then increased

in adulthood in females, reaching similar values to those in the youngest age groups. In contrast, the lower transcription at PND 3 than during gestation in males remained unchanged until adulthood (p = 0.0001). For both male and females, liver *RNASEH2A* expression showed the highest expression values on GD 84–86, an initial drop in expression on GD 108, and a second one on PND 28 (p = 0.0001). In general, these ontogeny profiles in the biobank samples are in accordance with the expression patterns seen in the in vivo study samples (Figure S3.4C).

3.4 Discussion

In the present study, the safety, exposure, and pharmacological effect of a model LNA gapmer, RTR5001, were assessed in a limited number of juvenile Göttingen Minipigs after repeated SC dosing. The rapid growth and development of the pediatric population can influence the pharmacokinetics and pharmacodynamics of therapeutic agents, leading to potential adverse effects [65–67]. RTR5001 was previously tested in adult minipigs, in which the liver and kidney were the main target organs of distribution/toxicity, and its pharmacologic effect (i.e., reduced total and LDL cholesterol) was demonstrated [31]. Similar clinical chemistry and toxicity findings were observed in the juvenile minipigs in our study. However, differences in plasma and tissue exposure, as well as pharmacologic activity, were seen compared with the adult data. To elucidate these findings, the expression and activity of nucleases involved in ASO metabolism and pharmacologic activity were assessed in the blood, kidney, and liver of juvenile Göttingen Minipigs. For clarity, we will discuss our results following the order in which ASOs interact in the animal. First, we will discuss the metabolism and exposure in the blood compartment, followed by distribution, metabolism, and finally toxicities in the tissue compartments. The remainder of the discussion will be devoted to other relevant toxicities and the pharmacologic effect of the model LNA gapmer.

The nuclease activity profiles in the blood and tissue compartments were assessed using isosequential PO, all-PS, and RTR5001 (LNA/PS/LNA gapmer) ASOs. Our findings for the three isosequential ASOs were similar in the blood and tissue compartments, with RTR5001 showing excellent stability for nucleases, followed by all-PS, and with the PO sequence being very susceptible to degradation. This is in accordance with previous results in adult rodents, NHPs, and humans for the blood compartment [56,68], liver [69–71], and kidney [72]. PO ASOs are degraded within minutes in the blood and tissue compartments by endogenous nucleases, and thus,

chemistry modifications of the phosphate bonds and sugar moiety of the oligonucleotide sequence are warranted to improve nuclease stability [6,22,73–75]. In addition to ASO chemistry modifications, sequence length also influences the rate of metabolism, as shorter sequences are digested more slowly [71]. Therefore, initial degradation products from nuclease digestion compete with full-length sequences and contribute to their stability [76]. This can influence the rate of nucleolytic metabolism in vitro, as shown by the plateau in our activity assay between 6 and 24h incubation.

For the blood compartment, no age-related differences in nuclease activity were observed for any of the investigated ASOs. 3'-Exonuclease is the main nuclease that acts on PS-modified ASOs in the blood compartment similar to PO [77], with the former having more significant enzymatic stability due to its backbone modification [77–80]. Differences in the ontogeny profile of the three 3'-exonucleases regarding their gene expression were observed. Among those three nucleases, ENPP1 is secreted in the plasma [81] and has been implicated in the degradation of ASOs in adult human plasma [20]. In contrast, PDE1B and TREX1 are localized mainly intracellularly [58,82], which suggests that they generally play a role in ASO metabolism in white blood cells and tissues. Although we have seen differences in *ENPP1* expression among different age groups, this did not translate to differences in activity in plasma. As discrepancies between RNA and protein abundance have been described before [83,84], mRNA is not always a good indicator of activity [85,86]. On the other hand, the additional flank modifications using other generations of chemistry modification, such as LNA leading to a gapmer design, provide additional/sufficient protection against exonucleases. Endonucleases can degrade LNA gapmers but do this over a more extended incubation period [56,68] in the plasma. However, due to increased plasma protein binding and excellent biodistribution properties of gapmer ASOs [87–89], they are quickly distributed to target organs. In the case of RTR5001, these are the kidneys and the liver. Thus, the main factor for plasma clearance is the initial rapid tissue distribution [87,90] instead of ASO metabolism.

The rapid elimination of RTR5001 from the circulation, i.e., within 24 h post-administration, was similar to the data in adult minipigs [31]. The short distribution half-life in the plasma of around 2–5 h for the various juvenile age groups complied with data on second-generation ASOs [91,92]. The biodistribution of ASOs from the plasma to other tissue compartments is related to plasma protein binding as well as to cell-surface proteins in the target organs [87,93–96], with plasma albumin

being the main plasma protein responsible for protein binding in the blood compartment [87,97–100], preventing renal clearance [76,101]. In our study, plasma albumin concentrations in the juvenile age groups were in accordance with already published reference values, and they were 10 to 60% lower than in 6-month-old minipigs [62]. Therefore, the lower plasma albumin concentration observed in the younger age groups could partly explain the lower C_{max} and $AUC_{0–24h}$ values seen at PND 2 to 23 compared to the adult minipig (Figure S3.6A-B) [31]. Of note, the juvenile minipigs were dosed up to eight times at a weekly interval, whereas all the adult minipigs were dosed only four times with a 5-day interval. After the first administration, the C_{max} of RTR5001 was 43% lower in juvenile (at PND 2) minipigs than in adult minipigs, whereas the $AUC_{0–24h}$ was 78% lower. After four doses, these values were still lower in juvenile compared to the adult minipigs. As the peak levels of ASOs do not tend to increase with repeated administration due to their wide tissue distribution [88,102,103], no differences were observed between the first and fourth dose. However, after the eighth and final dose in the juvenile minipigs, both parameters gradually increased, with C_{max} being 29% higher than the adult values (after four doses), whereas the $AUC_{0–24h}$ was still 50% lower than the adult values. This lower $AUC_{0–24h}$ could be due to a faster renal clearance of RTR5001 in the juvenile age groups than in the adult. On the other hand, the plasma trough levels after each weekly dose remained relatively very low, which is in contrast to the behavior in older juvenile age groups where at the end of the experimental period, trough levels were slightly higher and indicative of tissue saturation, as has been described before for ASOs after repeated administration [16,21,50,101,104,105].

The highest concentrations of RTR5001 were seen in the kidney and liver and were similar in the various juvenile age groups, with the kidney showing higher exposure than the liver. This has been demonstrated for the biodistribution of LNA gapmers [12,106,107]. However, the relative kidney exposure in the juvenile minipigs was less than the 5-fold difference observed in the adult minipig after the fourth dose (Figure S3.6C) [31]. This could be explained by the use of different bioanalytical methods. While in our study, LC-MS/MS was used, for the published adult minipig exposure data, a hybridization enzyme-linked immunosorbent assay (hELISA) was used to measure the tissue concentrations of RTR5001. Although this method has good sensitivity to the parent compound, it can cross-react with 3’- and 5’-end putative metabolites [108–110]. As we noted that RTR5001 was metabolized at a higher rate in the adult kidney homogenate than in the younger age groups, the

higher concentration in the adult kidney could be a cumulative concentration of the parent RTR5001 and its metabolites resulting from the relatively unspecific hELISA.

After repeated dosing, there was no apparent accumulation of the ASO [16,104] in the kidney. The presence of RTR5001 was confirmed in the cytoplasm of renal tubular cells by ISH and IHC immediately after the first dose, and it was similar with successive dosing. This stable exposure observed in the youngest age groups (PND 2, 9, and 16) might be due to the immaturity of the renal cortex [63] resulting in reduced uptake of ASOs. This finding is in line with current knowledge that completion of nephrogenesis occurs at PND 21 in pigs [111]. In contrast, the lower exposure values observed at PND 43 and PND 51 could be due to the high degree of tubular degeneration/regeneration and minimal to moderate renal fibrosis and glomerulosclerosis observed in these age groups. Hence, these injured tubules might have limited capacity to take up LNA ASOs further. Moreover, the distinct basophilic cytoplasmic granules in renal tubular cells previously seen in the adult minipig [31] and other species [13,112,113] were observed only at PND 51. The administration of RTR5001 resulted in degenerative/regenerative changes in the kidneys, similar to what was observed in adult minipigs [31]. However, the glomerulosclerosis seen in minipigs at PND 43 and 51, which received seven and eight doses respectively, was not previously observed in the adult minipigs that were dosed only four times. Despite these histological findings, clinical chemistry did not suggest a decrease in kidney function in the juvenile minipigs as opposed to what was observed in the adult minipig.

For the liver, an increasing exposure was observed after repeated dosing, suggesting accumulation. This coincided with the highest plasma trough level in the two oldest age groups, suggesting higher tissue accumulation than in the younger age groups. ISH and IHC confirmed the accumulation of RTR5001 in the liver, i.e., in the Kupffer cells. However, no distinct basophilic cytoplasmic granules were seen, unlike in the adult minipig and in other species [13,31,112,113]. Furthermore, in contrast to the adult minipig, no hepatocellular single-cell necrosis/apoptosis was seen, although a minimal to mild increase in serum transaminase was observed in some age groups, indicating liver insult.

In both kidney and liver homogenates, differences in activity among the different age groups were observed toward each isosequential ASO. In the kidney, PO degradation appeared quicker in the

youngest age groups than in the adult, whereas for the liver, slower degradation was observed at PND 1. Although PO are metabolized mainly by 3'-exonucleases in tissues [71,72,114,115], the activity profile for both tissues does not correlate with any of the three 3'-exonuclease expression patterns. Furthermore, no difference was seen in the degradation of the all-PS sequence across all the age groups. PS degradation appears to be more variable and cell-type specific, with either having 3'- or 5'-degradation profiles, with endonuclease-mediated degradation not generally observed [69,71,77,78]. Regarding RTR5001 degradation, the highest metabolism in the kidney was seen in the adult group, and the lowest was seen after birth until PND 3. This observation fits the expression profile of both endonucleases (*DNASE1* and *DNASE2*) and one of the 3'-exonucleases (*TREX1*).

Similarly, the nuclease activity in the liver fits the liver endonuclease (*DNASE1* and *DNASE2*) expression pattern, for which the highest activity was seen in the GD 108 group and the lowest activity was seen in the weaning and adult groups. However, this does not fit with any of the 3'-exonucleases' expression patterns. As ASO gapmers are protected at the 3'- and 5'-end from exonuclease degradation by the additional flank modifications, they are known to be initially cleaved by endonucleases in the tissue [69,70,116] of different species [16,50], leading to short fragments that exonucleases may degrade further. As such, this supports the correlation between liver nuclease activity and endonuclease expression pattern, indicating that the nuclease activity in the liver of minipigs initially proceeds through endonucleases. As this correlation was not observed for the kidney, the nuclease activity seen in the kidney seems to be mainly due to 3'-exonucleolytic degradation and not by initial cleavage by endonucleases. Accordingly, it was observed after LNA gapmer administration in rats that only the parent compound and a metabolite with one nucleotide cleaved at the 3'-end were detected in the kidney [117]. In contrast, further degradation from the 3'-end to shorter metabolites was observed in the liver. These findings support our hypothesis regarding the metabolism of LNA gapmer in the kidney discussed above and the higher kidney-liver exposure ratio seen previously in adult minipigs [31], as metabolites with only one cleaved nucleotide cross-react more than shorter metabolites in an hELISA [108]. Hence, the differential abundance and activity of endo- and exonucleases in different organs and species can affect the metabolic pathway of LNA gapmers. Moreover, as a disparity between *in vitro* incubation and animal models can be observed [69,118], careful interpretation of these data, together with metabolite profiling, is warranted.

ASO degradation differed between the two organs in juvenile minipigs; i.e., unmodified ASOs were degraded faster in the kidney, whereas the LNA gapmer was degraded faster in the liver. As ASO metabolism serves to be the critical driver for its tissue elimination [101,119], the different nuclease activity in both organs and juvenile age groups relative to the adult poses a concern of potential toxicity and underdosing. However, our observation regarding the nuclease gene expression and activity is not enough to explain the exposure profile seen in the different age groups of minipigs. Other factors, such as plasma and cell-surface protein binding, extracellular matrix binding, tissue saturation, and organ maturity, should be considered and further investigated [76,101,104,120–122].

In general, the juvenile minipigs showed a similar toxicity profile after RTR5001 administration as in the adult minipig [31]. Clinical observations, clinical pathology, gross, and histopathological findings were similar to those observed in adult minipigs. In addition to renal tubular degeneration/regeneration, glomerulosclerosis was observed in the piglets at PND 43 and 51, which was considered to be due to repeated dosing of the test compound. Accumulation of LNA ASO in the lymph nodes as evidenced by IHC and ISH was observed, which was similar to that seen in the adult minipig and other species [13,31,112]. Likewise, no clinical or gross post-mortem observations were noted aside from the expected inflammatory reaction regarding the injection site, as in adult minipigs [31].

There was no apparent decrease in the total complement after each RTR5001 administration compared to the pre-dose levels, which corresponds to previous findings in adults of other species and humans [123,124]. This is also in accordance with the findings in the adult minipig, suggesting a lower sensitivity of minipigs for this parameter than NHPs, which are known to be over-predictive for man [31,125,126]. The total complement level was not detectable at PND 1, but the adult (control) level [31] was approximately reached from PND 8 onwards. This observation is in line with what has been seen in newborn humans [127]. On the other hand, the increase in total complement level measured pre-dose at PND 29 until 51 after repeated administration of LNA ASO could be due to chronic inflammation [127]. ASOs exhibit proinflammatory characteristics [13,29,128], which are seen in the juvenile minipigs as inflammatory changes in the kidneys, the accumulation of mononuclear cells in the lymph nodes, and chronic inflammation with fibrosis at the injection sites.

Regarding pharmacologic action, binding to the RNA target is critical for the activity of ASOs [129]. Moreover, the nonclinical safety package of ASOs should include a pharmacologically cross-reactive species. Therefore, the selected species should express a homologous RNA target. In this respect, the Göttingen Minipig is a potential alternative non-rodent model due to its phylogenetic proximity with humans, and this is made possible by its recent genome annotation. Despite the fact that RTR5001 has a single-end mismatch to the minipig RNA target, its location in the sequence does not ablate its pharmacologic activity [31]. The pharmacologic activity of RTR5001, i.e., decreasing total cholesterol and LDL cholesterol, was similar in the juvenile and adult minipig, but only from PND 43 onwards when compared to the controls and previous published data [62]. The higher total cholesterol values observed for the treated groups at PND 29 and 37 are within the range of historical control data for minipigs [62]. However, the total cholesterol values seen for the treated PND 23 piglets are higher than the available PND 28 data in minipigs. As these published cholesterol values were observed to increase gradually from PND 2 and peak at PND 28, we hypothesize that the actual peak is somewhere in between PND 21 and 28, requiring further investigation to address this observation.

The late onset of pharmacologic effect in the juvenile minipig could be due to several factors. Particular cell-type-specific nucleic acid-binding surface proteins [93,94,121] have been identified and were noted to be essential for cellular uptake. The presence and abundance of these proteins can affect the tissue disposition of ASOs [76,130,131]. Moreover, once inside the cell, ASOs could bind to specific proteins and get sequestered away from the target RNA and RNase H [121,132–135]. More broadly, aside from binding to ASOs inside the cell, some proteins also contribute to their activity [22,136]. Therefore, we hypothesize that the specific proteins involved in the uptake and trafficking [137] of ASO are also under-expressed in the neonate. Thus, further investigation is needed on the ontogeny of these proteins. Moreover, other factors such as the turn-over kinetics of protein translation [101,138,139] and rate of ASO-directed RNase H activity (usually minutes to hours) [121] can have an impact on the degradation of the target RNA. As such, these factors could influence the dose to be used.

In addition, the abundance of RNase H1 is another critical component that can affect the ASO-driven cleavage mechanism [121]. Both *RNASEH1* and RN*ASEH2* were included in our panel of genes for expression analysis, even though RNase H1 is considered responsible for RNA degradation in

the RNA–DNA heteroduplex [52] in both the cytoplasm and nucleus [140]. On the other hand, RNase H2 has been reported to be mainly localized in the nucleus and associated with chromatin, which would impede its participation in the antisense effects of ASOs [8]. However, the 15PC3 cell line presents RNase H2 in both the cytoplasm and nucleus instead of the strict nuclear localization in other cell lines [53]. This suggests that depending on cell type, the subcellular localization of RNase H2 can have catalytic activity toward the RNA in duplex. As we were supposed to do an *in vitro* RNase H assay using tissue homogenates, seeing the link between RNase H1 and H2 expression with degradation of ASO substrate would be necessary, since RNase H2 is fully capable of degrading ASO in cell lysates [8,53]. However, no activity was seen in vitro (data not shown) with our biobank samples. This could be due to the low abundance of both enzymes or unspecific reaction binding in the homogenate itself from other proteins [121,132–135].

The expression of *RNASEH1* showed a different ontogeny profile for kidney and liver, with its expression level gradually increasing in the kidney and decreasing until weaning in the liver followed by an increased again toward adulthood for females. The *PCSK9*, the RNA targeted by RTR5001, is found abundantly in the liver and was successfully knocked down previously by LNA ASOs in the adult minipig, human, and several other species [26,31,47,141,142]. The higher expression level of *RNASEH1* observed in the liver of adult females than the other juvenile age–sex groups suggests that the RNase H1 level may play a role in the delayed pharmacologic effect seen in the juvenile minipigs, since the data on adults were only from females.

3.4.1 Study limitations

In our in vivo study, we were limited in sample size for the treated and the control animals, which could cause sample bias and reduced power. Therefore, we recommend cautious interpretation and extrapolation of these results. Despite the small group size, we still observed differences in ASO exposure and pharmacodynamic activity in the different age groups of Göttingen Minipigs, which was one of the goals of our study. For the ontogeny analysis, the inclusion of biobank samples was needed to increase the power of our study. This clearly shows that the correct sample size in a study is dependent on the (variability of the) endpoints that are investigated.

3.5 Conclusions

In conclusion, a similar toxicity profile was noted in juvenile minipigs as previously reported in adult minipigs following repeated ASO administration. Lower plasma and tissue exposure to RTR5001 were noted in younger minipigs up to weaning than in older or adult minipigs. Differences in the pharmacodynamic profile were also noted between minipigs of various ages. These differences in exposure and pharmacologic activity were partly explained by our nuclease ontogeny data, indicating that the juvenile Göttingen Minipig is a promising nonclinical model for the pediatric safety assessment of ASOs. Although we have to acknowledge the limited number of animals used in the in vivo study, our results highlight the importance of considering maturational factors in ASO dose setting in the pediatric population.

3.6 Supplementary Materials

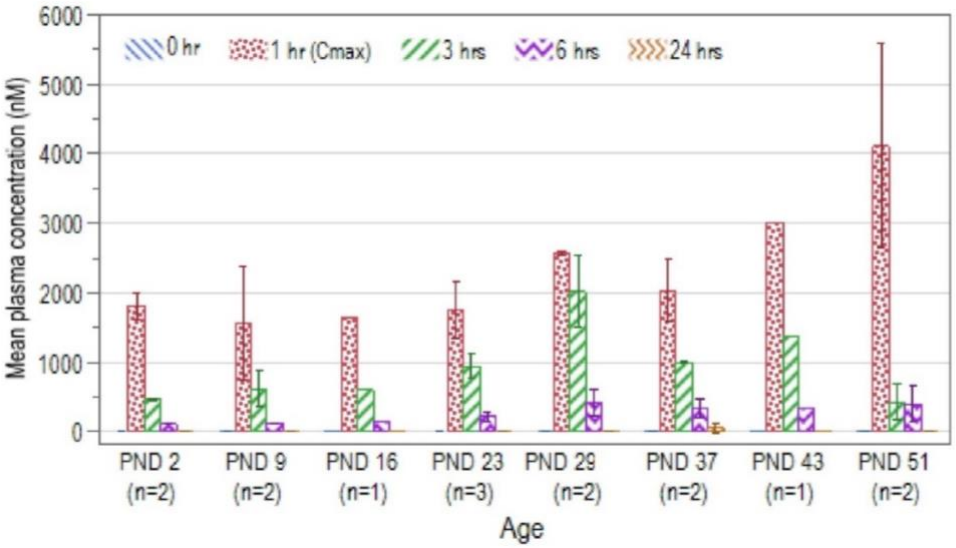

Figure S3.1. Mean ± SD plasma concentration after SC administration of RTR5001 to juvenile minipigs at 20mg/kg dose level. 0 h: trough level; C_{max}: maximum concentration.

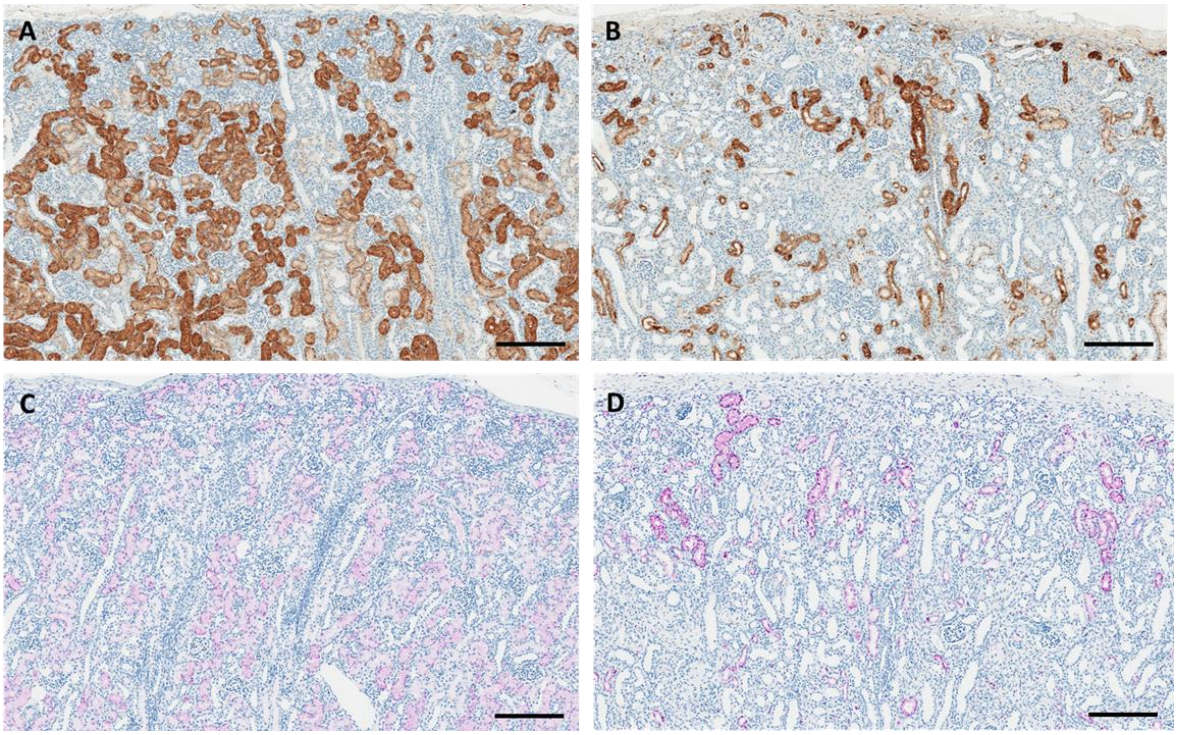

Figure S3.2. Immunohistochemistry and in situ hybridization. (**A**) Kidney, PND 30; Immunohistochemistry for RTR5001. Accumulation of RTR5001 into the proximal tubular cells (brown staining). (**B**) Kidney, PND 51, accumulation of RTR5001 in proximal tubular cells, fewer tubules and irregularly stained renal tubuli (brown staining). (**C**) Kidney, PND 51; in situ hybridization for RTR5001. Accumulation of RTR5001 into the proximal tubular cells (purple staining). (**D**) Kidney, PND 51, accumulation of RTR5001 in proximal tubular cells, fewer tubules and irregularly stained renal tubuli (purple staining). (Scale bar: A, B, C, and D = 200 µM).

A

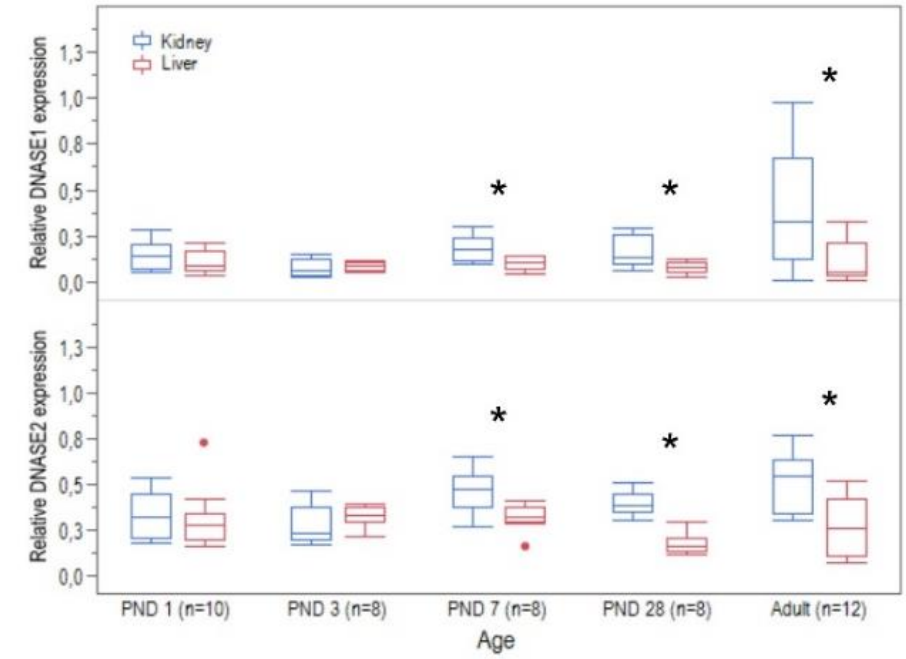
Kidney
Liver
Relative DNASE1 expression
Relative DNASE2 expression
1,3
1,0
0,8
0,5
0,3
0,0
PND 1 (n=10)
PND 3 (n=8)
PND 7 (n=8)
PND 28 (n=8)
Adult (n=12)
Age

B

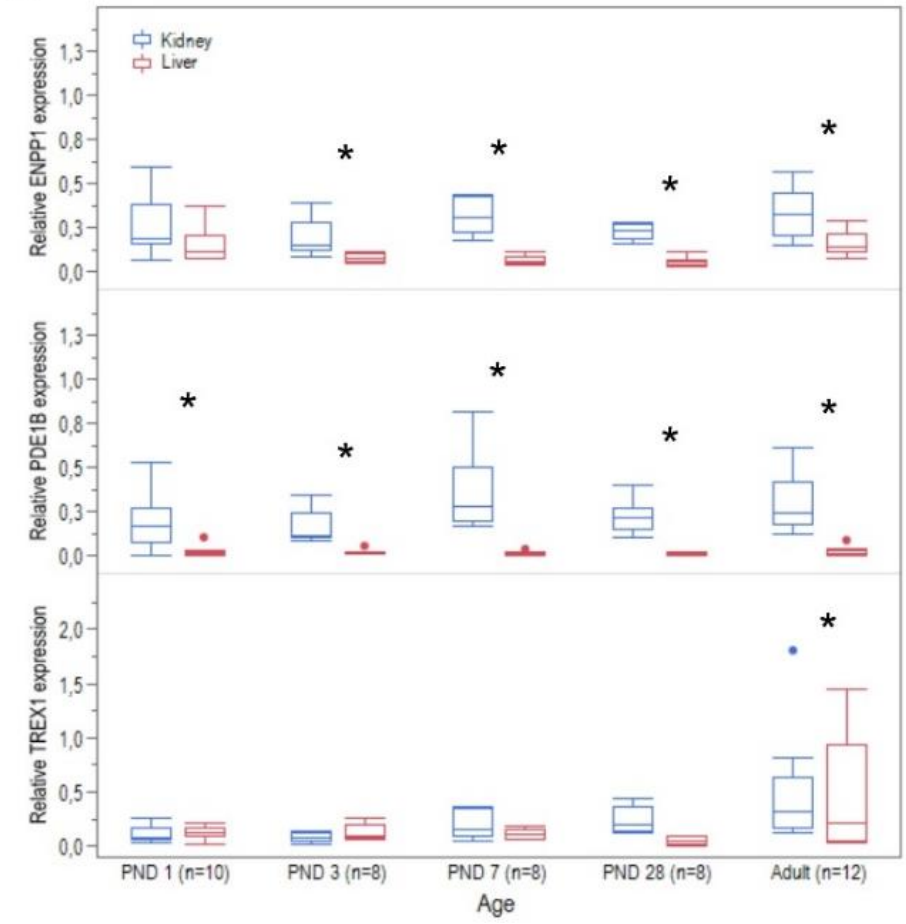
Kidney
Liver
Relative ENPP1 expression
Relative PDE1B expression
Relative TREX1 expression
1,3
1,0
0,8
0,5
0,3
0,0
2,0
1,5
PND 1 (n=10)
PND 3 (n=8)
PND 7 (n=8)
PND 28 (n=8)
Adult (n=12)
Age

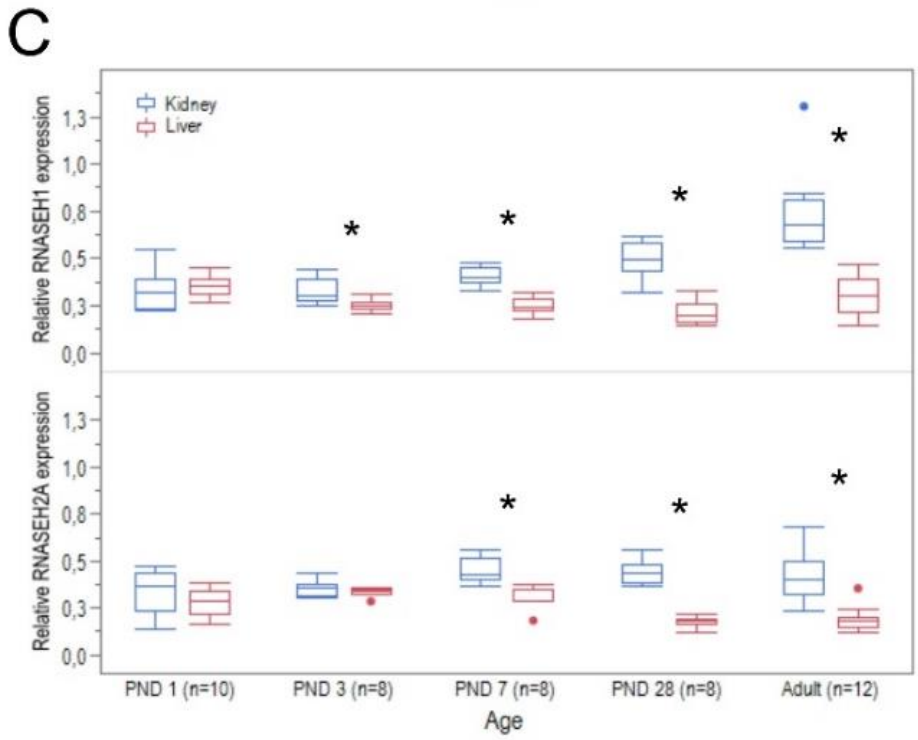

Figure S3.3. Relative gene expression of nucleases for ASO metabolism and pharmacologic activity between kidney and liver over time in post-natal and adult Göttingen Minipig. Endonucleases: *DNASE1*, and *DNASE2* (**A**); 3'-exonucleases: *ENPP1*, *PDE1B*, and *TREX1* (**B**); and *RNASEH1* and *RNASEH2A* (**C**) expression difference between the kidney and liver was considered significant (*) if $p < 0.05$.

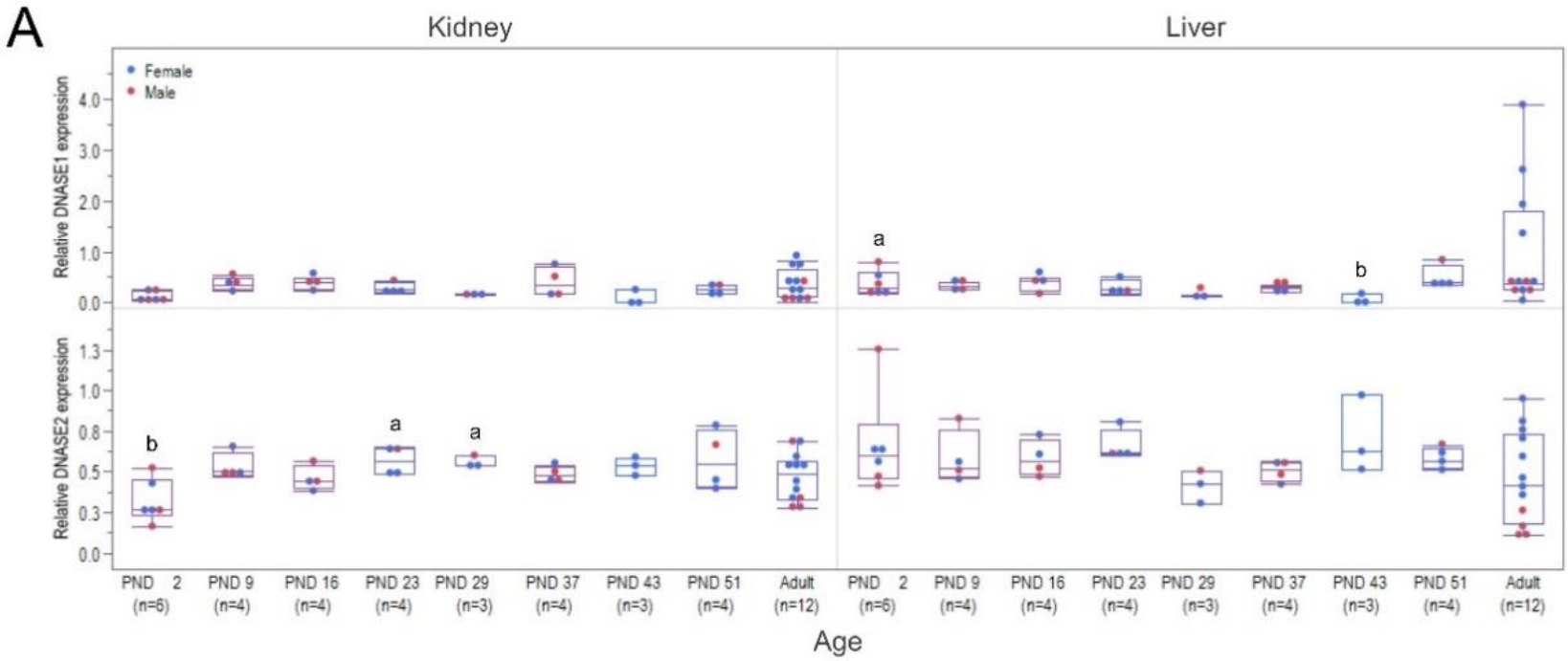
A
Kidney
Liver
Female
Male
Relative DNASE1 expression
Relative DNASE2 expression
a
b
a
a
b
PND 2 (n=6)
PND 9 (n=4)
PND 16 (n=4)
PND 23 (n=4)
PND 29 (n=3)
PND 37 (n=4)
PND 43 (n=3)
PND 51 (n=4)
Adult (n=12)
Age

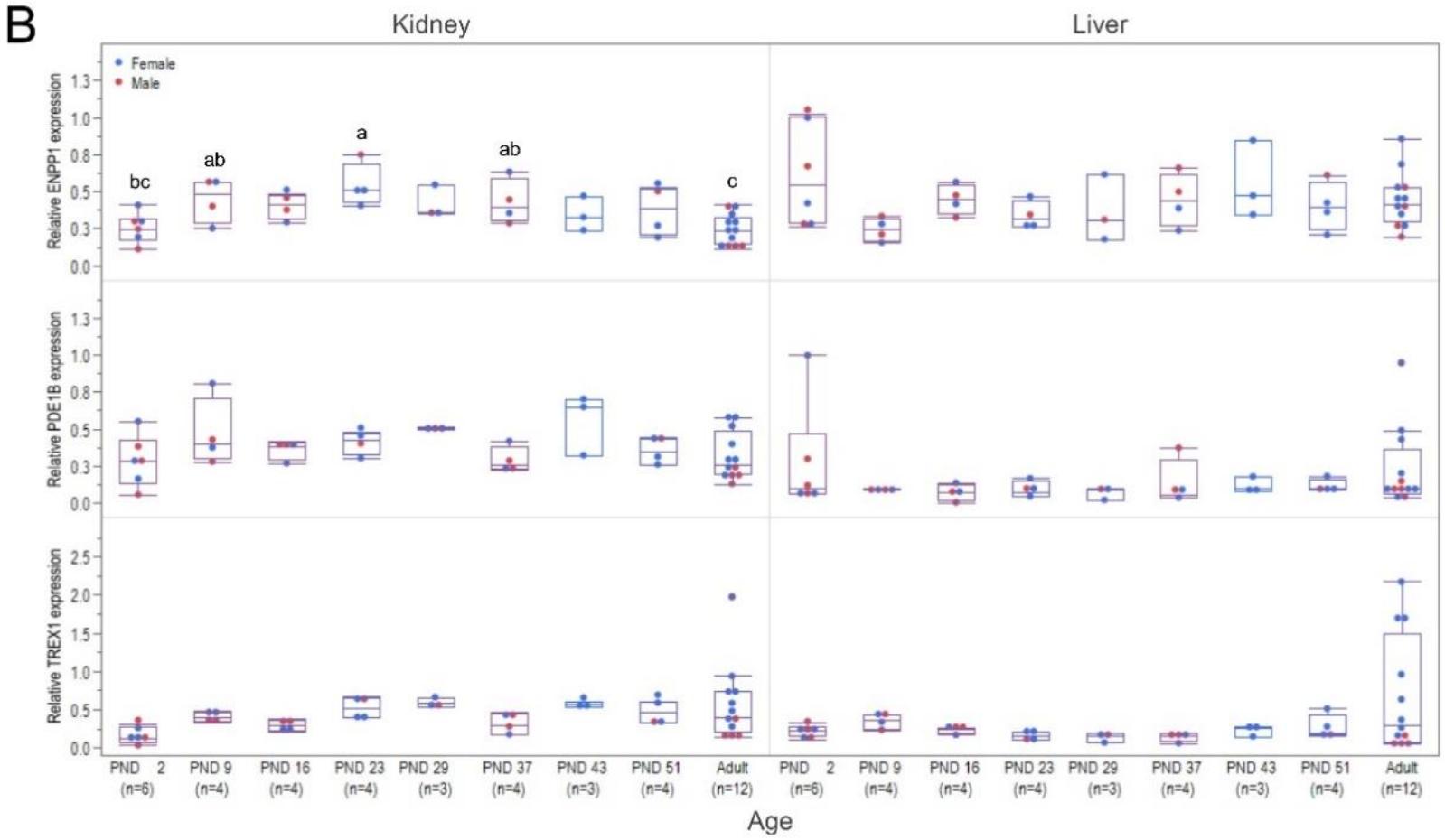
B
Kidney
Liver
Female
Male
Relative ENPP1 expression
Relative PDE1B expression
Relative TREX1 expression
bc
ab
a
ab
c
PND 2 (n=6)
PND 9 (n=4)
PND 16 (n=4)
PND 23 (n=4)
PND 29 (n=3)
PND 37 (n=4)
PND 43 (n=3)
PND 51 (n=4)
Adult (n=12)
Age

C

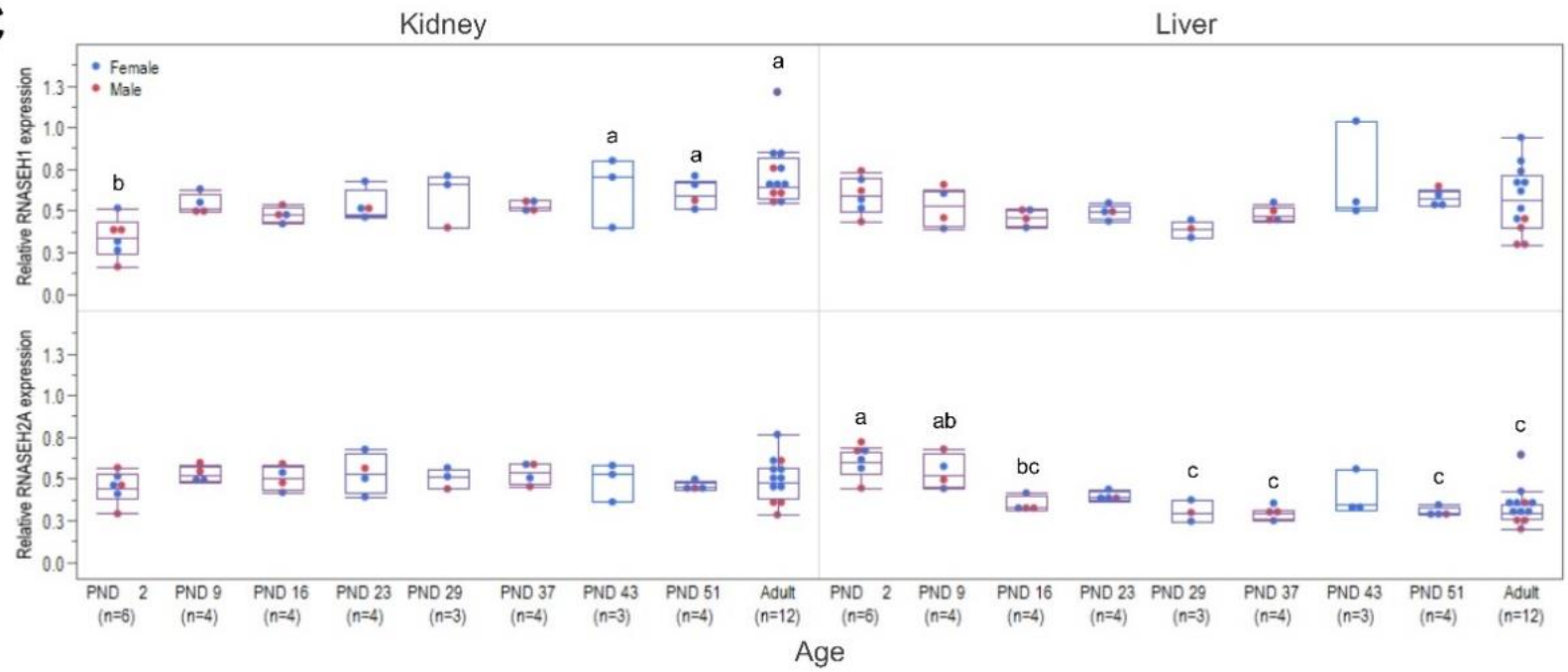
Kidney
Liver
Female
Male
Relative RNASEH1 expression
Relative RNASEH2A expression
0.0
0.3
0.5
0.8
1.0
1.3
a
b
ab
bc
c
PND 2 (n=6)
PND 9 (n=4)
PND 16 (n=4)
PND 23 (n=4)
PND 29 (n=3)
PND 37 (n=4)
PND 43 (n=3)
PND 51 (n=4)
Adult (n=12)
Age

Figure S3.4. Relative gene expression of nucleases for ASO metabolism and pharmacologic activity over time in the developing and adult Göttingen Minipig samples from the investigational toxicity study. Endonucleases: *DNASE1*, and *DNASE2* (**A**); 3'-exonucleases: *ENPP1*, *PDE1B*, and *TREX1* (**B**); and *RNASEH1* and *RNASEH2A* (**C**) were evaluated in the kidney and liver samples from the investigational toxicity study. Different letters indicate significantly different expression in the age groups. Gene expression difference was considered significant if $p < 0.05$. Statistical analysis on liver *DNASE2*, *TREX1*, and *RNASEH1*, and kidney *TREX1* was not performed as sex-age interaction was detected on previous analysis of the biobank samples.

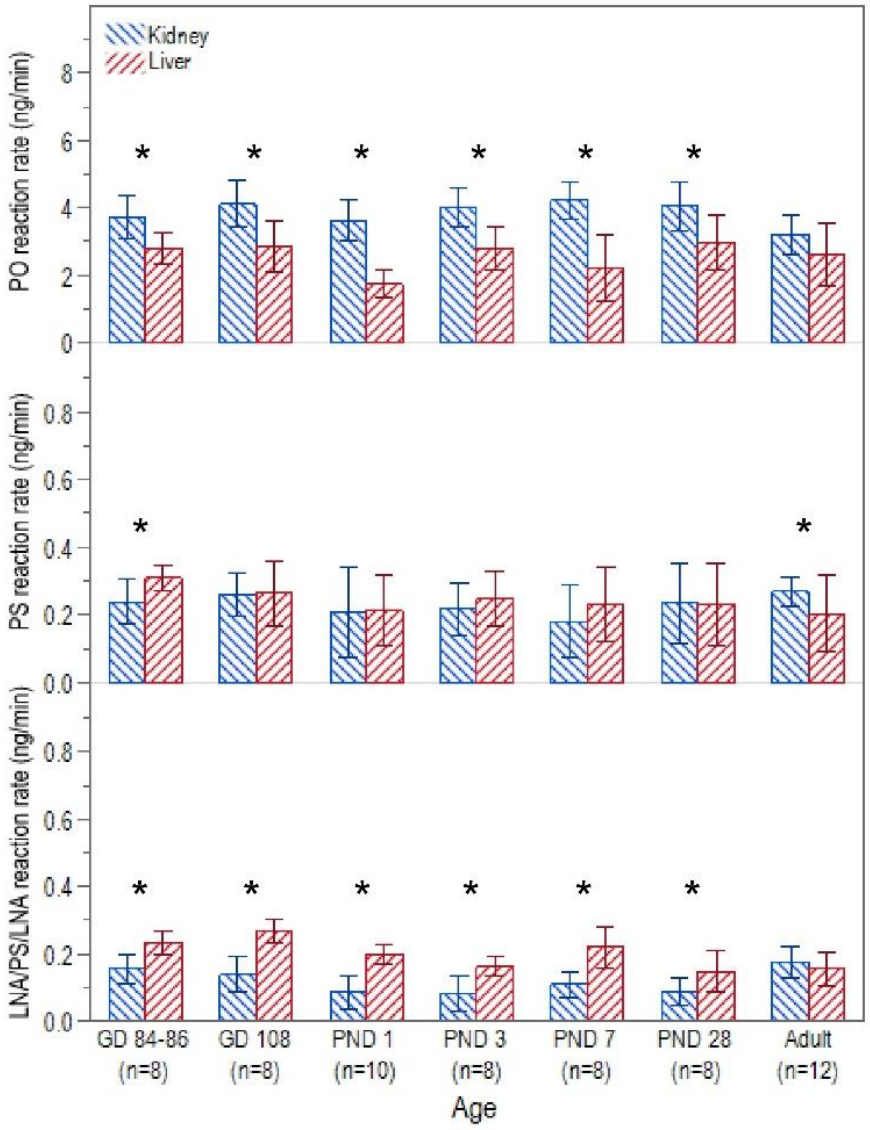

Figure S3.5. Estimated reaction rate towards the isosequential ASOs: unmodified (PO), all-PS (PS), and LNA/PS/LNA gapmer in the kidney and liver homogenates from the developing and adult Göttingen Minipig. Difference between the kidney and liver was considered significant (*) if $p < 0.05$.

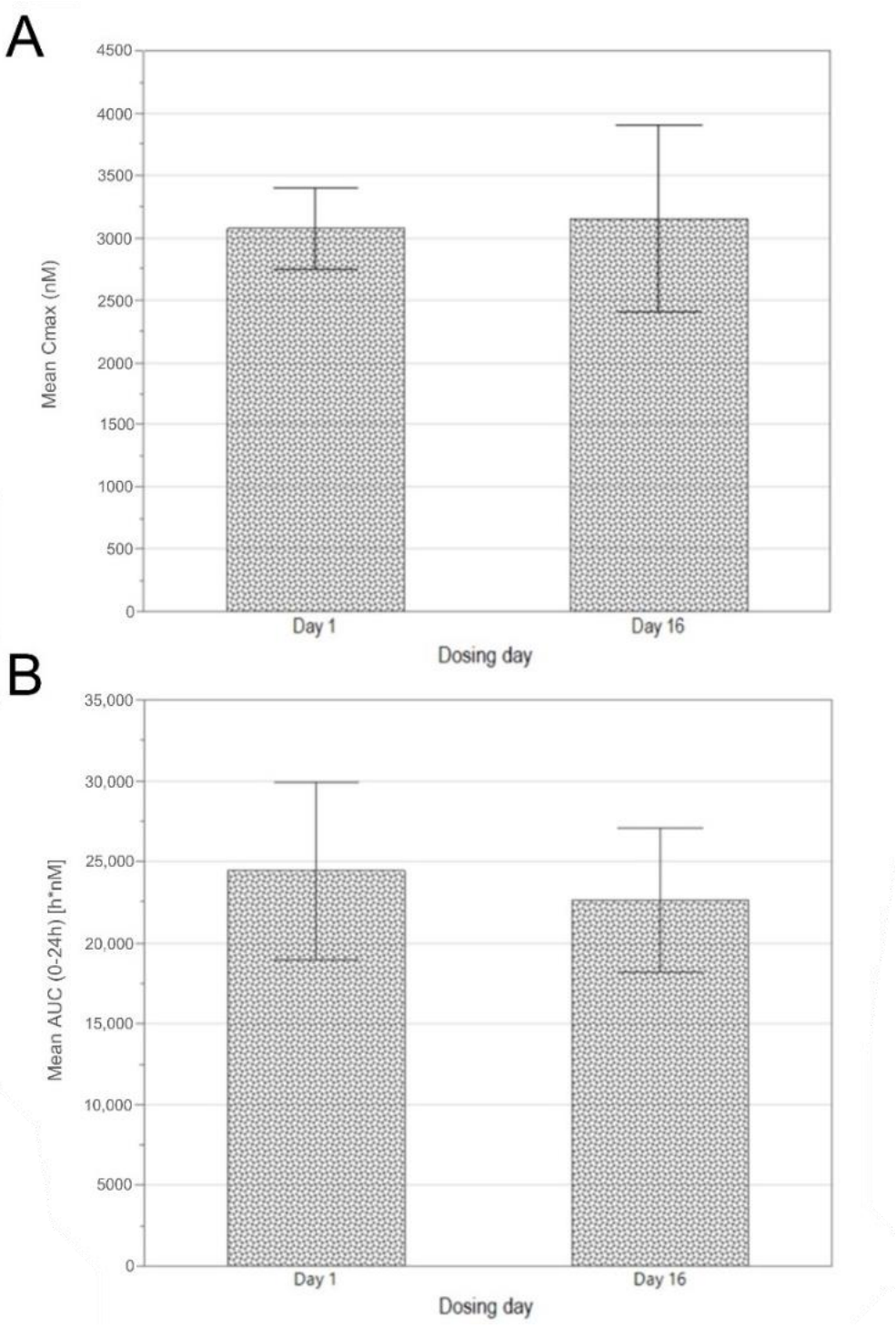
A
4500
4000
3500
3000
2500
2000
1500
1000
500
0
Mean Cmax (nM)
Day 1
Day 16
Dosing day
B
35,000
30,000
25,000
20,000
15,000
10,000
5000
0
Mean AUC (0-24h) [h*nM]
Day 1
Day 16
Dosing day

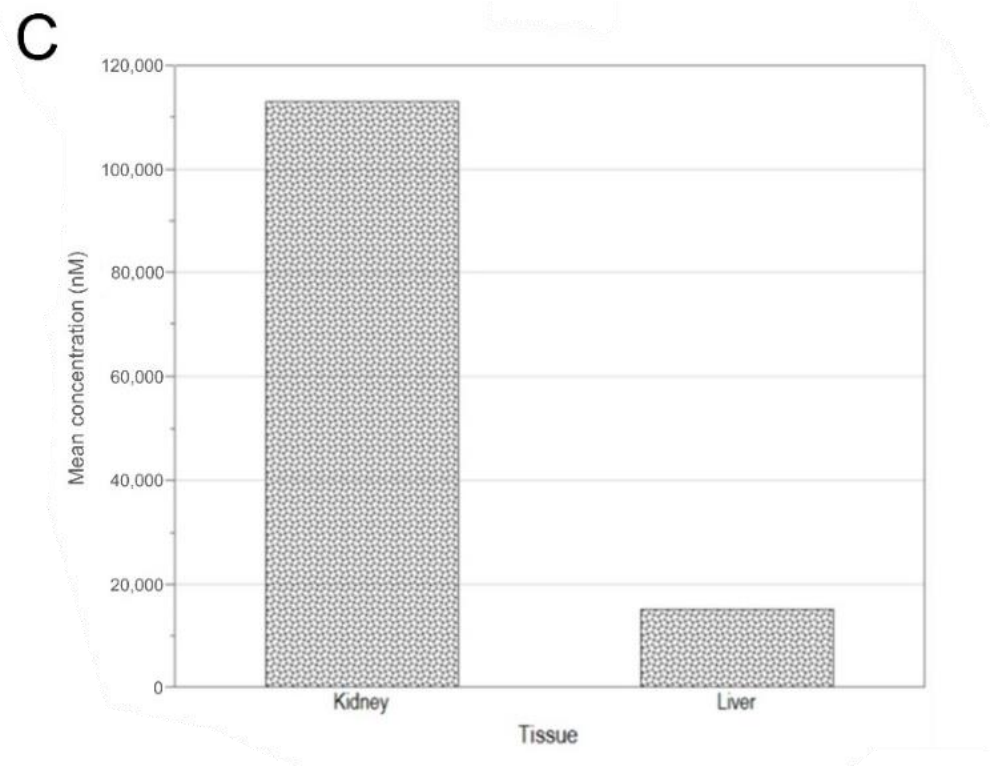

Figure S3.6. Published mean ± SD exposure levels in the plasma (**A**); mean ± SD maximum plasma concentration (C_{max}) (**B**); and mean exposure levels in the kidney and liver (**C**) data of adult Göttingen Minipig after RTR5001 administration [31]. C_{max}: Maximum concentration; AUC: Area under the curve.

3.7 References

1. Dias, N.; Stein, C.A. Antisense oligonucleotides: Basic concepts and mechanisms. *Mol. Cancer Ther.* **2002**, *1*, 347–355.
2. Mustonen, E.K.; Palomäki, T.; Pasanen, M. Oligonucleotide-based pharmaceuticals: Non-clinical and clinical safety signals and non-clinical testing strategies. *Regul. Toxicol. Pharmacol.* **2017**, *90*, 328–341, doi:10.1016/j.yrtph.2017.09.028.
3. Xiong, H.; Veedu, R.N.; Diermeier, S.D. Recent advances in oligonucleotide therapeutics in oncology. *Int. J. Mol. Sci.* **2021**, *22*, 3295, doi:10.3390/ijms22073295.
4. Quemener, A.M.; Bachelot, L.; Forestier, A.; Donnou-Fournet, E.; Gilot, D.; Galibert, M.D. The powerful world of antisense oligonucleotides: From bench to bedside. *Wiley Interdiscip. Rev. RNA* **2020**, *11*, e1594, doi:10.1002/wrna.1594.
5. Crooke, S.T. Molecular Mechanisms of Antisense Oligonucleotides. *Nucleic Acid Ther.* **2017**, *27*, 70–77, doi:10.1089/nat.2016.0656.
6. Dhuri, K.; Bechtold, C.; Quijano, E.; Pham, H.; Gupta, A.; Vikram, A.; Bahal, R. Antisense Oligonucleotides: An Emerging Area in Drug Discovery and Development. *J. Clin. Med.* **2020**, *9*, 2004, doi:10.3390/jcm9062004.
7. Yin, W.; Rogge, M. Targeting RNA: A Transformative Therapeutic Strategy. *Clin. Transl. Sci.* **2019**, *12*, 98–112, doi:10.1111/cts.12624.
8. Lima, W.; Wu, H.; Crooke, S.T. The RNase H mechanism. In *Antisense Drug Technology: Principles, Strategies, and Applications,* 2nd ed.; Crooke, S.T., Ed.; CRC Press: Boca Raton, FL, USA, 2007; pp. 47–74.
9. Henry, S.P.; Johnson, M.; Zanardi, T.A.; Fey, R.; Auyeung, D.; Lappin, P.B.; Levin, A.A. Renal uptake and tolerability of a 2'-O-methoxyethyl modified antisense oligonucleotide (ISIS 113715) in monkey. *Toxicology* **2012**, *301*, 13–20, doi:10.1016/j.tox.2012.06.005.

10. Brown, D.A.; Kang, S.H.; Gryaznov, S.M.; DeDionisio, L.; Heidenreich, O.; Sullivan, S.; Xu, X.; Nerenberg, M.I. Effect of phosphorothioate modification of oligodeoxynucleotides on specific protein binding. *J. Biol. Chem.* **1994**, *269*, 26801–26805, doi:https://doi.org/10.1016/S0021-9258(18)47090-1.
11. Geary, R.S.; Watanabe, T.A.; Truong, L.; Freier, S.; Lesnik, E.A.; Sioufi, N.B.; Sasmor, H.; Manoharan, M.; Levin, A.A. Pharmacokinetic properties of 2′-O-(2-methoxyethyl)-modified oligonucleotide analogs in rats. *J. Pharmacol. Exp. Ther.* **2001**, *296*, 890–897.
12. Geary, R.S.; Norris, D.; Yu, R.; Bennett, C.F. Pharmacokinetics, biodistribution and cell uptake of antisense oligonucleotides. *Adv. Drug Deliv. Rev.* **2015**, *87*, 46–51, doi:10.1016/j.addr.2015.01.008.
13. Frazier, K.S. Antisense Oligonucleotide Therapies:The Promise and the Challenges from a Toxicologic Pathologist's Perspective. *Toxicol. Pathol.* **2015**, *43*, 78–89, doi:10.1177/0192623314551840.
14. Yu, R.Z.; Geary, R.S.; Flaim, J.D.; Riley, G.C.; Tribble, D.L.; VanVliet, A.A.; Wedel, M.K. Lack of pharmacokinetic interaction of mipomersen sodium (ISIS 301012), a 2′-O-methoxyethyl modified antisense oligonucleotide targeting apolipoprotein B-100 messenger RNA, with simvastatin and ezetimibe. *Clin. Pharmacokinet.* **2009**, *48*, 39–50, doi:10.2165/0003088-200948010-00003.
15. Kazmi, F.; Yerino, P.; McCoy, C.; Parkinson, A.; Buckley, D.B.; Ogilvie, B.W. An assessment of the in vitro inhibition of cytochrome P450 enzymes, UDP-glucuronosyltransferases, and transporters by phosphodiester- or phosphorothioate-linked oligonucleotides. *Drug Metab. Dispos.* **2018**, *46*, 1066–1074, doi:10.1124/dmd.118.081729.
16. Yu, R.Z.; Kim, T.W.; Hong, A.; Watanabe, T.A.; Gaus, H.J.; Geary, R.S. Cross-species pharmacokinetic comparison from mouse to man of a second-generation antisense oligonucleotide, ISIS 301012, targeting human apolipoprotein B-100. *Drug Metab. Dispos.* **2007**, *35*, 460–468, doi:10.1124/dmd.106.012401.
17. Griffey, R.H.; Greig, M.J.; Gaus, H.J.; Liu, K.; Monteith, D.; Winniman, M.; Cummins, L.L. Characterization of oligonucleotide metabolism in vivo via liquid chromatography/electrospray tandem mass spectrometry with a quadrupole ion trap mass spectrometer. *J. Mass Spectrom.* **1997**, *32*, 305–313, doi:10.1002/(SICI)1096-9888(199703)32:3<305::AID-JMS482>3.0.CO;2-R.
18. Yang, W. Nucleases: Diversity of structure, function and mechanism. *Q. Rev. Biophys.* **2011**, *44*, 1–93, doi:10.1017/S0033583510000181.
19. Eder, P.S.; Devine, R.J.; Dagle, J.M.; Walder, J.A. Substrate Specificity and Kinetics of Degradation of Antisense Oligonucleotides by a 3′ Exonuclease in Plasma. *Antisense Res. Dev.* **1991**, *1*, 141–151, doi:10.1089/ard.1991.1.141.
20. Wójcik, M.; Cieślak, M.; Stec, W.J.; Goding, J.W.; Koziołkiewicz, M. Nucleotide Pyrophosphatase/Phosphodiesterase 1 Is Responsible for Degradation of Antisense Phosphorothioate Oligonucleotides. *Oligonucleotides* **2007**, *17*, 134–145, doi:10.1089/oli.2007.0021.
21. Geary, R.S. Antisense oligonucleotide pharmacokinetics and metabolism. *Expert Opin. Drug Metab. Toxicol.* **2009**, *5*, 381–391, doi:10.1517/17425250902877680.
22. Watts, J.K. The Medicinal Chemistry of Antisense Oligonucleotides. In *Oligonucleotide-Based Drugs and Therapeutics*; Ferrari, N.; Seguin, R., Eds.; John Wiley & Sons, Inc.: Hoboken, NJ, USA, 2018; pp. 39–69.
23. Krishnan, A.V.; Mishra, D. Antisense Oligonucleotides: A Unique Treatment Approach. *Indian Pediatr.* **2020**, *57*, 165–171, doi:10.1007/s13312-020-1736-7.
24. Laxton, C.; Brady, K.; Moschos, S.; Turnpenny, P.; Rawal, J.; Pryde, D.C.; Sidders, B.; Corbau, R.; Pickford, C.; Murray, E.J. Selection, optimization, and pharmacokinetic properties of a novel, potent antiviral locked nucleic acid-based antisense oligomer targeting hepatitis C virus internal ribosome entry site. *Antimicrob. Agents Chemother.* **2011**, *55*, 3105–3114, doi:10.1128/AAC.00222-11.
25. Kuespert, S.; Heydn, R.; Peters, S.; Wirkert, E.; Meyer, A.L.; Siebörger, M.; Johannesen, S.; Aigner, L.; Bogdahn, U.; Bruun, T.H. Antisense oligonucleotide in LNA-gapmer design targeting TGFBR2—A key single gene target for safe and effective inhibition of TGFβ signaling. *Int. J. Mol. Sci.* **2020**, *21*, 1–25, doi:10.3390/ijms21061952.
26. Gupta, N.; Fisker, N.; Asselin, M.C.; Lindholm, M.; Rosenbohm, C.; Ørum, H.; Elmén, J.; Seidah, N.G.; Straarup, E.M. A locked nucleic acid antisense oligonucleotide (LNA) silences PCSK9 and enhances LDLR expression In Vitro and In Vivo. *PLoS ONE* **2010**, *5*, 1–9, doi:10.1371/journal.pone.0010682.
27. Abewe, H.; Deshmukh, S.; Mukim, A.; Beliakova-Bethell, N. Use of GapmeRs for gene expression knockdowns in human primary resting CD4+ T cells. *J. Immunol. Methods* **2020**, *476*, 112674, doi:10.1016/j.jim.2019.112674.
28. Roberts, T.C.; Langer, R.; Wood, M.J.A. Advances in oligonucleotide drug delivery. *Nat. Rev. Drug Discov.* **2020**, *19*, 673–694.
29. Hammond, S.M.; Aartsma-Rus, A.; Alves, S.; Borgos, S.E.; Buijsen, R.A.M.; Collin, R.W.J.; Covello, G.; Denti, M.A.; Desviat, L.R.; Echevarría, L.; et al. Delivery of oligonucleotide-based therapeutics: Challenges and opportunities. *EMBO Mol. Med.* **2021**, *13*, 1-23, doi:10.15252/emmm.202013243.
30. European Medicine Agency; Committee for Medicinal Products for Human Use; International Council for Harmonisation of Technical Requirements for Pharmaceuticas for Human Use. *ICH Guideline M3 (R2) on Non-Clinical Safety Studies for the Conduct of Human Clinical Trials and Marketing Authorization for Pharmaceuticals, Step 5, EMA/CHMP/ICH/286/95*; European Medicines Agency, London, UK, 11 February 2013, Available online: https://www.ema.europa.eu/en/documents/scientific-guideline/ich-guideline-m3r2-non-clinical-safety-studies-conduct-human-clinical-trials-marketing-authorisation_en.pdf (accessed on 11 June 2021).

31. Braendli-Baiocco, A.; Festag, M.; Erichsen, K.D.; Persson, R.; Mihatsch, M.J.; Fisker, N.; Funk, J.; Mohr, S.; Constien, R.; Ploix, C.; et al. The minipig is a suitable non-rodent model in the safety assessment of single stranded oligonucleotides. *Toxicol. Sci.* **2017**, *157*, 112–128, doi:10.1093/toxsci/kfx025.
32. Heckel, T.; Schmucki, R.; Berrera, M.; Ringshandl, S.; Badi, L.; Steiner, G.; Ravon, M.; Küng, E.; Kuhn, B.; Kratochwil, N.A.; et al. Functional analysis and transcriptional output of the Göttingen minipig genome. *BMC Genomics* **2015**, *16*, 1–19, doi:10.1186/s12864-015-2119-7.
33. Vamathevan, J.J.; Hall, M.D.; Hasan, S.; Woollard, P.M.; Xu, M.; Yang, Y.; Li, X.; Wang, X.; Kenny, S.; Brown, J.R.; et al. Minipig and beagle animal model genomes aid species selection in pharmaceutical discovery and development. *Toxicol. Appl. Pharmacol.* **2013**, *270*, 149–157, doi:10.1016/j.taap.2013.04.007.
34. Scoto, M.; Finkel, R.; Mercuri, E.; Muntoni, F. Genetic therapies for inherited neuromuscular disorders. *Lancet Child Adolesc. Heal.* **2018**, *2*, 600–609, doi:10.1016/S2352-4642(18)30140-8.
35. Abreu, N.J.; Waldrop, M.A. Overview of gene therapy in spinal muscular atrophy and Duchenne muscular dystrophy. *Pediatr. Pulmonol.* **2021**, *56*, 710–720, doi:10.1002/ppul.25055.
36. Aoki, Y.; Wood, M.J.A. Emerging Oligonucleotide Therapeutics for Rare Neuromuscular Diseases. *J. Neuromuscul. Dis.* **2021**, 1–16, doi:10.3233/jnd-200560.
37. Osredkar, D.; Jílková, M.; Butenko, T.; Loboda, T.; Golli, T.; Fuchsová, P.; Rohlenová, M.; Haberlova, J. Children and young adults with spinal muscular atrophy treated with nusinersen. *Eur. J. Paediatr. Neurol.* **2021**, *30*, 1–8, doi:10.1016/j.ejpn.2020.11.004.
38. Hoffman, E.P. Pharmacotherapy of duchenne muscular dystrophy. *Handb. Exp. Pharmacol.* **2020**, *261*, 25–37, doi:10.1007/164_2019_256.
39. Martinovich, K.M.; Shaw, N.C.; Kicic, A.; Schultz, A.; Fletcher, S.; Wilton, S.D.; Stick, S.M. The potential of antisense oligonucleotide therapies for inherited childhood lung diseases. *Mol. Cell. Pediatr.* **2018**, *5*, 3, doi:10.1186/s40348-018-0081-6.
40. Ashrafi, M.R.; Amanat, M.; Garshasbi, M.; Kameli, R.; Nilipour, Y.; Heidari, M.; Rezaei, Z.; Tavasoli, A.R. An update on clinical, pathological, diagnostic, and therapeutic perspectives of childhood leukodystrophies. *Expert Rev. Neurother.* **2020**, *20*, 65–84, doi:10.1080/14737175.2020.1699060.
41. Oren, Y.S.; Irony-Tur Sinai, M.; Golec, A.; Barchad-Avitzur, O.; Mutyam, V.; Li, Y.; Hong, J.; Ozeri-Galai, E.; Hatton, A.; Leibson, C.; et al. Antisense oligonucleotide-based drug development for Cystic Fibrosis patients carrying the 3849+10 kb C-to-T splicing mutation. *J. Cyst. Fibros.* **2021**, doi:10.1016/j.jcf.2021.06.003.
42. European Medicine Agency; Committee for Medicinal Products for Human Use; International Council for Harmonisation of Technical Requirements for Pharmaceuticas for Human Use. *ICH Guideline S11 on Noncliniclinical Safety Testing in Support of Development of Pediatric Pharmaceuticals, Step 5, EMA/CHMP/ICH/616110/2018*; European Medicines Agency/ Amsterdam, The Netherlands, 31 March 2020, Available online: https://www.ema.europa.eu/en/documents/scientific-guideline/ich-guideline-s11-nonclinical-safety-testing-support-development-paediatric-pharmaceuticals-step-5_en.pdf (accessed on 11 June 2021).
43. Barrow, P.C.; Barbellion, S.; Stadler, J. Preclinical evaluation of juvenile toxicity. *Methods Mol. Biol.* **2011**, *691*, 17–35, doi:10.1007/978-1-60761-849-2_2.
44. Ayuso, M.; Buyssens, L.; Stroe, M.; Valenzuela, A.; Allegaert, K.; Smits, A.; Annaert, P.; Mulder, A.; Carpentier, S.; Van Ginneken, C.; et al. The neonatal and juvenile pig in pediatric drug discovery and development. *Pharmaceutics* **2021**, *13*, 44, doi:10.3390/pharmaceutics13010044.
45. Bode, G.; Clausing, P.; Gervais, F.; Loegsted, J.; Luft, J.; Nogues, V.; Sims, J. The utility of the minipig as an animal model in regulatory toxicology. *J. Pharmacol. Toxicol. Methods* **2010**, *62*, 196–220, doi:10.1016/j.vascn.2010.05.009.
46. Forster, R.; Bode, G.; Ellegaard, L.; van der Laan, J.W. The RETHINK project on minipigs in the toxicity testing of new medicines and chemicals: Conclusions and recommendations. *J. Pharmacol. Toxicol. Methods* **2010**, *62*, 236–242, doi:10.1016/j.vascn.2010.05.008.
47. Lindholm, M.W.; Elmén, J.; Fisker, N.; Hansen, H.F.; Persson, R.; Møller, M.R.; Rosenbohm, C.; Ørum, H.; Straarup, E.M.; Koch, T. PCSK9 LNA antisense oligonucleotides induce sustained reduction of LDL cholesterol in nonhuman primates. *Mol. Ther.* **2012**, *20*, 376–381, doi:10.1038/mt.2011.260.
48. Lin, X.L.; Xiao, L.L.; Tang, Z.H.; Jiang, Z.S.; Liu, M.H. Role of PCSK9 in lipid metabolism and atherosclerosis. *Biomed. Pharmacother.* **2018**, *104*, 36–44, doi:10.1016/j.biopha.2018.05.024.
49. Van Peer, E.; Downes, N.; Casteleyn, C.; Van Ginneken, C.; Weeren, A.; Van Cruchten, S. Organ data from the developing Göttingen minipig: First steps towards a juvenile PBPK model. *J. Pharmacokinet. Pharmacodyn.* **2016**, *43*, 179–190, doi:10.1007/s10928-015-9463-8.
50. Geary, R.S.; Yu, R.Z.; Watanabe, T.; Henry, S.P.; Hardee, G.E.; Chappell, A.; Matson, J.; Sasmor, H.; Cummins, L.; Levin, A.A. Pharmacokinetics of a tumor necrosis factor-α phosphorothioate 2′-O-(2-methoxyethyl) modified antisense oligonucleotide: Comparison across species. *Drug Metab. Dispos.* **2003**, *31*, 1419–1428, doi:10.1124/dmd.31.11.1419.
51. Stein, H.; Hausen, P. Enzyme from calf thymus degrading the RNA moiety of DNA-RNA hybrids: Effect on DNA-dependent RNA polymerase. *Science* **1969**, *166*, 393–395, doi:10.1126/science.166.3903.393.

52. Wu, H.; Lima, W.F.; Zhang, H.; Fan, A.; Sun, H.; Crooke, S.T. Determination of the Role of the Human RNase H1 in the Pharmacology of DNA-like Antisense Drugs. *J. Biol. Chem.* **2004**, *279*, 17181–17189, doi:10.1074/jbc.M311683200.
53. Ten Asbroek, A.L.M.A.; Van Groenigen, M.; Nooij, M.; Baas, F. The involvement of human ribonucleases H1 and H2 in the variation of response of cells to antisense phosphorothioate oligonucleotides. *Eur. J. Biochem.* **2002**, *269*, 583–592, doi:10.1046/j.0014-2956.2001.02686.x.
54. Nygard, A.B.; Jørgensen, C.B.; Cirera, S.; Fredholm, M. Selection of reference genes for gene expression studies in pig tissues using SYBR green qPCR. *BMC Mol. Biol.* **2007**, *8*, 67, doi:10.1186/1471-2199-8-67.
55. Vandesompele, J.; De Preter, K.; Pattyn, F.; Poppe, B.; Van Roy, N.; De Paepe, A.; Speleman, F. Accurate normalization of real-time quantitative RT-PCR data by geometric averaging of multiple internal control genes. *Genome Biol.* **2002**, *3*, 1–12, doi:10.1186/gb-2002-3-7-research0034.
56. Wahlestedt, C.; Salmi, P.; Good, L.; Kela, J.; Johnsson, T.; Ho, T.; Broberger, C.; Porreca, F.; Lai, J.; Ren, K.; et al. Potent and nontoxic antisense oligonucleotides. *Proc. Natl. Acad. Sci. USA.* **2000**, *97*, 5633–5638, doi:https://doi.org/10.1073/pnas.97.10.5633.
57. Gilar, M.; Belenky, A.; Smisek, D.L.; Bourque, A.; Cohen, A.S. Kinetics of phosphorothioate oligonucleotide metabolism in biological fluids. *Nucleic Acids Res.* **1997**, *25*, 3615–3620, doi:10.1093/nar/25.18.3615.
58. Mazur, D.J.; Perrino, F.W. Identification and expression of the TREX1 and TREX2 cDNA sequences encoding mammalian 3'→5' exonucleases. *J. Biol. Chem.* **1999**, *274*, 19655–19660, doi:10.1074/jbc.274.28.19655.
59. Kavanagh, D.; Spitzer, D.; Kothari, P.H.; Shaikh, A.; Liszewski, M.K.; Richards, A.; Atkinson, J.P. New roles for the major human 3'–5' exonuclease TREX1 in human disease. *Cell Cycle* **2010**, *7*, 1718–1725, doi:10.4161/cc.7.12.6162.
60. Kishi, K.; Yasuda, T.; Ikehara, Y.; Sawazaki, K.; Sato, W.; Ida, R. Human serum deoxyribonuclease I (DNase I) polymorphism: Pattern similarities among isozymes from serum, urine, kidney, liver, and pancreas. *Am. J. Hum. Genet.* **1990**, *47*, 121–126.
61. Evans, C.J.; Aguilera, R.J. DNase II: Genes, enzymes and function. *Gene* **2003**, *322*, 1–15, doi:10.1016/j.gene.2003.08.022.
62. Grossi, A.B.; Zeltner, A.; Christoffersen, C.; Søndergaard, A.C. Reference data of clinical chemistry and hematology in juvenile Göttingen Minipigs. *Toxicol. Lett.* **2016**, *258*, s234, doi:10.1016/j.toxlet.2016.06.1838.
63. Seely, J.C. A brief review of kidney development , maturation , developmental abnormalities , and drug toxicity: Juvenile animal relevancy. *J. Toxicol. Pathol.* **2017**, *30*, 125–133, doi:10.1293/tox.2017-0006.
64. Szudzik, M.; Starzyński, R.R.; Jończy, A.; Mazgaj, R.; Lenartowicz, M.; Lipiński, P. Erratum: Iron supplementation in suckling piglets: An ostensibly easy therapy of neonatal iron deficiency anemia, *Pharmaceuticals* **2019**, *12*, 22, doi:10.3390/ph12010022.
65. O'Hara, K. Paediatric pharmacokinetics and drug doses. *Aust. Prescr.* **2016**, *39*, 208–210, doi:10.18773/austprescr.2016.071.
66. van Donge, T.; Evers, K.; Koch, G.; van den Anker, J.; Pfister, M. Clinical pharmacology and pharmacometrics to better understand physiological changes during pregnancy and neonatal life. *Handb. Exp. Pharmacol.* **2020**, *261*, 325–337, doi:10.1007/164_2019_210.
67. Bueters, R.; Bael, A.; Gasthuys, E.; Chen, C.; Schreuder, M.F.; Frazier, K.S. Ontogeny and Cross-species Comparison of Pathways Involved in Drug Absorption, Distribution, Metabolism, and Excretion in Neonates (Review): Kidney. *Drug Metab. Dispos.* **2020**, *48*, 353–367, doi:10.1124/DMD.119.089755.
68. Kurreck, J.; Wyszko, E.; Gillen, C.; Erdmann, V.A. Design of antisense oligonucleotides stabilized by locked nucleic acids. *Nucleic Acids Res.* **2002**, *30*, 1911–1918, doi:10.1093/nar/30.9.1911.
69. Kim, J.; Basiri, B.; Hassan, C.; Punt, C.; van der Hage, E.; den Besten, C; Bartlett, M.G. Metabolite Profiling of the Antisense Oligonucleotide Eluforsen Using Liquid Chromatography-Mass Spectrometry. *Mol. Ther. Nucleic Acid* **2019**, *17*, 714–725, doi:10.1016/j.omtn.2019.07.006.
70. Baek, M.; Yu, R.Z.; Gaus, H.; Grundy, J.S.; Geary, R.S. In Vitro Metabolic Stabilities and Metabolism Antisense Oligonucleotides in Preincubated Rat or Human Whole Liver Homogenates. *Oligonucleotides* **2010**, *20*, 309–316, doi:10.1089/oli.2010.0252.
71. Crooke, R.M.; Graham, M.J.; Martin, M.J.; Lemonidis, K.M.; Wyrzykiewiecz, T.A.D.; Cummins, L.L. Metabolism of Antisense Oligonucleotides in Rat Liver Homogenates. *J. Pharmacol. Exp. Ther.* **2000**, *292*, 140–149.
72. Sands, H.; Gorey-Feret, L.J.; Cocuzza, A.J.; Hobbs, F.W.; Chidester, D.; Trainor, G.L. Biodistribution and metabolism of internally 3H-labeled oligonucleotides. I. Comparison of a phosphodiester and a phosphorothioate. *Mol. Pharmacol.* **1994**, *45*, 932–943.
73. Walder, R.Y.; Walder, J.A. Role of RNase H in hybrid-arrested translation by antisense oligonucleotides. *Proc. Natl. Acad. Sci. USA* **1988**, *85*, 5011–5015, doi:10.1073/pnas.85.14.5011.
74. Lin, M.; Hu, X.; Chang, S.; Chang, Y.; Bian, W.; Hu, R.; Wang, J.; Zhu, Q.; Qiu, J. Advances of Antisense Oligonucleotide Technology in the Treatment of Hereditary Neurodegenerative Diseases. *Evidence-based Complement. Altern. Med.* **2021**, 2021, 6678422, doi:10.1155/2021/6678422.
75. Chen, S.; Le, B.T.; Chakravarthy, M.; Kosbar, T.R.; Veedu, R.N. Systematic evaluation of 2'-Fluoro modified chimeric antisense oligonucleotide-mediated exon skipping in vitro. *Sci. Rep.* **2019**, *9*, 6078, doi:10.1038/s41598-019-42523-0.

76. Dirin, M.; Winkler, J. Tissue Distribution, Metabolism, and Clearance. In *Oligonucleotide-Based Drugs and Therapeutics*; Ferrari, N., Seguin, R., Eds.; John Wiley & Sons, Inc.: Hoboken, NJ, USA, 2018; pp. 137–151.
77. Levin, A.A. A review of issues in the pharmacokinetics and toxicology of phosphorothioate antisense oligonucleotides. **1999**, *1489*, 69–84.
78. Gaus, H.J.; Owens, S.R.; Winniman, M.; Cooper, S.; Cummins, L.L. On-Line HPLC Electrospray Mass Spectrometry of Phosphorothioate Oligonucleotide Metabolites. *Anal. Chem.* **1997**, *69*, 313–319, doi:https://doi.org/10.1021/ac960557q.
79. Shaw, J.; Kent, K.; Bird, J.; Fishback, J.; Froehler, B. Modified deoxyoligonucleotides stable to exonuclease degradation in serum. *Nucleic Acids Res.* **1991**, *19*, 747–750, doi:10.1093/nar/19.4.747.
80. Østergaard, M.E.; De Hoyos, C.L.; Wan, W.B.; Shen, W.; Low, A.; Berdeja, A.; Vasquez, G.; Murray, S.; Migawa, M.T.; Liang, X.H.; et al. Understanding the effect of controlling phosphorothioate chirality in the DNA gap on the potency and safety of gapmer antisense oligonucleotides. *Nucleic Acids Res.* **2020**, *48*, 1691–1700, doi:10.1093/nar/gkaa031.
81. Belli, S.I.; van Driel, I.R.; Goding, J.W. Identification and characterization of a soluble form of the plasma cell membrane glycoprotein PC-1 (5′-nucleotide phosphodiesterase). *Eur. J. Biochem.* **1993**, *217*, 421–428, doi:10.1111/j.1432-1033.1993.tb18261.x.
82. Loughney, K.; Ferguson, K. Identification and Quantification of PDE Isoenzymes and Subtypes by Molecular Biological Methods. In *Phosphodiesterase Inhibitors*; Schudt, C., Dent, G., Rabe, K., Eds.; Academic Press Ltd: San Diego, CA, USA, 1996; pp. 1–14.
83. Wang, D. Discrepancy between mRNA and protein abundance: Insight from information retrieval process in computers. *Comput. Biol. Chem.* **2008**, *32*, 462–468, doi:10.1016/j.compbiolchem.2008.07.014.
84. Bruckmueller, H.; Martin, P.; Kähler, M.; Haenisch, S.; Ostrowski, M.; Drozdzik, M.; Siegmund, W.; Cascorbi, I.; Oswald, S. Clinically Relevant Multidrug Transporters Are Regulated by microRNAs along the Human Intestine. *Mol. Pharm.* **2017**, *14*, 2245–2253, doi:10.1021/acs.molpharmaceut.7b00076.
85. Zapalska-Sozoniuk, M.; Chrobak, L.; Kowalczyk, K.; Kankofer, M. Is it useful to use several “omics” for obtaining valuable results? *Mol. Biol. Rep.* **2019**, *46*, 3597–3606, doi:10.1007/s11033-019-04793-9.
86. Kamaliddin, C.; Guillochon, E.; Salnot, V.; Rombaut, D.; Huguet, S.; Guillonneau, F.; Houzé, S.; Cot, M.; Deloron, P.; Argy, N.; et al. Comprehensive Analysis of Transcript and Protein Relative Abundance during Blood Stages of Plasmodium falciparum Infection. *J. Proteome Res.* **2021**, *20*, 1206–1216, doi:10.1021/acs.jproteome.0c00496.
87. Yu, R.Z.; Geary, R.S.; Levin, A.A. Pharmacokinetics and Pharmacodynamics of Antisense Oligonucleotides. In *Pharmacokinetics and Pharmacodynamics of Biotech Drugs: Principles and Case Studies in Drug Development*; Meibohm, B., Ed.; Wiley-VCH: Weinheim, Germany, 2006; pp. 93–115.
88. Lundin, K.E.; Hansen, B.R.; Persson, R.; Bramsen, J.B.; Koch, T.; Wengel, J.; Smith, C.I.E. Biological Activity and Biotechnological Aspects of Locked Nucleic Acids. *Adv. Genet.* **2013**, *82*, 47–107, doi:10.1016/B978-0-12-407676-1.00002-0.
89. Post, N.; Yu, R.; Greenlee, S.; Gaus, H.; Hurh, E.; Matson, J.; Wang, Y. Metabolism and disposition of volanesorsen, a 29-O-(2 methoxyethyl) antisense oligonucleotide, across species. *Drug Metab. Dispos.* **2019**, *47*, 1164–1173, doi:10.1124/dmd.119.087395.
90. Tillman, L.G.; Geary, R.S.; Hardee, G.E. Oral delivery of antisense oligonucleotides in man. *J. Pharm. Sci.* **2008**, *97*, 225–236, doi:10.1002/jps.21084.
91. Crooke, S.T.; Geary, R.S. Clinical pharmacological properties of mipomersen (Kynamro), a second generation antisense inhibitor of apolipoprotein B. *Br. J. Clin. Pharmacol.* **2013**, *76*, 269–276, doi:10.1111/j.1365-2125.2012.04469.x.
92. Yu, R.Z.; Grundy, J.S.; Geary, R.S. Clinical pharmacokinetics of second generation antisense oligonucleotides. *Expert Opin. Drug Metab. Toxicol.* **2013**, *9*, 169–182, doi:10.1517/17425255.2013.737320.
93. Schmidt, K.; Prakash, T.P.; Donner, A.J.; Kinberger, G.A.; Gaus, H.J.; Low, A.; Østergaard, M.E.; Bell, M.; Swayze, E.E.; Seth, P.P. Characterizing the effect of GalNAc and phosphorothioate backbone on binding of antisense oligonucleotides to the asialoglycoprotein receptor. *Nucleic Acids Res.* **2017**, *45*, 2294–2306, doi:10.1093/nar/gkx060.
94. Miller, C.M.; Donner, A.J.; Blank, E.E.; Egger, A.W.; Kellar, B.M.; Østergaard, M.E.; Seth, P.P.; Harris, E.N. Stabilin-1 and Stabilin-2 are specific receptors for the cellular internalization of phosphorothioate-modified antisense oligonucleotides (ASOs) in the liver. *Nucleic Acids Res.* **2016**, *44*, 2782–2794, doi:10.1093/nar/gkw112.
95. Hvam, M.L.; Cai, Y.; Dagnæs-Hansen, F.; Nielsen, J.S.; Wengel, J.; Kjems, J.; Howard, K.A. Fatty Acid-Modified Gapmer Antisense Oligonucleotide and Serum Albumin Constructs for Pharmacokinetic Modulation. *Mol. Ther.* **2017**, *25*, 1710–1717, doi:10.1016/j.ymthe.2017.05.009.
96. Migawa, M.T.; Shen, W.; Wan, W.B.; Vasquez, G.; Oestergaard, M.E.; Low, A.; De Hoyos, C.L.; Gupta, R.; Murray, S.; Tanowitz, M.; et al. Site-specific replacement of phosphorothioate with alkyl phosphonate linkages enhances the therapeutic profile of gapmer ASOs by modulating interactions with cellular proteins. *Nucleic Acids Res.* **2019**, *47*, 5465–5479, doi:10.1093/nar/gkz247.
97. Srinivasan, S.K.; Tewary, H.K.; Iversen, P.L. Characterization of Binding Sites, Extent of Binding, and Drug Interactions of Oligonucleotides with Albumin. *Antisense Res. Dev.* **1995**, *5*, 131–139, doi:10.1089/ard.1995.5.131.

98. Watanabe, T.A.; Geary, R.S.; Levin, A.A. Plasma protein binding of an antisense oligonucleotide targeting human ICAM-1 (ISIS 2302). *Oligonucleotides* **2006**, *16*, 169–180, doi:10.1089/oli.2006.16.169.
99. Wartlick, H.; Spänkuch-Schmitt, B.; Strebhardt, K.; Kreuter, J.; Langer, K. Tumour cell delivery of antisense oligonuclceotides by human serum albumin nanoparticles. *J. Control. Release* **2004**, *96*, 483–495, doi:10.1016/j.jconrel.2004.01.029.
100. Gaus, H.J.; Gupta, R.; Chappell, A.E.; Østergaard, M.E.; Swayze, E.E.; Seth, P.P. Characterization of the interactions of chemically-modified therapeutic nucleic acids with plasma proteins using a fluorescence polarization assay. *Nucleic Acids Res.* **2019**, *47*, 1110–1122, doi:10.1093/nar/gky1260.
101. Lightfoot, H.; Schneider, A.; Hall, J. Pharmacokinetics and Pharmacodynamics of Antisense Oligonucleotides. In *Oligonucleotide-Based Drugs and Therapeutics*; Ferrari, N., Seguin, R., Eds.; John Wiley & Sons, Inc.: Hoboken, NJ, USA, 2018; pp. 107–136.
102. Lanford, R.E.; Hildebrandt-Eriksen, E.S.; Petri, A.; Persson, R.; Lindow, M.; Munk, M.E.; Kauppinen, S.; Rum, H. Therapeutic silencing of microRNA-122 in primates with chronic hepatitis C virus infection. *Science.* **2010**, *327*, 198–201, doi:10.1126/science.1178178.
103. Weidolf, L.; Björkbom, A.; Dahlén, A.; Elebring, M.; Gennemark, P.; Hölttä, M.; Janzén, D.; Li, X.Q.; Andersson, S. Distribution and biotransformation of therapeutic antisense oligonucleotides and conjugates. *Drug Discov. Today* **2021**, doi:10.1016/j.drudis.2021.04.002.
104. Goemans, N.M.; Tulinius, M.; van den Akker, J.T.; Burm, B.E.; Ekhart, P.F.; Heuvelmans, N.; Holling, T.; Janson, A.A.; Platenburg, G.J.; Sipkens, J.A.; et al. Systemic Administration of PRO051 in Duchenne's Muscular Dystrophy. *N. Engl. J. Med.* **2011**, *364*, 1513–1522, doi:10.1056/nejmoa1011367.
105. Levin, A.A.; Yu, R.Z.; Geary, R.S. Basic principles of the pharmacokinetics of antisense oligonucleotide drugs. In *Antisense Drug Technology: Principles, Strategies, and Applications,* 2nd ed.; Crooke, S.T., Ed.; CRC Press: Boca Raton, FL, USA, 2007; pp. 183–216.
106. Straarup, E.M.; Fisker, N.; Hedtjärn, M.; Lindholm, M.W.; Rosenbohm, C.; Aarup, V.; Hansen, H.F.; Ørum, H.; Hansen, J.B.R.; Koch, T. Short locked nucleic acid antisense oligonucleotides potently reduce apolipoprotein B mRNA and serum cholesterol in mice and non-human primates. *Nucleic Acids Res.* **2010**, *38*, 7100–7111, doi:10.1093/nar/gkq457.
107. Hagedorn, P.H.; Persson, R.; Funder, E.D.; Albæk, N.; Diemer, S.L.; Hansen, D.J.; Møller, M.R.; Papargyri, N.; Christiansen, H.; Hansen, B.R.; et al. Locked nucleic acid: Modality, diversity, and drug discovery. *Drug Discov. Today* **2018**, *23*, 101–114, doi:10.1016/j.drudis.2017.09.018.
108. Wei, X.; Dai, G.; Marcucci, G.; Liu, Z.; Hoyt, D.; Blum, W.; Chan, K.K. A specific picomolar hybridization-based ELISA assay for the determination of phosphorothioate oligonucleotides in plasma and cellular matrices. *Pharm. Res.* **2006**, *23*, 1251–1264, doi:10.1007/s11095-006-0082-3.
109. Deverre, J.R.; Boutet, V.; Boquet, D.; Ezan, E.; Grassi, J.; Grognet, J.M. A competitive enzyme hybridization assay for plasma determination of phosphodiester and phosphorothioate antisense oligonucleotides. *Nucleic Acids Res.* **1997**, *25*, 3584–3589, doi:10.1093/nar/25.18.3584.
110. Andersson, S.; Antonsson, M.; Elebring, M.; Jansson-Löfmark, R.; Weidolf, L. Drug metabolism and pharmacokinetic strategies for oligonucleotide- and mRNA-based drug development. *Drug Discov. Today* **2018**, *23*, 1733–1745, doi:10.1016/j.drudis.2018.05.030.
111. Frazier, K.S. Species Differences in Renal Development and Associated Developmental Nephrotoxicity. *Birth Defects Res.* **2017**, *109*, 1243–1256, doi:10.1002/bdr2.1088.
112. Hildebrandt-Eriksen, E.S.; Aarup, V.; Persson, R.; Hansen, H.F.; Munk, M.E.; Ørum, H. A locked nucleic acid oligonucleotide targeting microRNA 122 is well-tolerated in cynomolgus monkeys. *Nucleic Acid Ther.* **2012**, *22*, 152–161, doi:10.1089/nat.2011.0332.
113. Koch, T.; Ørum, H. Locked nucleic acid. In *Antisense Drug Technology: Principles, Strategies, and Applications,* 2nd ed.; Crooke, S.T., Ed.; CRC Press: Boca Raton, FL, USA, 2007; pp. 519–564.
114. Graham, M.J.; Crooke, S.T.; Monteith, D.K.; Cooper, S.R.; Lemonidis, K.M.; Stecker, K.I.M.K.; Martin, M.J.; Crooke, R.M. In Vivo Distribution and Metabolism of a Phosphorothioate Oligonucleotide within Rat Liver after Intravenous Administration. *J. Pharmacol. Exp.* **1998**, *286*, 447–458.
115. Altmann, K.H.; Dean, N.M.; Fabbro, D.; Freier, S.M.; Geiger, T.; Hanera, R.; Hiisken, D.A.; Martina, P.; Monia, P.B.; Miiller, M.; et al. Second generation of antisense oligonucleotides: From nuclease resistance to biological efficacy in animals. *Chim. Int. J. Chem.* **1996**, *50*, 168–176.
116. Kim, J.; El Zahar, N.M.; Bartlett, M.G. In vitro metabolism of 2'-ribose unmodified and modified phosphorothioate oligonucleotide therapeutics using liquid chromatography mass spectrometry. *Biomed. Chromatogr.* **2020**, *34*, e4839, doi:10.1002/bmc.4839.
117. Romero-Palomo, F.; Festag, M.; Lenz, B.; Schadt, S.; Brink, A.; Kipar, A.; Steinhuber, B.; Husser, C.; Koller, E.; Sewing, S.; et al. Safety, Tissue Distribution, and Metabolism of LNA-Containing Antisense Oligonucleotides in Rats. *Toxicol. Pathol.* **2021**, *49*, 1174–1192, doi:10.1177/01926233211011615.
118. Kilanowska, A.; Studzińska, S. In vivo and in vitro studies of antisense oligonucleotides—a review. *RSC Adv.* **2020**, *10*, 34501–34516, doi:10.1039/d0ra04978f.
119. White, P.J.; Anastasopoulos, F.; Pouton, C.W.; Boyd, B.J. Overcoming biological barriers to in vivo efficacy of antisense oligonucleotides. *Expert Rev. Mol. Med.* **2009**, *11*, 1–19, doi:10.1017/S1462399409001021.

120. Yu, R.Z.; Lemonidis, K.M.; Graham, M.J.; Matson, J.E.; Crooke, R.M.; Tribble, D.L.; Wedel, M.K.; Levin, A.A.; Geary, R.S. Cross-species comparison of in vivo PK/PD relationships for second-generation antisense oligonucleotides targeting apolipoprotein B-100. *Biochem. Pharmacol.* **2009**, *77*, 910–919, doi:10.1016/j.bcp.2008.11.005.
121. Crooke, S.T.; Liang, X.H.; Baker, B.F.; Crooke, R.M. Antisense technology: A review. *J. Biol. Chem.* **2021**, *296*, 100416, doi:10.1016/j.jbc.2021.100416.
122. Geary, R.S.; Yu, R.Z.; Siwkowski, A.; Levin, A.A. Pharmacokinetic/Pharmacodynamic Properties of Phosphorothioate 2′-O-(2-Methoxyethyl)-Modified Antisense Oligonucleotides in Animals and Man. In *Antisense Drug Technology: Principles, Strategies, and Applications,* 2nd ed.; Crooke, S.T., Ed.; CRC Press: Boca Raton, FL, USA, 2007; pp. 305–326.
123. Henry, S.P.; Jagels, M.A.; Hugli, T.E.; Manalili, S.; Geary, R.S.; Giclas, P.C.; Levin, A.A. Mechanism of alternative complement pathway dysregulation by a phosphorothioate oligonucleotide in monkey and human serum. *Nucleic Acid Ther.* **2014**, *24*, 326–335, doi:10.1089/nat.2014.0491.
124. Shen, L.; Engelhardt, J.A.; Hung, G.; Yee, J.; Kikkawa, R.; Matson, J.; Tayefeh, B.; Machemer, T.; Giclas, P.C.; Henry, S.P. Effects of Repeated Complement Activation Associated with Chronic Treatment of Cynomolgus Monkeys with 2′-O-Methoxyethyl Modified Antisense Oligonucleotide. *Nucleic Acid Ther.* **2016**, *26*, 236–249, doi:10.1089/nat.2015.0584.
125. Henry, S.P.; Seguin, R.; Cavagnaro, J.; Berman, C.; Tepper, J.; Kornbrust, D. Considerations for the Characterization and Interpretation of Results Related to Alternative Complement Activation in Monkeys Associated with Oligonucleotide-Based Therapeutics. *Nucleic Acid Ther.* **2016**, *26*, 210–215, doi:10.1089/nat.2015.0593.
126. Andersson, P.; Den Besten, C. Preclinical and Clinical Drug-metabolism, Pharmacokinetics and Safety of Therapeutic Oligonucleotides. In *RSC Drug Discovery Series: Advances in Nucleic Acid Therapeutics*; Agrawal, S., Gait, M., Eds.; Royal Society of Chemistry: UK, 2019; pp. 474–517.
127. Mcgreal, E.P.; Hearne, K.; Spiller, O.B. Immunobiology Off to a slow start : Under-development of the complement system in term newborns is more substantial following premature birth. *Immunobiology* **2012**, *217*, 176–186, doi:10.1016/j.imbio.2011.07.027.
128. Seguin, R. Class-Related Proinflammatory Effects. In *Oligonucleotide-Based Drugs and Therapeutics*; Ferrari, N., Seguin, R., Eds.; John Wiley & Sons, Inc.: Hoboken, NJ, USA, 2018; pp. 227–242.
129. Aartsma-Rus, A.; Jackson, A.L.; Levin, A.A. Mechanisms of Oligonucleotide Actions. In *Oligonucleotide-Based Drugs and Therapeutics*; Ferrari, N., Seguin, R., Eds.; John Wiley & Sons, Inc.: Hoboken, NJ, USA, 2018; pp. 1–38.
130. Geary, R.S.; Wancewicz, E.; Matson, J.; Pearce, M.; Siwkowski, A.; Swayze, E.; Bennett, F. Effect of dose and plasma concentration on liver uptake and pharmacologic activity of a 2′-methoxyethyl modified chimeric antisense oligonucleotide targeting PTEN. *Biochem. Pharmacol.* **2009**, *78*, 284–291, doi:10.1016/j.bcp.2009.04.013.
131. Koller, E.; Vincent, T.M.; Chappell, A.; De, S.; Manoharan, M.; Bennett, C.F. Mechanisms of single-stranded phosphorothioate modified antisense oligonucleotide accumulation in hepatocytes. *Nucleic Acids Res.* **2011**, *39*, 4795–4807, doi:10.1093/nar/gkr089.
132. Liang, X.H.; Sun, H.; Shen, W.; Crooke, S.T. Identification and characterization of intracellular proteins that bind oligonucleotides with phosphorothioate linkages. *Nucleic Acids Res.* **2015**, *43*, 2927–2945, doi:10.1093/nar/gkv143.
133. Pollak, A.J.; Hickman, J.H.; Liang, X.H.; Crooke, S.T. Gapmer Antisense Oligonucleotides Targeting 5S Ribosomal RNA Can Reduce Mature 5S Ribosomal RNA by Two Mechanisms. *Nucleic Acid Ther.* **2020**, *30*, 312–324, doi:10.1089/nat.2020.0864.
134. Vickers, T.A.; Crooke, S.T. Antisense oligonucleotides capable of promoting specific target mRNA reduction via competing RNase H1-dependent and independent mechanisms. *PLoS ONE* **2014**, *9*, e108625, doi:10.1371/journal.pone.0108625.
135. Vickers, T.A.; Sabripour, M.; Crooke, S.T. U1 adaptors result in reduction of multiple pre-mRNA species principally by sequestering U1snRNP. *Nucleic Acids Res.* **2011**, *39*, e71, doi:10.1093/nar/gkr150.
136. Crooke, S.T.; Wang, S.; Vickers, T.A.; Shen, W.; Liang, X.H. Cellular uptake and trafficking of antisense oligonucleotides. *Nat. Biotechnol.* **2017**, *35*, 230–237.
137. Liang, X.H.; Sun, H.; Nichols, J.G.; Allen, N.; Wang, S.; Vickers, T.A.; Shen, W.; Hsu, C.W.; Crooke, S.T. COPII vesicles can affect the activity of antisense oligonucleotides by facilitating the release of oligonucleotides from endocytic pathways. *Nucleic Acids Res.* **2018**, *46*, 10225–10245, doi:10.1093/nar/gky841.
138. Ramanathan, M.; Macgregor, R.D.; Hunt, C.A. Predictions of Effect for Intracellular Antisense Oligodeoxyribonucleotides from a Kinetic Model. *Antisense Res. Dev.* **1993**, *3*, 3–18, doi:10.1089/ard.1993.3.3.
139. Spiller, D.G.; Giles, R.V.; Broughton, C.M.; Grzybowski, J.; Ruddell, C.J.; Tidd, D.M.; Clark, R.E. The influence of target protein half-life on the effectiveness of antisense oligonucleotide analog-mediated biologic responses. *Antisense Nucleic Acid Drug Dev.* **1998**, *8*, 281–293, doi:10.1089/oli.1.1998.8.281.
140. Liang, X.H.; Sun, H.; Nichols, J.G.; Crooke, S.T. RNase H1-Dependent Antisense Oligonucleotides Are Robustly Active in Directing RNA Cleavage in Both the Cytoplasm and the Nucleus. *Mol. Ther.* **2017**, *25*, 2075–2092, doi:10.1016/j.ymthe.2017.06.002.
141. Van Poelgeest, E.P.; Swart, R.M.; Betjes, M.G.H.; Moerland, M.; Weening, J.J.; Tessier, Y.; Hodges, M.R.; Levin, A.A.; Burggraaf, J. Acute kidney injury during therapy with an antisense oligonucleotide directed against PCSK9. *Am. J. Kidney Dis.* **2013**, *62*, 796–800, doi:10.1053/j.ajkd.2013.02.359.

142. Van Poelgeest, E.P.; Hodges, M.R.; Moerland, M.; Tessier, Y.; Levin, A.A.; Persson, R.; Lindholm, M.W.; Dumong Erichsen, K.; Ørum, H.; Cohen, A.F.; et al. Antisense-mediated reduction of proprotein convertase subtilisin/kexin type 9 (PCSK9): A first-in-human randomized, placebo-controlled trial. *Br. J. Clin. Pharmacol.* **2015**, *80*, 1350–1361, doi:10.1111/bcp.12738.

Chapter 4

Platelet Activation by Antisense Oligonucleotides in the Göttingen Minipig, Including an Evaluation of Glycoprotein VI and Platelet Factor 4 Ontogeny

Allan Paulo Valenzuela, Miriam Ayuso Hernando, Laura Buyssens, Chloé Bars, Chris Van Ginneken, Yann Tessier, and Steven Van Cruchten.

Adapted from *Pharmaceutics 2023, 15(4), 1112*.

Abstract: Antisense oligonucleotide (ASO) is a therapeutic modality that enables selective modulation of undruggable protein targets. However, dose- and sequence-dependent platelet count reductions have been reported in nonclinical studies and clinical trials. The adult Göttingen Minipig is an acknowledged nonclinical model for ASO safety testing, and the juvenile Göttingen Minipig has been recently proposed for the safety testing of pediatric medicines. This study assessed the effects of various ASO sequences and modifications on Göttingen Minipig platelets using in vitro platelet activation and aggregometry assays. The underlying mechanism was investigated further to characterize this animal model for ASO safety testing. In addition, the protein abundance of glycoprotein VI (GPVI) and platelet factor 4 (PF4) was investigated in the adult and juvenile minipigs. Our data on direct platelet activation and aggregation by ASOs in adult minipigs are remarkably comparable to human data. Additionally, PS ASOs bind to platelet collagen receptor GPVI and directly activate minipig platelets in vitro, mirroring the findings in human blood samples. This further corroborates the use of the Göttingen Minipig for ASO safety testing. Moreover, the differential abundance of GPVI and PF4 in minipigs provides insight into the influence of ontogeny in potential ASO-induced thrombocytopenia in pediatric patients.

4.1 Introduction

Antisense oligonucleotides (ASOs) are an acknowledged drug modality for treating specific diseases by selectively modulating the gene expression of disease-associated proteins. Currently, over a dozen RNA-targeting therapeutics have marketing approval, and many are in development for various conditions with limited or unavailable treatment options [1–3]. Recent rapid advancements in the medicinal chemistry of ASOs have led to a steep increase in RNA-targeted therapeutics entering clinical trials for a wide variety of diseases [4,5]. Backbone modification of the oligonucleotide sequence improves stability and increases resistance to endogenous nucleases, resulting in better bioavailability and potency [5–9]. ASOs that contain a phosphorothioated (PS) backbone together with additional sugar moiety modifications, e.g., 2'-O-methoxyethyl (2'-MOE) or locked nucleic acid (LNA), have further reduced ASO metabolism and enhanced affinity toward their target mRNA [10–13]. In addition, these sugar moiety modifications reduce some class-related toxicities [10,12–14]. The adverse effects caused by ASOs are categorized either as hybridization-dependent (i.e., exaggerated pharmacology and off-target effects) or as hybridization-independent toxicities (i.e., class-related effects due to interactions between ASOs and proteins) [15]. Such ASO class-related toxicities are usually the result of uptake and accumulation-induced changes in parenchymatous tissues [16]. Blood-born adverse effects have also been described, including dose-dependent thrombocytopenia [17–21].

Thrombocytopenia induced by ASOs can be caused by several mechanisms [19,22,23]. Due to the polyanionic nature of ASOs with PS backbone linkages, their nonspecific affinity to plasma and cellular surface proteins is enhanced [24–26]. Therefore, one mechanism by which platelets can be activated directly by ASOs is through nonspecific binding to platelet collagen receptor glycoprotein VI (GPVI), which then leads to platelet aggregation [22,27,28]. Moreover, ASOs can bind to platelet factor 4 (PF4), inducing a humoral response to the ASO-PF4 complex, similar to heparin-induced thrombocytopenia (HIT) [23,28]. Incubation of human platelets with ODN2395, a proinflammatory oligonucleotide with PS backbone modification without sugar moiety modification, causes direct platelet activation (P-selectin surface expression and alpha granule content release) and subsequent platelet aggregation [22,27,28]. The PS backbone modification of ODN2395 is the central mediator of its platelet-activating effects through GPVI receptor activation and enhances its responsiveness via GPVI clustering/dimerization [22]. Concentration-dependent platelet activation

by PS ASOs is related to length and PS load in the ASO sequence [28]. Furthermore, sugar modifications such as LNA are also shown to reduce binding to GPVI protein and dampen platelet activation [28]. Dose-dependent and sequence-specific alterations in platelet count have also been observed after ASO treatment in humans [21] and nonhuman primates (NHPs) [18]. However, the reduced platelet count in the peripheral blood of cynomolgus monkeys treated with ISIS104838, a 2'-MOE-modified ASO, was suggested to be due to the overall increase in natural IgM and monocyte activation, leading to an increased platelet sequestration in the spleen and liver [19]. Accordingly, no increase in P-selectin surface expression was observed in vitro, and no specific PF4-ASO antibodies were detected in this study, suggesting that no direct platelet activation occurred and no induction of the HIT-like humoral response developed in the study animals. On the other hand, the same sequence (ISIS104838) and other 2'MOE-modified and PS ASOs activated human platelets in vitro (release of alpha granule markers and P-selectin surface expression) through the GPVI binding mechanism [27]. On the other hand, a previous study in adult Göttingen Minipigs treated with various LNA-based PS ASOs did not show a fall in platelet count following four weeks of treatment [29]. This is also in line with the repeat-dose toxicity study conducted in juvenile Göttingen minipigs treated with RTR5001, an LNA-modified PS ASO, in which no fall in platelet count was seen after a drug exposure of up to eight weeks [30]. However, the effect of different types of ASOs on Göttingen minipig platelets, including their potential activation mechanism, has not yet been characterized.

The adult Göttingen Minipig is an acceptable nonclinical model for the safety testing of ASOs [29]. The present study aims to further characterize the Göttingen Minipig as a safety testing model for ASO therapeutics with particular attention to the platelet count alteration by ASOs. For that purpose, we investigated the effect of a panel of ASOs (with known and unknown platelet-related effects in humans and NHPs) on adult minipig platelets in vitro and compared it with previous data in humans and NHPs. Accordingly, an enzyme-linked immunosorbent assay (ELISA) was used to determine the in vitro fold-change increase of the activation marker, Thrombospondin 1 (TSP-1). TSP-1 is a highly abundant (up to 25%) protein contained in platelet alpha-granules that are secreted upon platelet activation [31,32]. It is a sensitive and stable marker in detecting in vitro platelet activation in humans and could also be used in future in vivo studies to differentiate in vivo platelet activation from in vitro artifacts during blood processing [33]. Furthermore, as platelet

aggregation usually follows platelet activation [34], we also measured the degree of aggregation of the different ASOs induced.

Recently, the juvenile minipig has also been evaluated as a pediatric safety testing model, and similar clinical chemistry and toxicity findings were observed in juveniles as in adult animals. However, differences in plasma and tissue exposures, as well as pharmacologic activity, were observed in the juvenile animals compared with the adult data, which could also potentially be present in the pediatric population and have an impact on the dose setting. For instance, the differential nuclease expression and activity across various ages of Göttingen Minipigs affect the metabolic pathway and pharmacologic effect of ASOs in different tissues and age groups [30]. As such, the ontogeny pattern of the platelet proteins implicated in ASO-induced thrombocytopenia could be different between various age groups and between minipigs and humans. Moreover, as there are concerns that treatment with ASOs could precipitate the already low platelet count in human neonates and juvenile animals [35,36], an investigation of potential platelet-related effects by ASOs is crucial. To help better understand and support the use of minipigs as an alternative model to NHPs for the safety testing of ASOs, we also aimed to characterize the same mechanism of direct platelet activation by ASOs in the Göttingen minipig through platelet GPVI binding and downstream signaling and activation as seen in human samples. Furthermore, ontogeny data for proteins implicated in ASO-induced thrombocytopenia mechanisms, such as GPVI and PF4, are pivotal to extending the work to juvenile minipigs as a nonclinical safety model for pediatric drug development. The GPVI level affected the intensity of platelet activation and was proposed as a screening biomarker to identify patients at a higher risk of ASO-induced thrombocytopenia [27]. On the other hand, PF4 in the plasma serves as a binding partner to ASOs, inducing a humoral response that leads to platelet clearance and thus could either be a precipitating or limiting factor in the mechanism. Therefore, this study also aimed to evaluate the changes in abundance of GPVI and PF4 in juvenile minipigs throughout postnatal development, and this could help explain and predict potential pediatric safety issues of ASOs.

4.2 Materials and Methods

4.2.1 Antisense Oligonucleotides (ASOs)

Seven tool ASOs were assessed to investigate their effects on adult Göttingen minipig platelets (Table 4.1). Accordingly, ODN2395 (PS oligonucleotide known to cause platelet activation and aggregation) and its unmodified isosequential variant [22,27,28]; ISIS104838 (2'MOE/PS/2'MOE gapmer that causes thrombocytopenia in NHPs and humans) [18,19,21,27] and its all-PS variant; and RTR5001 (LNA/PS/LNA gapmer that does not cause platelet count alteration) [29,30,37,38] together with its all-PS and unmodified variant were included and described in Table 4.1. In particular, RTR5001 targets the human *PCSK9* transcript (NCBI reference sequence: NM_174936.3) and has a single end-standing mismatch to the minipig sequence, which did not ablate its pharmacologic effects in the minipigs [29,30]. On the other hand, ISIS104838 targets the human TNF-α transcript (NCBI reference sequence: NM_000594.4) and does not align with the porcine transcript [39], whereas ODN2395 is an immunostimulatory (Toll-like receptor 9 agonist) CpG oligonucleotide containing only phosphorothioated bonds and DNA nucleotides [40]. All ASOs were synthesized and purchased in desalted form from Integrated DNA Technologies (Leuven, Belgium), except RTR5001, which was provided by the Roche Innovation Center, Copenhagen (Denmark). The oligonucleotides were purified by high-performance liquid chromatography and reconstituted in DPBS (14190-094, Gibco™, Thermo-Fischer, Waltham, MA, USA) to a stock of 100 µM. Four of these ASOs: ODN2395, ODN2395-PO, ISIS104838, and ISIS104838-PS, were synthesized and conjugated with biotin, and procured from Integrated DNA Technologies (Leuven, Belgium).

Table 4.1. Tool ASOs. Three ASO sequences with varying modifications were included in this study to investigate their effects in minipig platelets.

ASO	Modifications	Sequence (5'-3')	Length	PS Load	Platelet Effect
ODN2395	PS	t*c*g*t*c*g*t*t*t*t*c*g*g*c*g*c*g*c*g*c*c*g*	22	21	platelet activation
ODN2395-PO	unmodified	tcgtcgttttcggcgcgcgccg	22	0	no effect
ISIS104838	2'-MOE/PS/2'-MOE	G*C*T*G*A*t*t*a*g*a*g*a*g*a*g*G*T*C*C*C*	20	19	platelet activation
ISIS104838-PS	PS	g*c*t*g*a*t*t*a*g*a*g*a*g*a*g*g*t*c*c*c*	20	19	unknown
RTR5001	LNA/PS/LNA	T*G*C*t*a*c*a*a*a*a*c*C*C*A*	14	13	no effect
RTR5001-PS	PS	t*g*c*t*a*c*a*a*a*a*c*c*c*a*	14	13	unknown
RTR5001-PO	unmodified	tgctacaaaaccca	14	0	unknown

Phosphorothioate (PS) backbone modification position is indicated with *. Upper-case letters indicate the location of the 2'-O-methoxyethyl (2'-MOE)-modified sugar residues. Uppercase underlined letters indicate the location of the locked-nucleic-acid oligonucleotide in the sequence. ODN2395 isosequences contain unmethylated CpG dinucleotide-rich motifs (bold).

4.2.2 Study design

To assess platelet activation and aggregation, blood samples from five control adult female Göttingen Minipigs were provided by Janssen (Beerse, Belgium). Additional blood samples from juvenile minipigs (vehicle control and treated) that participated in an in vivo eight-week repeat-dose toxicity study of a model ASO (RTR5001) that is known not to cause platelet count alteration [30] were included to assess the ontogeny of GPVI and PF4 protein abundance (Supplementary Table S4.1). Furthermore, additional samples from four adult males provided by Ellegaard Göttingen minipig A/S (Dalmose, Denmark) and four adult females provided by Charles River Laboratories France Safety Assessment SAS (Saint Germain-Nuelles, France) were also included in the ontogeny investigation to increase statistical power. Blood sampling was approved by the ethics committees of Janssen (Beerse, Belgium), Charles River Laboratories France Safety Assessment SAS (Saint Germain-Nuelles, France), and Ellegaard Göttingen Minipig A/S (Dalmose, Denmark). We analyzed the animals (control and treated, male and female) per age group in our investigation of platelet count and the ontogeny of the two platelet-related proteins. Therefore, the following age groups were investigated for the ontogeny study: post-natal day (PND) 2 (n = 4), 9 (n = 4), 16 (n = 4), 23 (n = 4), 29–30 (n = 3), 37 (n = 4), 43 (n = 3), 51 (n = 4), and adults ranging from 1.5 to 3 years old (female (n = 9); male (n = 4)).

4.2.3 Blood collection and sample preparation

Blood was collected by venipuncture into citrated tubes (363080, BD Vacutainer®, Franklin Lakes, NJ, USA) and tubes without anticoagulant (20.1290, Sarstedt-Microvette® 200, Nümbrecht, Germany). Citrated blood samples were centrifuged at 200× *g* for 10 min at room temperature (RT) to isolate the platelet-rich plasma (PRP). The PRP was taken from the upper 2/3 of the supernatant to avoid contamination from the buffy coat layer. Platelet concentration in respective PRP was counted using KOVA® Glasstic 10 (22-270141, Thermo-Fischer, Waltham, MA, USA). Platelet-poor plasma (PPP) (either citrated or without anticoagulant) was prepared by centrifugation at 4000× *g* for 5 min at RT. Whole blood (WB) and plasma samples for the platelet activation and aggregation experiment were processed and assayed within 3 h after collection. Samples for the ontogeny study were snap-frozen and stored at −80 °C until processing. Washed platelet samples for the pull-down assay were subsequently prepared by two additional washing steps at 500× *g* for 10 min at RT using acid-citrate-dextrose (ACD) buffer (C3821-50ML, Sigma Aldrich, Tokyo, Japan) with 0.01 U/mL apyrase (A6237-100UN, Sigma-Aldrich).

4.2.4 Platelet activation assay in platelet-rich plasma and whole blood

PRP and WB were stimulated with either 20 µM adenosine diphosphate (ADP) (A2754-100MG, Sigma-Aldrich) as the positive control [22,28] or with the seven tool ASOs (Table 4.1) at two final concentrations (1 and 5 µM) to investigate platelet activation. ADP, as a positive control, allows comparison with the results of the aggregometry experiment (described below). DPBS was used as vehicle control. Accordingly, an aliquot of 90 µL PRP or WB was incubated with 10 µL of ADP, and tool ASOs for 30 min [27] in a cell culture incubator at 37 °C, with 5% CO_2 without agitation. After incubation, the PRP and WB samples were centrifuged at 1000× *g* for 15 min, and the supernatant per sample was aliquoted and stored at −80 °C until performing the thrombospondin 1 (TSP-1) immunoassay. To evaluate the role of GPVI protein in platelet activation, WB was pretreated with 10 µM spleen tyrosine kinase (SYK) inhibitor (PRT-060318, Abmole M5252) to prevent the downstream signaling of GPVI [27] or vehicle (0.1% DMSO) for 10 min at 37°C, followed by treatment with vehicle DPBS, or 5 µM ASOs (ODN2395 and ISIS104838) for 30 min at 37 °C. After incubation, the samples were centrifuged, aliquoted, and stored until processing as described above.

4.2.5 Thrombospondin 1 (TSP-1) immunoassay

Platelet activation was determined by an increase in TSP-1 level upon stimulation, as it is considered a validated marker to monitor in vitro platelet activation in humans [33]. TSP-1 level in the supernatant after the platelet activation assay was measured using an ELISA kit that is reactive to the full-length TSP-1 (MBS2511835, MyBioSource, San Diego, CA, USA) following the manufacturer's instructions. Plates were read using a Tecan Infinite M200 Pro (Tecan Group Ltd., Männedorf, Switzerland). Results were analyzed using a four-parameter logistic curve to determine TSP-1 levels and are presented as fold-change from the vehicle control.

4.2.6 96-well plate platelet aggregometry in platelet-rich plasma

This method was adapted from a previous study by Flierl et al. [22] with some modifications. Citrated PRP and PPP were collected as described above. After 30 min of resting at 37 °C in 5% CO_2 without agitation, 90 µL PRP was added to the wells of a 96-well plate, prepared with the different agonists; 5 µM ADP (positive control) and 5 µM of the different tool ASOs (Table 4.1). DPBS was used as vehicle control, whereas 0.01 U/mL apyrase was used as a negative control to inhibit platelet aggregation. The plate was then immediately placed in an absorbance monochromator (EnVision, Waltham, MA, USA), and optical density (OD) was determined at 595 nm every minute for 30 min (as no further aggregation was observed thereafter) between vortex shaking (1200 rpm) of the plates at 37 °C [41]. As a reference for maximal and minimal aggregation concerning the OD, PPP (100%) and PRP (0%) were used [42]. Data are presented as % change in OD through time which was established based on the change in OD values from the start of the experiment.

4.2.7 GPVI pull-down with ASO-coated streptavidin beads

The assay was run according to the protocol of Flierl et al. [22]. Accordingly, washed platelets were lysed in RIPA lysis buffer (50 mM Tris, 150 mM NaCl, 0.1% SDS, 1% Nonidet™ P-40 (21-3277, Sigma-Aldrich, Darmstadt, Germany), 1× Halt™ Protease Inhibitor (78430, Thermo Scientific, Waltham, MA, USA), pH 7.5), and total protein concentration was estimated using a Pierce BCA protein assay kit (23225, Thermo-Fischer). The lysate was precleared by incubation with Dynabeads™ Streptavidin T1 beads (65801D, MyOne™, Thermo-Fischer) for 20 min at RT to remove biotinylated proteins that might interact with the streptavidin beads to be used after. Fresh streptavidin beads

(100 µL) coated with 400 pmol ODN2395, ODN2395-PO, ISIS104838, and ISIS104838-PS were incubated with the cleared platelet lysates (devoid of biotinylated proteins) for 30 min at RT. Beads were then pelleted and washed three times with DPBS. Proteins pulled down by the beads coated with tool ASOs were eluted into a 5× SDS-PAGE loading buffer (MBS176755, MyBioSource, San Diego, CA, USA) and heated for 10 min at 96 °C before the downstream qualitative Western blot. The eluents were then separated by 12% SDS-PAGE and electrotransferred to a polyvinylidene difluoride membrane (1620174, Immun-Blot®, Bio-Rad Laboratories, Hercules, CA, USA). Ponceau staining of the membrane was performed to confirm protein transfer from the gel. As the nature of the PS backbone modification includes nonspecific interaction with different proteins [26], and this assay may pull down other proteins, the blots were incubated with an anti-GPVI (1/2000, PA5-20582, Thermo Scientific) primary antibody (reactive to human, mouse, rat, and pig) overnight at 4 °C to demonstrate GPVI protein binding with the tool ASOs. Immunoreactivity was revealed by incubating with HRP-conjugated anti-rabbit secondary antibody (1/5000, P0448, Dako, Denmark) for 60 min at RT and was detected by chemiluminescence. The size of the identified protein was compared to the Reference Sequence (https://www.ncbi.nlm.nih.gov/protein/XP_005656014.2, accessed on 23 September 2021) of predicted swine GPVI protein calculated on a protein MW calculator (https://www.genecorner.ugent.be/protein_mw.html, accessed on 23 September 2021).

4.2.8 GPVI and PF4 quantification by ELISA

The level of GPVI and PF4 proteins were measured in the different juvenile and adult age groups to characterize their ontogeny. GPVI was measured in citrated PRP samples, whereas PF4 was measured in PPP samples (without anticoagulant) as we are interested in free PF4 in the plasma, where it could serve as a binding partner for ASOs and result in the HIT-like mechanism of thrombocytopenia. Samples that were hemolyzed (PND 2) were excluded from our investigation. GPVI protein abundance was quantified using an ELISA kit (MBS743059, MyBioSource) following the manufacturer's instructions. The GPVI level was adjusted to a 1×10^8 platelets/mL final platelet count to allow a relative comparison between samples. Afterward, to assess the relative amount of GPVI protein per ml of blood in the juvenile minipigs, the GPVI level was adjusted using the platelet concentration in WB, as differential platelet concentration was expected in the developing animals. The corresponding platelet count for the juvenile minipig samples was determined previously [30] on an ADVIA 120/2120 system (Siemens, Erlangen, Germany) is and provided as supplementary

data (Supplementary Table S4.1). The abundance of PF4 was measured from plasma using an ELISA kit (MBS2701434, MyBioSource) as per manufacturer's protocol.

4.2.9 Statistical analysis

The TSP-1 fold change data were fitted first to a linear mixed model. ASO treatment was used as a fixed factor in this model to evaluate the treatment effect on platelet activation. The animal was set as a random effect to account for the dependence between observations among each treatment per animal. The role of SYK in the downstream signaling of GPVI was also evaluated using a linear mixed model with SYK inhibitor treatment, ASO treatment, and their interaction as fixed factors. Animal nested with SYK inhibitor treatment groups was included as a random effect. The Student's t-test for pairwise comparison was used as a post hoc analysis. On the other hand, to evaluate the treatment effect on platelet aggregation, the data on aggregation through time were fitted to a mixed model for repeated measures. The fixed factors for the model for this analysis consisted ASO treatment and time, together with their interaction. The animal was also set as a random effect, and the residual was used as a repeated structure to represent the compound symmetry covariance. The analysis was limited to only include the % change in OD data from the last 10 min of the assay in this model to satisfy the sphericity assumption based on Mauchly's test for sphericity. Post hoc analysis with Dunnett's test for multiple comparisons was used when comparing with the vehicle control group. Nevertheless, to determine if the sample size included in the ontogeny study comprising vehicle control and RTR5001-treated animal samples was sufficient, and whether we could remove the effect of treatment and sex in our analysis as no treatment-related and sex-related differences that were previously seen [30,43–45], we adopted two approaches. First, we conducted a principal component analysis to see if treatment and sex are significant contributors to variability in the principal components of the data. Second, we performed a linear regression with fixed effects of age, treatment or sex, and their interactions. The starting models were gradually simplified using stepwise backward modeling, wherein all non-significant effects were removed step by step. No significant effect of treatment, sex, and their interactions was detected in either approach. A simplified linear regression model with age as a fixed effect and laboratory source of blood as a random effect was used to examine age-related differences in GPVI and PF4 protein abundance and the platelet count. Tukey's honest significance difference was used post hoc to identify differences between groups for the protein abundance, and Student's t-test for a pairwise comparison was used for the platelet concentration data. A non-

parametric Spearman rank correlation test was performed to identify the correlation between platelet activation in PRP and WB; platelet activation and aggregation in PRP; GPVI and PF4 abundance with platelet concentration; and GPVI abundance with platelet activation and aggregation data. A *p*-value smaller than 0.05 was considered statistically significant. Variables were log- or square-root-transformed when needed to meet normality and homoscedasticity assumptions. Statistical analysis and graphs were performed using JMP® Pro 16 (SAS Institute, Cary, NC, USA).

4.3 Results

4.3.1 ASO-induced platelet activation in platelet-rich plasma and whole blood

To establish whether ASOs activate minipig platelets directly, we investigated the effects on the platelet activation marker, TSP-1 level, after incubating the PRP samples with ASOs (Figure 4.1A). Compared to the vehicle control, PRP treated with ADP as positive control showed a significant increase in TSP-1 ($p = 0.0095$). In general, none of the PRP samples treated with 1 µM ASOs showed a significant increase in TSP-1. Samples treated with 5 µM ODN2395 ($p < 0.0001$), ISIS104838 ($p = 0.0002$), RTR5001-PS ($p = 0.0053$), and ISIS104838-PS ($p = 0.0056$) triggered a robust release of TSP-1. On the other hand, no significant TSP-1 release was observed for ODN2395-PO, RTR5001, and RTR5001-PO, even at a 5 µM concentration.

We also studied the platelet activation in WB (Figure 4.1B), in which treatment with the platelet agonist ADP also showed a significant increase in TSP-1 level ($p = 0.0110$). Again, no considerable stimulation was detected for the WB samples treated with 1 µM ASOs. Consistent with the robust increase in TSP-1 level in PRP, 5 µM ODN2395 also stimulated the highest release ($p < 0.0001$) of TSP-1 in the WB, followed by ISIS104838 ($p = 0.0048$) and RTR5001-PS ($p = 0.0210$), respectively. Interestingly, 5 µM ODN2395-PO also triggered a significant increase in TSP-1 level ($p = 0.0323$), while we failed to detect a significant increase in TSP-1 for the WB samples treated with 5 µM ISIS104818-PS ($p = 0.0630$). On the other hand, Spearman's rank correlation analysis on all treatment groups showed a moderate correlation between TSP-1 activity levels in the WB and PRP ($p < 0.0001$, $r = 0.5633$).

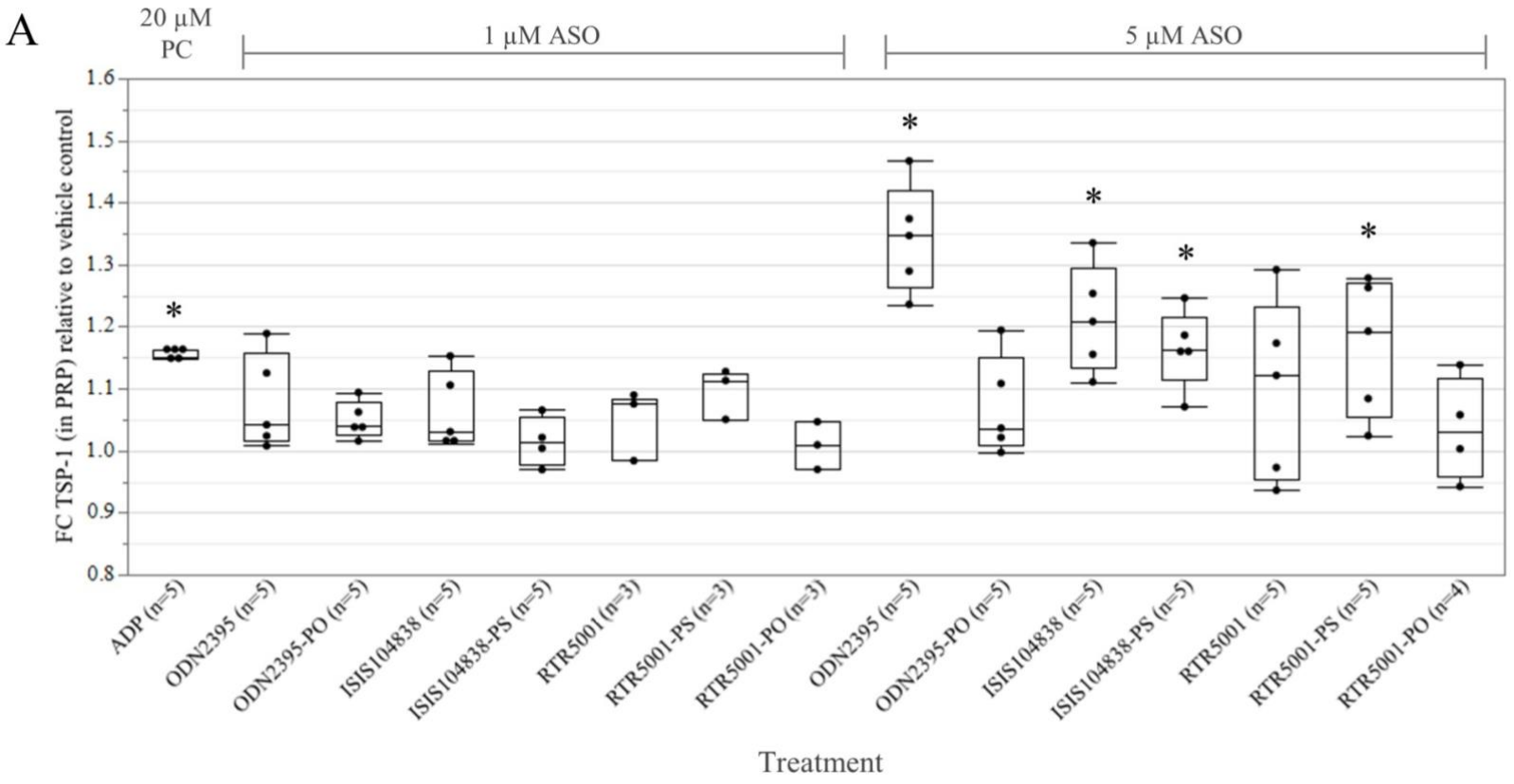
A
20 µM PC
1 µM ASO
5 µM ASO
FC TSP-1 (in PRP) relative to vehicle control
1.6
1.5
1.4
1.3
1.2
1.1
1.0
0.9
0.8
ADP (n=5)
ODN2395 (n=5)
ODN2395-PO (n=5)
ISIS104838 (n=5)
ISIS104838-PS (n=5)
RTR5001 (n=3)
RTR5001-PS (n=3)
RTR5001-PO (n=3)
ODN2395 (n=5)
ODN2395-PO (n=5)
ISIS104838 (n=5)
ISIS104838-PS (n=5)
RTR5001 (n=5)
RTR5001-PS (n=5)
RTR5001-PO (n=4)
Treatment

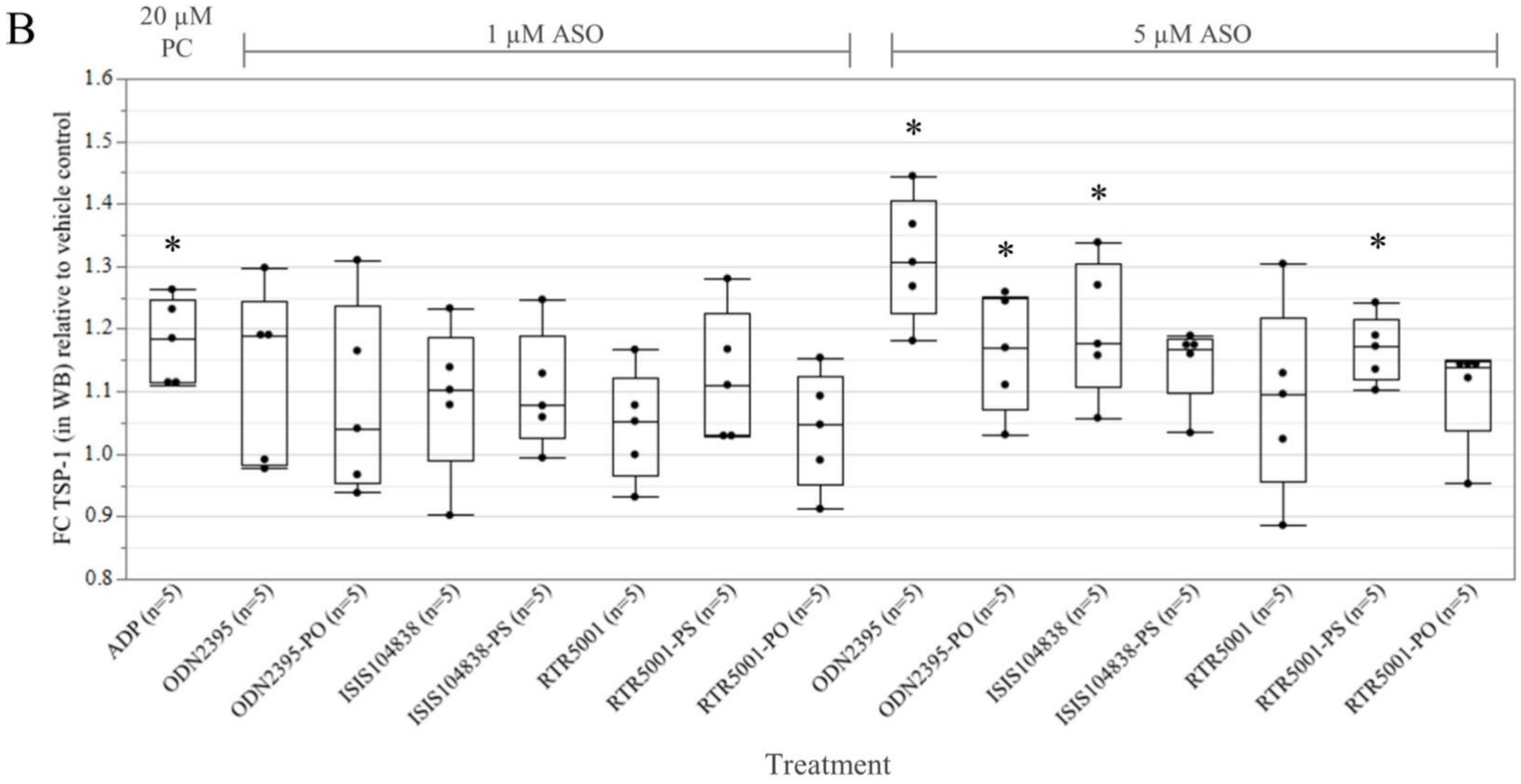
B
20 µM PC
1 µM ASO
5 µM ASO
FC TSP-1 (in WB) relative to vehicle control
1.6
1.5
1.4
1.3
1.2
1.1
1.0
0.9
0.8
*
ADP (n=5)
ODN2395 (n=5)
ODN2395-PO (n=5)
ISIS104838 (n=5)
ISIS104838-PS (n=5)
RTR5001 (n=5)
RTR5001-PS (n=5)
RTR5001-PO (n=5)
ODN2395 (n=5)
ODN2395-PO (n=5)
ISIS104838 (n=5)
ISIS104838-PS (n=5)
RTR5001 (n=5)
RTR5001-PS (n=5)
RTR5001-PO (n=5)
Treatment

Figure 4.1. Effects of 1 and 5 µM antisense oligonucleotides (ASOs) on the platelet activation marker, thrombospondin 1 (TSP-1) in Göttingen minipig (**A**) platelet-rich plasma and (**B**) whole blood. An amount of 20 µM ADP as positive control (PC) in parallel with the panel of ASOs was incubated for 30 min with either platelet-rich plasma or whole blood from adult minipigs. Change in TSP-1 level in each treatment group is expressed as fold change (FC) with respect to the vehicle control (DPBS). * $p < 0.05$ compared with the vehicle by linear mixed model, with Dunnett post hoc test.

4.3.2 ASO-induced platelet aggregation in platelet-rich plasma

To investigate whether the observed platelet activation (see Figure 4.1) would translate into platelet aggregation, we performed a 96-well plate aggregometry assay wherein a reduction in OD values reflects platelet aggregation in the samples (Figure 4.2). The OD of the vehicle- (Figure 4.2A) and 0.01 U/mL apyrase-treated (Figure 4.2C) PRP samples remained unchanged throughout the assay. The positive control, ADP, triggered a significant decrease in OD ($p < 0.0001$), which was already observed in the initial five minutes of the experiment (Figure 4.2B). Samples treated with ODN2395 triggered the highest reduction in OD throughout time ($p < 0.0001$) (Figure 4.2D). Two samples showed a maximum reduction of around 80% in OD values. This is followed by RTR5001-PS, for which a significant decline in OD values was observed ($p < 0.0001$) (Figure 4.2I). Two samples in this group decreased by around 60–80% in their OD values. A minimal decrease in OD was observed for ISIS104838 ($p = 0.0392$) (Figure 4.2F) and its all-PS variant, ISIS104838-PS ($p = 0.0387$) (Figure 4.2G), after an erratic increase in the OD of some samples observed at different time points. No significant change in OD was observed for samples treated with ODN2395-PO, RTR5001, and its unmodified variant (Figure 4.2E,H,J). There was no significant correlation between the aggregometry results (% OD change after 30 min) and TSP-1 activity marker level in PRP.

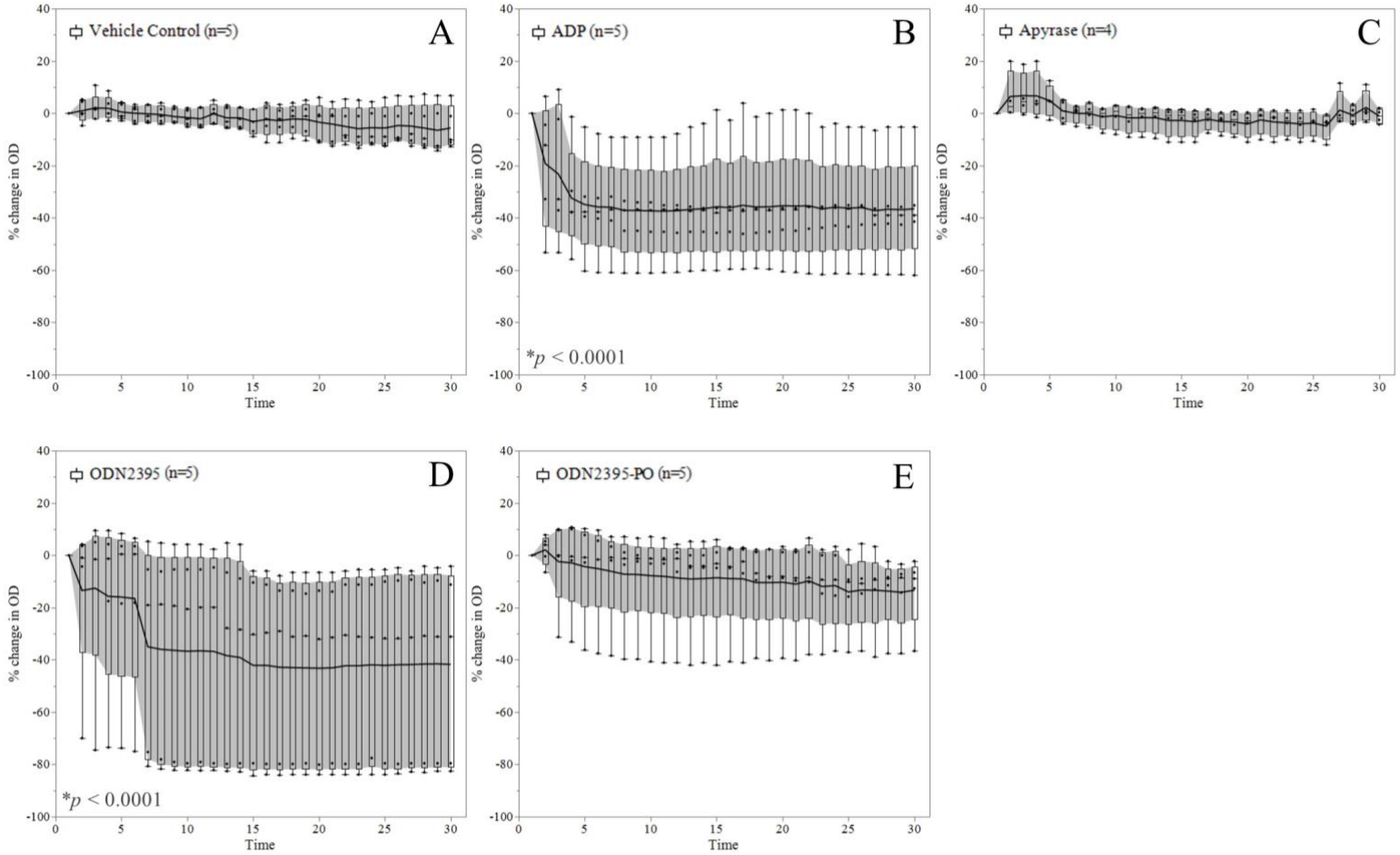
Vehicle Control (n=5)
A
ADP (n=5)
B
*p < 0.0001
Apyrase (n=4)
C
ODN2395 (n=5)
D
*p < 0.0001
ODN2395-PO (n=5)
E
% change in OD
Time

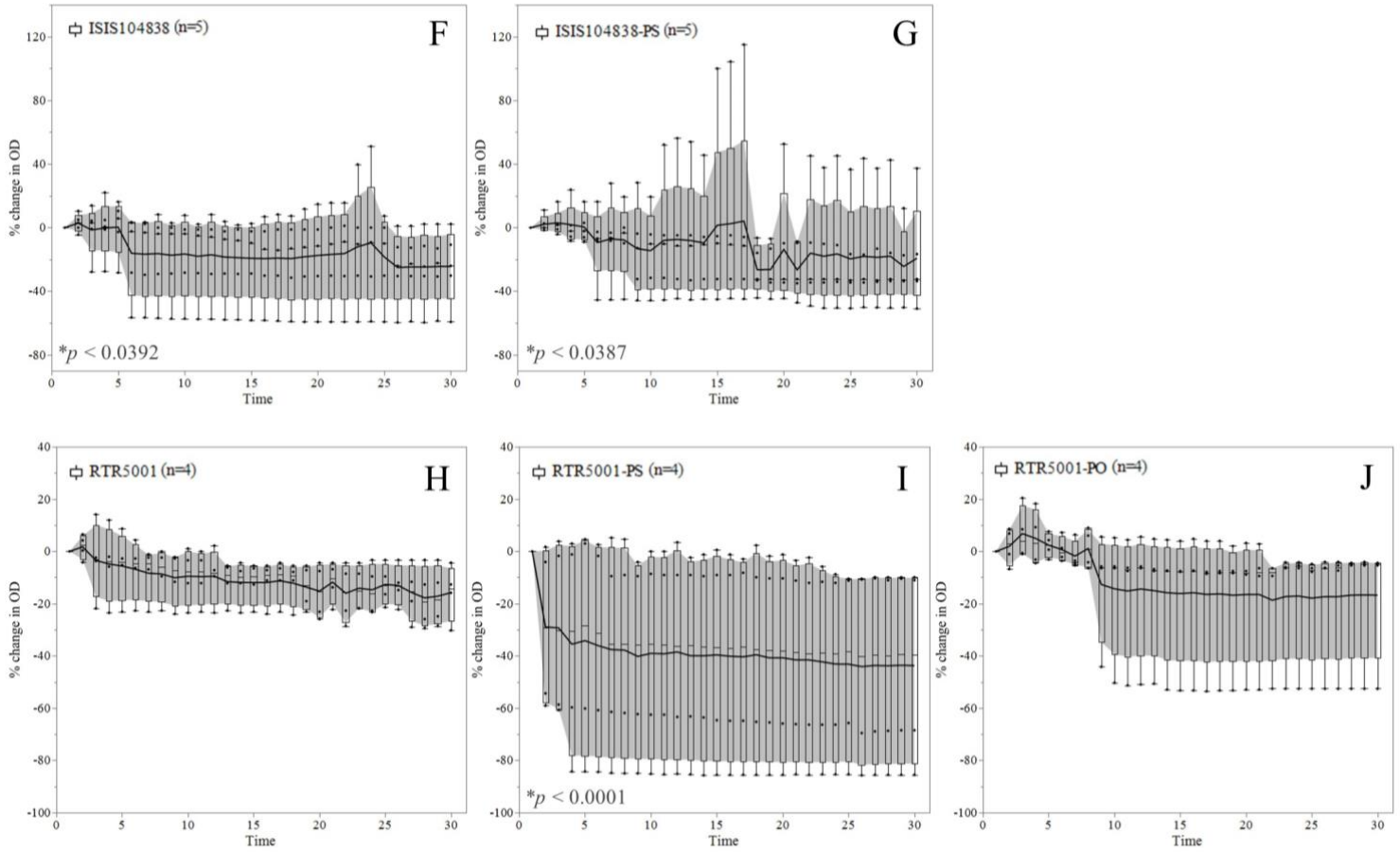
ISIS104838 (n=5)
F
% change in OD
Time
*p < 0.0392
ISIS104838-PS (n=5)
G
*p < 0.0387
RTR5001 (n=4)
H
RTR5001-PS (n=4)
I
*p < 0.0001
RTR5001-PO (n=4)
J

Figure 4.2. Platelet aggregation in platelet-rich plasma (PRP) after ASO stimulation. The mean trend line of % change in OD for the (**A**) vehicle control (DPBS), (**B**) 5 µM ADP (positive control), and (**C**) 0.01 U/mL apyrase (negative control) incubated in parallel with the seven tool ASOs (**D**–**J**) are presented together with the interquartile range highlighted as bands. Time is presented in minutes (min). Detailed representation of the % change in OD values across time for each 5 µM ASO treatment: (**D**) ODN2395 and (**E**) ODN2395-PO; (**F**) ISIS104838 and (**G**) ISIS104838-PS; and (**H**) RTR5001, (I) RTR5001-PS, and (**J**) RTR5001-PO are shown in different panels. * $p < 0.05$ compared with the vehicle by a linear mixed model for repeated measures during the last 10 min of the assay (between 21 and 30 min), with the Dunnett post hoc test.

4.3.3 GPVI protein binding and signaling in Göttingen Minipig platelets

The pull-down experiment using streptavidin beads coated with ASOs confirmed GPVI as a binding partner for the three ASOs (ODN2395, ISIS104838, and ISIS104838-PS) that caused activation and aggregation in the minipig platelets (Figure 4.3A). Accordingly, these three ASOs containing PS-backbone modifications successfully pulled down an approximately 75-kDa protein identified as GPVI using Western blot. Nonetheless, other nonspecific proteins were detected (using Ponceau stain) to be pulled down as well. Conversely, no binding was observed with the ODN2395-PO that lacks the PS-modification in its backbone, even with the eluent volume increased by two-fold. Subsequently, to further define the role of GPVI as a receptor that mediates platelet activation by PS-modified ASOs, we investigated the role of SYK in the downstream signaling of GPVI. Pre-treatment with SYK inhibitor abolished the increase in platelet activation marker, TSP-1, in ODN2395- and ISIS104838-treated samples (Figure 4.3B).

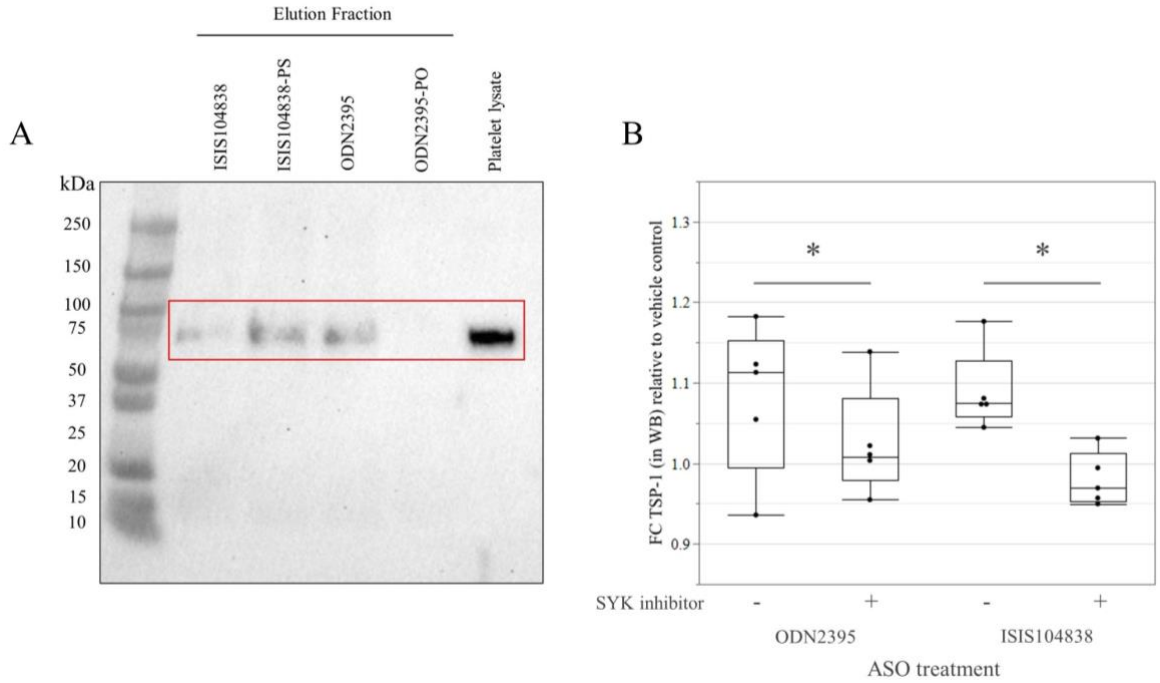

Figure 4.3. (**A**) Pull-down assay identified GPVI protein as a binding partner for PS-modified ASOs (contained in the red box with the positive control, platelet lysate); representative of Western blot detecting GPVI (n = 3). (**B**) Whole blood (n = 5) pretreated or not with the spleen tyrosine kinase (SYK) inhibitor PRT-060318 (10 µM) before the addition of vehicle (DPBS), or 5 µM ASOs (ODN2395 and ISIS104838). Change in TSP-1 level in the different treatment groups is expressed as fold change (FC) with respect to the vehicle control. * $p < 0.05$ by linear mixed model with paired Student's t-test as post hoc for the effect of the SYK inhibitor.

4.3.4 Platelet count and protein abundance of GPVI and PF4

To permit a comparison between platelet count ontogeny with platelet GPVI and PF4 protein abundance, we show in Figure 4.4 the previous platelet concentration data from the in vivo eight-week repeat-dose toxicity study in juvenile Göttingen minipigs (PND 2, 9, 16, 23, 29–30, 37, 43, and 51) [30] (Supplementary Table S4.1), together with the normal platelet count range in the juvenile Göttingen minipigs (Figure 4.4A) [43,46–48]. Accordingly, a sinusoidal pattern of ontogeny was observed for the platelet concentration in the different juvenile age groups ($p < 0.0001$), wherein the lowest mean platelet concentration was observed at PND 2. Two peaks of higher platelet concentration were observed at PND 9 and PND 43–51, whereas intermediate platelet concentrations were observed from PND 16 to PND 37. The ontogeny profiles of the two platelet-related proteins involved in platelet activation in humans showed two different patterns in the

juvenile (PND 9, 16, 23, 29–0, 37, 43, and 51) and adult minipigs (Figure 4.4B-C). GPVI presented a stable protein abundance with no statistically significant differences among various age groups (Figure 4.4B). Likewise, no difference was observed among the different age groups when GPVI abundance was adjusted according to the differential platelet concentration in the WB (Supplementary Table S4.1). On the other hand, a significantly higher PF4 abundance was detected for PND 9, 43, and 51 compared to adult samples, while PND 16 to 37 showed intermediate values (p = 0.0124) (Figure 4.4C). The Spearman's rank correlation analysis on all age groups (except PND 2 as it was not included to determine protein abundance due to hemolysis in the sample) showed a moderate correlation between platelet concentration and PF4 abundance in plasma (p = 0.0010, r = 0.6075). In contrast, no correlation was seen between platelet concentration and GPVI abundance. A strong correlation was seen between platelet activation in the WB treated with ODN2395 and GPVI abundance in PRP (p = 0.0374, r = 0.9); and between the platelet aggregation data on ISIS104838-PS and GPVI abundance in PRP (p = 0.0374, r = 0.9).

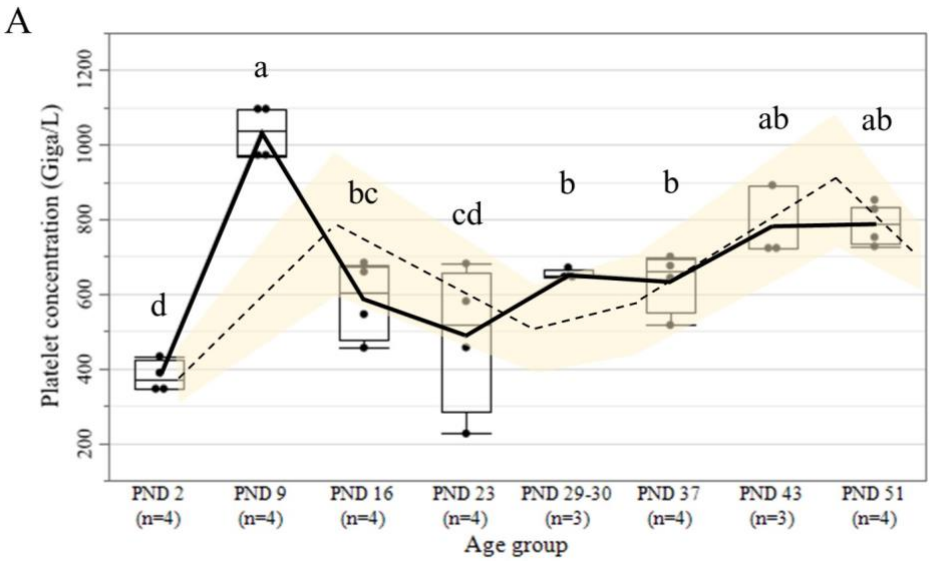

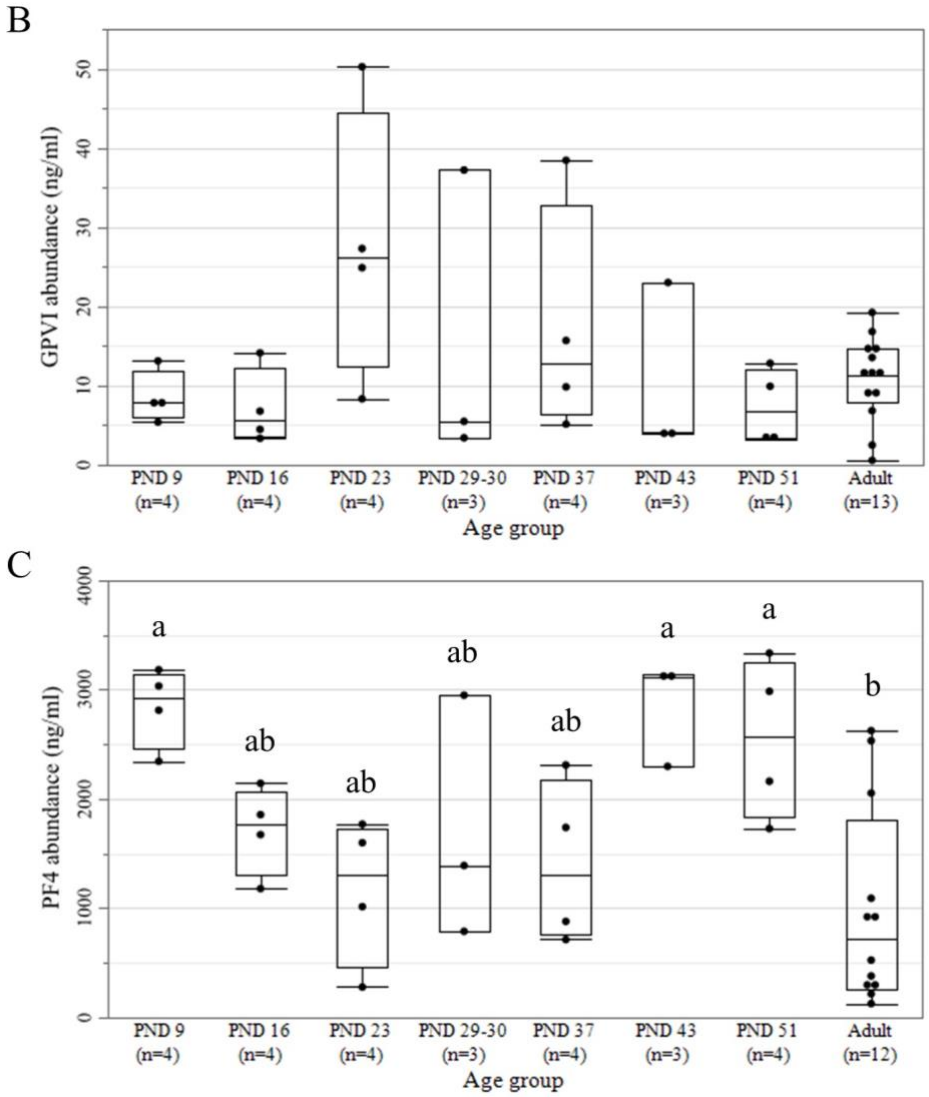

Figure 4.4. (**A**) Platelet concentration. The full trend line represents the platelet count from the juvenile minipig samples [30], whereas the broken trend line (mean) represents the normal platelet concentration range (yellow band) previously reported in the Göttingen minipig [43,46–48]. (**B**) GPVI, and (**C**) PF4 protein abundance over time in the juvenile and adult Göttingen minipigs. Age groups not sharing the same letter are significantly different by a linear mixed model, with Tukey's honest significance difference post hoc ($p < 0.05$).

4.4 Discussion

The present study aimed to assess the effects of a panel of ASOs on minipig platelets and investigate the underlying mechanisms for the observed platelet activation and aggregation. An overview of the complete platelet response pattern is presented for both non-rodent species (minipig and NHP)

and humans for all seven different ASOs in Table 4.2. As rapid growth and development in the pediatric population can influence the pharmacodynamics of a therapeutic agent [49], the ontogeny of GPVI and PF4 protein abundance was also assessed together with the platelet counts. Both proteins were previously seen to interact with ASOs, and either directly activate platelets [22,27,28] or cause an immune-mediated effect [23,28], potentially leading to late-onset thrombocytopenia. The main findings of our study are: (i) adult minipig platelets are activated and aggregated by PS- and/or 2'-MOE-modified ASOs (Table 4.2); (ii) GPVI plays a role in the direct activation of Göttingen Minipig platelets by ASOs; and (iii) GPVI and PF4 show a differential pattern in their protein abundance during the postnatal development of the Göttingen Minipig.

Direct activation of platelets by ASOs was previously investigated in vitro in human PRP and WB samples and shown to be concentration-dependent [22,27,28]. Dose-dependent changes in platelet counts have also been observed in vivo after ASO treatment in humans and NHPs [18,19,21]. Our results align with these data, as the platelet activation marker (TSP-1) increased after ASO incubation was seen at 5 µM. The therapeutically relevant dose of ASOs given subcutaneously in humans produces a plasma maximum concentration (C_{max}) of around 1–2 µM [50], which falls within the concentration range used in the current study.

In general, incubating human platelets with PS-modified ASOs led to platelet activation and aggregation [22,27,28,51], with a greater activation seen in sequences containing CpG motifs [27,28]. The tool ASOs with PS-modified backbone in this study also induced the activation and aggregation of minipig platelets (Table 4.2). Accordingly, ODN2395 (CpG-rich PS-ASO) produced the biggest release of the TSP-1 marker, also compared to the samples treated with ADP [22,27,28]. Moreover, subsequent platelet activation also correlates with ON length and the number of PS bonds in the sequence [28]. However, RTR5001-PS induced a slightly higher activation than ISIS104838-PS, even though the latter has a longer sequence and more PS bonds. Hence, the platelet activation observed in this regard appears to be sequence-specific. In contrast, RTR5001 did not cause platelet activation in our study, and this agrees with the in vivo findings in Göttingen minipigs [29,30], NHPs [38], or humans [37], in spite of the context of relatively short-term treatments (13 weeks in NHPs, 4–8 weeks in minipigs, and 2 weeks in humans). Therefore, our minipig data confirm the observation in human samples [28] that sugar modification, such as LNA, reduces the risk of platelet activation. Although it is difficult to argue based on this data that LNA is

less platelet activating than 2'-MOE, the lower doses afforded by the greater potency of LNA-modified ASOs [10] are likely to reduce the thrombocytopenic risk. Overall, it seemed that the tool ASOs were weak agonists in terms of platelet activation in the minipig samples, as evidenced by the mean maximum of about 1.3 fold change in the TSP-1 marker. Nevertheless, this marker was sensitive enough to detect platelet activation, and this was in line with previous papers in human samples; thus, further evaluation using other markers of platelet activation (i.e., P-selectin expression by flow cytometry) and an in vivo study would be useful to confirm these findings in the Göttingen Minipigs.

Our study noted a discrepancy in the activity marker results between the PRP and WB samples concerning ISIS104838-PS and ODN2395-PO. The non-activation of the platelets in the WB by ISIS104838-PS could be due to the higher variability in WB samples. The slightly higher activation level seen with ISIS104838 compared to its all-PS variant could be due to the added negative charge brought about by the additional 2'-MOE modifications [52] that could result in a higher binding affinity to some proteins [53]. Further investigation is needed to understand the detailed mechanism of 2'-MOE-ASO–protein interaction leading to platelet activation and if ISIS104838-PS could interact less with GPVI, leading to weaker platelet activation. On the other hand, we noted an increase in the platelet activation marker when co-incubating ODN2395-PO with WB. This might be due to the unmethylated CpG motifs in its sequence that could have either induced immune activation through the activation of Toll-like receptor 9 (TLR 9) [54], which is predominant in immune cells [55], or through the activation of the complement cascade [56]. Systemic effects such as these have been considered factors for thrombocytopenia, either through platelet activation, sequestration, or secondary effects on platelet production [19,28,57]. Further investigation is needed to differentiate the inflammatory state and the role of the complement cascade in platelet activation by ASOs, and whether both mechanisms interact to have a synergistic effect [58]. Moreover, since ODN2395-PO has not been evaluated in terms of platelet activation in the WB of humans or NHPs, questions remain about how this observation in the minipig model could be translated to humans. Differences in the innate immune response of juveniles and adults [59] should also be considered during juvenile animal studies of ASOs with compound-specific effects. As such, the stringent screening of specific sequence motifs and strategic modifications in the sequence proves to be beneficial [60] for mitigating proinflammatory effects and improving the overall tolerability of ASOs.

Table 4.2. Overview of in vivo and in vitro platelet response in Göttingen minipig, NHP, and humans for all the seven different tool ASOs, including the modifications used for each sequence, its length, and PS load [18,19,21,22,27,28,30,37,38].

ASO	Modifications	Length	PS Load	Platelet Effect			
				Human, NHP, Göttingen minipig		Göttingen minipig	
				In Vivo	In Vitro [H]	In Vitro	
					Activation Assay, Aggregometry	Activation Assay	Aggregometry
ODN2395	PS	22	21	unknown	activation, aggregation	activation	aggregation
ODN2395-PO	unmodified	22	0	unknown	no effect	PRP: no effect WB: activation	no effect
ISIS104838	2′-MOE/PS/2′-MOE	20	19	thrombocytopenia [H,N]	activation	activation	aggregation
ISIS104838-PS	PS	20	19	unknown	unknown	PRP: no effect WB: activation	aggregation
RTR5001	LNA/PS/LNA	14	13	no effect [H,N,M]	unknown	no effect	no effect
RTR5001-PS	PS	14	13	unknown	unknown	activation	aggregation
RTR5001-PO	unmodified	14	0	unknown	unknown	no effect	no effect

Abbreviations: PS, phosphorothioate; 2′-MOE, 2′-O-methoxyethyl; LNA, locked nucleic acid; [H], humans; NHP/[N], nonhuman primates; [M], Göttingen Minipigs; PRP, platelet-rich plasma; WB, whole blood.

In terms of platelet aggregation, ASOs also seem to be very weak agonists, with the effects of some ASOs in the tested panel appearing to be negligible. ODN2395, which had the highest release of TSP-1, seemed only to have a weak impact on platelet aggregation. This observation toward ODN2395 and its unmodified variant, relative to ADP, is in accordance with previous findings in human PRP [22]. In a general sense, the results of the aggregometry experiment are in line with the platelet activity data discussed above (Table 4.2), as platelet activation is usually followed by subsequent platelet aggregation [34]. However, we have not seen a correlation between the TSP-1 level and aggregation intensity in the Göttingen Minipig PRP samples treated with the different ASOs. This could be related to the response variability in aggregation among the different ASO tools and between samples [61]. On the other hand, the initial increase in OD after stimulation with ISIS104838 and its all-PS variant was due to the change in the shape of platelets when activated and their subsequent binding with fibrinogen providing "bridges" with other platelets [62]. Furthermore, interindividual platelet responsiveness to different agonists is highly variable [63–66] due to genetic and environmental factors [67]. Therefore, it is recommended to have a larger sample size to catch the anticipated effects. Although we saw a disparate level of variability between samples per treatment group, we still observed differences in responses between the different tool ASOs, as shown in the activity assay results.

Several mechanisms for causing thrombocytopenia have been identified after drug administration [68]. For ASOs, the direct activation of platelets after the interaction of PS-modified ASOs and GPVI protein has been proven in several in vitro studies with human platelets [22,27,28]. We also observed this in our study, as a protein of around 75-kDa was identified as GPVI by Western blot and served as a binding partner for all the tested ASOs containing PS modifications. Furthermore, the role of GPVI was defined by abolishing the increase in TSP-1 level of samples pretreated with SYK inhibitor [22,27,28]. This confirmed that the Göttingen Minipig platelets undergo the same mechanism as those in humans by direct platelet activation through GPVI. Therefore, it is recommended for future studies specific to platelet activation by ASOs through GPVI binding to use collagen-related peptides or convulxin as a positive control [69]. On the other hand, as other nonspecific proteins from the platelet lysates were detected to bind to the PS-modified ASOs in our study, further investigation would be needed to identify these proteins and to define if their interaction with ASOs leads to a different mechanism of platelet activation in the minipigs. Likewise, other mechanisms await in vivo evaluation in Göttingen Minipigs, such as the immune-mediated

mechanism through PF4 [23,28] or through natural IgM in concert with monocyte activation, leading to increased platelet sequestration in the liver and spleen as has been shown in vivo in NHPs [19]. Nevertheless, if direct activation is asserted as the prevailing mechanism, the effects in life would tend to be acute in onset [70,71]. In contrast, the immune-mediated model similar to HIT can have either a rapid (if clinically significant levels of antibodies are present) or delayed onset [72]. However, while dose-dependency is in favor of a direct activation mechanism such as that described in Flierl et al., 2015, the late onset, as well as the rare occurrence in humans [21] are more in favor of an immune mechanism (Sewing et al., 2017). Further investigation is needed as several potential factors could (inter)play a role in platelet count reduction.

Considering that responsiveness to ASO treatment was observed to be strongly correlated to individual GPVI levels, assessing platelet GPVI abundance could be a useful screening marker to identify patients at a higher risk of ASO-induced platelet side effects [27]. For instance, platelet GPVI levels have been shown to vary between healthy individuals [73] and can be elevated in patients with underlying conditions, e.g., obesity [45,74] and cancers [75]. Moreover, certain individuals may be predisposed to platelet-related adverse effects in relation to their disease state [76]. Therefore, response to ASO treatment may differ between healthy and diseased animal models, and this applies to individual human patients as well. In this study, we detected a strong correlation to individual GPVI levels with ODN2395 and ISIS104838-PS treatments, which is in line with the potency of these compounds. Since ASO-relevant proteins undergo maturational changes in the Göttingen Minipigs [30], we also investigated the ontogeny of GPVI protein in minipigs. Accordingly, no GPVI abundance differences were seen between the different juvenile and adult minipigs. Thus, no difference in GPVI-mediated platelet reactivity toward ASOs is expected between the different age groups, with no increased risk of platelet depletion in the youngest population.

The observed ontogenic pattern in platelet count was in line with earlier data in the different age groups of minipigs [43,46–48]. This corresponds to the sinusoidal trend in humans with low platelet concentration for neonates and peaks at 2 to 3 weeks and 6 to 7 weeks [35]. Therefore, neonatal trends in platelet counts should be considered when analyzing nonclinical data from juvenile minipig studies. Intriguingly, the sinusoidal pattern of platelet count ontogeny seems to not influence the relative platelet GPVI abundance adjusted to the platelet concentration measured in WB. As the GPVI protein is essentially uncleaved on normal circulating platelets and shed from the

platelet surface upon activation [77], it is expected that the relationship between GPVI level in plasma and platelet count after in vitro activation should be direct. On the other hand, when GPVI shedding is elevated due to, for instance, thrombocytopenia caused by an increased immune clearance rather than a low platelet production, the expected relationship with platelet count would be inverse in vivo [78]. Moreover, compared with adult platelets, neonatal platelets are hyporeactive [79–83]. This is further supported by transcriptomic data showing the downregulation of genes related to platelet reactivity and cell-signaling [84], which could lead to a lowered protein abundance. Therefore, we hypothesize that GPVI could be downregulated during the period of physiologic thrombocytosis, thus regulating platelet function during this developmental period until the platelet count reaches a steady state of maturity. However, this still could not explain why we found the same levels of GPVI relative to platelet concentration in all age groups. Moreover, it is unclear whether the high variability in GPVI levels in some age groups could influence platelet reactivity to ASOs in the clinical setting. Therefore, further research is needed to address this observation, including the measurement of GPVI density on platelet surfaces in the different juvenile age groups.

Unlike GPVI, the PF4 abundance appeared to correlate with platelet concentration. PF4 is released from developing megakaryocytes [85]. However, the positive correlation between the two datasets is in sharp contrast to the negative autocrine effect of PF4 on megakaryopoiesis, for which PF4 abundance is inversely related to platelet count [85,86]. However, we noted a decline of approximately 50% in the platelet count between PND 9 and 16, which is similar to the 50% decrease in the number of megakaryocyte-containing colonies after supplementation of hPF4 in previous in vitro studies using cultures of human marrow progenitor cells [87]. It should be noted that the described negative autocrine effect of PF4 occurred during steady-state platelet count and not during the active developmental stages. Therefore, the negative autocrine in vivo regulation by megakaryopoiesis proceeds differently during this developmental period. The low-density lipoprotein receptor-related protein 1 (LRP1) is responsible for this auto-downregulation, and it undergoes a transient expression during megakaryopoiesis before platelet release [86]. Hence, LRP1 might be undergoing a developmental expression ontogeny to regulate the negative autocrine effect. We postulate that the receptor is lowly expressed between birth and postnatal week 2 and weeks 6–7, allowing an increase in platelet production (with a corresponding rise in PF4 released by developing megakaryocytes), leading to the two peaks in platelet concentration observed.

Therefore, future attention should be given during these developmental periods with observed peak PF4 abundance as the availability of PF4 could influence the risk for the generation of PF4/ASO immune response that could lead to platelet count alteration in minipigs.

4.5 Conclusion

In conclusion, our study showed remarkably comparable results in the activation and aggregation of platelets in the adult Göttingen Minipig as in humans, which further supports the use of the Göttingen Minipig as a nonclinical safety testing model for ASOs. Moreover, we also provided insight into the potential role of the ontogeny of the two platelet proteins, GPVI and PF4, implicated in platelet activation, possibly leading to thrombocytopenia. However, activity assays using samples from the different juvenile age groups and/or in vivo studies in juvenile minipigs are recommended to further characterize and extend the juvenile Göttingen Minipig as a safety testing model for pediatrics.

4.6 Supplementary material

Table S4.1. Juvenile Göttingen Minipig sample overview from the in vivo 8-week repeat-dose toxicity study (Chapter 4).

Animal	Age	Sex	Treatment	Platelet count (Giga/L)	GPVI abundance (ng/ml)		PF4 abundance (ng/ml)
					Adjusted to 1 x 10^8 platelets/ml	Adjusted to platelet count in WB	
501	PND 2	male	control	433	h	h	h
511	PND 2	female	control	389	h	h	h
521	PND 2	male	treated	348	h	h	h
531	PND 2	female	treated	344	h	h	h
503	PND 9	male	control	1096	13.14	144.04	2814
513	PND 9	female	control	977	7.81	76.26	3184
523	PND 9	male	treated	969	5.42	52.53	3036
535	PND 9	female	treated	1097	7.93	86.95	2346
504	PND 16	male	control	456	3.38	15.40	2154
517	PND 16	female	control	677	6.80	46.05	1676
524	PND 16	male	treated	546	4.39	23.99	1858
537	PND 16	female	treated	660	14.15	93.42	1182
512	PND 23	female	control	457	24.90	113.79	1017
522	PND 23	male	treated	226	27.32	61.74	1602
532	PND 23	female	treated	581	8.35	48.52	1771
534	PND 23	female	treated	682	50.26	342.77	280
515	PND 29-30	female	control	666	3.44	22.90	2952

527	PND 29-30	male	treated	643	5.51	35.46	790
533	PND 29-30	female	treated	650	37.23	241.97	1392
505	PND 37	male	control	644	5.16	33.23	715
518	PND 37	female	control	517	38.45	198.80	1741
525	PND 37	male	treated	699	9.86	68.91	881
538	PND 37	female	treated	676	15.72	106.23	2313
519	PND 43	female	control	724	23.03	166.75	2300
520	PND 43	female	control	723	4.15	29.98	3113
539	PND 43	female	treated	892	3.86	34.46	3141
514	PND 51	female	control	751	12.84	96.45	1731
516	PND 51	female	control	835	9.94	82.99	2164
526	PND 51	male	treated	828	3.77	31.19	3337
536	PND 51	female	treated	728	3.25	23.69	2987

Abbreviations: WB, whole blood; h, hemolyzed; PND, postnatal day; GPVI, glycoprotein VI; PF4, platelet factor 4.

4.7 References

1. Hill, S.F.; Meisler, M.H. Antisense Oligonucleotide Therapy for Neurodevelopmental Disorders. *Dev. Neurosci.* **2021**, *43*, 247–252.
2. Quemener, A.M.; Bachelot, L.; Forestier, A.; Donnou-Fournet, E.; Gilot, D.; Galibert, M.D. The Powerful World of Antisense Oligonucleotides: From Bench to Bedside. *Wiley Interdiscip. Rev. RNA* **2020**, *11*, e1594. https://doi.org/10.1002/wrna.1594.
3. Xiong, H.; Veedu, R.N.; Diermeier, S.D. Recent Advances in Oligonucleotide Therapeutics in Oncology. *Int. J. Mol. Sci.* **2021**, *22*, 3295. https://doi.org/10.3390/ijms22073295.
4. Schoch, K.M.; Miller, T.M. Antisense Oligonucleotides: Translation from Mouse Models to Human Neurodegenerative Diseases. *Neuron* **2017**, *94*, 1056–1070.
5. Watts, J.K. The Medicinal Chemistry of Antisense Oligonucleotides. In *Oligonucleotide-Based Drugs and Therapeutics*; Ferrari, N., Seguin, R., Eds.; John Wiley & Sons, Inc.: Hoboken, NJ, USA, 2018; pp. 39–69, ISBN 9781119070290.
6. Krishnan, A.V.; Mishra, D. Antisense Oligonucleotides: A Unique Treatment Approach. *Indian Pediatr.* **2020**, *57*, 165–171.
7. Swayze, E.; Bhat, B. The Medicinal Chemistry of Oligonucleotides. In *Antisense Drug Technology: Principles, Strategies, and Applications*; Crooke, S., Ed.; CRC Press: Boca Raton, FL, USA, 2007; pp. 143–182.
8. Bennett, C.F.; Baker, B.F.; Pham, N.; Swayze, E.; Geary, R.S. Pharmacology of Antisense Drugs. *Annu. Rev. Pharmacol. Toxicol.* **2017**, *57*, 81–105.
9. Østergaard, M.E.; de Hoyos, C.L.; Wan, W.B.; Shen, W.; Low, A.; Berdeja, A.; Vasquez, G.; Murray, S.; Migawa, M.T.; Liang, X.H.; et al. Understanding the Effect of Controlling Phosphorothioate Chirality in the DNA Gap on the Potency and Safety of Gapmer Antisense Oligonucleotides. *Nucleic Acids Res.* **2020**, *48*, 1691–1700. https://doi.org/10.1093/nar/gkaa031.
10. Laxton, C.; Brady, K.; Moschos, S.; Turnpenny, P.; Rawal, J.; Pryde, D.C.; Sidders, B.; Corbau, R.; Pickford, C.; Murray, E.J. Selection, Optimization, and Pharmacokinetic Properties of a Novel, Potent Antiviral Locked Nucleic Acid-Based Antisense Oligomer Targeting Hepatitis C Virus Internal Ribosome Entry Site. *Antimicrob. Agents Chemother.* **2011**, *55*, 3105–3114. https://doi.org/10.1128/AAC.00222-11.
11. Wahlestedt, C.; Salmi, P.; Good, L.; Kela, J.; Johnsson, T.; Ho, T.; Broberger, C.; Porreca, F.; Lai, J.; Ren, K.; et al. Potent and Nontoxic Antisense Oligonucleotides. *Proc. Natl. Acad. Sci. USA* **2000**, *97*, 5633–5638. https://doi.org/10.1073/pnas.97.10.5633.
12. Rinaldi, C.; Wood, M.J.A. Antisense Oligonucleotides: The next Frontier for Treatment of Neurological Disorders. *Nat. Rev. Neurol.* **2018**, *14*, 9–22. https://doi.org/10.1038/nrneurol.2017.148.
13. Bennett, C.F.; Swayze, E.E. RNA Targeting Therapeutics: Molecular Mechanisms of Antisense Oligonucleotides as a Therapeutic Platform. *Annu. Rev. Pharm. Toxicol.* **2010**, *50*, 259–293. https://doi.org/10.1146/annurev.pharmtox.010909.105654.
14. Shen, W.; de Hoyos, C.L.; Migawa, M.T.; Vickers, T.A.; Sun, H.; Low, A.; Bell, T.A.; Rahdar, M.; Mukhopadhyay, S.; Hart, C.E.; et al. Chemical Modification of PS-ASO Therapeutics Reduces Cellular Protein-Binding and Improves the Therapeutic Index. *Nat. Biotechnol.* **2019**, *37*, 640–650. https://doi.org/10.1038/s41587-019-0106-2.

15. Ferrari, N. Hybridization-Independent Effects. In *Oligonucleotide-Based Drugs and Therapeutics*; John Wiley & Sons, Inc.: Hoboken, NJ, USA, 2018.
16. Frazier, K.S. Antisense Oligonucleotide Therapies:The Promise and the Challenges from a Toxicologic Pathologist's Perspective. *Toxicol. Pathol.* **2015**, *43*, 78–89. https://doi.org/10.1177/0192623314551840.
17. Senín, L.D.; Garro, C.B.; Gómez, E.S.; Santos-Rubio, M.D. Inotersen and Severe Thrombocytopenia: 2 Case Reports and Review. *Int. J. Clin. Pharmacol. Ther.* **2022**, *60*, 311–316. https://doi.org/10.5414/cp204190.
18. Henry, S.P.; Narayanan, P.; Shen, L.; Bhanot, S.; Younis, H.S.; Burel, S.A. Assessment of the Effects of 2'-Methoxyethyl Antisense Oligonucleotides on Platelet Count in Cynomolgus Nonhuman Primates. *Nucleic Acid Ther.* **2017**, *27*, 197–208. https://doi.org/10.1089/nat.2017.0666.
19. Narayanan, P.; Shen, L.; Curtis, B.R.; Bourdon, M.A.; Nolan, J.P.; Gupta, S.; Hoffmaster, C.; Zhou, F.; Christian, B.; Schaubhut, J.L.; et al. Investigation into the Mechanism(s) That Leads to Platelet Decreases in Cynomolgus Monkeys during Administration of ISIS 104838, a 20-MoE-Modified Antisense Oligonucleotide. *Toxicol. Sci.* **2018**, *164*, 613–626. https://doi.org/10.1093/toxsci/kfy119.
20. Chi, X.; Gatti, P.; Papoian, T. Safety of Antisense Oligonucleotide and SiRNA-Based Therapeutics. *Drug Discov Today* **2017**, *22*, 823–833.
21. Crooke, S.T.; Baker, B.F.; Witztum, J.L.; Kwoh, T.J.; Pham, N.C.; Salgado, N.; McEvoy, B.W.; Cheng, W.; Hughes, S.G.; Bhanot, S.; et al. The Effects of 2'-O-Methoxyethyl Containing Antisense Oligonucleotides on Platelets in Human Clinical Trials. *Nucleic Acid Ther.* **2017**, *27*, 121–129. https://doi.org/10.1089/nat.2016.0650.
22. Flierl, U.; Nero, T.L.; Lim, B.; Arthur, J.F.; Yao, Y.; Jung, S.M.; Gitz, E.; Pollitt, A.Y.; Zaldivia, M.T.K.; Jandrot-Perrus, M.; et al. Phosphorothioate Backbone Modifications of Nucleotide-Based Drugs Are Potent Platelet Activators. *J. Exp. Med.* **2015**, *212*, 129–137. https://doi.org/10.1084/jem.20140391.
23. Jaax, M.E.; Krauel, K.; Marschall, T.; Brandt, S.; Gansler, J.; Fürll, B.; Appel, B.; Fischer, S.; Block, S.; Helm, C.A.; et al. Complex Formation with Nucleic Acids and Aptamers Alters the Antigenic Properties of Platelet Factor 4. *Blood* **2013**, *122*, 272–281. https://doi.org/10.1182/blood-2013-01-478966.
24. Andersson, S.; Antonsson, M.; Elebring, M.; Jansson-Löfmark, R.; Weidolf, L. Drug Metabolism and Pharmacokinetic Strategies for Oligonucleotide- and MRNA-Based Drug Development. *Drug Discov. Today* **2018**, *23*, 1733–1745. https://doi.org/10.1016/j.drudis.2018.05.030.
25. Lightfoot, H.; Schneider, A.; Hall, J. Pharmacokinetics and Pharmacodynamics of Antisense Oligonucleotides. In *Oligonucleotide-Based Drugs and Therapeutics*; Ferrari, N., Seguin, R., Ed.; John Wiley & Sons, Inc.: Hoboken, NJ, USA, 2018; pp. 107–136, ISBN 9781119070290.
26. Crooke, S.T.; Vickers, T.A.; Liang, X.H. Phosphorothioate Modified Oligonucleotide-Protein Interactions. *Nucleic Acids Res.* **2021**, *48*, 5235–5253.
27. Slingsby, M.H.L.; Vijey, P.; Tsai, I.T.; Roweth, H.; Couldwell, G.; Wilkie, A.R.; Gaus, H.; Goolsby, J.M.; Okazaki, R.; Terkovich, B.E.; et al. Sequence-Specific 2'-O-Methoxyethyl Antisense Oligonucleotides Activate Human Platelets through Glycoprotein VI, Triggering Formation of Platelet-Leukocyte Aggregates. *Haematologica* **2022**, *107*, 519–531. https://doi.org/10.3324/haematol.2020.260059.
28. Sewing, S.; Roth, A.B.; Winter, M.; Dieckmann, A.; Bertinetti-Lapatki, C.; Tessier, Y.; McGinnis, C.; Huber, S.; Koller, E.; Ploix, C.; et al. Assessing Single-Stranded Oligonucleotide Drug-Induced Effects in Vitro Reveals Key Risk Factors for Thrombocytopenia. *PLoS ONE* **2017**, *12*, e0187574. https://doi.org/10.1371/journal.pone.0187574.
29. Braendli-Baiocco, A.; Festag, M.; Erichsen, K.D.; Persson, R.; Mihatsch, M.J.; Fisker, N.; Funk, J.; Mohr, S.; Constien, R.; Ploix, C.; et al. The Minipig Is a Suitable Non-Rodent Model in the Safety Assessment of Single Stranded Oligonucleotides. *Toxicol. Sci.* **2017**, *157*, 112–128. https://doi.org/10.1093/toxsci/kfx025.
30. Valenzuela, A.; Tardiveau, C.; Ayuso, M.; Buyssens, L.; Bars, C.; van Ginneken, C.; Fant, P.; Leconte, I.; Braendli-Baiocco, A.; Parrott, N.; et al. Safety Testing of an Antisense Oligonucleotide Intended for Pediatric Indications in the Juvenile Göttingen Minipig, Including an Evaluation of the Ontogeny of Key Nucleases. *Pharmaceutics* **2021**, *13*, 1442. https://doi.org/10.3390/pharmaceutics13091442.
31. Baenziger, N.L.; Brodie, G.N.; Majerus, P.W. Isolation and Properties of a Thrombin-Sensitive Protein of Human Platelets. *J. Biol. Chem.* **1972**, *247*, 2723–2731. https://doi.org/10.1016/s0021-9258(19)45271-x.
32. Ruggeri, Z.M.; Jackson, S.P. Platelet Thrombus Formation in Flowing Blood. In *Platelets*; Academic Press: Cambridge, MA, USA, 2013. https://doi.org/10.1016/b978-0-12-387837-3.00020-1.
33. Starlinger, P.; Moll, H.P.; Assinger, A.; Nemeth, C.; Hoetzenecker, K.; Gruenberger, B.; Gruenberger, T.; Kuehrer, I.; Schoppmann, S.F.; Gnant, M.; et al. Thrombospondin-1: A Unique Marker to Identify in Vitro Platelet Activation When Monitoring in Vivo Processes. *J. Thromb. Haemost.* **2010**, *8*, 1809–1819. https://doi.org/10.1111/j.1538-7836.2010.03908.x.
34. Yun, S.H.; Sim, E.H.; Goh, R.Y.; Park, J.I.; Han, J.Y. Platelet Activation: The Mechanisms and Potential Biomarkers. *BioMed Res. Int.* **2016**, *2016*, 9060143.
35. Wiedmeier, S.E.; Henry, E.; Sola-Visner, M.C.; Christensen, R.D. Platelet Reference Ranges for Neonates, Defined Using Data from over 47000 Patients in a Multihospital Healthcare System. *J. Perinatol.* **2009**, *29*, 130–136. https://doi.org/10.1038/jp.2008.141.
36. Faustini, M.; Bronzo, V.; Maffeo, G.; Russo, V.; Munari, E.; Vigo, D. Reference Intervals and Age-Related Changes for Platelet Count, Mean Platelet Volume and Plateletcrit in Healthy Pre-Weaning Piglets in Italy. *J. Vet. Med. Ser. A Physiol. Pathol. Clin. Med.* **2003**, *50*, 466–469. https://doi.org/10.1046/j.1439-0442.2003.00581.x.

37. van Poelgeest, E.P.; Hodges, M.R.; Moerland, M.; Tessier, Y.; Levin, A.A.; Persson, R.; Lindholm, M.W.; Dumong Erichsen, K.; Ørum, H.; Cohen, A.F.; et al. Antisense-Mediated Reduction of Proprotein Convertase Subtilisin/Kexin Type 9 (PCSK9): A First-in-Human Randomized, Placebo-Controlled Trial. *Br. J. Clin. Pharm.* **2015**, *80*, 1350–1361. https://doi.org/10.1111/bcp.12738.
38. Lindholm, M.W.; Elmén, J.; Fisker, N.; Hansen, H.F.; Persson, R.; Møller, M.R.; Rosenbohm, C.; Ørum, H.; Straarup, E.M.; Koch, T. PCSK9 LNA Antisense Oligonucleotides Induce Sustained Reduction of LDL Cholesterol in Nonhuman Primates. *Mol. Ther.* **2012**, *20*, 376–381. https://doi.org/10.1038/mt.2011.260.
39. Sewell, K.L.; Geary, R.S.; Baker, B.F.; Glover, J.M.; Mant, T.G.K.; Yu, R.Z.; Tami, J.A.; Dorr, F.A. Phase I Trial of ISIS 104838, a 2'-Methoxyethyl Modified Antisense Oligonucleotide Targeting Tumor Necrosis Factor-α. *J. Pharmacol. Exp. Ther.* **2002**, *303*, 1334–1343. https://doi.org/10.1124/jpet.102.036749.
40. Burel, S.A.; Machemer, T.; Baker, B.F.; Kwoh, T.J.; Paz, S.; Younis, H.; Henry, S.P. Early-Stage Identification and Avoidance of Antisense Oligonucleotides Causing Species-Specific Inflammatory Responses in Human Volunteer Peripheral Blood Mononuclear Cells. *Nucleic Acid Ther.* **2022**, *32*, 457–472. https://doi.org/10.1089/nat.2022.0033.
41. Chan, M.V.; Warner, T.D. Standardised Optical Multichannel (Optimul) Platelet Aggregometry Using High-Speed Shaking and Fixed Time Point Readings. *Platelets* **2012**, *23*, 404–408.
42. Vinholt, P.J.; Nybo, M.; Nielsen, C.B.; Hvas, A.M. Light Transmission Aggregometry Using Pre-Coated Microtiter Plates and a Victor X5 Plate Reader. *PLoS ONE* **2017**, *12*, e0185675. https://doi.org/10.1371/journal.pone.0185675.
43. Bollen, P.J.A.; Madsen, L.W.; Meyer, O.; Ritskes-Hoitinga, J. Growth Differences of Male and Female Göttingen Minipigs during Ad Libitum Feeding: A Pilot Study. *Lab. Anim.* **2005**, *39*, 80–93. https://doi.org/10.1258/0023677052886565.
44. Lambert, M.; Reznikov, A.; Nguyen, Y.; Rauova, L.; Poncz, M. Platelet Factor 4 Levels Inversely Correlate with Platelet Transfusion Needs In Pediatric Patients Treated for Standard Risk Acute Lymphoblastic Leukemia. *Blood* **2010**, *116*, 725. https://doi.org/10.1182/blood.v116.21.725.725.
45. Cabeza, N.; Li, Z.; Schulz, C.; Kremmer, E.; Massberg, S.; Bültmann, A.; Gawaz, M. Surface Expression of Collagen Receptor Fc Receptor-γ/Glycoprotein VI Is Enhanced on Platelets in Type 2 Diabetes and Mediates Release of CD40 Ligand and Activation of Endothelial Cells. *Diabetes* **2004**, *53*, 2117–2121. https://doi.org/10.2337/diabetes.53.8.2117.
46. Feyen, B.; Penard, L.; van Heerden, M.; Fant, P.; Marsden, E.; de Jonghe, S.; Desmidt, M.; Mousa, S.M.; Bailey, G.P. "All Pigs Are Equal" Does the Background Data from Juvenile Göttingen Minipigs Support This? *Reprod. Toxicol.* **2016**, *64*, 105–115. https://doi.org/10.1016/j.reprotox.2016.04.019.
47. Grossi, A.B.; Zeltner, A.; Christoffersen, C.; Søndergaard, A.C. Reference Data of Clinical Chemistry and Hematology in Juvenile Göttingen Minipigs. *Toxicol. Lett.* **2016**, *258*, S235. https://doi.org/10.1016/j.toxlet.2016.06.1838.
48. Pawlowsky, K.; Ernst, L.; Steitz, J.; Stopinski, T.; Kögel, B.; Henger, A.; Kluge, R.; Tolba, R. The Aachen Minipig: Phenotype, Genotype, Hematological and Biochemical Characterization, and Comparison to the Göttingen Minipig. *Eur. Surg. Res.* **2017**, *58*, 193–203. https://doi.org/10.1159/000471483.
49. van Donge, T.; Evers, K.; Koch, G.; van den Anker, J.; Pfister, M. Clinical Pharmacology and Pharmacometrics to Better Understand Physiological Changes during Pregnancy and Neonatal Life. *Handb. Exp. Pharm.* **2020**, *261*, 325–337. https://doi.org/10.1007/164_2019_210.
50. Yu, R.Z.; Grundy, J.S.; Geary, R.S. Clinical Pharmacokinetics of Second Generation Antisense Oligonucleotides. *Expert Opin. Drug Metab. Toxicol.* **2013**, *9*, 169–182. https://doi.org/10.1517/17425255.2013.737320.
51. Zaslavsky, A.; Adams, M.; Cao, X.; Yamaguchi, A.; Henderson, J.; Busch-Østergren, P.; Udager, A.; Pitchiaya, S.; Tourdot, B.; Kasputis, T.; et al. Antisense Oligonucleotides and Nucleic Acids Generate Hypersensitive Platelets. *Thromb. Res.* **2021**, *200*, 64–71. https://doi.org/10.1016/j.thromres.2021.01.006.
52. Karaki, S.; Paris, C.; Rocchi, P. Antisense Oligonucleotides, A Novel Developing Targeting Therapy. In *Antisense Therapy*; *BoD—Books on Demand* GmbH: Norderstedt, Germany, 2019.
53. Liang, X.H.; Shen, W.; Sun, H.; Kinberger, G.A.; Prakash, T.P.; Nichols, J.G.; Crooke, S.T. Hsp90 Protein Interacts with Phosphorothioate Oligonucleotides Containing Hydrophobic 2'-Modifications and Enhances Antisense Activity. *Nucleic Acids Res.* **2016**, *44*, 3892–3907. https://doi.org/10.1093/nar/gkw144.
54. Saitoh, S.I.; Miyake, K. CHAPTER 13: Nucleic Acid Innate Immune Receptors. In *RSC Drug Discovery Series*; The *Royal Society of Chemistry: London, UK,* 2019; Volume 2019-January.
55. Agrawal, S.; Kandimalla, E.R. CHAPTER 14: Synthetic Agonists of Toll-like Receptors and Therapeutic Applications. In *RSC Drug Discovery Series*; The *Royal Society of Chemistry: London, UK,* 2019; Volume 2019-January.
56. Mangsbo, S.M.; Sanchez, J.; Anger, K.; Lambris, J.D.; Ekdahl, K.N.; Loskog, A.S.; Nilsson, B.; Tötterman, T.H. Complement Activation by CpG in a Human Whole Blood Loop System: Mechanisms and Immunomodulatory Effects. *J. Immunol.* **2009**, *183*, 6724–6732. https://doi.org/10.4049/jimmunol.0902374.
57. Henry, S.P.; Kim, T.W.; Kramer-Stickland, K.; Zanardi, T.A.; Fey, R.A.; Levin, A.A. Toxicologic Properties of 2'-o-Methoxyethyl Chimeric Antisense Inhibitors in Animals and Man. In *Antisense Drug Technology: Principles, Strategies, and Applications*, 2nd ed.; CRC Press: Boca Raton, FL, USA, 2007.
58. Zhang, X.; Kimura, Y.; Fang, C.; Zhou, L.; Sfyroera, G.; Lambris, J.D.; Wetsel, R.A.; Miwa, T.; Song, W.C. Regulation of Toll-like Receptor-Mediated Inflammatory Response by Complement in Vivo. *Blood* **2007**, *110*, 228–236. https://doi.org/10.1182/blood-2006-12-063636.

59. Kollmann, T.R.; Kampmann, B.; Mazmanian, S.K.; Marchant, A.; Levy, O. Protecting the Newborn and Young Infant from Infectious Diseases: Lessons from Immune Ontogeny. *Immunity* **2017**, *46*, 350–363.
60. Andersson, P.; den Besten, C. Preclinical and Clinical Drug-Metabolism, Pharmacokinetics and Safety of Therapeutic Oligonucleotides. In *RSC Drug Discovery Series*; Agrawal, Sudhir, Gait, M., Eds.; Royal Society of Chemistry: London, UK, 2019; Volume 2019-Januaay, pp. 474–517, ISBN 978-1-78801-571-4.
61. Chan, M.V.; Armstrong, P.C.; Warner, T.D. 96-Well Plate-Based Aggregometry. *Platelets* **2018**, *29*, 650–655.
62. Filkova, A.A.; Martyanov, A.A.; Garzon Dasgupta, A.K.; Panteleev, M.A.; Sveshnikova, A.N. Quantitative Dynamics of Reversible Platelet Aggregation: Mathematical Modelling and Experiments. *Sci. Rep.* **2019**, *9*, 6217. https://doi.org/10.1038/s41598-019-42701-0.
63. O'Donnell, C.J.; Larson, M.G.; Feng, D.L.; Sutherland, P.A.; Lindpaintner, K.; Myers, R.H.; D'Agostino, R.A.; Levy, D.; Tofler, G.H. Genetic and Environmental Contributions to Platelet Aggregation: The Framingham Heart Study. *Circulation* **2001**, *103*, 3051–3056. https://doi.org/10.1161/01.CIR.103.25.3051.
64. Yee, D.L.; Sun, C.W.; Bergeron, A.L.; Dong, J.F.; Bray, P.F. Aggregometry Detects Platelet Hyperreactivity in Healthy Individuals. *Blood* **2005**, *106*, 2723–2729. https://doi.org/10.1182/blood-2005-03-1290.
65. Jones, C.I.; Garner, S.F.; Angenent, W.; Bernard, A.; Berzuini, C.; Burns, P.; Farndale, R.W.; Hogwood, J.; Rankin, A.; Stephens, J.C.; et al. Mapping the Platelet Profile for Functional Genomic Studies and Demonstration of the Effect Size of the GP6 Locus. *J. Thromb. Haemost.* **2007**, *5*, 1756–1765. https://doi.org/10.1111/j.1538-7836.2007.02632.x.
66. Panzer, S.; Höcker, L.; Koren, D. Agonists-Induced Platelet Activation Varies Considerably in Healthy Male Individuals: Studies by Flow Cytometry. *Ann. Hematol.* **2006**, *85*, 121–125. https://doi.org/10.1007/s00277-005-0029-5.
67. Kunicki, T.J.; Nugent, D.J. The Genetics of Normal Platelet Reactivity. *Blood* **2010**, *116*, 2627–2634.
68. Narayanan, P.K.; Henry, S.; Li, N. Drug-Induced Thrombocytopenia: Mechanisms and Relevance in Preclinical Safety Assessment. *Curr. Opin. Toxicol.* **2019**, *17*, 23–30.
69. Jung, S.M.; Moroi, M.; Soejima, K.; Nakagaki, T.; Miura, Y.; Berndt, M.C.; Gardiner, E.E.; Howes, J.M.; Pugh, N.; Bihan, D.; et al. Constitutive Dimerization of Glycoprotein VI (GPVI) in Resting Platelets Is Essential for Binding to Collagen and Activation in Flowing Blood. *J. Biol. Chem.* **2012**, *287*, 30000–30013. https://doi.org/10.1074/jbc.M112.359125.
70. Curtis, B.R.; Swyers, J.; Divgi, A.; McFarland, J.G.; Aster, R.H. Thrombocytopenia after Second Exposure to Abciximab Is Caused by Antibodies That Recognize Abciximab-Coated Platelets. *Blood* **2002**, *99*, 2054–2059. https://doi.org/10.1182/blood.V99.6.2054.
71. Santostefano, M.J.; Kirchner, J.; Vissinga, C.; Fort, M.; Lear, S.; Pan, W.J.; Prince, P.J.; Hensley, K.M.; Tran, D.; Rock, D.; et al. Off-Target Platelet Activation in Macaques Unique to a Therapeutic Monoclonal Antibody. *Toxicol. Pathol.* **2012**, *40*, 899–917. https://doi.org/10.1177/0192623312444029.
72. Warkentin, T.E. Heparin-Induced Thrombocytopenia: Pathogenesis and Management. *Br. J. Haematol.* **2003**, *121*, 535–555.
73. Furihata, K.; Clemetson, K.J.; Deguchi, H.; Kunicki, T.J. Variation in Human Platelet Glycoprotein VI Content Modulates Glycoprotein VI-Specific Prothrombinase Activity. *Arter. Thromb. Vasc. Biol.* **2001**, *21*, 1857–1863. https://doi.org/10.1161/hq1001.096643.
74. Barrachina, M.N.; Sueiro, A.M.; Izquierdo, I.; Hermida-Nogueira, L.; Guitián, E.; Casanueva, F.F.; Farndale, R.W.; Moroi, M.; Jung, S.M.; Pardo, M.; et al. GPVI Surface Expression and Signalling Pathway Activation Are Increased in Platelets from Obese Patients: Elucidating Potential Anti-Atherothrombotic Targets in Obesity. *Atherosclerosis* **2019**, *281*, 62–70. https://doi.org/10.1016/j.atherosclerosis.2018.12.023.
75. Mammadova-Bach, E.; Gil-Pulido, J.; Sarukhanyan, E.; Burkard, P.; Shityakov, S.; Schonhart, C.; Stegner, D.; Remer, K.; Nurden, P.; Nurden, A.T.; et al. Platelet Glycoprotein VI Promotes Metastasis through Interaction with Cancer Cell–Derived Galectin-3. *Blood* **2020**, *135*, 1146–1160. https://doi.org/10.1182/blood.2019002649.
76. Narayanan, P.K.; Curtis, B.R.; Shen, L.; Schneider, E.; Tami, J.A.; Paz, S.; Burel, S.A.; Tai, L.J.; Machemer, T.; Kwoh, T.J.; et al. Underlying Immune Disorder May Predispose Some Transthyretin Amyloidosis Subjects to Inotersen-Mediated Thrombocytopenia. *Nucleic Acid Ther.* **2020**, *30*, 94–103. https://doi.org/10.1089/nat.2019.0829.
77. Al-Tamimi, M.; Mu, F.T.; Moroi, M.; Gardiner, E.E.; Berndt, M.C.; Andrews, R.K. Measuring Soluble Platelet Glycoprotein VI in Human Plasma by ELISA. *Platelets* **2009**, *20*, 143–149. https://doi.org/10.1080/09537100802710286.
78. Al-Tamimi, M.; Arthur, J.F.; Gardiner, E.E.; Andrews, R.K. Focusing on Plasma Glycoprotein VI. *Thromb. Haemost.* **2012**, *107*, 648–655.
79. Rajasekhar, D.; Kestin, A.S.; Bednarek, F.J.; Ellis, P.A.; Barnard, M.R.; Michelson, A.D. Neonatal Platelets Are Less Reactive than Adult Platelets to Physiological Agonists in Whole Blood. *Thromb. Haemost.* **1994**, *72*, 957–963. https://doi.org/10.1055/s-0038-1648990.
80. Rajasekhar, D.; Barnard, M.R.; Bednarek, F.J.; Michelson, A.D. Platelet Hyporeactivity in Very Low Birth Weight Neonates. *Thromb. Haemost.* **1997**, *77*, 1002–1007. https://doi.org/10.1055/s-0038-1656093.
81. Israels, S.J.; Daniels, M.; McMillan, E.M. Deficient Collagen-Induced Activation in the Newborn Platelet. *Pediatr. Res.* **1990**, *27*, 337–343. https://doi.org/10.1203/00006450-199004000-00004.
82. Ferrer-Marin, F.; Liu, Z.J.; Gutti, R.; Sola-Visner, M. Neonatal Thrombocytopenia and Megakaryocytopoiesis. *Semin. Hematol.* **2010**, *47*, 281–288. https://doi.org/10.1053/j.seminhematol.2010.04.002.

83. Corby, D.G.; O'Barr, T.P. Decreased Alpha-Adrenergic Receptors in Newborn Platelets: Cause of Abnormal Response to Epinephrine. *Dev. Pharm.* **1981**, *2*, 215–225. https://doi.org/10.1159/000481016.
84. Caparrós-Pérez, E.; Teruel-Montoya, R.; López-Andreo, M.J.; Llanos, M.C.; Rivera, J.; Palma-Barqueros, V.; Blanco, J.E.; Vicente, V.; Martínez, C.; Ferrer-Marín, F. Comprehensive Comparison of Neonate and Adult Human Platelet Transcriptomes. *PLoS ONE* **2017**, *12*, e0183042. https://doi.org/10.1371/journal.pone.0183042.
85. Lambert, M.P.; Rauova, L.; Bailey, M.; Sola-Visner, M.C.; Kowalska, M.A.; Poncz, M. Platelet Factor 4 Is a Negative Autocrine in Vivo Regulator of Megakaryopoiesis: Clinical and Therapeutic Implications. *Blood* **2007**, *110*, 1153–1160. https://doi.org/10.1182/blood-2007-01-067116.
86. Lambert, M.P.; Wang, Y.; Bdeir, K.H.; Nguyen, Y.; Kowalska, M.A.; Poncz, M. Platelet Factor 4 Regulates Megakaryopoiesis through Low-Density Lipoprotein Receptor-Related Protein 1 (LRP1) on Megakaryocytes. *Blood* **2009**, *114*, 2290–2298. https://doi.org/10.1182/blood-2009-04-216473.
87. Gewirtz, A.; Calabretta, B.; Rucinski, B.; Niewiarowski, S.; Xu, W.Y. Inhibition of Human Megakaryocytopoiesis in Vitro by Platelet Factor 4 (PF4) and a Synthetic COOH-Terminal PF4 Peptide. *J. Clin. Investig.* **1989**, *83*, 1477–1486. https://doi.org/10.1172/JCI114041.

Chapter 5

General Discussion

In this doctoral thesis, the juvenile Göttingen Minipig was evaluated for its use as a pediatric safety testing model for ASOs. In addition, ASO-induced direct platelet activation and aggregation were evaluated in adult minipig samples to elucidate the platelet response phenotype towards ASOs in this animal model. The body of data from this initiative is fundamental for the selection of the juvenile Göttingen Minipig in assessing safety concerns for ASOs intended for the human pediatric population. This chapter will discuss the main findings of the doctoral project and will put them into a broader perspective by addressing the following questions:

1. **What are the implications of the current PK/PD findings in the juvenile Göttingen Minipig, and how can we relate the differences observed in this work to a clinical perspective?**

   In the first section of this chapter, a general view of the current PK/PD findings in the juvenile Göttingen Minipig concerning its nonclinical and clinical applications will be presented. We will also provide a broad understanding of the differences seen in the PK/PD profile of juveniles compared to adult minipigs, as well as to NHPs and humans. These should be considered when using the model in pediatric safety testing of ASOs.

2. **What do the toxicological findings in juvenile Göttingen Minipigs tell us about this model in response to ASO treatment, and how would these findings contribute to the knowledge in pediatric safety testing of ASOs?**

   This section will present the results regarding the safety concerns in the juvenile Göttingen Minipigs and they will be compared to what is known about this ASO class in nonclinical (i.e., NHPs) and clinical contexts. Moreover, this section will provide an overview of how these data will contribute to the safety assessment of ASOs indicated for pediatrics.

3. **How do the current findings support the selection of the juvenile Göttingen Minipig as an alternative animal model for the safety testing of ASOs intended for pediatrics?**

The section will summarize the main findings from the previous chapters with particular emphasis on the animal test system selection according to the ICH S11 guideline on nonclinical safety testing in support of the development of pediatric pharmaceuticals. This section will also highlight how our data supports the acceptance of this juvenile animal model by health authorities.

4. **What is still missing information regarding the juvenile Göttingen Minipig as a safety testing model for ASOs?**

We will recapitulate the future research perspectives discussed throughout the chapter and generally conclude on the potential selection and use of the juvenile Göttingen Minipig as an animal model for future pediatric safety testing of ASOs.

5.1 Understanding differences: clinical perspectives on the PK/PD findings

In this doctoral thesis, an LNA PS gapmer (i.e., RTR5001) with known PK and safety profile in the adult minipig (and NHPs and humans) was used as a model compound in an eight-week repeat-dose toxicity study (Chapter 3) to assess potential differences in its exposure/toxicity and pharmacologic effect in the juvenile Göttingen Minipig. As described in Chapter 3, differences in various PK/PD parameters were observed after the systemic (SC) administration of RTR5001 in juvenile minipigs compared to adults. In this section, we will discuss these differences and their potential nonclinical (i.e., versus NHPs) and clinical implications. For the first part, we will discuss specific findings related to plasma and tissue exposure, the factors affecting them, and the pharmacologic activity of ASOs. Afterwards, the results of ASO metabolism evaluation will be tackled. Although this thesis is limited to the evaluation of only one ASO (class) in the juvenile minipig, certain findings could be extrapolated to other ASO classes.

As the plasma exposure of RTR5001 (see Figures 3.2 and S3.1) correlates to the maturation of plasma albumin in the juvenile minipigs (see Figure 3.5 and Table 5.1), we could assert that the ontogeny of plasma proteins served as an essential factor to its PK in the juvenile animals. Moreover, we could argue that in contrast to adult animals in which ASO plasma clearance is particularly linked to its rapid tissue biodistribution, rapid renal elimination could have more bearing on the systemic clearance of ASOs in juvenile animals due to the limited plasma albumin binding. However, this is only true for ASO classes that tend to bind to plasma proteins like those designed with PS backbone modification (e.g., RTR5001). For ASO classes that utilize neutral chemistries with no plasma protein binding capacity (e.g., splice-switching ONs with phosphorodiamidate morpholino oligomer modifications), glomerular filtration is the main factor regarding their clearance in the plasma, both in juveniles and adults [1]. Therefore, the development of the renal system, particularly the maturation of glomerular filtration rate (GFR) (see section 5.3) rather than the maturation of plasma albumin, is a critical factor for the PK of neutral ASO chemistries.

Table 5.1. Albumin concentration in different age groups of Göttingen Minipigs [2], humans [3], and cynomolgus monkeys [4–6].

Age	Sex	Plasma albumin concentration (g/L)	Total protein concentration (g/L)	Albumin concentration (% of total protein)
Göttingen Minipigs				
2 d	male	17.62 ± 3.36	58.59 ± 14.20	30
	female	18.48 ± 2.64	54.33 ± 9.58	34
1 wk	male	31.31 ±2.93	49.63 ± 4.93	63
	female	30.67 ± 3.43	47.26 ± 4.20	65
2 wk	male	36.14 ± 2.70	51.39 ± 2.12	70
	female	37.54 ± 4.30	52.64 ± 8.06	71
4 wk	male	43.79 ± 1.21	54.36 ± 2.71	81
	female	43.17 ± 1.68	54.67 ± 3.14	79
5 wk	male	47.46 ± 2.62	59.53 ± 3.07	80
	female	45.01 ± 2.09	59.00 ± 4.78	76
7 wk	male	36.43 ± 2.48	53.37 ± 2.73	68
	female	37.75 ± 2.02	55.78 ± 2.75	68
3 mo	male	39.12 ± 8.09	52.32 ± 11.23	75
	female	38.76 ± 8.33	52.76 ± 10.13	74
6 mo	male	40.35 ± 8.75	53.01 ± 11.76	76
	female	43.24 ± 8.04	60.17 ± 12.95	72
Humans				
0 – 1 wk	both	28.00 ± 1.00	43.00 ± 1.00	65
> 1 wk – 4 wk	both	29.00 ± 0.50	53.00 ± 1.00	55
> 4 wk – 1 y	both	29.00 ± 4.00	54.00 ± 2.00	54
> 1 y – 3 y	both	31.00 ± 2.00	59.00 ± 1.00	52
> 3 y – 6 y	both	31.00 ± 11.00	62.00 ± 1.00	50
> 6 y – 18 y	both	32.00 ± 6.00	59.00 ± 1.00	54
Adult	both	40.00 ± 2.00	63.00 ± 1.00	63
Cynomolgus monkeys				
~2 y	male	49.70 ± 1.50	83.00 ± 3.70	60
	female	48.90 ± 2.84	83.00 ± 4.40	59
≤ 4 y	male	41.96 ± 2.27	62.63 ± 3.61	67
	female	41.22 ± 4.10	62.58 ± 4.24	66
≥ 4 y	male	40.50 ± 3.67	65.99 ± 4.04	61
	female	38.00 ± 4.16	67.63 ± 5.46	56
4 – 8 y	male	38.70 ± 4.90	66.80 ±6.60	58
	female	38.50 ± 3.80	67.20 ± 6.00	57

Abbreviations: d, day; wk, week; mo, months; y, year. Data represents mean ± SD. Common grey color represent comparative age groups.

Regarding the plasma albumin concentrations, a peak concentration was observed at PND 37 (around 5 weeks of age) among the different juvenile minipigs. These values align with previous data in Göttingen Minipigs and are within the reference range for adults [2]. On the other hand, the

values for the other juvenile age groups are generally lower. In contrast, a maturation profile of the plasma albumin was reported in humans, with lower levels for neonates and infants under 1-3 years of age resulting in increased amounts of free drug (e.g., diazepam, cyclosporine, and deltamethrin) in the circulation [3]. Therefore, this suggests that younger age groups of animals/pediatrics could be predisposed to toxic protein interactions by ASOs (see section 1.1.7.2) while in the plasma compartment due to the higher level of unbound drugs.

In comparison to minipigs and humans, the published reference ranges for juvenile cynomolgus monkeys (< 4 years) are generally greater than in adults (≥ 4 years) [4–6]. Still, a more comprehensive study is recommended to explore the effect of age on plasma albumin maturation in neonatal to pubescent NHPs, and to what extent these interspecies differences seen in plasma albumin ontogeny between cynomolgus monkeys and Göttingen Minipigs could affect PK translation to human pediatrics. In this regard, physiologic-based pharmacokinetic (PBPK) modeling for ASOs in juvenile animals and pediatric patients would be valuable to predict the ADME processes for ASOs [7]. However, a lesser plasma albumin level could mean more unbound ASOs in circulation, leading to inefficient ASO tissue distribution and faster renal clearance. We observed that the plasma half-life of RTR5001 (see Table 5.2) in juvenile minipigs was shortest at PND 22 and 29 (3 and 4 weeks of age) and longest at PND 36 (around 5 weeks of age). These values during minipig's weaning period seemed to be influenced by tissue distribution, as completion of nephrogenesis occurred three weeks after birth [8]. Therefore, from that age onwards more mature tubules had the capacity to take up the model ASO from the circulation resulting in faster plasma clearance at PND 22 and 29. On the other hand, the longest half-life at PND 36 could be related to the peak plasma albumin level observed (see Figure 3.5 and Table 5.1), which also corresponds to the age group having the relatively highest liver and kidney RTR5001 exposure (tissue saturation) (see Figure 3.2B-C). Although it could be expected that plasma half-life would either increase (due to observed liver saturation and kidney tubular changes leading to non-uptake of ASOs) or at least remain at this rate for the two oldest age groups in our study, shorter half-lives were observed. We speculate that this could be due to the lower plasma albumin in these two oldest age groups (relative to PND 36) and/or faster renal clearance. Hence, measuring the parent ASO concentration in the urine would allow us to test this hypothesis.

Table 5.2. Toxicokinetic parameters in plasma, liver, and kidneys of juvenile minipigs after subcutaneous RTR5001 administration at 20 mg/kg weekly.

Age (PND)	Plasma C_{max} (nM)	Plasma RTR5001 concentration (nM), 24 h; (% of C_{max})	Plasma RTR5001 concentration (nM), 7 d; (% of C_{max})	Plasma half-life (h)	Kidney to plasma ratio	Liver to plasma ratio	Kidney to liver ratio
1	1810	4.30 (0.23)	0.00 (n.a.)	3.33	4090	1800	2.28
8	1570	7.31 (0.46)	3.36 (0.21)	3.54	2810	1310	2.04
15	1640	8.04 (0.49)	13.1 (0.79)	3.66	2040	1430	1.43
22	1750	4.84 (0.28)	0.00 (0.00)	2.94	4980	2370	2.12
28-29	2570	9.51 (0.37)	1.50 (0.06)	2.91	2110	1490	1.43
36	2030	53.1 (2.62)	4.28 (0.21)	5.02	1800	1420	1.43
42	3010	9.34 (0.31)	13.6 (0.45)	3.09	1090	2010	0.54
50	4110	12.9 (0.31)	10.6 (0.26)	4.12	1160	1110	1.20

Abbreviations: PND, postnatal day; C_{max}, maximum concentration; nM, nanomolar; d, day; h, hour; n.a., not applicable.

The ontogeny evaluation of other plasma proteins (e.g., α2-macroglobulin) would also give us an idea on their role on the distribution and cellular uptake of ASOs during early development. Parallel to this, the fraction of the other plasma proteins regarding total plasma protein concentration could evolve among the different juvenile minipig age groups as seen in pediatrics (i.e., 50% for infants 3 to 6 years old vs. adults with 37%) (Table 5.1) [3]. It was shown with gapmer ASOs that a two-fold enhancement in potency in α-2-macroglobin-knockout mice occurred, which might indicate that association with such proteins may steer the ASO towards other tissue compartments or to less productive cellular uptake pathway [9]. Therefore, the ontogeny and relative fraction of plasma proteins could influence ASOs' binding predisposition leading to less productive cellular uptake or deviated target cell/tissue distribution. This could be a possible reason for the delayed onset of pharmacologic response seen in juvenile minipigs. The decrease in plasma cholesterol profile was only observed in the juvenile minipigs after the seventh and eighth dose (PND 43 and 51) (see Figure 3.4 and Table 3.2), compared to adult minipigs (after 4 doses within 16 days), NHPs (after 5 doses within 28 days), and humans (after 3 doses within 15 days) [10–12]. However, more investigation is needed to draw firm conclusions.

Considering that several factors could affect plasma exposure (and tissue exposure afterward) in juvenile animals/pediatric patients, dose adjustments seem warranted. Given the lowered plasma albumin binding in the youngest juvenile minipigs and the adverse effects of administering higher ASO doses (see sections 1.1.7.2 and 5.2), increasing the dosing frequency with lower dose

concentration seems to be a more suitable choice. As an alternative, targeted delivery approaches (e.g., GalNAc conjugation) (see section 1.1.4.3) could also be an option but evaluations on the ontogeny of proteins involved in the uptake of formulated ASOs (e.g., ASGR1) is warranted. Both of these could help improve the lower RTR5001 exposure in the liver (target organ of pharmacology) and/or productive uptake of hepatocytes (target cell of pharmacology) in the youngest juvenile minipigs.

Regarding the delayed onset of the pharmacologic response to RTR5001 (i.e., decrease in total and LDL cholesterol in the plasma) by the juvenile minipigs, an additional mRNA ISH was done to qualitatively assess the abundance of *PCSK9* in the liver tissue sections from the different juvenile age groups of minipigs [10] (see Figure 5.1). A relative decrease in the *PCSK9* level with an increasing number of RTR5001 weekly administrations can be observed, which correlates (at least in the last two age groups) with the decrease in plasma cholesterol. Although qualitatively, *PCSK9* expression in the youngest age group (PND 2) appeared to be higher than in the older age groups. Therefore, *PCSK9* expression seemed to be undergoing ontogeny in the juvenile minipigs, which could explain the differential level of plasma cholesterol observed in the control juvenile minipigs (see Figure 3.4), wherein both plasma total and LDL cholesterol levels increased until the third week of life, then decreased afterward. This could be another factor affecting the delayed onset of RTR5001 pharmacologic activity. In line with this, maturational factors affecting the target transcript and molecular pathways by which ASOs exert their pharmacologic effect should be considered when performing nonclinical safety packages for pediatric ASOs.

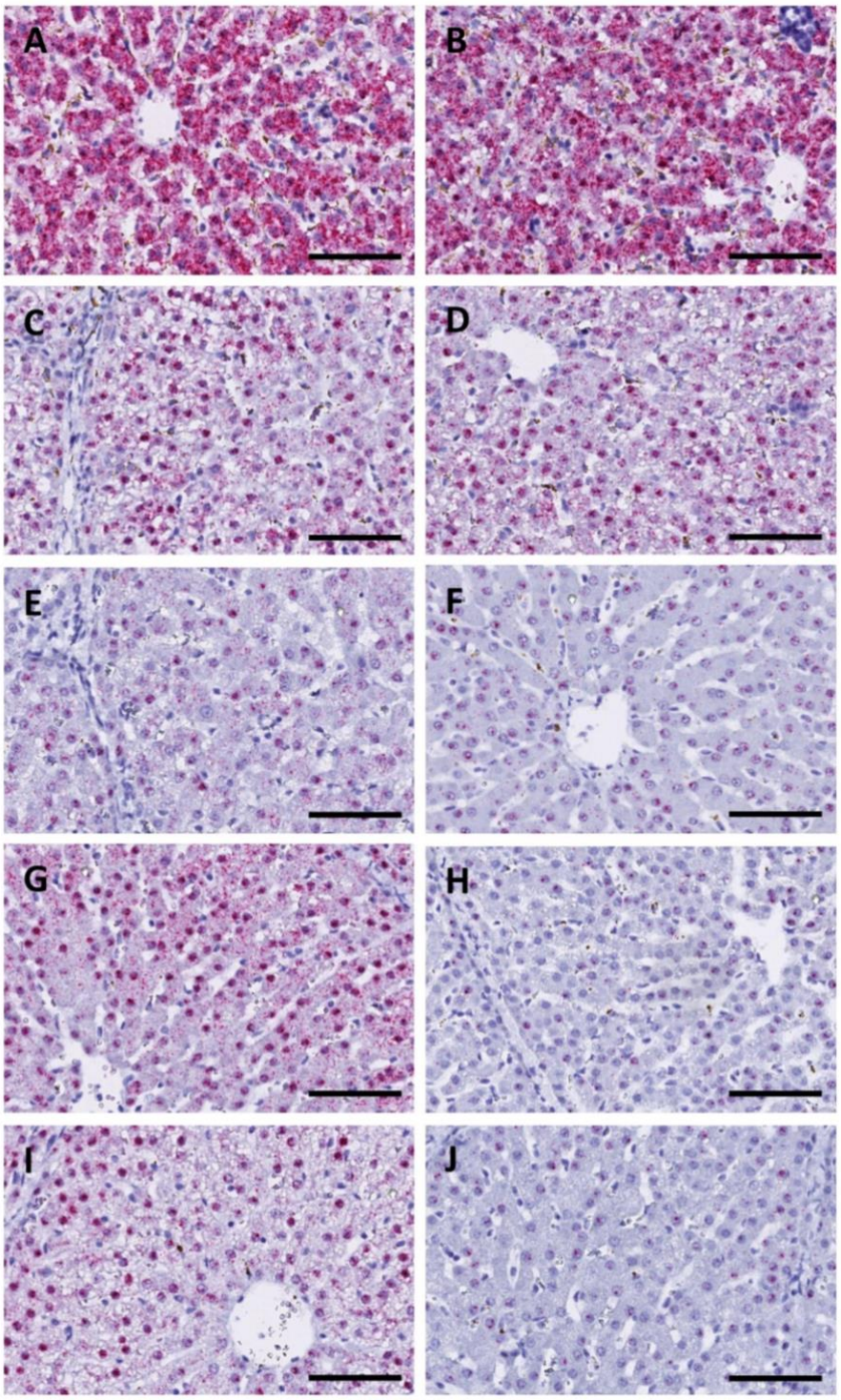

Figure 5.1. In situ hybridization (ISH) for PCSK9 (red staining) of liver sections from control (left panels) and RTR5001 treated (right panels) juvenile minipigs aged PND 2 (**A,B**), PND 16 (**C, D**), PND 30 (**E, F**), PND 43 (**G, H**) and PND 51 (**I, J**). Scale bar = 50 µM.

As mentioned in Chapters 1 and 3, the ontogeny and role of proteins (not just in the discussed PK components but also for the cellular uptake, trafficking, and pharmacologic activity of ASOs) are pivotal in understanding the difference in pharmacologic response seen in the juvenile minipigs compared to adults. Hence, future work focused on this specific research is necessary. For instance, the age and sex differences observed in liver *RNase H* relative expression (see Figures 3.10C and S3.4C) illuminated us its potential implication on the delayed RTR5001 pharmacology in the juvenile minipigs (Chapter 3). Based on this, proper translation of results from juvenile animal studies warrants similar ontogeny investigation in pediatrics, for which this is currently largely unexplored. Expanding this work to characterize other ASO modalities require additional ontogeny study for proteins unique to each of their intended MOA (e.g., Dicer enzyme for siRNAs [13]). The maturational factors discussed in this section and Chapter 3 for the potential reasons for the delayed pharmacologic response in the juvenile minipigs should also be taken into consideration when monitoring potential on- and off-target effects in animal models as these factors could also retard these toxicities in juvenile animals and pediatrics.

In terms of tissue exposure, we saw that the liver exposure showed an accumulation profile after repeated dosing of ASOs (Chapter 3, see Figure 3.2C). The degree of ASO metabolism in the liver could have also contributed to this exposure profile: when liver nuclease activity is higher (i.e., preterm) (see Figure 3.9C), underdosing could occur. As the exposure in the liver in the youngest juvenile minipigs is below the adult minipig values [10], dose regimen adjustments should be considered. As expected, the therapeutically-relevant dose should be determined by dose-range finding studies. On the other hand, another difference observed in the current work is the absence of basophilic granules in the liver tissue of juvenile minipigs. This was seen previously in adult minipigs after ASO administration [10], which signifies deposition and clearance of ASOs [14]. We speculate that this could also be related to a different uptake (less) and trafficking of ASOs in the juvenile minipig liver (e.g., Kupffer cells, hepatocytes), which resulted in the non-accumulation of the model ASO inside liver cells. This also depends on the amount of ASOs accumulated in the liver tissue and the clearance capacity of Kupffer cells.

Regarding the kidney, wherein developmental milestone differences occur between minipigs and humans (see section 5.3), proper age selection depending on the intended pediatric age is crucial [15]. For instance, weaned minipigs could be opted for human neonates in general, while neonatal

minipigs could be selected for premature infants if nephrotoxicity is the main safety concern for a candidate ASO. Since the lowest nuclease activity towards RTR5001 using kidney homogenates was observed after birth (PND 1 and 3) (see Figure 3.9B), the kidney tissue half-life of LNA PS gapmers could be longer for this age group and might influence the dose to be used during this neonatal period, as the excess would just get eliminated in the urine. However, due to the discrepancy in the adult kidney exposure values [10] and the current juvenile data (due to the different bioanalytical methods used), a direct comparison could not be made for dose adjustment considerations. This could be seen when we look at the kidney-to-liver concentration ratio after RTR5001 administration in juveniles (0.5-2.28) (Table 5.2) as compared to the 7.5 ratio in adult minipigs [10]. Parameters to estimate tissue exposure are prone to misinterpretation in juvenile minipigs. Although we observed an increase in plasma trough concentrations (Table 5.2) in the older juvenile minipigs that could be argued as a sign of liver tissue saturation [16], other parameters such as liver-to-plasma and kidney-to-plasma concentration ratio showed disparate results (Table 5.2) that could be attributed to plasma albumin maturation, and organ immaturity and histopathological changes (in kidneys) resulting to non-uptake of candidate ASOs. As such, we observed that RTR5001 accumulation in the kidney is limited to mature nephrons below the outer cortical region, and the kidney RTR5001 concentration remained the same, even after three doses (Chapter 3). This means that no uptake and accumulation occurred in the immature region of the kidneys. Accordingly, accumulation-related changes are not expected in immature nephrons. Several factors are involved in the cellular uptake of ASOs (both productive and unproductive), e.g., plasma protein and cell surface protein interactions (see section 1.1.5.4). This supports the notion that the maturation of specific cellular proteins responsible for the uptake of ASOs does not only dictate activity in the target cell population (pharmacology) but also toxicities that could occur after ASO treatment (e.g., accumulation-related changes).

A large part of this thesis evaluated the ontogeny of key nucleases responsible for ASO metabolism in juvenile minipigs (Chapter 3). For the following part, we will tackle in detail several related findings in view of the results from both the in vivo juvenile animal study and the in vitro nuclease assays. Accordingly, we have mentioned briefly that tissue nuclease activity could influence ASO tissue exposure and their corresponding half-life, leading to their ultimate elimination from the urine. As we saw a correlation of endonuclease gene expression with activity in the liver, while exonuclease activity appeared to fit more for the kidneys (Chapter 3), the metabolite profile is

expected to differ between these two organs. ASO metabolites after endonuclease degradation would be inactive as they are shorter in length and, therefore, easier to re-equilibrate out of the circulation and be ultimately excreted [17]. Putative exonuclease metabolites, as they are shorter – usually by one nucleotide at the end, could still be active [18]. As such, these metabolites could still cause on- and off-target activities. Hence, further investigation is needed (between organs and species) as the value of metabolite profiling could elucidate potential differences in on- and off-target activities in juvenile animals/pediatrics.

For the kidney compartment, both the exo- and endonuclease expression and activity data (see Figures 3.9B, 3.10A-B, and S3.4A-B) are generally lowest in the youngest age groups before they increase upon weaning and towards adulthood. This might suggest potential overdosing in the youngest population regarding kidney exposure. However, it should be mentioned that the assays for the nuclease gene expression and activity were nonspecific to mature and immature nephrons in the kidneys. Therefore, these values represent the mixture of the two cellular developmental conditions and warrant careful interpretation, as ASOs only accumulate in mature tubular cells in the kidneys. Although it is not known whether the nuclease gene expression and activity of these nucleases differ or to what extent they differ between immature and mature renal cells, future research should be performed using specific assays targeting each cell population to give us a more comprehensive view when interpreting results from in vitro assays. Likewise, the recovery phase in the in vivo study is needed to observe any delayed effect in developing organs as putative exonuclease metabolites can still be active together in function of LNA PS ASOs' longer half-life [19].

For the liver compartment, the general trend of nuclease activity in the liver of minipigs is higher during the perinatal period and lower during adulthood. Regarding *DNASE1* expression (correlated to liver nuclease activity), the highest expression was observed after birth and the lowest at PND 43 (see Figure S3.4A). Thus, the youngest age groups (with the lowest liver exposure) could be argued to have the potential to be underdosed, while at PND 43 (highest liver exposure) they could be overdosed. Although these findings could be incidental and only related to the inherent ASO accumulation associated with development, this still highlights the value of knowing the metabolic profile of the ASO in the different tissue compartments of developing animals. Care should also be given to this liver data as the nuclease expression and activity were done using liver tissue and not specific liver cell types. Therefore, nuclease activity differences between cell types (Kupffer cells vs.

hepatocytes) should be looked into in the future for better extrapolation of results from in vitro and in vivo assays as differences in ASO cellular uptake and accumulation occurs within certain tissues. If endonuclease was seen as the predominant nuclease active for ASO metabolism in this tissue compartment, inactivity of the metabolites is expected for this class of ASOs as they are shorter to produce activity (on- and off-target).

Our findings about nuclease expression in the blood, are valuable for future research on diseases in which ASO target transcripts are located in leukocytes such as in cases of blood-borne genetic conditions or cancers [20,21]. Our findings show that *PDE1B* and *TREX1* are higher in adults compared to juveniles (see Figure 3.8), which could indicate lower exonuclease activity in the youngest population. However, activity assays and metabolite profiling in these cells are warranted to further characterize the implications of this data.

5.2 Seen and not seen: safety signals in the juvenile minipig and what do they tell us

In Chapter 1, we reviewed the key toxicological elements of ASO therapies. As pointed out, most ASO-induced toxicities are hybridization-independent [22]. They are generally due to tissue accumulation, proinflammatory effects, and protein binding, which are usually related to the physicochemical properties of the candidate ASOs. As predictive "class toxicities" can be identified for ASOs depending on their design and chemistry [23], findings in this work could be applied within the same ASO class and may also be extrapolated to other ASO class and OND modalities. Likewise, previous nonclinical and clinical experience with this ASO class will be referred to assimilate our findings in the juvenile minipig. An emphasis on how these findings could contribute to the knowledge expansion of ASO pediatric safety testing will also be made throughout this section.

In general, the safety signals seen in the different juvenile age groups of minipigs are in accordance with what was seen previously in adult minipigs after the same LNA PS gapmer administration [10] (Chapter 3). In line with the consistent tissue distribution of LNA PS gapmers, changes in high-exposure organs, such as the kidneys (see section 1.1.7.2.5), were observed in the juvenile minipigs. In contrast, no novel accumulation-related changes were observed in other organs with limited

exposure. In analogy, it would be easy to argue that the consistent ASO tissue distribution in the juvenile minipigs and adults resulted in the same target organs of toxicities.

Table 5.3. Overview of toxicity findings for RTR5001 in juvenile and adult minipigs [10], adult NHPs [11], and adult humans [12,24].

Toxicity findings	Juvenile minipigs	Adult minipigs	Adult NHPs	Humans	Remarks
Renal tubular degeneration/ regeneration	Observed	Observed	Not observed	Not observed	Accumulation-related change
Acute tubular necrosis	Not observed	Not observed	Not observed	Observed	Possibly off-target effect
Glomerulosclerosis	Observed in older age groups that received more dose over a longer period of time	Not observed	Not observed	Not observed	Related to chronic dosing
Kidney function tests	No observed change	Elevation in plasma chemistry (BUN, creatinine) and urinary changes	No observed change	Transient increase in plasma chemistry (creatinine)	Related to structural changes in the kidneys
Basophilic granules and hypertrophy of Kupffer cells	Not observed	Minimal	Not observed	Not observed	Accumulation-related change and ASO proinflammatory effect
Single-cell necrosis	Not observed	Minimal	Not observed	Not observed	Associated to ASO proinflammatory effect
Liver function tests	Minimal increase in AST	No change	No observed change	No observed change	Related to structural changes in the liver
Injection site reaction	Similar NHP	Similar to NHP	Not predictive of human injection site reactions	Mild to moderate	Proinflammatory effect of ASOs
Thrombocytopenia	Not observed	Not observed	Not observed	Not observed	Toxic ASO-protein interaction or immune-mediated
Complement activation	Not observed	Not observed	Not observed	Not observed	Toxic ASO-protein interaction
Coagulation cascade inhibition	Not observed	Not observed	Not observed	Not observed	Toxic ASO-protein interaction

Abbreviations: NHP, nonhuman primate; BUN, blood urea nitrogen ; AST, aspartate aminotransferase.

The renal tubular degeneration/regeneration observed in the juvenile minipigs after treatment with RTR5001 was considered non-adverse, as no change in kidney function was observed (see Table 5.3). In contrast, a concomitant increase in serum creatinine and blood urea nitrogen (BUN), as well as urinary changes, which consisted of an increase in urinary volume and an increase in urinary N-acetyl-beta-D-glucosaminidase and calcium normalized to creatine were observed in adult minipigs [10]. In NHPs, RTR5001 treatment was well tolerated with no observed effects on kidney toxicological parameters (histology and serum BUN and creatinine). It should be mentioned that in the adult minipig study, these results were only observed in the high dose group (20 mg/kg on days 1, 6, 11, and 16), while for the NHP study, animals were given an initial loading dose of 20 mg/kg, followed by four weekly maintenance dose of 5 mg/kg. Hence, this difference in renal findings between the adult minipig and NHPs may be dose-related, as histopathological changes concurrent with functional alterations occur above a concentration threshold [25,26]. Regarding the difference in renal findings between juvenile and adult minipigs, we hypothesized that due to the lower exposure of the juvenile minipigs' kidneys (due to renal immaturity and lower plasma albumin binding in the youngest age groups resulting in faster renal elimination), the degree of accumulation-related changes did not result in functional alterations as the former generally correlates with serum clinical chemistry elevations. Moreover, the elevation of serum biochemical parameters could sometimes have a late onset [27], and could explain why it was not observed later on in the older juvenile minipigs even though they developed a higher degree of tubular degeneration/regeneration. Therefore, other kidney injury biomarkers detectable in the urine, such as kidney injury molecule 1 (KIM-1), could be used to potentially detect tubular toxicity during nonclinical development [27]. On the other hand, glomerulosclerosis was observed in the juvenile minipigs, which is related to the longer treatment duration of the present work. Thus, caution is needed in future juvenile studies regarding this glomerular toxicity and its possible sequelae. Likewise, this should also be differentiated accordingly from tubular toxicity. The reversibility of such findings post-treatment and the appearance of delayed after-treatment effects should also be looked at.

Similar to the kidneys, the liver also received a high fraction of the dose after the systemic administration of RTR5001, consistent with previous knowledge of its ASO class [28,29]. For this reason, accumulation-related changes in the liver are expected, such as the presence of basophilic granules, and hypertrophy of Kupffer cells related to their function for ASO clearance [14,30–32].

In contrast to the findings in adult minipigs, basophilic granules and Kupffer cell hypertrophy were not seen in the liver of the juvenile minipigs (see Table 5.3). Although lower liver exposure was seen initially in juvenile minipigs, adult liver RTR5001 concentration [10] was reached after five doses. We speculate that the juvenile minipig's Kupffer cells have limited capacity to clear ASOs early in postnatal development as the Kupffer cell's phagocytic activity increases with age [33]. This is supported by the morphological differences (e.g., less extensive dendritic processes) seen in Kupffer cells of mice during early postnatal development compared to adults [34]. In line with this, the minimal single-cell necrosis observed in adult minipigs [10] was absent in the juveniles, similarly to the findings in NHPs [11]. Again, the lower dose used in the NHP study could be responsible for this difference with the adult minipig as reflected by the lower liver exposure in NHPs [11]. Observation of this histopathological change in the liver that correlates with increased serum transaminase activities is not unusual [14], as it was seen after the administration of two other model LNA PS gapmers in adult minipigs, as well as in NHPs in similar study designs [10,21]. As single-cell necrosis is associated with the proinflammatory class effect of PS-containing ASOs [35], we hypothesized that the proinflammatory potential of ASOs in the minipig liver is also affected by age, as a response to this inflammatory stimuli could still be immature in younger individuals [36]. On the other hand, the inflammatory reaction in the injection site, is similar between the juvenile and adult minipigs (and NHPs) [10](see Table 5.3). Therefore, the previous hypothesis and its translation to human pediatrics warrant further investigation. Future research should also be devoted to the proinflammatory effects of ASOs in other organs of the juvenile minipigs, including those that are targeted by local ASO administration (e.g., CNS, lung).

In view of their PK, newer generation high-affinity ASO gapmers have been linked to causing on- and off-target pharmacologic effects, especially in the liver and the kidneys (see section 1.1.7.2.6-7). This is a critical safety signal of concern for ASO therapeutics in pediatrics, since developing animals may present differences in gene transcription of the target and off-targets in function of age. On this account, no hybridization-related effects (on- and off-target effects) were observed in our work with juvenile minipigs.

It should be mentioned that RTR5001 caused acute nephrotoxicity in adult humans (see Table 5.3), resulting in its clinical development being terminated [12]. A highly sequence-dependent acute multifocal tubular necrosis was seen in a healthy volunteer following three doses (5 mg/kg) of

RTR5001 [24]. Although no symptoms of renal toxicities being present in the pivotal mouse and NHP nonclinical toxicity packages, a retrospective high-dose study in rats confirmed the tubular toxicity for this sequence [27]. Thus, it was postulated that, like the sequence-dependent liver toxicities of high-affinity gapmers (see section 1.1.7.2.7), similar mechanisms of RNase H-dependent off-target toxicity [37,38] might be involved in this sequence-dependent renal toxicity of RTR5001 in humans [22]. However, this phenotype of nephrotoxicity was not observed in both adult and juvenile minipigs, as in mice and NHPs after RTR5001 administration. Despite the advances in safety assessment, this demonstrates that it remains difficult to predict human toxicity from animal models [39], although the value of animal models was still proven in detecting toxicities secondary to exaggerated pharmacology, i.e., mipomersen and ALN-AAT (siRNA) [22].

The failure to predict the acute kidney injury induced by RTR5001 in its clinical trial suggested the need for additional nonclinical models to complement animal toxicity studies. Accordingly, the utility of in vitro systems is being explored. For instance, a human renal proximal tubule-on-a-chip demonstrated its translational potential through the induction of nephrotoxicity and kidney injury biomarkers by RTR5001 [40]. Furthermore, as LNA gapmers that cause renal toxicity in vivo were shown to impair epidermal growth factor (EGF) receptor signaling in primary and immortalized human proximal tubules in vitro, a robust EGF-based assay that contributes to the in vitro safety profiling of this class of ONDs was developed [27]. Besides in vitro models, the computational predictions of ASO unintended targeting are continuously progressing [41–43]. This should markedly reduce the risk of encountering unexpected adverse effects related to off-target pharmacology that could go undetected in nonclinical animal toxicity packages, even with relevant animal species, e.g., off-target transcripts could have a different degree of homology, mainly if occurring in intronic sequences.

Aside from accumulation-related changes and on- and off-target pharmacological effects, toxic protein interactions by ASOs are another potential safety signal of concern in pediatrics, as proteins implicated in each specific mechanism could also undergo ontogeny. For instance, the value of understanding platelet GPVI and PF4 ontogeny related to potential ASO-induced thrombocytopenia in the juvenile minipigs was described in Chapter 4. In that chapter, additional tool ASOs with various sequences and modifications (unmodified, all PS, 2'-MOE) were used to evaluate their effects on minipig platelets. This was to expand the knowledge on platelet response phenotype to

ASOs by the Göttingen Minipig, as only LNA PS gapmers were characterized in the previous study by Braendli-Baiocco et al. (2017) [10] in adult minipigs and in the present repeat-dose toxicity study in juvenile animals. As discussed, a similar platelet response was observed in vitro as in NHPs and humans. Moreover, concentration-dependent direct platelet activation was seen in line with previous findings in human samples. For this, an appropriate dosing regimen (e.g., SC administration or longer lower-dose IV infusions) should be implemented to reduce the risk for this adverse effect. A similar approach applies to candidate ASOs with an increased propensity to cause coagulation cascade inhibition and alternative complement system activation. Both are also brought on by nonspecific ASO–protein toxic interactions. On the other hand, the model ASO (RTR5001) did not cause platelet count reduction, prolongation of coagulation, and complement activation in the (juvenile and adult) minipig, NHP, and human studies [10–12,24] (see Table 5.3). Therefore, RTR5001 alone is not enough to characterize these adverse effects, and other tool ASOs should be used in vivo in juvenile minipigs. In respect of this, future research should also be done to determine if the proteins involved in the coagulation and complement systems undergo ontogeny in juvenile minipigs similar to what was done in Chapter 4.

Although we had an idea of the ontogeny of total complement factors in the juvenile minipigs (Chapter 3), differential ontogeny profiles for each complement system protein component could occur during early development. This could impact the inhibition of complement factor H by ASOs resulting in either heightened or decreased adverse effect sequelae. As minipigs seemed to be less sensitive to ASO complement activation (similar to humans) than NHPs, the value of the Göttingen Minipig as an animal model for safety testing of candidate ASOs with increased complement activation should be taken into account, since NHPs overpredict findings related to this adverse effect [31,44–46] (see section 1.1.7.2.1). With regards to the coagulopathy related to ASOs administration, the adult minipigs showed similar results as NHPs [10]. However, although the porcine coagulation and fibrinolytic systems are in many aspects comparable to those of humans, the intrinsic coagulation system, seems to be hyperactive (aPTT is shorter in porcine than in humans) [47]. This is in accordance with the fact that the levels of several coagulation factors are higher in porcine plasma (e.g., factor X, 50-289% higher) [47]. Therefore, further research is needed to determine if coagulation abnormalities to be observed in minipigs (e.g., including diseased models) could represent coagulation profiles in (sick) patients [48].

In conclusion, we have not seen novel toxicities (aside from the glomerulosclerosis related to more chronic ASO exposure) in juvenile minipigs exposed to RTR5001 compared to adult minipigs. Still, our findings serve as a basis for future pediatric safety testing of similar ASO classes due to their class-related PK and safety properties. The selection of a relevant model (both for adults and pediatrics) for off-target effects is more difficult, as sequence homology for these off-target sequences and their transcription ontogeny are largely unknown. However, as in vitro and in silico models for this aspect continuously improve, it is likely that the risk of encountering off-target effects in the clinics will be reduced in the future.

5.3 Choosing wisely: selection of the juvenile Göttingen Minipig as a model for pediatric safety testing of ASOs

In this section, we will discuss the selection of the juvenile Göttingen Minipig as an animal model for ASO pediatric safety testing. The ICHS11 guideline clearly stipulates that a juvenile animal study should be performed in a pharmacologically relevant species. In our in vivo study, the Göttingen Minipig showed an inherent pharmacologic cross-reactivity for the model ASO, RTR5001, and this definitely substantiates the selection of this species as a relevant alternative animal model to NHPs. However, other factors should also be considered when selecting a species for juvenile animal studies [15].

Firstly, conducting a study in the selected species should be technically/practically feasible. This was evidenced in the 8-week investigational repeat-dose toxicity study of RTR5001 by the SC route in the juvenile minipig (Chapter 3). Minipigs present many technical and practical advantages in pediatric drug discovery and development [49]. For instance, its large litter size (especially for high parity sows) allows fewer animals to be kept for breeding purposes, which is further aided by their short reproductive cycle [50]. This also enables placing littermates into various experimental groups. Likewise, minipigs are also relatively easy to handle (in view of size) and train [51,52], and their larger birth size, permits sampling at early stages compared to dogs or NHPs. All routes of administration are also feasible. Although the clinical features of human injection site reactions were not predicted well by the juvenile and adult minipigs after SC administration of ASOs (see Table 5.3), histopathological similarities were observed between minipigs and NHPs [10]. In cases of chronic JAS, dosing up to maturity is usually tricky or not feasible in NHPs due to the large

interindividual differences in the onset of maturity, whereas this is possible in minipigs as they reach maturity faster and with relative consistency [15]. On the other hand, the fast growth and size of minipigs could, from a practical point of view, be a disadvantage when compared with the dog and other nonclinical species in terms of compound consumption and availability during repeat-dose toxicity studies. However, this may represent an advantage when sampling at very early stages [49]. In view of this, blood sampling could be challenging as their peripheral veins are not easily accessible. However, with experienced personnel, approaching the jugular and cranial vena cava for blood collection is feasible [53] and was done in the in vivo study in this thesis. Although microsampling was not performed for the toxicokinetic part of this work due to the less sophisticated method available for the model ASO (dead compound), its value in such studies would improve animal welfare [54]. Moreover, additional toxicity biomarkers (e.g., urinary β2-microglobulin and KIM-1 by ELISA; CD62P, and PAC-1 platelet activation markers by flow cytometry) should be included in the panel of predictive assays to assess potential toxicity by ASOs during nonclinical studies [39]. Regarding additional endpoints to address identified safety concerns, such as localization of accumulated ASOs in tissues by staining methods (e.g., IHC) and to assess target knockdown (i.e., qPCR), the administration of iron dextran after birth in minipigs could pose a challenge in processing the tissue samples where the iron supplement would be deposited (e.g., liver, lymph nodes). In this study, an additional clean-up step was necessary for the RNA extraction, whereas brown staining of the hemosiderin (iron deposits) in IHC tissue sections could be confused with DAB-positive staining.

Another factor that should be considered when selecting an animal model is its similarity to humans in view of PK profile (ADME characteristics). Several attempts to further characterize ADME processes in (mini)pigs have been made for their use in pharmaceutical research [50,55,56]. In particular, further exploration of pig models has been of interest in the development of biopharmaceuticals [57], e.g., growth hormones [58], and vaccines [59–63]. Likewise, studies on small molecules have been published in recent years addressing the PK of antibiotics, anesthetic drugs [64–66], and nonsteroidal anti-inflammatory drugs [67] in juvenile pigs. Moreover, the pig showed higher similarities with humans in ontogenic changes in PK (with rifampin as a model compound) than other species, including the dog [68].

With regards to ASOs, the PK profile of LNA PS gapmers in adult minipigs showed a high degree of similarity with NHPs [10] (see section 1.3.1). However, no data on the ADME of ASOs in the juvenile Göttingen Minipig had been published before the conduct of this thesis, thus the value of this pioneering work is fundamental. In brief, we observed a similar PK behavior between the juvenile and adult minipigs [10]: the model ASO (RTR5001) was quickly absorbed following SC administration in adult and juvenile minipigs. This has also been observed after weekly SC administration of drisapersen (2'-OMe PS ASO) in ≥ 5-yr-old boys, wherein T_{max} was recorded two hours post-systemic administration [69]. Moreover, rapid tissue distribution was observed in 5-16-yr old boys, with a decline in plasma levels of drisapersen to approximately 18% of C_{max} after 24 h and 0.6% at the end of dose intervals (7 days) [70]. A faster tissue distribution of RTR5001 was observed in juvenile minipigs, at 0.23-2.62% (after 24 h) and 0.00-0.79% (end of dose intervals) (see Table 5.2). On the other hand, $AUC_{0\text{-}24h}$ showed no increase after repeated dosing of drisapersen in 5-16-yr-old boys, but plasma trough levels increased with the increasing number of dosing [70]. A similar increase in plasma trough levels was observed in our work and could be related to tissue saturation. The $AUC_{0\text{-}24h}$ increased after repeated RTR5001 dosing in the juvenile minipigs. The probable reason for the observed differences in AUC and the % decline in plasma levels (relative to C_{max}) described between the boys dosed with drisapersen and minipigs dosed with RTR5001 could be linked to the degree of plasma albumin level maturation (and its overall influence in plasma clearance, tissue distribution, and elimination, see section 5.1) in the selected age groups exposed in both studies. Other factors, such as the physicochemical properties of the ASO itself (2'-OMe PS ASO vs. LNA PS ASO) and the age differences between the animal model and target pediatric population linked with potential differences in ADME processes could have further contributed to this. Therefore, ADME characterization of specific sequence design and modifications should be done in the juvenile minipig to allow proper extrapolation of results between this animal model and pediatrics. With regard to tissue distribution and metabolism of ASOs, due to the limited published data on systematically administered ASOs in pediatrics and on human nuclease ontogeny, a comparison of our in vivo and in vitro findings in the juvenile minipigs with human pediatrics' PK profile is not feasible. However, data from this doctoral thesis emphasizes the importance of considering the maturational factors of the ADME processes between the juvenile minipig and the pediatric target population in view of future pediatric ASO safety testing and its translation.

To facilitate the comparison of systemic exposure profiles and toxicities between juveniles and adult animals, the same species used in adult repeat-dose studies should initially be considered as the species for JAS. Thus, adult repeat-dose study considerations could dictate the test animal selection for JAS. An active challenge in considering the use of the juvenile Gottingen Minipig as an alternative animal model for safety assessment of pediatric pharmaceuticals is its limited available historical data compared to dogs and NHPs [15], especially from earlier complementary safety studies (minipig-based) conducted in the drug development plan. In view of this, pharmaceutical companies scarcely employ adult (mini)pigs in repeat-dose toxicity tests. However, this trend is changing, and minipigs are increasingly used as alternatives to dogs or NHPs [49]. Defining comprehensive animal selection criteria in the current regulatory guidelines for adult repeat-dose toxicity studies, such as which relevant species to be considered (e.g., similar pathophysiology, target homology), would also convince pharmaceutical companies to include the Göttingen Minipig in their nonclinical testing strategies, including those for pediatric use [49].

With the characterization of the adult Göttingen Minipig as a suitable animal model for safety assessment of ASOs (due to the similarities shown in terms of PK/PD and safety profiles with NHPs [10]), together with the increasing drive to limit the use of NHPs [71], extending the use of juvenile minipigs in pediatric safety testing of ASOs has been put forward. However, a survey has reported the limited use of minipigs as non-rodent species for ASO toxicity studies (14% for RNase H-dependent ASOs) across 22 companies developing therapeutic ONs performed in 2018 [72]. Against this background, respondents who are open to using alternative non-rodent relevant species to NHPs mentioned cross-species homology. This is a valid criterion, as monitoring on-target pharmacology and toxicity is crucial in JAS for ASOs due to their high target specificity. Although mismatches on the target sequence could be tolerated to some degree, depending on the location of these mismatches, antisense activity could be abolished (end-standing versus mid-standing for RNAse H-dependent ASOs) as seen with the different model LNA PS gapmers tested in the adult minipig study by Braendli-Baiocco and colleagues (2017) [10]. Even with exact target sequence homology, it does not mean it will reflect the same ASO activity in animal models. Therefore, proofs (e.g., additional complementary studies to show antisense activity) should be provided to justify the selection of an animal model as relevant species for safety testing, especially for new drug modalities with high specificities.

On the other hand, the juvenile animal's relative stage of target organ/system development compared to the targeted pediatric population should also be considered. As such, this corresponds to the animal model's capacity to identify toxicity endpoints of concern. In the pediatric population, EMA has defined several age groups [73], and significant parallels in organ development between humans and Göttingen Minipigs (the reference breed used in the pharmaceutical sector [49]) are reported in the ICH S11 guideline [15]. These data are illustrated in Figure 5.2. At the same time, a summary of the main similarities and differences in the maturation of different organ systems in pigs and humans is presented in Table 5.4.

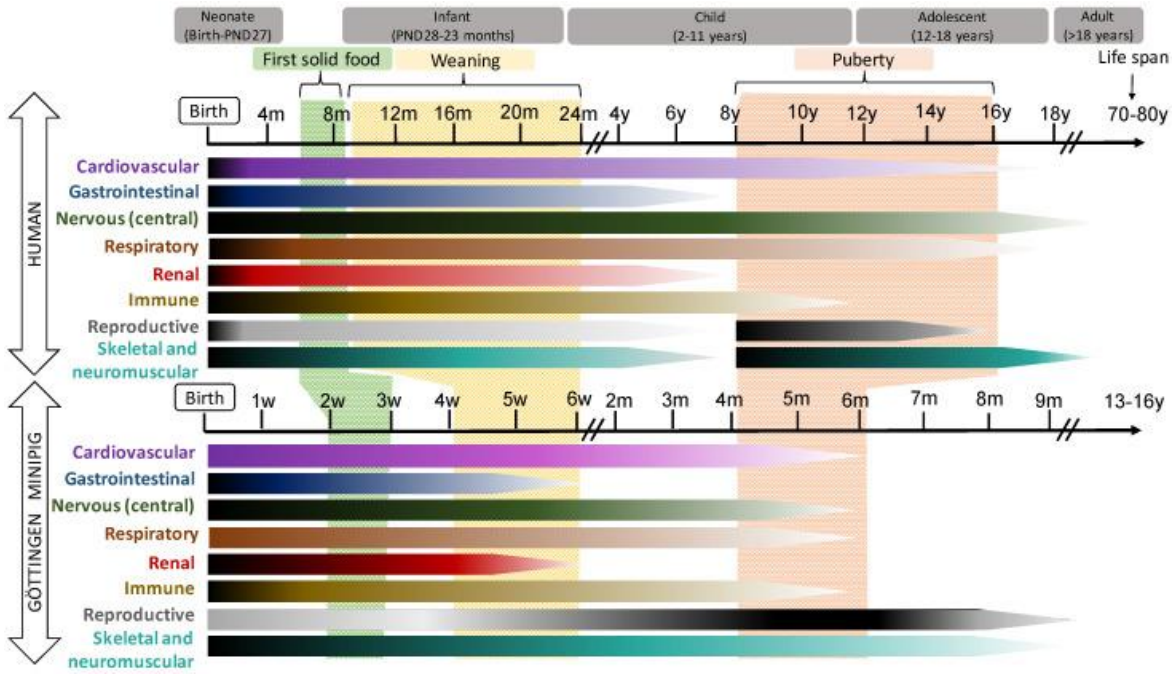

Figure 5.2. Schematic representation of the postnatal development of different organ systems in human (top) and Göttingen Minipig. In the horizontal bars, the intensity of the maturation process is represented by dark (more intense) and light (less intense) tones. The time bar represents weeks (w, months (m), or year (y) of life. This figure is reproduced from Ayuso et al. (2020) [49]

Specifically for ASOs, of which class-specific toxicities could be well predicted, the toxicological target organs remain relatively the same. This was demonstrated in the repeat-dose toxicity study conducted wherein the toxicological target organs were similar in the different juvenile age groups as in former results in adult minipigs [10] and NHPs [11,25,26,74–78]. For instance, accumulation-

related changes specific to the kidneys were observed and discussed in Chapter 3 and section 5.2. As briefly indicated before, the nephrogenesis in the pig is slower that in the human, despite the gross anatomy and several functional aspects being quite comparable (Table 5.4). This has to be considered, particularly when evaluating ASOs, having a primarily renal excretion mechanism. In addition, human GFR is reported to be lower (between 55 and 80% of pigs), but GFR maturation seems to be similar [79]. Additionally, it is essential to note that a high incidence of inflammatory cell infiltration has been seen in many minipig strains [80], which is also worth considering when evaluating nephrotoxicity by ASOs due to their proinflammatory potential (see section 1.1.7.2.4).

In contrast, accumulation-related changes in the adult minipig liver were not observed in the different juvenile minipigs and were previously related to possible maturation of inflammatory response within the organ itself (see section 5.2). Nonetheless, there is a high degree of similarity between the pig and human immune systems [81–83]. With regard to the other systems with increased safety concerns after systemic ASO administration (discussed in sections 1.1.7 and 5.2), future work is needed to fully characterize the mechanism through which ASO could induce potential toxicities during early developmental stages in the minipigs.

Lastly, an understanding of the ontogeny of toxicological (i.e., off-target transcripts and proteins related to toxic ASO-protein interactions) and pharmacological targets (i.e., on-target transcript) in animals in comparison to that in the intended pediatric population is crucial in the selection of a relevant test animal species. In general, as potential off-target effects could also be a safety concern in pediatrics (similar to RTR5001 causing acute nephrotoxicity in an adult human volunteer, see section 5.2), the ontogeny of the potential off-target sequences should also be evaluated (given the off-target sequence was identified by complementary studies before in vivo toxicity evaluations). This information from humans regarding the RTR5001-induced acute nephrotoxicity still needs to be clarified, and whether translatability from animal models would be informative. On the other hand, the ontogeny of proteins related to toxic ASO-protein interactions was already discussed in section 5.2.

Table 5.4. Summary of main simmilarities and differences in maturation of different organ systems in pigs and humans. This table is adapted from Ayuso et al. (2020) [49].

Organ System	Feature	Similarity
Cardiovascular	Drainage	Different
	Main central vessels	Different relative importance
	Cardiac output	Different
	Cardiac myocyte maturation	Similar (compared to other species)
	Serum proteins (albumins and globulins)	Different in neonatal pigs and humans, but even at infant stages
Gastrointestinal	Physiology of digestion	Very similar
	Ontogeny of digestive enzymes	Similar in most cases (more than the rat)
	Neonatal gastric pH	Different: pigs show adult-like values early in life (five days of age) and humans reach that point at two years of age
	Gastric emptying	Maturation of gastric emptying with age has not been established in pigs. Prolonged emptying is expected in newborn pigs, as observed in humans
	Intestinal transit	Similar: longer in neonates than juvenile/adults
	Intestinal surface	Similar: smaller than juvenile/adults, leads to similar nutrient absorption
	Microbiome	Similar: mainly consists of Firmicutes and Bacteriodetes phyla
	Liver	Similar relation to body weight in adults (about 2%) Slightly higher ratio in human (around 5%) than minipig (3%) neonates
Central nervous	Anatomical complexity	Similar
	Distribution of grey and white matter	Similar
	Brain growth pattern	Similar
Respiratory	Anatomy and histology	Similar
	Maturation	Faster
	Alveoli multiplication	Earlier in pigs
Renal	Nephrogenesis	Different: completes after weaning (three weeks of age) in pig and 34-36 weeks gestational age in humans
	Glomerular filtration rate	Similar maturation: adult levels at 8 weeks (pig) and one year (human) of age
	Effective renal plasma flow Urinary pH	Within the same range in growing pigs and children
Immune	Immune genes	High similarity (>80%)
Skeletal and neuromuscular	Development	Different: faster in pigs, in which locomotion patterns reach mature levels as early as eight hours after birth

Knowledge of the target transcript ontogeny would help us assess potential differences in ASO activity between the chosen animal model and pediatrics, especially in the case of the delayed pharmacologic response, as seen with RTR5001 in the juvenile minipigs (Chapter 3). Although a qualitative assessment of *PCSK9* expression was done by ISH (see section 5.2), a corresponding quantitative evaluation of the target transcript was not performed between the control and treated juvenile minipigs. The *PCSK9* expression appeared to undergo ontogeny, supported by the observations in the endpoint plasma biomarker (plasma total and LDL cholesterol levels) in the juvenile minipigs (see Figure 3.4). However, as RNase H-dependent ASO's MOA is to degrade the target transcript, a decrease in the two lipid profile panels is expected even if the target transcript is undergoing ontogeny. We hypothesize that a different mechanism for lipid/cholesterol homeostasis could be involved aside from the factors mentioned in section 5.1 and Chapter 3. Regardless, the delay in pharmacologic activity observed in our work still highlights the possibility of altered ASO pharmacologic response in juvenile animals and/or pediatric humans. This further supports that the juvenile minipig model can detect such differences compared to adult populations.

In conclusion, the selection of the (juvenile) Gottingen Minipig as a relevant animal model for (pediatric) ASO safety testing can be clearly justified to health authorities if the drug candidate cross-reacts with this animal model. We have discussed several advantages (technical and practical feasibility) regarding the conduct of juvenile animal studies in the Gottingen Minipig. Although further efforts have to be made to advance the translational knowledge on ASO ADME and PD processes in juvenile minipigs, our data clearly showed the importance of considering maturational factors for better data interpretation and translation between the juvenile animal and/or pediatric target populations. Based on the data generated in this thesis, the development of target organs/systems in the model compared to the pediatric population and the ontogeny of the toxicological and pharmacological targets should be carefully considered. Finally, since (adult) minipigs are increasingly used as an alternative to dogs or NHPs in drug discovery and drug development, this will aid in convincing regulatory authorities to also accept the juvenile minipig as a model for pediatric drug safety testing of drug candidates.

5.4 Future perspectives and general conclusions

In the course of the general discussion, the main findings related to PK/PD and safety profiles of ASOs in the juvenile Göttingen Minipig were discussed. Accordingly, several points that warrant further research evaluations in the future were highlighted to ultimately characterize this animal model for the pediatric safety testing of ASOs. Some key aspects include the further assessment of the ADME and PD processes regarding ASO administration in juvenile minipigs, such as those involving proteins that may undergo ontogeny. In addition, future characterization of nucleases (and metabolite profiling) in other developing organs that may be targeted by ASOs, using specific cell-type assays, were also mentioned. As such, both will facilitate the development of PBPK modeling in this animal model to predict ASO exposure. Likewise, future research focus should also be extended to the components of organ systems undergoing development with ASO toxicity concerns, such as the inflammatory response maturation in the liver and ontogeny of proteins implicated in toxic ASO-protein interaction mechanisms. Moreover, issues such as developing nonclinical models (minipig-based) that will complement animal studies were tackled, including those that can assess off-target effects amongst other toxicities. Together with this, the characterization of appropriate toxicity biomarkers that are translatable to the human scenario would be crucial in selecting the Göttingen Minipig as an animal model for ASO safety testing.

Overall, this thesis provides a solid foundation for future pediatric safety testing in minipigs using LNA PS gapmers and for the justification of selecting this juvenile animal model in regulatory submissions. Although we only looked at the profile of one model ASO in the juvenile minipig (with the known class-related properties of ASOs in terms of PK/PD and safety), extrapolation of our findings to other candidate ASOs belonging to the same class is simpler to carry out as compared to small molecules and biologics. On the other hand, extending the knowledge from this doctoral thesis to other OND modalities, although possible, is limited. Therefore, future characterization of other nucleic acid-based modalities with various physicochemical properties and general MOA should be done in juvenile minipigs for its timely use as a juvenile animal model for the safety assessment of these emerging drug modalities. In line with this, further characterization of other components of the ADME process in the juvenile minipigs should also be done (e.g., the role of glomerular filtration maturation for siRNA with neutral chemistries). Furthermore, as the trend for newer drug modalities that target tissues outside the usual ASO distribution repertoire, ASO

delivery systems would be more of the approach in the near future. Therefore, ontogeny characterization of the processes involved in such delivery processes should be included in future works concerning the characterization of this animal model. Nevertheless, based on the data presented in this dissertation, we conclude that there is no constraint in using juvenile minipigs as the non-rodent species in pediatric ASO candidate nonclinical safety packages and in convincing health authorities to accept this juvenile animal model.

5.5 References

1. Aartsma-Rus, A.; Jackson, A.L.; Levin, A.A. Mechanisms of Oligonucleotide Actions. In *Oligonucleotide-Based Drugs and Therapeutics*; Ferrari, N, Seguin, R., Ed.; John Wiley & Sons, Inc.: New Jersey, 2018; pp. 1–38 ISBN 9781119070290.
2. Grossi, A.B.; Zeltner, A.; Christoffersen, C.; Søndergaard, A.C. Reference Data of Clinical Chemistry and Hematology in Juvenile Göttingen Minipigs. *Toxicol Lett* **2016**, *258*, doi:10.1016/j.toxlet.2016.06.1838.
3. Sethi, P.K.; White, C.A.; Cummings, B.S.; Hines, R.N.; Muralidhara, S.; Bruckner, J. V. Ontogeny of Plasma Proteins, Albumin and Binding of Diazepam, Cyclosporine, and Deltamethrin. *Pediatr Res* **2016**, *79*, doi:10.1038/pr.2015.237.
4. Bakker, J.; Maaskant, A.; Wegman, M.; Zijlmans, D.G.M.; Hage, P.; Langermans, J.A.M.; Remarque, E.J. Reference Intervals and Percentiles for Hematologic and Serum Biochemical Values in Captive Bred Rhesus (Macaca Mulatta) and Cynomolgus Macaques (Macaca Fascicularis). *Animals* **2023**, *13*, doi:10.3390/ani13030445.
5. Bonfanti, U.; Lamparelli, D.; Colombo, P.; Bernardi, C. Hematology and Serum Chemistry Parameters in Juvenile Cynomolgus Monkeys (Macaca Fascicularis) of Mauritius Origin: Comparison between Purpose-Bred and Captured Animals. *J Med Primatol* **2009**, *38*, doi:10.1111/j.1600-0684.2009.00345.x.
6. Koo, B.-S.; Lee, D.-H.; Kang, P.; Jeong, K.-J.; Lee, S.; Kim, K.; Lee, Y.; Huh, J.-W.; Kim, Y.-H.; Park, S.-J.; et al. Reference Values of Hematological and Biochemical Parameters in Young-Adult Cynomolgus Monkey (Macaca Fascicularis) and Rhesus Monkey (Macaca Mulatta) Anesthetized with Ketamine Hydrochloride. *Lab Anim Res* **2019**, *35*, doi:10.1186/s42826-019-0006-0.
7. Shadid, M.; Badawi, M.; Abulrob, A. Antisense Oligonucleotides: Absorption, Distribution, Metabolism, and Excretion. *Expert Opin Drug Metab Toxicol* 2021, *17*.
8. Frazier, K.S. Species Differences in Renal Development and Associated Developmental Nephrotoxicity. *Birth Defects Res* **2017**, *109*, 1243–1256, doi:10.1002/bdr2.1088.
9. Shemesh, C.S.; Yu, R.Z.; Gaus, H.J.; Seth, P.P.; Swayze, E.E.; Bennett, F.C.; Geary, R.S.; Henry, S.P.; Wang, Y. Pharmacokinetic and Pharmacodynamic Investigations of ION-353382, a Model Antisense Oligonucleotide: Using Alpha-2-Macroglobulin and Murinoglobulin Double-Knockout Mice. *Nucleic Acid Ther* **2016**, *26*, doi:10.1089/nat.2016.0607.
10. Braendli-Baiocco, A.; Festag, M.; Erichsen, K.D.; Persson, R.; Mihatsch, M.J.; Fisker, N.; Funk, J.; Mohr, S.; Constien, R.; Ploix, C.; et al. The Minipig Is a Suitable Non-Rodent Model in the Safety Assessment of Single Stranded Oligonucleotides. *Toxicological Sciences* **2017**, *157*, 112–128, doi:10.1093/toxsci/kfx025.

11. Lindholm, M.W.; Elmén, J.; Fisker, N.; Hansen, H.F.; Persson, R.; Møller, M.R.; Rosenbohm, C.; Ørum, H.; Straarup, E.M.; Koch, T. PCSK9 LNA Antisense Oligonucleotides Induce Sustained Reduction of LDL Cholesterol in Nonhuman Primates. *Molecular Therapy* **2012**, *20*, 376–381, doi:10.1038/mt.2011.260.
12. Van Poelgeest, E.P.; Hodges, M.R.; Moerland, M.; Tessier, Y.; Levin, A.A.; Persson, R.; Lindholm, M.W.; Dumong Erichsen, K.; Ørum, H.; Cohen, A.F.; et al. Antisense-Mediated Reduction of Proprotein Convertase Subtilisin/Kexin Type 9 (PCSK9): A First-in-Human Randomized, Placebo-Controlled Trial. *Br J Clin Pharmacol* **2015**, *80*, 1350–1361, doi:10.1111/bcp.12738.
13. Carthew, R.W.; Sontheimer, E.J. Origins and Mechanisms of MiRNAs and SiRNAs. *Cell* 2009, *136*.
14. Ferrari, N. Hybridization-Independent Effects. In *Oligonucleotide-Based Drugs and Therapeutics*; 2018.
15. ICH S11 NONCLINICAL SAFETY TESTING IN SUPPORT OF DEVELOPMENT OF PAEDIATRIC PHARMACEUTICALS. *ICH Consensus Guideline* **2020**.
16. Yu, R.Z.; Lemonidis, K.M.; Graham, M.J.; Matson, J.E.; Crooke, R.M.; Tribble, D.L.; Wedel, M.K.; Levin, A.A.; Geary, R.S. Cross-Species Comparison of in Vivo PK/PD Relationships for Second-Generation Antisense Oligonucleotides Targeting Apolipoprotein B-100. *Biochem Pharmacol* **2009**, *77*, 910–919, doi:10.1016/j.bcp.2008.11.005.
17. Geary, R.S. Antisense Oligonucleotide Pharmacokinetics and Metabolism. *Expert Opin Drug Metab Toxicol* **2009**, *5*, 381–391, doi:10.1517/17425250902877680.
18. Lightfoot, H.; Schneider, A.; Hall, J. Pharmacokinetics and Pharmacodynamics of Antisense Oligonucleotides. In *Oligonucleotide-Based Drugs and Therapeutics*; Ferrari, N, Seguin, R., Ed.; John Wiley & Sons, Inc.: New Jersey, 2018; pp. 107–136 ISBN 9781119070290.
19. Lundin, K.E.; Hansen, B.R.; Persson, R.; Bramsen, J.B.; Koch, T.; Wengel, J.; Smith, C.I.E. Biological Activity and Biotechnological Aspects of Locked Nucleic Acids. *Adv Genet* **2013**, *82*, 47–107, doi:10.1016/B978-0-12-407676-1.00002-0.
20. Xiong, H.; Veedu, R.N.; Diermeier, S.D. Recent Advances in Oligonucleotide Therapeutics in Oncology. *Int J Mol Sci* **2021**, *22*, 3295, doi:10.3390/ijms22073295.
21. Koch, T.; Ørum, H. Locked Nucleic Acid. In *Antisense Drug Technology: Principles, Strategies, and Applications, Second Edition*; Crooke, S.T., Ed.; CRC Press: USA, 2007; pp. 519–564 ISBN 9780849387968.
22. Andersson, P.; Den Besten, C. Preclinical and Clinical Drug-Metabolism, Pharmacokinetics and Safety of Therapeutic Oligonucleotides. In *RSC Drug Discovery Series*; Agrawal, Sudhir, Gait, M., Ed.; Royal Society of Chemistry: UK, 2019; Vol. 2019-Janua, pp. 474–517 ISBN 978-1-78801-571-4.
23. Andersson, P. Preclinical Safety Assessment of Therapeutic Oligonucleotides. In *Methods in Molecular Biology*; 2022; Vol. 2434.
24. Van Poelgeest, E.P.; Swart, R.M.; Betjes, M.G.H.; Moerland, M.; Weening, J.J.; Tessier, Y.; Hodges, M.R.; Levin, A.A.; Burggraaf, J. Acute Kidney Injury during Therapy with an Antisense Oligonucleotide Directed against PCSK9. *American Journal of Kidney Diseases* **2013**, *62*, 796–800, doi:10.1053/j.ajkd.2013.02.359.
25. Henry, S.P.; Johnson, M.; Zanardi, T.A.; Fey, R.; Auyeung, D.; Lappin, P.B.; Levin, A.A. Renal Uptake and Tolerability of a 2'-O-Methoxyethyl Modified Antisense Oligonucleotide (ISIS 113715) in Monkey. *Toxicology* **2012**, *301*, 13–20, doi:10.1016/j.tox.2012.06.005.
26. Monteith, D.K.; Horner, M.J.; Gillett, N.A.; Butler, M.; Geary, R.; Burckin, T.; Ushiro-Watanabe, T.; Levin, A.A. Evaluation of the Renal Effects of an Antisense Phosphorothioate Oligodeoxynucleotide in Monkeys. *Toxicol Pathol* **1999**, *27*, doi:10.1177/019262339902700306.
27. Moisan, A.; Gubler, M.; Zhang, J.D.; Tessier, Y.; Dumong Erichsen, K.; Sewing, S.; Gérard, R.; Avignon, B.; Huber, S.; Benmansour, F.; et al. Inhibition of EGF Uptake by Nephrotoxic Antisense Drugs In Vitro and Implications for Preclinical Safety Profiling. *Mol Ther Nucleic Acids* **2017**, *6*, doi:10.1016/j.omtn.2016.11.006.

28. Laxton, C.; Brady, K.; Moschos, S.; Turnpenny, P.; Rawal, J.; Pryde, D.C.; Sidders, B.; Corbau, R.; Pickford, C.; Murray, E.J. Selection, Optimization, and Pharmacokinetic Properties of a Novel, Potent Antiviral Locked Nucleic Acid-Based Antisense Oligomer Targeting Hepatitis C Virus Internal Ribosome Entry Site. *Antimicrob Agents Chemother* **2011**, *55*, 3105–3114, doi:10.1128/AAC.00222-11.
29. Hagedorn, P.H.; Persson, R.; Funder, E.D.; Albæk, N.; Diemer, S.L.; Hansen, D.J.; Møller, M.R.; Papargyri, N.; Christiansen, H.; Hansen, B.R.; et al. Locked Nucleic Acid: Modality, Diversity, and Drug Discovery. *Drug Discov Today* **2018**, *23*, 101–114, doi:10.1016/j.drudis.2017.09.018.
30. Frazier, K.S. Antisense Oligonucleotide Therapies:The Promise and the Challenges from a Toxicologic Pathologist's Perspective. *Toxicol Pathol* **2015**, *43*, 78–89, doi:10.1177/0192623314551840.
31. Henry, S.P.; Kim, T.W.; Kramer-Stickland, K.; Zanardi, T.A.; Fey, R.A.; Levin, A.A. Toxicologic Properties of 2'-o-Methoxyethyl Chimeric Antisense Inhibitors in Animals and Man. In *Antisense Drug Technology: Principles, Strategies, and Applications, Second Edition*; 2007.
32. Monteith, D.K.; Levin, A.A. Synthetic Oligonucleotides: The Development of Antisense Therapeutics. In Proceedings of the Toxicologic Pathology; 1999; Vol. 27.
33. Hilmer, S.N.; Cogger, V.C.; Le Couteur, D.G. Basal Activity of Kupffer Cells Increases with Old Age. *Journals of Gerontology - Series A Biological Sciences and Medical Sciences* **2007**, *62*, doi:10.1093/gerona/62.9.973.
34. Lopez, B.G.; Tsai, M.S.; Baratta, J.L.; Longmuir, K.J.; Robertson, R.T. Characterization of Kupffer Cells in Livers of Developing Mice. *Comp Hepatol* **2011**, *10*, doi:10.1186/1476-5926-10-2.
35. Leeds, J.M.; Henry, S.P.; Geary, R.; Burckin, T.; Levin, A.A. Comparison of the Pharmacokinetics of Subcutaneous and Intravenous Administration of a Phosphorothioate Oligodeoxynucleotide in Cynomolgus Monkeys. *Antisense Nucleic Acid Drug Dev* **2000**, *10*, doi:10.1089/oli.1.2000.10.435.
36. Simon, A.K.; Hollander, G.A.; McMichael, A. Evolution of the Immune System in Humans from Infancy to Old Age. *Proceedings of the Royal Society B: Biological Sciences* 2015, *282*.
37. Dieckmann, A.; Hagedorn, P.H.; Burki, Y.; Brügmann, C.; Berrera, M.; Ebeling, M.; Singer, T.; Schuler, F. A Sensitive In Vitro Approach to Assess the Hybridization-Dependent Toxic Potential of High Affinity Gapmer Oligonucleotides. *Mol Ther Nucleic Acids* **2018**, *10*, doi:10.1016/j.omtn.2017.11.004.
38. Burel, S.A.; Hart, C.E.; Cauntay, P.; Hsiao, J.; Machemer, T.; Katz, M.; Watt, A.; Bui, H.H.; Younis, H.; Sabripour, M.; et al. Hepatotoxicity of High Affinity Gapmer Antisense Oligonucleotides Is Mediated by RNase H1 Dependent Promiscuous Reduction of Very Long Pre-MRNA Transcripts. *Nucleic Acids Res* **2015**, *44*, 2093–2109, doi:10.1093/nar/gkv1210.
39. Goyenvalle, A.; Jimenez-Mallebrera, C.; Van Roon, W.; Sewing, S.; Krieg, A.M.; Arechavala-Gomeza, V.; Andersson, P. Considerations in the Preclinical Assessment of the Safety of Antisense Oligonucleotides. *Nucleic Acid Ther* 2023, *33*.
40. Nieskens, T.T.G.; Magnusson, O.; Andersson, P.; Söderberg, M.; Persson, M.; Sjögren, A.K. Nephrotoxic Antisense Oligonucleotide SPC5001 Induces Kidney Injury Biomarkers in a Proximal Tubule-on-a-Chip. *Arch Toxicol* **2021**, *95*, doi:10.1007/s00204-021-03062-8.
41. Kitson, J.D.A.; Kamola, P.J.; Kane, L. Hybridization-Dependent Effects. In *Oligonucleotide-Based Drugs and Therapeutics*; 2018.
42. Lindow, M.; Vornlocher, H.P.; Riley, D.; Kornbrust, D.J.; Burchard, J.; Whiteley, L.O.; Kamens, J.; Thompson, J.D.; Nochur, S.; Younis, H.; et al. Assessing Unintended Hybridization-Induced Biological Effects of Oligonucleotides. *Nat Biotechnol* 2012, *30*.
43. Hagedorn, P.H.; Hansen, B.R.; Koch, T.; Lindow, M. Managing the Sequence-Specificity of Antisense Oligonucleotides in Drug Discovery. *Nucleic Acids Res* 2017, *45*.

44. Shen, L.; Frazer-Abel, A.; Reynolds, P.R.; Giclas, P.C.; Chappell, A.; Pangburn, M.K.; Younis, H.; Henry, S.P. Mechanistic Understanding for the Greater Sensitivity of Monkeys to Antisense Oligonucleotide-Mediated Complement Activation Compared with Humans. *Journal of Pharmacology and Experimental Therapeutics* **2014**, *351*, doi:10.1124/jpet.114.219378.
45. Henry, S.P.; Beattie, G.; Yeh, G.; Chappel, A.; Giclas, P.; Mortari, A.; Jagels, M.A.; Kornbrust, D.J.; Levin, A.A. Complement Activation Is Responsible for Acute Toxicities in Rhesus Monkeys Treated with a Phosphorothioate Oligodeoxynucleotide. *Int Immunopharmacol* **2002**, *2*, doi:10.1016/S1567-5769(02)00142-X.
46. Henry, S.P.; Giclas, P.C.; Leeds, J.; Pangburn, M.; Auletta, C.; Levin, A.A.; Kornbrust, D.J. Activation of the Alternative Pathway of Complement by a Phosphorothioate Oligonucleotide: Potential Mechanism of Action. *Journal of Pharmacology and Experimental Therapeutics* **1997**, *281*.
47. Olsen, A.K.; Hansen, A.K.; Jespersen, J.; Marckmann, P.; Bladbjerg, E.M. The Pig as a Model in Blood Coagulation and Fibrinolysis Research. *Scandinavian Journal of Laboratory Animal Science* **1999**, *26*.
48. Kessler, U.; Grau, T.; Gronchi, F.; Berger, S.; Brandt, S.; Bracht, H.; Marcucci, C.; Zachariou, Z.; Jakob, S.M. Comparison of Porcine and Human Coagulation by Thrombelastometry. *Thromb Res* **2011**, *128*, doi:10.1016/j.thromres.2011.03.013.
49. Ayuso, M.; Buyssens, L.; Stroe, M.; Valenzuela, A.; Allegaert, K.; Smits, A.; Annaert, P.; Mulder, A.; Carpentier, S.; Van Ginneken, C.; et al. The Neonatal and Juvenile Pig in Pediatric Drug Discovery and Development. *Pharmaceutics* **2021**, *13*, 44, doi:10.3390/pharmaceutics13010044.
50. Forster, R.; Bode, G.; Ellegaard, L.; van der Laan, J.W. The RETHINK Project on Minipigs in the Toxicity Testing of New Medicines and Chemicals: Conclusions and Recommendations. *J Pharmacol Toxicol Methods* **2010**, *62*, 236–242, doi:10.1016/j.vascn.2010.05.008.
51. Van Peer, E.; Downes, N.; Casteleyn, C.; Van Ginneken, C.; Weeren, A.; Van Cruchten, S. Organ Data from the Developing Göttingen Minipig: First Steps towards a Juvenile PBPK Model. *J Pharmacokinet Pharmacodyn* **2016**, *43*, 179–190, doi:10.1007/s10928-015-9463-8.
52. Stricker-Krongrad, A.; Shoemake, C.R.; Bouchard, G.F. The Miniature Swine as a Model in Experimental and Translational Medicine. *Toxicol Pathol* **2016**, *44*, doi:10.1177/0192623316641784.
53. Swindle, M.M.; Smith, A.C. *Swine in the Laboratory: Surgery, Anesthesia, Imaging, and Experimental Techniques*; 2016;
54. Prior, H.; Blunt, H.; Crossman, L.; McGuire, A.; Stow, R.; Sewell, F. Refining Procedures within Regulatory Toxicology Studies: Improving Animal Welfare and Data. *Animals* **2021**, *11*, doi:10.3390/ani11113057.
55. Suenderhauf, C.; Parrott, N. A Physiologically Based Pharmacokinetic Model of the Minipig: Data Compilation and Model Implementation. *Pharm Res* 2013, *30*.
56. Summerfield, A.; Rziha, H.J.; Saalmüller, A. Functional Characterization of Porcine CD4+CD8+ Extrathymic T Lymphocytes. *Cell Immunol* **1996**, *168*, doi:10.1006/cimm.1996.0078.
57. Ulrich, P.; Blaich, G.; Baumann, A.; Fagg, R.; Hey, A.; Kiessling, A.; Kronenberg, S.; Lindecrona, R.H.; Mohl, S.; Richter, W.F.; et al. Biotherapeutics in Non-Clinical Development: Strengthening the Interface between Safety, Pharmacokinetics-Pharmacodynamics and Manufacturing. *Regulatory Toxicology and Pharmacology* **2018**, *94*, doi:10.1016/j.yrtph.2018.01.013.
58. Thygesen, P.; Andersen, H.S.; Behrens, C.; Fels, J.J.; Nørskov-Lauritsen, L.; Rischel, C.; Johansen, N.L. Nonclinical Pharmacokinetic and Pharmacodynamic Characterisation of Somapacitan: A Reversible Non-Covalent Albumin-Binding Growth Hormone. *Growth Hormone and IGF Research* **2017**, *35*, doi:10.1016/j.ghir.2017.05.006.

59. Gala, R.P.; Popescu, C.; Knipp, G.T.; McCain, R.R.; Ubale, R. V.; Addo, R.; Bhowmik, T.; Kulczar, C.D.; D'Souza, M.J. Physicochemical and Preclinical Evaluation of a Novel Buccal Measles Vaccine. *AAPS PharmSciTech* **2017**, *18*, doi:10.1208/s12249-016-0566-3.
60. Starbæk, S.M.R.; Brogaard, L.; Dawson, H.D.; Smith, A.D.; Heegaard, P.M.H.; Larsen, L.E.; Jungersen, G.; Skovgaard, K. Animal Models for Influenza A Virus Infection Incorporating the Involvement of Innate Host Defenses: Enhanced Translational Value of the Porcine Model. *ILAR J* 2018, *59*.
61. Rajao, D.S.; Vincent, A.L. Swine as a Model for Influenza Avirus Infection and Immunity. *ILAR J* **2015**, *56*, doi:10.1093/ilar/ilv002.
62. Busignies, V.; Simon, G.; Mollereau, G.; Bourry, O.; Mazel, V.; Rosa-Calatrava, M.; Tchoreloff, P. Development and Pre-Clinical Evaluation in the Swine Model of a Mucosal Vaccine Tablet for Human Influenza Viruses: A Proof-of-Concept Study. *Int J Pharm* **2018**, *538*, doi:10.1016/j.ijpharm.2018.01.021.
63. Ramos, L.; Obregon-Henao, A.; Henao-Tamayo, M.; Bowen, R.; Izzo, A.; Lunney, J.K.; Gonzalez-Juarrero, M. Minipigs as a Neonatal Animal Model for Tuberculosis Vaccine Efficacy Testing. *Vet Immunol Immunopathol* **2019**, *215*, doi:10.1016/j.vetimm.2019.109884.
64. Kajimoto, M.; Atkinson, D.B.; Ledee, D.R.; Kayser, E.B.; Morgan, P.G.; Sedensky, M.M.; Isern, N.G.; Des Rosiers, C.; Portman, M.A. Propofol Compared with Isoflurane Inhibits Mitochondrial Metabolism in Immature Swine Cerebral Cortex. *Journal of Cerebral Blood Flow and Metabolism* **2014**, *34*, doi:10.1038/jcbfm.2013.229.
65. Boudreaux, J.P.; Schieber, R.A.; Cook, D.R. Hemodynamic Effects of Halothane in the Newborn Piglet. *Anesth Analg* **1984**, *63*, doi:10.1213/00000539-198408000-00005.
66. Rai, A.; Bhalla, S.; Rebello, S.S.; Kastrissios, H.; Gulati, A. Disposition of Morphine in Plasma and Cerebrospinal Fluid Varies during Neonatal Development in Pigs. *Journal of Pharmacy and Pharmacology* **2010**, *57*, doi:10.1211/0022357056505.
67. Millecam, J.; Van Bergen, T.; Schauvliege, S.; Antonissen, G.; Martens, A.; Chiers, K.; Gehring, R.; Gasthuys, E.; Walle, J. Vande; Croubels, S.; et al. Developmental Pharmacokinetics and Safety of Ibuprofen and Its Enantiomers in the Conventional Pig as Potential Pediatric Animal Model. *Front Pharmacol* **2019**, *10*, doi:10.3389/fphar.2019.00505.
68. Roth, W.J.; Kissinger, C.B.; McCain, R.R.; Cooper, B.R.; Marchant-Forde, J.N.; Vreeman, R.C.; Hannou, S.; Knipp, G.T. Assessment of Juvenile Pigs to Serve as Human Pediatric Surrogates for Preclinical Formulation Pharmacokinetic Testing. *AAPS Journal* **2013**, *15*, doi:10.1208/s12248-013-9482-6.
69. McDonald, C.M.; Wong, B.; Flanigan, K.M.; Wilson, R.; de Kimpe, S.; Lourbakos, A.; Lin, Z.; Campion, G.; Iannaccone, S.T.; Karachunski, P.I.; et al. Placebo-Controlled Phase 2 Trial of Drisapersen for Duchenne Muscular Dystrophy. *Ann Clin Transl Neurol* **2018**, *5*, doi:10.1002/acn3.579.
70. Goemans, N.M.; Tulinius, M.; Van Den Hauwe, M.; Kroksmark, A.K.; Buyse, G.; Wilson, R.J.; Van Deutekom, J.C.; De Kimpe, S.J.; Lourbakos, A.; Campion, G. Long-Term Efficacy, Safety, and Pharmacokinetics of Drisapersen in Duchenne Muscular Dystrophy: Results from an Open-Label Extension Study. *PLoS One* **2016**, *11*, doi:10.1371/journal.pone.0161955.
71. Union, E. Directive 2010/63/EU of the European Parliament and of the Council of 22 September 2010 on the Protection of Animals Used for Scientific Purposes. *Official Journal of the European Union* **2010**.
72. Tessier, Y.; Achanzar, W.; Mihalcik, L.; Amuzie, C.; Andersson, P.; Parry, J.D.; Moggs, J.; Whiteley, L.O. Outcomes of the European Federation of Pharmaceutical Industries and Associations Oligonucleotide Working Group Survey on Nonclinical Practices and Regulatory Expectations for Therapeutic Oligonucleotide Safety Assessment. *Nucleic Acid Ther* **2021**, *31*, doi:10.1089/nat.2020.0892.

73. Baber, N. Guide to Paediatric Clinical Research. *Br J Clin Pharmacol* **2008**, *65*, 282–282, doi:10.1111/j.1365-2125.2007.03011.x.
74. Montieth, D.K.; Horner, M.J.; Gillett, N.A.; Butler, M.; Geary, R.; Burckin, T.; Ushiro-watanabe, T.; Levin, A.A. Oligodeoxynucleotide Antisense Phosphorothioate in Monkeys. *Toxicology Pathology* **1999**, *27*, 307–317.
75. Fey, R.A.; Templin, M. V.; McDonald, J.D.; Yu, R.Z.; Hutt, J.A.; Gigliotti, A.P.; Henry, S.P.; Reed, M.D. Local and Systemic Tolerability of a 2'O-Methoxyethyl Antisense Oligonucleotide Targeting Interleukin-4 Receptor-α Delivery by Inhalation in Mouse and Monkey. *Inhal Toxicol* **2014**, *26*, doi:10.3109/08958378.2014.907587.
76. Hildebrandt-Eriksen, E.S.; Aarup, V.; Persson, R.; Hansen, H.F.; Munk, M.E.; Ørum, H. A Locked Nucleic Acid Oligonucleotide Targeting MicroRNA 122 Is Well-Tolerated in Cynomolgus Monkeys. *Nucleic Acid Ther* **2012**, *22*, 152–161, doi:10.1089/nat.2011.0332.
77. Webb, M.S.; Tortora, N.; Cremese, M.; Kozlowska, H.; Blaquiere, M.; Devine, D. V.; Kornbrust, D.J. Toxicity and Toxicokinetics of a Phosphorothioate Oligonucleotide against the C-Myc Oncogene in Cynomolgus Monkeys. *Antisense Nucleic Acid Drug Dev* **2001**, *11*, doi:10.1089/108729001300338681.
78. Zanardi, T.A.; Han, S.C.; Jeong, E.J.; Rime, S.; Yu, R.Z.; Chakravarty, K.; Henry, S.P. Pharmacodynamics and Subchronic Toxicity in Mice and Monkeys of ISIS 388626, a Second-Generation Antisense Oligonucleotide That Targets Human Sodium Glucose Cotransporter 2. *Journal of Pharmacology and Experimental Therapeutics* **2012**, *343*, doi:10.1124/jpet.112.197426.
79. Dhondt, L.; Croubels, S.; De Paepe, P.; Wallis, S.C.; Pandey, S.; Roberts, J.A.; Lipman, J.; De Cock, P.; Devreese, M. Conventional Pig as Animal Model for Human Renal Drug Excretion Processes: Unravelling the Porcine Renal Function by Use of a Cocktail of Exogenous Markers. *Front Pharmacol* **2020**, *11*, doi:10.3389/fphar.2020.00883.
80. Helke, K.L.; Nelson, K.N.; Sargeant, A.M.; Jacob, B.; McKeag, S.; Haruna, J.; Vemireddi, V.; Greeley, M.; Brocksmith, D.; Navratil, N.; et al. Background Pathological Changes in Minipigs: A Comparison of the Incidence and Nature among Different Breeds and Populations of Minipigs. *Toxicol Pathol* **2016**, *44*.
81. Butler, J.E.; Wertz, N.; Sinkora, M. Antibody Repertoire Development in Swine. *Annu Rev Anim Biosci* 2017, *5*.
82. Comstock, S.S.; Reznikov, E.A.; Contractor, N.; Donovan, S.M. Dietary Bovine Lactoferrin Alters Mucosal and Systemic Immune Cell Responses in Neonatal Piglets. *Journal of Nutrition* **2014**, *144*, doi:10.3945/jn.113.190264.
83. Butler, J.E.; Lager, K.M.; Splichal, I.; Francis, D.; Kacskovics, I.; Sinkora, M.; Wertz, N.; Sun, J.; Zhao, Y.; Brown, W.R.; et al. The Piglet as a Model for B Cell and Immune System Development. *Vet Immunol Immunopathol* 2009, *128*.

Summary

Antisense oligonucleotides (ASOs) belong to a large group of nucleic acid-based therapeutic modalities that utilize synthetic oligomers of nucleotides to modulate RNA translation to proteins. This is of interest in cases of cancers, viral infections, and rare genetic conditions wherein the disease-causing or disease-related proteins are difficult or even impossible to target by small molecule drugs. In **Chapter 1**, we introduced the common classes and mechanisms of actions (e.g., RNase H dependent) that ASOs utilize, as well as the common chemistry modifications and designs that could influence their pharmacokinetic and pharmacodynamic profiles. In general, predictive class behavior in terms of drug metabolism, pharmacokinetics, and toxicity profiles is demonstrated. This facilitates certain extrapolations since their class behavior is only marginally influenced by a particular sequence. With previous experience and overall predictable behavior of ASOs, stringent screening processes can be applied.

Currently, there is no specific guideline for this emerging drug modality. The nonclinical development and general safety assessment of ASOs usually follows the nonclinical testing guidelines for small molecules, while some principles of the biotechnology-derived pharmaceutical guideline could be considered in a hybrid approach on a case-by-case basis. As ASOs need to hybridize to their complementary target RNA, nonhuman primates (NHPs) are the preferred non-rodent model for this class of compounds due to their close genetic homology and pharmacokinetics with humans. Nonetheless, the adult Göttingen Minipig appears to be a suitable alternative to NHPs, as it showed similar pharmacokinetic, pharmacodynamic, and safety profiles in a previous study. Since ASOs are usually indicated to rare genetic conditions that could start early in life, and as the rapid growth and development of the pediatric population can influence the pharmacokinetics and pharmacodynamics of therapeutic agents, leading to potential adverse effects, extending the previous work to the juvenile minipigs was deemed necessary. Therefore, the aim and objectives of this doctoral thesis were to evaluate the juvenile Göttingen Minipig as a pediatric safety testing model for ASOs (see **Chapter 2).**

In **Chapter 3**, we assessed potential differences in exposure/toxicity and pharmacologic effect of a model LNA/PS/LNA gapmer ASO (RTR5001) in the juvenile Göttingen Minipig in an 8-week repeat-

dose toxicity study (weekly subcutaneous dosing starting on postnatal day 1 for up to 8 weeks). Accordingly, the model ASO that had been previously characterized in adult Göttingen Minipigs and NHPs, in which the kidney and the liver were the primary target organs, showed comparable clinical chemistry and toxicity profiles in the juvenile minipigs. However, differences in plasma and tissue exposures as well as pharmacologic activity, were observed when compared with the adult data. On the other hand, as ASOs neither act as substrates for phase I nor phase II metabolizing enzymes but rather metabolize by endogenous nucleases, the ontogeny evaluation of the key nucleases responsible for ASO metabolism and pharmacologic activity (i.e., RNase H) revealed a differential nuclease expression and activity, which could affect the metabolic pathway and pharmacologic effect of ASOs in different tissues and age groups.

In the context of mechanisms and species translatability, a number of recurring ASO class safety concerns are well understood. No additional toxicities or clinically relevant toxicological target organs have been added to the possible risks associated with ASOs, aside from the sporadic occurrences of thrombocytopenia. In **Chapter 4**, to further understand the species translatability of ASO-induced thrombocytopenia, in vitro platelet activity and aggregometry assays were performed in Göttingen Minipigs using a panel of ASOs with different sequences and modifications with known platelet response phenotypes in NHPs and humans were employed as tool ASOs. Our data on direct platelet activation and aggregation by ASOs in adult minipigs are remarkably comparable to human data. Moreover, phosphorothioated ASOs bind to platelet collagen receptor glycoprotein VI (GPVI) and directly activate minipig platelets in vitro, mirroring the findings in human blood samples. In addition, the differential abundance of GPVI (and platelet factor 4) in minipigs provides insight into the influence of ontogeny in potential ASO-induced thrombocytopenia in pediatric patients.

The body of data from Chapters 3 and 4 is fundamental for selecting the juvenile Göttingen Minipig in assessing safety concerns for ASOs intended for the human pediatric population. **Chapter 5** discussed the main findings of this thesis and put them into broader nonclinical and clinical perspectives to conclude that there is no constraint in using juvenile minipigs as non-rodent species in pediatric ASO candidate nonclinical safety packages and this may convince health authorities in accepting this juvenile animal model.

Samenvatting

Antisense oligonucleotiden (ASO's) behoren tot een grote groep op nucleïnezuur gebaseerde therapeutische modaliteiten die gebruik maken van synthetische oligomeren van nucleotiden om RNA-translatie naar eiwitten te moduleren. Dit is van belang bij kanker, virale infecties en zeldzame genetische aandoeningen waarbij de ziekte-veroorzakende of ziekte-gerelateerde eiwitten moeilijk of zelfs onmogelijk kunnen worden behandeld door conventionele geneesmiddelen. In **Hoofdstuk 1** hebben we de meest voorkomende klassen en werkingsmechanismen geïntroduceerd (bijv. RNase H-afhankelijk) die ASO's gebruiken, evenals de meest voorkomende chemische aanpassingen en structuren die hun farmacokinetische en farmacodynamische profielen zouden kunnen beïnvloeden. Over het algemeen wordt zijn deze structuren en aanpassingen predictief mbt hun geneesmiddelmetabolisme, farmacokinetiek en toxiciteitsprofiel. Deze laatsten worden slechts marginaal beïnvloed door een bepaalde sequentie. Aan de hand van eerdere ervaringen en algemeen voorspelbaar gedrag van ASO's kunnen strikte screeningprocessen worden toegepast.

Momenteel bestaat er geen specifieke richtlijn voor deze opkomende therapeutische interventie. De preklinische ontwikkeling en algemene veiligheidsbeoordeling van ASO's volgt meestal de preklinische testrichtlijnen voor kleine moleculen, terwijl sommige principes van de biotechnologie-afgeleide farmaceutische richtlijn kunnen worden overwogen in een hybride benadering van geval tot geval. Aangezien ASO's moeten hybridiseren met hun complementaire doel-RNA, zijn apen (NHP's) het geprefereerde niet-knaagdiermodel voor deze klasse van verbindingen vanwege hun nauwe genetische homologie en farmacokinetiek met mensen. Desalniettemin lijkt het volwassen Göttingen minivarken een geschikt alternatief te zijn voor NHP's, aangezien het vergelijkbare farmacokinetische, farmacodynamische en veiligheidsprofielen vertoonde in een eerdere studie. Aangezien ASO's meestal geïndiceerd zijn voor zeldzame genetische aandoeningen die vroeg in het leven kunnen ontstaan, en aangezien de snelle groei en ontwikkeling van de pediatrische populatie de farmacokinetiek en farmacodynamiek van therapeutische middelen kan beïnvloeden, wat kan leiden tot mogelijke nadelige effecten, was het noodzakelijk om het eerdere werk uit te breiden naar juveniele minivarkens. Daarom evalueerde dit proefschrift het juveniele Göttingen minivarken als een pediatrisch veiligheidstestmodel voor ASO's (zie doelstellingen in **Hoofdstuk 2).**

In **Hoofdstuk 3** hebben we mogelijke verschillen in blootstelling/toxiciteit en farmacologisch effect van een model LNA/PS/LNA gapmer ASO (RTR5001) in het juveniele Göttingen minivarken onderzocht in een 8 weken durende toxiciteitsstudie met herhaalde dosering (wekelijkse subcutane toediening bij een leeftijd van dag 1 tot 8 weken). De ASO die eerder was gekarakteriseerd in volwassen Göttingen minivarkens en NHP's, waarbij de nier en de lever de primaire doelorganen waren, vertoonde vergelijkbare klinische chemie- en toxiciteitsprofielen bij de juveniele minivarkens. Er werden echter verschillen waargenomen in plasma- en weefselblootstelling en in farmacologische activiteit in vergelijking met de data voor volwassenen. Aangezien ASO's niet fungeren als substraten voor fase I- of fase II-metaboliserende enzymen, maar eerder worden gemetaboliseerd door endogene nucleasen, onthulde de ontogenie-evaluatie van de belangrijkste nucleasen die verantwoordelijk zijn voor het ASO-metabolisme en de farmacologische activiteit (d.w.z. RNase H) een verschillende nuclease expressie en activiteit, die de metabole route en het farmacologische effect van ASO's in verschillende weefsels en leeftijdsgroepen kunnen beïnvloeden.

Met betrekking tot mechanismen en de translatie tussen verschillende diersoorten en de mens, zijn er een aantal duidelijke veiligheidsproblemen bij RTR5001. In onze eerdere studie (Chapter 3) werden geen bijkomende klinisch relevante toxicologische doelorganen gedecteerd afgezien van sporadische gevallen van trombocytopenie. Om deze ASO-geïnduceerde trombocytopenie en de mogelijke translatie naar de mens beter te begrijpen, werden in **Hoofdstuk 4** s in vitro bloedplaatjesactiviteit- en aggregometrie-assays uitgevoerd in Göttingen minivarken met behulp van een panel van ASO's met verschillende sequenties en aanpassingen. Deze ASO’s hadden reeds gekende bloedplaatjesresponsfenotypes in NHP's en mensen. Onze gegevens over directe activering en aggregatie van bloedplaatjes door ASO's bij volwassen minivarkens zijn opmerkelijk vergelijkbaar met de gegevens bij mensen. Bovendien binden gefosforothioiseerde ASO's aan bloedplaatjescollageenreceptorglycoproteïne VI (GPVI) en activeren ze rechtstreeks minivarken-bloedplaatjes in vitro, een weerspiegeling van de bevindingen in menselijke bloedmonsters. Bovendien geeft de differentiële abundantie van GPVI (en bloedplaatjesfactor 4) bij minivarkens inzicht in de invloed van ontogenie bij potentiële ASO-geïnduceerde trombocytopenie bij pediatrische patiënten.

Het geheel aan gegevens uit de hoofdstukken 3 en 4 is van fundamenteel belang voor het selecteren van de juveniele Göttingen Minipig bij het beoordelen van veiligheidsrisico's voor ASO's die bedoeld zijn voor de pediatrische populatie. **Hoofdstuk 5** bespreekt de belangrijkste bevindingen van dit proefschrift en plaatst ze in bredere preklinische en klinische perspectieven. Er kan geconcludeerd worden dat er geen beperkingen zijn voor het gebruik van juveniele minivarkens als de niet-knaagdiersoort in preklinische studies voor pediatrische ASO-kandidaten. Dit kan regelgevende organisaties overtuigen om dit juveniele diermodel te aanvaarden voor preklinische studies.

Acknowledgements

The conduct of this doctoral research and the drafting of this thesis is only possible with the contributions of several people/organizations. Therefore, let me take this chance to acknowledge them and express my deepest gratitude and appreciation for their time, guidance, and support.

Foremost, to my promotor, Prof. Dr. Steven Van Cruchten. For believing in me and entrusting this doctoral project under his supervision. Thank you for your valuable guidance, advice, time, and support. This also goes well for my co-promotor, Dr. Miriam Ayuso Hernando, for her relentless supervision and who is always there to answer my questions. I have not mentioned it before, but I consider myself lucky to had this opportunity to work with both of you on a project that I am genuinely passionate about and which allowed me to develop and mature as a researcher, regardless of whatever challenges present themselves (either scientific, technical, practical, even public speaking, which I find the most taxing).

To my colleagues in the Comparative Perinatal Development group (UAntwerpen); Prof. Dr. Chris Van Ginneken, Katty Huybrechts, Gunther Vrolix, Sara Prims, Dr. Lieselotte Van Bockstal, Marlotte Loyens, Jente Hoyberghs, Axelle Coppens, Steve Van Bienst, Kevin Van Tichelen, Marjan Lauwers, Fien Verhaert, Ellen Goossenaerts, and Marleen Cools, thank you for everything.

I am also grateful to Marina Stroe and Michiel Tubeeckx for providing pig blood samples from their experiments, allowing me to optimize my assays. And, of course, to Laura Buyssens and Chloé Bars, who became not just the best colleagues but terrific friends with whom I could share not only my frustrations about this research but my milestones and achievements as well (including outside this research domain). Thank you for keeping me sane with your chitchats, brainstorming sessions, and whatever in between.

I would also like to acknowledge the contributions of the following people/organizations:

- The team from Roche Pharmaceutical Research and Early Development (Basel, Switzerland) and Charles River Laboratories France Safety Assessment SAS (Saint-Germain-Nuelles,

France) that is behind this collaborative project (from the conception, funding, to the conduct of this research). My gratitude goes to Dr. Claire Tardiveau, Dr. Pierluigi Fant, Isabelle Leconte, Dr. Annamaria Braendli-Baiocco, Dr. Neil Parrott, Dr. Georg Schmitt, Dr. Paul Barrow, and Dr. Yann Tessier.

- Ellegaard Göttingen Minipigs A/S (Dalmose, Denmark) and Janssen (Beerse, Belgium) for their warm accommodation and kind donation of animals and blood and tissue samples.
- The members of the jury: Prof. Dr. Louis Maes, Dr. Aurélie Goyenvalle, Dr. Peter van Meer, and Prof. Dr. Dries Knappen, for their constructive review.

I would also like to express my sincerest appreciation to my friends, my family (Alfonso, Josephine, Allan Joseph, and Allan Philip), and Marko (and his/my [second] family). Thank you for believing in me and for your unconditional love and support during this journey.

To those people whom I failed to mention specifically but became part of my life as a Ph.D. student (both academic and nonacademic-related).

Thank you. Dank u wel. Merci. Hvala. Maraming salamat!